การแยกนีโอดิเมียมจากโลหะหายากผ่านระบบเยื่อแผ่นเหลวที่พยุงด้วยเส้นใยกลวง

นางสาวธนพร วรรณโชติ

วิทยานิพนธ์นี้เป็นส่วนหนึ่งของการศึกษาตามหลักสูตรปริญญาวิศวกรรมศาสตรดุษฎีบัณฑิต
สาขาวิชาวิศวกรรมเคมี ภาควิชาวิศวกรรมเคมี
คณะวิศวกรรมศาสตร์ จุฬาลงกรณ์มหาวิทยาลัย
ปีการศึกษา 2558
ลิขสิทธิ์ของจุฬาลงกรณ์มหาวิทยาลัย

SEPARATION OF NEODYMIUM FROM RARE EARTH METALS VIA HOLLOW
FIBER SUPPORTED LIQUID MEMBRANE

Miss Thanaporn Wannachod

A Dissertation Submitted in Partial Fulfillment of the Requirements

for the Degree of Doctor of Engineering Program in Chemical Engineering

Department of Chemical Engineering

Faculty of Engineering

Chulalongkorn University

Academic Year 2015

Thesis Title	SEPARATION OF NEODYMIUM FROM RARE EARTH METALS VIA HOLLOW FIBER SUPPORTED LIQUID MEMBRANE
By	Miss Thanaporn Wannachod
Field of Study	Chemical Engineering
Thesis Advisor	Professor Ura Pancharoen, D.Eng.Sc.

Accepted by the Faculty of Engineering, Chulalongkorn University in Partial Fulfillment of the Requirements for the Doctoral Degree

--Dean of the Faculty of Engineering

(Professor Bundhit Eua-arporn, Ph.D.)

THESIS COMMITTEE

--Chairman

(Professor Paisan Kittisupakorn, Ph.D.)

--Thesis Advisor

(Professor Ura Pancharoen, D.Eng.Sc.)

--Examiner

(Assosiate Professor Kasidit Nootong, Ph.D.)

--Examiner

(Associate Professor Soorathep Kheawhom, Ph.D.)

--External Examiner

(Doctor Suwat Soonglerdsongpha, Ph.D.)

CONTENTS

LIST OF TABLES

LIST OF FIGURES

Page

จุฬาลงกรณ์มหาวิทยาลัย
CHULALONGKORN UNIVERSITY

CHAPTER 1

1.1   Introduction

Rare earth metals (REMs) consist of three elements i.e. Sc, Y, La and fourteen lanthanides, namely, from cerium to lutetium. The total member of REMs is thus 17. They are divided conventionally into two groups: the light group (Sc, La, Ce, Pr, Nd, Pm, Sm, Eu, Gd) and the heavy group (Y, Tb, Dy, Ho, Er, Tm, Yb, Lu) [1].

Rare earth metals, alone or in the form of mischmetal, are of increasing economic importance. The performance of alloys can be greatly improved by the addition of an appropriate amount of rare earth metals or their compounds [1]. For example, when an amount of rare earth elements is added to steel, the plasticity, heat resistance, toughness, oxidation resistance, abrasive resistance and corrosion resistance of the steel can be increased. Rare earths can be used to make pyrophoric alloys, permanent magnetic materials, dyeing materials, superconducting materials, luminescent materials, trace element fertilizers, and so on. Rare earth metals have been widely used, not only in the petrochemical industry and in metallurgy, glass ceramics, fluorescent materials, electronic materials, medicine and agriculture but

also have gradually penetrated into many other areas of modern science and technology. With ever more extensive applications, the separation and enrichment of rare earth elements has become increasingly important [2]. Due to their similar chemical nature owing to the common oxidation state of (III), rare earth metals are very difficult to separate from each other [3].

The selective separation of mixed rare earth metals, including neodymium, poses a glaring challenge to industry. Recently, numerous attempts have been made to develop efficient separation and concentration processes for RE metals. Owing to their unique physical and chemical properties, RE metals are in great demand and are best suited for the creation of advanced materials for high-technology devices.

Originally, the technique of fractionation and ion exchange was used for the separation of RE metals. However, this technique complicated the industry because it was tedious and time consuming. Subsequently, solvent extraction became renowned as an effective technique for separating RE metals. Yet, solvent extraction requires a large number of stages in a series of mixer-settlers to obtain high-purity products of RE metals since the chemical and physical properties of their adjacent elements are very similar. Therefore, an alternative technique to the use of solvent

extraction to overcome these complications has been introduced i.e. hollow fiber supported liquid membrane (HFSLM).

HFSLM has many advantages over traditional solvent extraction processes namely (1) low capital and operating costs (2) low energy consumption (3) economic use of expensive tailor-made extractants and solvents because only an extremely small amount of membrane liquid is required for filling the pores (4) low maintenance costs due to fewer moving parts and (5) the possibility of achieving a high overall separation factor [2, 3]. This method allows for both simultaneous extraction and stripping of target ions in one single-step operation. In recent years, the separation of ions with very low concentration has focused on liquid membrane (LM) techniques. HFSLM, especially, is an excellent method for extraction of ions in highly diluted solution at part-per-trillion (ppt) concentration levels. LM's can carry out simultaneous extraction and stripping processes in one stage and benefits a non-equilibrium mass transfer and up-hill effect where the solute can move from low to high concentration solution [4–7]. Therefore, HFSLM can be suitably applied for the treatment of neodymium (III) ions.

This study investigated the extraction of neodymium (III) ions by using HFSLM due to its low operating costs and its wide application in many industries. The feed solution was mixed rare earth nitrate solution provided by courtesy of the Rare Earth Research and Development Center, Office of Atoms for Peace, Bangkok, Thailand. The source of neodymium for study was supplied in nitrate solutions $RE(NO_3)_3$ – the digestion product of monazite ores processing. Monazite ore is a phosphate mineral containing rare earth metals e.g. lanthanum and cerium as well as small amounts of uranium and thorium [8, 9]. In general, uranium is a radioactive element which is useful at the front and back ends of the nuclear fuel cycle. However, uranium is known to cause serious environmental damage and has an acute effect on mammals. Monazite processing is shown in Fig. 1.1. It is made up of five units: ore digestion unit, tri sodium phosphate crystallization unit, dissolution unit, initial precipitation unit and cerium separation unit [10]. Researchers need to develop more efficient techniques in order to separate uranium from monazite processing directly or from tri-sodium phosphate. It is of vital importance to discover new ways to separate uranium safely and economically.
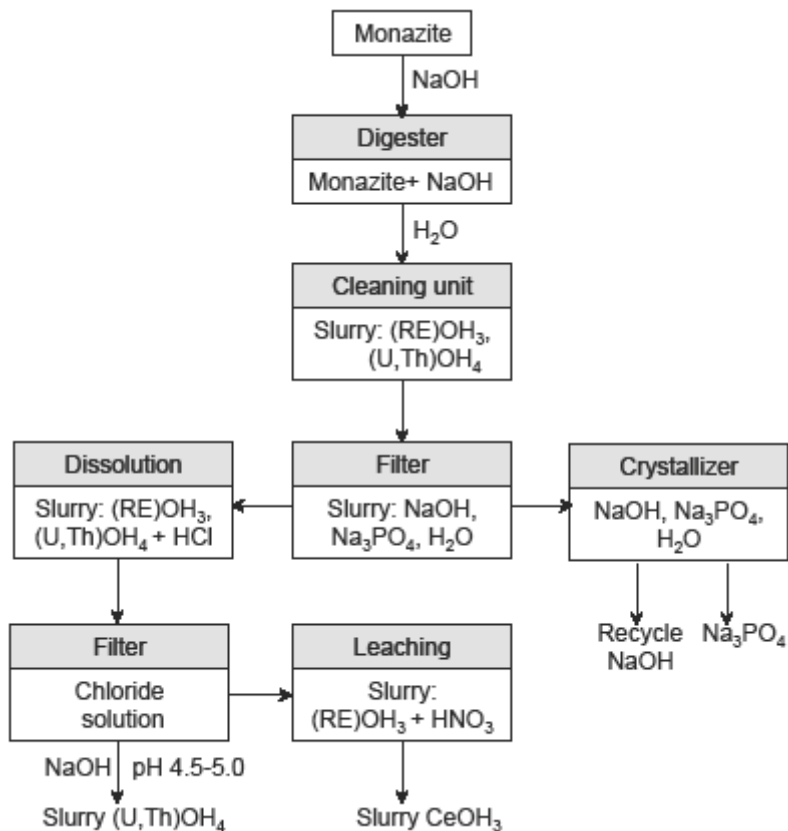
Figure 1.1 Monazite processing

1.1.1 Extractants

Extractants for the HFSLM system are grouped into 5 classes according to extraction mechanism, functional groups and types of metal ions extracted (cation, anion and neutral complex) i.e. acidic extractants, chelating extractants, neutral

extractants (or solvating type extractants), ligand substitution extractants, and basic extractants (or ion-pair extractants) [4, 5].

Acidic Extractants

Acidic extractants contain a functional group of phosphate ($HOPO(OR)_2$), carboxyl ($RCOOH$) or sulfo (RSO_3H) where R is alkyl group [4, 5]. An acidic extractant reacts with metal cation in the feed phase. In organic solvent or liquid membrane, the phosphate groups carboxyl or sulfo of the acidic extractant deprotonates to an anion species $OPO(OR)_2^-$, $RCOO^-$ or RSO_3^- ,respectively. The anion species subsequently form organo-metal complexes with the cation species. An acidic extractant which is widely used is D2EHPA (di-2-ethylhexylphosphoric acid, $HOPO(OC_8H_{17})_2$) [4]. The extraction of Nd^{3+} by D2EHPA is shown as follows in Eq. (1.1) [6].
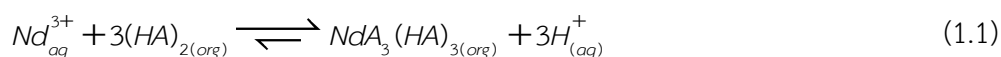
$$Nd^{3+}_{aq} + 3(HA)_{2(org)} \rightleftharpoons NdA_3(HA)_{3(org)} + 3H^+_{(aq)} \tag{1.1}$$

where (aq) is the species in the aqueous phase and (org) is the species in the liquid membrane phase.

Chelating extractants

Chelating extractants are often derived from analytical reagents, such as 2'-hydroxy-5'-nonylacetophenone ketoxime ($C_{17}H_{27}NO_2$) or LIX 84-I. They react with cation species same as acidic extractants. Chelating extractants chemically bond to cation species at two sites in a manner similar to holding an object between the ends of the thumb and the index finger [4]. When chelating extractants bond to cation species, they release hydrogen ion (H^+) into the feed solution. When pH of feed solution is increased, the extractability of chelating extractants increased. Decreasing of the pH promotes back-extraction or stripping. The extraction of Cu^{2+} is shown below in Eq. (1.2) [7].

$$Cu^{2+}_{aq} + 2C_{17}H_{27}NO_{2(org)} \rightleftharpoons (C_{17}H_{26}NO_2)_2 Cu_{(org)} + 2H^+_{(aq)} \qquad (1.2)$$
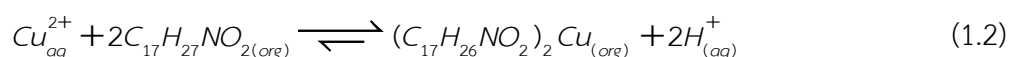
Neutral extractants (solvating type extractants)

Neutral extractants contain a functional group of phosphate ester ($PO(OR)_3$), phosphine sulphide (R_3PS) or phosphine oxide (R_3PO). Tributyl phosphate (L=TBP, $PO(OC_4H_9)_3$) or tri-isobutylphosphine ulphide (Cyanex 471, $(C_4H_9)_3PS$) is a good example

as a neutral extractant. Neutral extractants are basic in nature and will coordinate with certain neutral metal ions in the feed solution by replacing water molecules of hydration around neutral metal ions; thereby altering the targeted metal to hydrophobic ions [4]. The neutral donor (L) captures the inorganic anion (NO_3^-) in the feed phase to form the extractant. Subsequently, it reacts with Nd(III) to produce complex ions [6]. The extraction reaction of Nd(III) with neutral donor is shown in Eq. (1.3):

$$Nd_{(aq)}^{3+} + 3NO_{3(aq)}^- + 3L_{(org)} \rightleftharpoons Nd(NO_3)_3 \cdot L_{3(org)} \qquad (1.3)$$
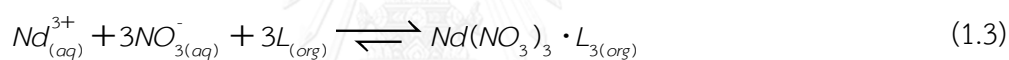
Ligand substitution extractants

Ligand substitution extractants donate an electrical pair to metal anion ions in similar mechanism to the neutral extractants. However, it forms an inner shell complex and subsequently displaces other ligands. A ligand substitution extractant includes mono-oxime (R_2CNOH) and dialkyl sulfides (R_2S). The extraction of $PdCl_4^{2-}$ using mono-oxime is shown as follows in Eq. (1.4) [11].

$$PdCl_{4(aq)}^{2-} + 2R_2CNOH_{(org)} \rightleftharpoons (R_2CNOH)_2PdCl_{2(org)} + 2Cl^{-} \qquad (1.4)$$

Basic extractants (ion-pair extractants)

Basic extractants contain a functional group of primary amine (RNH_2) or secondary amine (R_2NH) or tertiary amine (R_3N) or quaternary amine (R_4N^+). In general, commercial basic extractants contain a functional group of tertiary amine or quaternary amine. Quaternary amines are usually in the form of alkyl ammonium salts or amine salts. Metal anions in the feed solution can react with quaternary amine to form organo-metal complexes by replacing the common anions (e.g. Cl^-, F^- and SO_4^-) of the quaternary amines [4, 12]. The extraction of $HgCl_4^{2-}$ by Aliquat 336 [13] is shown as follows in Eq. (1.5).

$$HgCl_{4(aq)}^{2-} + 2(R_3N^+CH_3)Cl_{(org)}^{-} \xrightarrow{k_f} (R_3N^+CH_3)_2HgCl_{4\ (org)}^{2-} + 2Cl_{(aq)}^{-} \qquad (1.5)$$
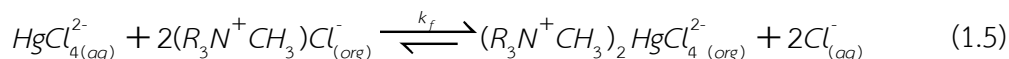
1.1.2   Feed solution

$RE(OH)_3$ from the Rare Earth Research and Development Center, Office of Atom for Peace, Bangkok, Thailand was supplied as a raw material for the experiments. The

RE hydroxide was digested with nitric acid solution. Then, RE oxide without cerium was obtained. After removing cerium, the colour changed from yellow to pale yellow as shown in Table 1.1 (analyzed by ICP). In this work, nitrate solution from monazite processing was again obtained from the Rare Earth Research and Development Center, Office of Atoms for Peace, Bangkok.

Table 1.1 Composition of mixed rare earth

Metal ions	Y	La	Ce	Pr	Nd	Sm	Eu	Gd	Dy	Yb
Concentration (mg/L)	13.6	12.8	1.8	23	106.7	1.3	0. 3	7.7	2.5	0.2

1.1.3   Diluents

A diluent is necessary for extraction via the HFSLM process. Generally, a diluent is a solvent that shall be inert, has a high boiling point and low toxicity [14]. Its application is to dissolve an extractant which is either a solid or viscous liquid that will render it suitable in terms of mobility and capillary tension for working in micro-porous hollow fibers. Diluents, such as kerosene, heptane, octane, nitrobenzene, dichloromethane, chloroform, xylene and toluene, are widely used for this HFSLM application [15]. The percentage of extraction of metal ions varies with the nature of

the diluents e.g. polarity indexes. Generally, when the dielectric constant and the dipole moment of diluents decrease, extraction increases. This can be explained by the fact that the interaction of diluents, having a high dielectric constant with the extractant, are generally stronger than those of low dielectric constant e.g. octane. Strong interaction of diluents with an extractant can result in lower extraction of metal ions.

1.1.4   Stripping solutions

The selection of stripping solution for removal of metal ions from the organo-metal complexes depends on the type of metal ions extracted (cation, anion and neutral complex) and type of extractants (acidic extractants, chelating extractants, neutral extractants, ligand substitution extractants and basic extractants) used in the extraction of metal ions.

In the extraction of metal cations, an acidic extractant or a chelating extractant is used. In order to strip metal cations from the organo-metal complexes, an acidic stripping solution is required. Hydrogen ions from the acidic stripping solution work to replace metal cations in the (organo) metal complex. As a

consequence, the metal cations will become free and captured by the stripping solution.

In the case of extraction of metal anions, a basic extractant or a neutral extractant is used. In order to strip metal anions from the organo-metal complexes, a basic stripping solution is required. Anions from the basic stripping solution replace metal anions in the organo-metal complexes. As a result, metal anions are released to the stripping solution.

For the extraction of neutral metal complexes, a neutral extractant is used. Neutral metal complexes can be stripped from the organo-metal complexes by a neutral stripping solution.

1.1.5   Transport in Hollow Fiber Supported Liquid Membrane

The HFSLM module, deployed in this study, is engineered from micro-porous polypropylene woven into fabric and wrapped around a central-tube feeder to supply the shell side fluid. It thus creates an immiscible layer between feed and stripping phases to form an organic extractant in the micro-porous hollow fibers. It is

supplied by CELGARD LLC (Charlotte, NC; formerly Hoechst Celanese). It has properties as shown in Table 1.2.

Table 1.2 Properties of the hollow fiber module

Properties	Description
Material	Polypropylene
Inside diameter of hollow fiber (cm)	0.024
Outside diameter of hollow fiber (cm)	0.03
Effective length of hollow fiber (cm)	15
Number of hollow fibers	35,000
Average pore size (cm)	3×10^{-6}
Porosity (%)	25
Effective surface area (cm^2)	1.4×10^4
Area per unit volume (cm^2/cm^3)	29.3
Module diameter (cm)	6.3
Module length (cm)	20.3
Tortuosity factor	2.6
Operating temperature (K)	273–333

The target component is dissolved in the liquid membrane at the interface and then preferentially diffuses through that immiscible layer to the stripping solution where it is recovered. This phenomenon of diffusion transport can be either a simple facilitated transport or coupled facilitated transport. Simple facilitated transport

occurs when the transport is independent of any other ions. It normally takes place in an application of neutral species extraction. Coupled facilitated transport will occur in the case of ionic species extraction to maintain the solution electro neutrality [16]. The driving force to determine transport rate is dependent on co-ion concentration in the feed.

Fig. 1.2 schematically explains the transport of each case. The schema depicts (A) as the target component (B) co-ions (C) the organic extractant and (A-C or B-C or A-B-C) the organic complex. In our study, the target component (A) can be arsenic and/or mercury ions. The straightforward mechanism is observed with the simple facilitated transport (Fig. 1.2 (a)) since the organic complex (A-C) is produced from the reaction between (A) and (C). Then, (A-C) is decomposed at the interface between the liquid membrane and the stripping phase and (A) is recovered to the stripping solution. The coupled facilitated transport can be classified into co-transport (Fig. 1.2 (b)) and counter-transport (Fig. 1.2 (c)). For the coupled facilitated co-transport, the extractant reacts with the target component (A) and co-ion (B) to form the organic complex (ABC). The organic complex (ABC) diffuses across the liquid membrane to the stripping interface where both target component and co-ion are simultaneously

recovered. This mechanism has co-ion transporting along with the target component from feed phase to stripping phase.
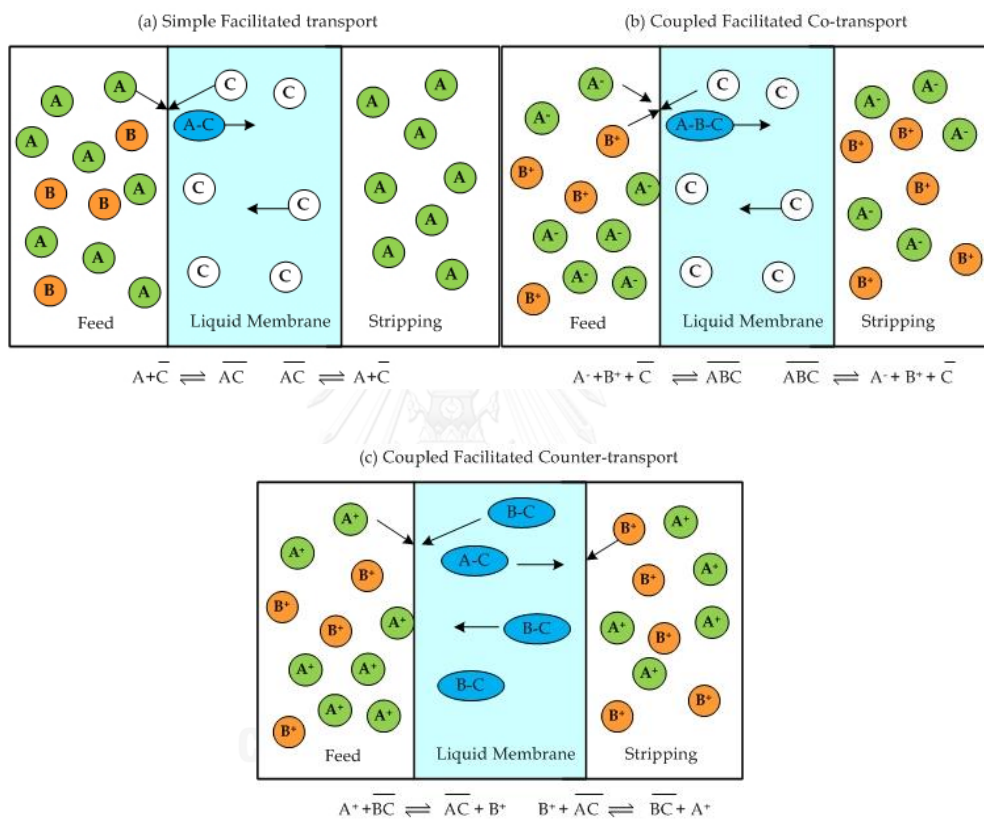
Figure 1.2 Schema of liquid membrane systems [15]

This coupled facilitated co-transport is common for neutral and basic extraction as schematized in Eq. (1.6) for the reaction with neutral organic extractant and Eq. (1.7) for the reaction with the basic organic extractant.

Coupled co-transport, neutral organic extractant:

$$A^+_{(aq)} + B^-_{(aq)} + C_{(org)} \rightleftharpoons ABC_{(org)} \tag{1.6}$$

Coupled co-transport, basic organic extractant:

$$A^{n+}_{(aq)} + mB^-_{(aq)} + (m-n)H^+_{(aq)} + (m-n)C_{(org)} \rightleftharpoons AB_m^{(m-n)-}((m-n)CH^+)_{(org)} \tag{1.7}$$
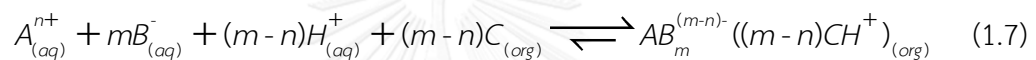
The coupled facilitated counter-transport has reverse mechanism from the co-transport. The co-ion (B) transports from the stripping phase to feed phase, against the transport direction of the target component (A). The mechanism starts with the reaction between (A) and the organic extractant (BC) to form the organic complex (AC) and to release co-ion (B) to the feed phase. Subsequently, the organic complex (AC) diffuses across the liquid membrane to the stripping interface where the target component is released to the stripping phase and co-ion is recovered to the organic extractant. The common case of counter-transport is the reaction using acidic extractant as schematized below in Eq. (1.8).

Coupled counter-transport, acidic organic extractant:

$$A^+_{(aq)} + HC_{(org)} \rightleftharpoons AC_{(org)} + H^+_{(aq)} \tag{1.8}$$

Uphill transport where the target component can be transported across the membrane against the concentration gradient of the target component is usually observed from the coupled transport. The uphill effects can continue until the target component diffuses across the liquid membrane to the stripping solution as long as the driving force in the coupled transport system is maintained. The driving force is often acquired from the aqueous pH (H^+) and/or co-ion (B) gradient.

In this work, the separation of neodymium ions from mixed rare earths follows the mechanism of coupled facilitated transport and the uphill effects against the target component concentration is usually observed.

1.1.6   Patterns of HFSLM operations

The patterns of HFSLM operations for metal ions separation are mainly classified as follows: batch operation, continuous operation and semi-continuous operation.

I.   Batch operation

The separation of metal ions by batch operation consists of a single HFSLM module, a feed reservoir and a stripping reservoir. Feed and stripping solutions are circulated through the HFSLM module. Batch operation is suitable for the separation of metal ions from a small volume of feed solution, and slow extraction and stripping. By using batch operation, a high percentage of metal ions can be separated.

II.   Continuous operation

Continuous operation is suitable for the separation of metal ions from a large volume of feed solution and can be performed by connecting the HFSLM modules in

series or in parallel. The feed and stripping solutions are supplied in single-pass flow or one-through-mode.

Continuous operation by connecting the HFSLM modules in series needs a higher residence time of feed and stripping solutions in the HFSLM modules. Therefore, continuous operation with the HFSLM modules in series is recommended for slow extraction and stripping as they require a long residence time to complete the reaction.

On the other hand, continuous operation by connecting the HFSLM modules in parallel provides a shorter residence time than that in series. Therefore, continuous operation connecting the HFSLM modules in parallel is suitable for fast extraction and stripping.

III.   Semi-continuous operation

The separation of metal ions by semi-continuous operation is carried out by using a single-pass flow of feed solution but circulating flow of stripping solution. By

using this pattern operation, the metal ions in the stripping solution can be concentrated until its concentration is constant and the reaction reaches equilibrium.

Operation using HFSLM modules in series is preferable for selective separation of metal ions where the extraction reaction is slow. In the case of fast extraction reaction, separation of metal ions does not need a long residence time. Therefore, using HFSLM modules in parallel is suitable. From an application perspective, the semi-continuous setup offers continuous treatment of a large volume of feed solution.

1.1.7   The synergistic extractants

A synergistic extractant is a mixture of two types of extractants. The synergistic extraction of Nd(III) can be described below as in Eq. (1.9).

Phospho-organic extractants have functional groups with strong electron-donor oxygen atoms. They can form complexes of a diverse structure and also have an ability to interact with one another, creating various associated molecules [14]. Acid

phospho-organic extractants in solvents used for the extraction of metal ions occur in dimer form: $2(HA) \rightarrow (HA)_2$.

For the 1st extractant, the extraction reaction of Nd(III) with D2EHPA $((HA)_2)$ is as shown in Eq. (1.9) [2].
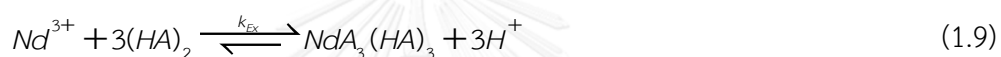
$$Nd^{3+} + 3(HA)_2 \xrightleftharpoons{k_{Ex}} NdA_3(HA)_3 + 3H^+ \qquad (1.9)$$

where $(HA)_2$ is the dimer from of D2EHPA and k_{Ex} is the reaction rate constant of extraction.

For the 2nd extractant, the extraction reaction of Nd(III) with neutral donor ligand (L=TOPO, TBPO, TPPO and TBP) is shown in Eq. (1.10). The neutral donor (L) captures the inorganic anion (NO_3^-) in the feed phase to form the 2nd extractant. Subsequently, it reacts with Nd(III) to produce complex ions $(NdA_3(HA)_3)$. The numbers of stoichiometry in this present work were determined by slope analysis method [18].
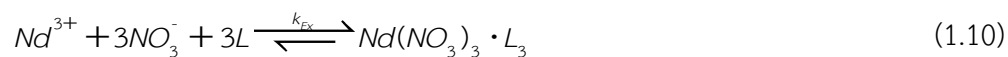
$$Nd^{3+} + 3NO_3^- + 3L \xrightleftharpoons{k_{Ex}} Nd(NO_3)_3 \cdot L_3 \qquad (1.10)$$

For synergistic extractants, the mixture of D2EHPA and the neutral donor ligand can be expressed by the following Eq. (1.11). Again, the stoichiometric numbers were also determined by slope analysis method [3].

$$Nd^{3+} + 3(HA)_2 + L \xrightleftharpoons{k_{Ex}} NdA_3(HA)_3 \cdot L + 3H^+ \qquad (1.11)$$
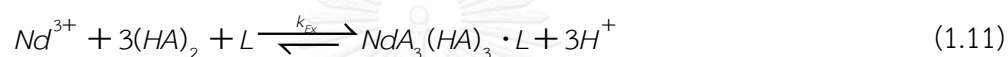
Luo et al.[19] determined the synergistic coefficient (S.C.) in terms of the distribution coefficient:

$$S.C. = \frac{K_{d12}}{K_{d1} + K_{d2}} \qquad (1.12)$$

If S.C. > 1, synergism is present.

For S.C. = 1, there is no synergism.

If S.C. < 1, an antagonistic effect happens.

where K_{d12} is the distribution coefficient of the synergistic system to extract the specified ions, K_{d1} is the distribution coefficient of D2EHPA and K_{d2} is the distribution coefficient of the neutral donor.

1.1.8   Analytical instrument

Inductively coupled plasma spectrometry (ICP)

An inductively coupled plasma spectrometry (ICP) was used. ICP Spectrometer–model Stroflame–ICP M from Spectro Co. can detect the elements of concentration higher than 1 ppm, in both acidic and basic states.

The analyzing method was comprised of:

(1)   Introducing 1 mL of sample into a volumetric flask of 10 mL

(2)   Adding 1% (v/v) HNO_3 volume to 10 mL and

(3)   Analyzing the amount of neodymium ions in the sample.

1.2   Objectives of the dissertation

1. To study the influence of variables on the efficiency of extraction and stripping of neodymium (III) ions via HFSLM from monazite ores processed from the Rare Earth Research and Development Center, Office of Atoms for Peace, Bangkok, Thailand.

2. To develop a model to predict the concentration of Nd(III) ions from feed and stripping solution on the conservation of mass which consisted of convection, diffusion, reaction and accumulation.

1.3   Scope of the dissertation

1. The experiments focused on the separation of neodymium (III) ions from monazite ores processing.

2. Feed and stripping solutions were supplied counter-currently with equal flow rates to tube and shell sides of the HFSLM, respectively.

3. Investigated parameters were as follows:

a) type and concentration of extractants

b) concentration of pH value (initial feed) in monazite ores processing

c) type and concentration of stripping solutions

d) synergistic extractants

e) patterns of HFSLM operations

f) operating time

g) flow rates of feed and stripping solutions

4. The model was developed for the extraction and stripping of neodymium (III) ions via HFSLM by considering the convection–diffusion–kinetic and accumulation of neodymium (III) ions.

5. The model was verified by comparing the model results with the experimental data.

1.4 Expected results

The expected results are as follows:

1. the outlet concentration of neodymium (III) ions from the HFSLM module

2. high stripping of neodymium (III) ions

3. high accuracy model

1.5   Description of dissertation

This dissertation is divided into VIII chapters. Chapter I give a brief introduction on the separation of metal ions via HFSLM. Chapter II presents the published articles showing the separation of uranium ions from monazite ores. Chapters III to VII present the published articles showing the separation of neodymium (III) ions from monazite ores processing via HFSLM. Chapter VIII is the conclusion of this dissertation. The studies in Chapters II to VII are involved and outlined as follows:

Chapter II

The mass transfer of synergistic extraction of uranium ions from monazite leach solution via HFSLM was examined. Optimum conditions for synergistic extraction were found to be pH 5 in the feed solution, 0.1 M Cyanex 272 + 0.1 M TOPO in the liquid membrane and 2 M H_2SO_4 in the stripping solution at 30°C. After a fourth cycle, the cumulative extraction and stripping of uranium ions reached 95% and 90%. Fractional resistance due to extraction reaction proved to be the highest value. This indicated that mass transfer resistance from the extraction was dominant. The

controlling step is the chemical reaction. Full details are available in Chapter II and the article in Journal of Industrial and Engineering Chemistry [20].

Chapter III

The separation of Nd(III) from lanthanide series via hollow fiber supported liquid membrane (HFSLM) using synergistic extractant was investigated. Optimum extraction and stripping obtained were 94.5% and 85.1% using D2EHPA and TOPO mixtures (0.5:0.5 M/M) as the synergistic extractant. Both extraction and stripping exhibited first-order reaction with rate constants of 1.444 and 1.338 min^{-1}, respectively. The experimental results were used to correlate with the models. Results showed that the concentration of Nd(III) from the experiment fitted in well with the model results. The average deviation was 1.95% and 2.18% for predictions in both feed and stripping sides, respectively. Details are available in Chapter III and the article in Journal of Industrial and Engineering Chemistry [21].

Chapter IV

The mass transfer of Nd(III) via hollow fiber supported liquid membrane was studied. At pH 4.5 using 0.5 M 2-ethylhexyl phosphonic acid mono-2-ethylhexyl ester as the extractant and 1 M H_2SO_4 as the stripping solution, optimum extraction and stripping reached 98% and 95%. Mass transfer resistance due to chemical reaction proved to be of the highest value i.e.$1/K_e$ = 5.871 × 10^2 s/cm. Thus, this indicated that the mass transfer resistance from the extraction was the most important. Further, the mass transfer model fitted in well with the experiment data. The average deviation in the feed side was below 5%. Full details are available in Chapter IV and the article in Journal of Industrial and Engineering Chemistry[22]

Chapter V

The separation of Nd(III) via hollow fiber supported liquid membrane (HFSLM) and mass transfer analysis was studied. At pH of 4.5, 0.5 M DNPPA as extractant, 3 M H_2SO_4 as stripping solution, flow rates of feed and stripping solutions of 100 mL/min and temperature of feed and stripping solutions of 313 K. optimum extraction and stripping reached 98% and 95%. The mass transfer due to chemical reaction is the

mass transfer–controlling step. The experiment data fitted in well with the mass transfer model. The average deviation in the feed side was below 2%. Full details are available in Chapter V and the article in Journal of Industrial and Engineering Chemistry [23].

Chapter VI

The extraction of neodymium ions from monazite leach solution was achieved by synergistic extraction via hollow fiber supported liquid membrane (HFSLM). Applying the results from central composite design (CCD) experiments, further optimization experiments were carried out using response surface methodology (RSM). Validation tests revealed optimum performance at 0.1 M Cyanex 272 and 0.05 M TOPO, 4 M HNO_3 as the stripping solution: flow rates of both feed and stripping solutions were 100 mL/min. The extraction of neodymium ions reached a maximum of 98%. Results indicated that the highest fractional resistance was a chemical reaction. This showed that mass transfer resistance due to chemical reaction was dominant for transport of neodymium ions through the hollow fiber supported liquid membrane system. For more detail and discussion, it is available in Chapter VI and the article in Mineral Engineering [24].

Chapter VII

The separation of Nd(III) from mixed rare earths via hollow fiber supported liquid membrane (HFSLM) was examined. Percentages of extraction and stripping of Nd(III) attained were 95% and 87%, respectively. Optimum condition was achieved using 4.5 pH of feed solution, 0.5 M 2-ethylhexyl-2-ethylhexyl phosphoric acid (HEHEPA) dissolved in octane as the extractant and 4 M HNO_3 of stripping solution. The flow rates of both feed and stripping phase were 100 mL/min. The mathematical model was developed on the conservation of mass which consisted of convection, diffusion, reaction and accumulation. The model results prediction proved to be in good agreement with the experimental data at an average Standard Deviation of 1.9% and 1.2%, respectively. Details are available in Chapter VII and the article in Chemical Engineering Journal [25].

CHAPTER 2

The synergistic extraction of uranium ions from monazite leach solution via HFSLM and its mass transfer

Thanaporn Wannachod[a], Thidarat Wongsawa[a], Prakorn Ramakul[b], Ura Pancharoen[a,*] and Soorathep Kheawhom[a,**]

[a]*Department of Chemical Engineering, Faculty of Engineering, Chulalongkorn University, Patumwan, Bangkok 10330, Thailand*
[b]*Department of Chemical Engineering, Faculty of Engineering and Industrial Technology, Silpakorn University, Nakhon Pathom 73000, Thailand*

2.1 Abstract

The mass transfer of synergistic extraction of uranium ions from monazite leach solution via HFSLM was examined. Optimum conditions for synergistic extraction were found to be pH 5 in the feed solution, 0.1 M Cyanex 272 + 0.1 M TOPO in the liquid membrane and 2 M H_2SO_4 in the stripping solution at 30°C. After a fourth cycle, the cumulative extraction and stripping of uranium ions reached 95% and 90%. Fractional resistance due to extraction reaction proved to be the highest value. This indicated that mass transfer resistance from the extraction was dominant. The controlling step is the chemical reaction.

Keywords: Mass transfer; Synergistic; Extraction; Uranium; HFSLM

2.2 Introduction

Monazite ore is a phosphate mineral containing rare earth metals e.g. lanthanum and cerium as well as small amounts of uranium and thorium [1]. Monazite processing is shown in Fig. 2.1. It is made up of five units: ore digestion unit, tri sodium phosphate crystallization unit, dissolution unit, initial precipitation unit and cerium separation unit [2]. In general, uranium is a radioactive element which is

useful at the front and back ends of the nuclear fuel cycle. However, uranium is known to cause serious environmental damage and has an acute effect on mammals: its compounds are potential carcinogens [3]. Thus, researchers need to develop more efficient techniques in order to separate uranium from monazite processing directly or from tri sodium phosphate. It is of vital importance to discover new ways to separate uranium safely and economically.

Various separation methods [4] including extraction chromatography [5] selective precipitation [6] solvent extraction [7, 8] ion exchange [9, 10] and a combination of these [11, 12] have been employed by many researchers for the separation of uranium. Liquid membrane (LM) techniques have begun to play a major role in the separation of metal ions with very low concentration. Membrane technology has recently gained much in influence for wastewater treatment. Hollow fiber supported liquid membrane (HFSLM) has proved to be excellent for extracting metal ions.

The HFSLM system has specific characteristics that allow simultaneous extraction and stripping processes of target ions in a single-step operation [13]. This system has several advantages over conventional methods. For example, it has lower

energy consumption, lower capital costs and less solvent used [14]. The high surface area of the HFSLM system attains a high separation rate [15]. In the separation of cerium (IV), tetravalent and trivalent lanthanide ions, HFSLM has achieved good results [15]. Ramakul et al. [16] reported that HFSLM was successful in separating uranium ions from nitrate media. Fontàs et al. [17] also affirmed that the HFSLM system was effective in separating Rh(III) from low level concentrations in the feed solution.

Synergistic extraction systems have been applied to separate radioactive metals numerous times. Consequently, there has been a large increase in extraction efficiency; a few synergistic systems have shown improved separation among radioactive metals [18]. Thus, the possible enhancement of separation was investigated via the concept of synergistic effect. Previous successful separations of uranium ions are shown in Table 2.1.

Table 2.1 Summary of previous research on uranium ions separation using a single extractant and synergistic extractant

Authors	Metals	Extractants	Diluents	Stripping	Method	% Ex	Ref.
Lothongkum et al.	$[UO_2(CO_3)_3]^{4-}$	Aliquat 336, TBP	kerosene	HNO_3	HFSLM	38	[1]
Panja et al.	U(VI)	T2EHDGA	dodecane	HNO_3	LM	N/A	[19]
Dogmane et al.	U(VI)	Cyanex 272	dodecane	HNO_3	L-L	85	[20]
Rao et al.	U_3O_8, UO_2	TBP	N/A	HNO_3	SFE	99	[21]
Biswas et al.	U(VI)	TEHP, TBP	paraffin	HNO_3	L-L	N/A	[22]
Joshi et al.	U(VI)	D2EHPA, TBP, DBBP, TOPO, Cyanex 923	dodecane	$(NH_4)_2CO_3$	SLM	N/A	[23]
Biswas et al.	U(VI)	DNPPA	paraffin	NH_2CO_3	SLM	N/A	[24]
Amaral et al.	U_3O_8	Alamine 336	kerosene	Na_2CO_3	L-L	83	[25]
Wannachod et al.	U(VI)	Cyanex 272, TOPO	dodecane	H_2SO_4	HFSLM	95	This study

Note: FSLM: flat sheet supported liquid membrane, HFSLM: hollow fiber supported liquid membrane, L-L: liquid liquid extraction, LM: liquid membrane and SFE: supercritical fluid extraction.

In the HFSLM system, mass transfer is the net diffusion of the mass of metal ions across the liquid membrane phase from feed phase to the stripping phase [26]. Many studies have been conducted on the mass transfer coefficient in terms of various dimensionless groups such as Leveque Equation [27] Sherwood–Graetz [28] as well as Damköhler [29]. Ramakul et al. separated Ce(IV) from sulfate media; Tri-n-octylamine (TOA) was used as extractant diluted in kerosene and sodium hydroxide was used as strip solution. The rate controlling step was the diffusion of cerium complex across the liquid membrane [30]. Kandwal et al. [31] developed a mathematical model for the transport of cesium through hollow fiber supported liquid membrane (HFSLM) containing calix-[4]-bis(2,3-naptho)-crown-6 (CNC) as the carrier extractant in NPOE and n-dodecane mixture as diluent.

The objective of this study is an investigation on the related mass transfer of synergistic extraction of uranium ions from monazite leach solution. Feed solution was obtained from the Rare Earth Research and Development Center, Office of Atoms for Peace, Bangkok, Thailand. Feed solution is shown in Table 2.2. Uranium ions in the presence of nitric acid exist in the form of UO_2^{2+} type species. The choice of extractant, diluent and stripping solution is vital for the successful separation of uranium ions as shown in previous works [23,24, 32]. The type and concentration of

acidic organo-phosphorous as well as neutral donors, synergistic extractant, concentration of stripping solution, flow rates of both feed and stripping solutions, operation of cycles and the mass transfer of synergistic extraction were investigated. Consecutive extraction via HFSLM was also carried out to enhance uranium ions flux by using synergistic extractant in the liquid membrane.
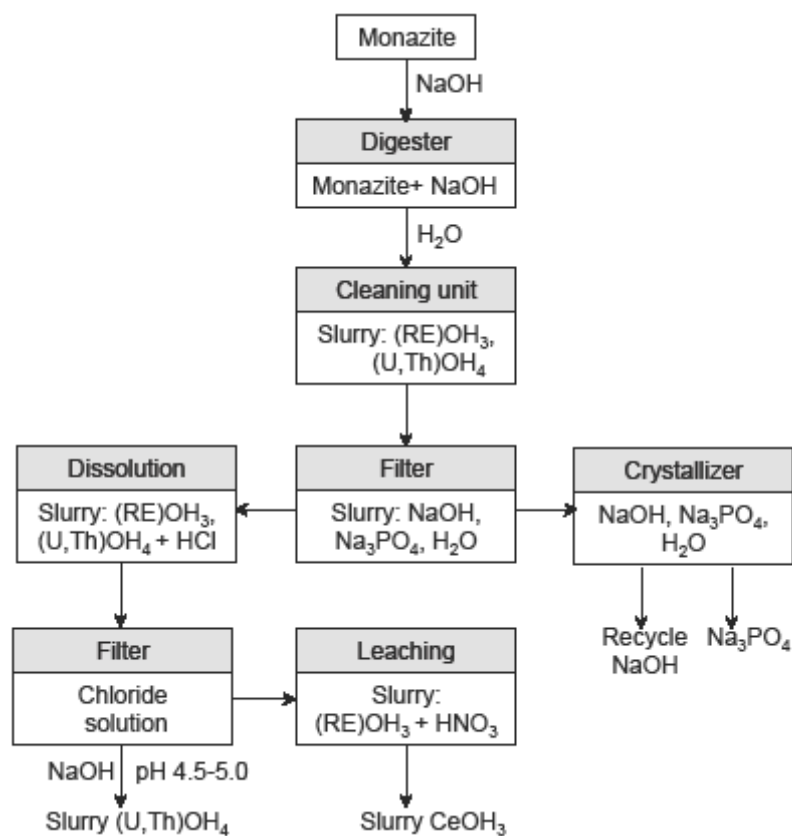
Figure 2.1 Monazite processing

Table 2.2 Typical composition of feed solutions (pH in the feed solution = 5)

Monazite ores processing	
Uranium ions (mg/L)	45 ± 0.015
Thorium ions (mg/L)	4 ± 0.012
Rare earth metal ions (mg/L)	5 ± 0.029
Nitric acid in the feed solution (M)	1×10^{-5}

2.3   Transport of uranium ions and mass transfer

The schematic mechanisms via HFSLM describe the counter transport between metal ions and hydrogen ions, as shown by Wannachod et al. [33]. The driving force of the process is the hydrogen ion concentration gradient in the feed phase and stripping phase. The concentration gradient of hydrogen ions yielded the high enrichment factors for metal ions [34]. Acidic organo-phosphorous and neutral donors act as the accelerator for the transport of specific components from the feed phase to the stripping phase. An analysis of the permeation rates of uranium ions via the HFSLM method was carried out in the same manner as reported by Wannachod et al [33].

The overall mass transfer resistance of uranium ions represents the mass-transfer resistances as in the feed phase, extraction reaction, liquid membrane phase,

shell-side, stripping reaction and strip-side resistance [35]. The overall mass transfer resistance can be modified by neglecting the transport resistances because the stripping reaction was completed almost instantaneously during the HFSLM process [35]. The individual mass transfer resistance was also determined in the same manner according to Wannachod et al. [36].

The relative contribution of each resistance to the overall resistance to mass transfer was obtained as follows:

$$\Delta_i = \frac{R_i}{R_{af} + R_e + R_m + R_o}$$

(2.1)

2.4 Experimental

2.4.1 The feed solution and reagents

Feed solution was supplied by courtesy of the Rare Earth Research and Development Centre, Office of Atoms for Peace, Bangkok, Thailand. Typical composition of feed solution is shown in Table 2.2. TOPO, Cyanex 272, Cyanex 923, TBP, TEHP, PC88A, D2EHPA and DNPPA were the extractants used. The extractants were diluted in n-dodecane and used for the preparation of the liquid membrane

phase. Sulphuric acid was used as stripping solution. The pH of feed solution was adjusted using HNO_3 solution: for all studies, the pH of feed solution of 5 was employed. The source and mass fraction purity of materials are listed in Table 2.3. All materials were used without further purification. All chemicals were of GR grade.

Table 2.3 Source and mass fraction purity of materials

Material name	Source	Purity/ % mass	Analysis method
TOPO	Cytec, Canada	97.0	HPLC
Cyanex 272	Cytec, Canada	99.9	HPLC
Cyanex 923	Cytec, Canada	99.0	HPLC
TBP	Cytec, Canada	99.8	GC
TEHP	Cytec, Canada	99.8	HPLC
PC88A	Cognis, USA	99.8	HPLC
D2EHPA	Cognis, USA	99.8	HPLC
DNPPA	Cognis, USA	99.8	HPLC
n-Dodecane	Aldrich, Singapore	99.8	GC
Sulphuric acid	Merck, Singapore	99.8	GC

Note: HPLC: high performance liquid chromatography and GC: gas chromatography

2.4.2   Apparatus

The hollow fiber module from Liqui–Cel® (Hoechst Celanese, Bridgewater, NJ) consists of micro-porous polypropylene fibers which are woven into fabric and wrapped around a central feeder tube in order to supply the shell–side fluid.

Properties of the hollow fiber module are shown in Table 2.4. All samples from the feed and stripping solutions were analyzed by ICP.

Table 2.4 Properties of the hollow fiber module

Properties	Description
Material	Polypropylene
Inside diameter of hollow fiber (cm)	0.024
Outside diameter of hollow fiber (cm)	0.03
Effective length of hollow fiber (cm)	15
Number of hollow fibers	35,000
Average pore size (cm)	3×10^{-6}
Porosity (%)	25
Effective surface area (cm^2)	1.4×10^4
Area per unit volume (cm^2/cm^3)	29.3
Module diameter (cm)	6.3
Module length (cm)	20.3
Tortuosity factor	2.6
Operating temperature (K)	273–333

2.4.3   Apparatus

The HFSLM system was carried out in the same manner as reported by Wannachod et al. [36]. First, the extractant was dissolved in n-dodecane. Then, it was circulated through the tube and shell sides of the HFSLM system for 40 min. in order

to embed the liquid membrane in the hollow-fiber micro-pores. Afterwards, the feed solution and the stripping solution were pumped counter-currently into the tube and shell sides of the HFSLM. Samples were collected in the feed and stripping reservoirs to determine the concentration of metals ions by ICP. The extractability of uranium ions in this work was calculated by the percentage of extraction and stripping and the synergistic coefficient (S.C.) was determined in the same manner according to Wannachod et al. [36]. If S.C. > 1, synergism is present, for S.C. = 1, there is no synergism and S.C. < 1, an antagonistic effect happens.

2.5   Results and discussion

2.5.1   Effect of type and concentration of acidic organo-phosphorous

In this work, concentration of acidic organo-phosphorous varied from 0.05 M to 0.3 M. Results are shown in Fig. 2.2. The extractability of uranium ions across HFSLM for the different extractants followed the order: Cyanex 272 > PC88A > D2EHPA > DNPPA. Results follow the *pKa* values of the acidic organo-phosphorous extractants [20, 37] as shown in Table 2.5. Similar observations have been reported on the extraction of uranium ions from nitric acid medium using different acidic

extractants [20]. The extraction of uranium ions in the feed phase using the acidic organo-phosphorous (H_2A_2) extractant, is shown in Eq. (2.2):

$$UO_{2\ (aq)}^{2+} + 2(H_2A_2)_{(org)} \rightleftharpoons UO_2(A_2H)_{2(org)} + 2H_{(aq)}^{+} \tag{2.2}$$
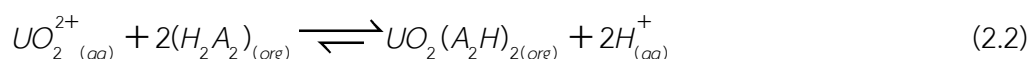
where the uranium ions from feed solution react with the extractant to form complex species. The uranium complex species diffuse to the interface between the liquid membrane phase and the stripping phase by the concentration gradient. Hydrogen ions from the stripping phase diffuse to the liquid membrane-stripping interface and react with the uranium complex species [34]. Consequently, uranium ions are released into the stripping phase. At Cyanex 272 concentration up to 0.1 M, it was noted that extraction of uranium ions increased to 60% and the stripping of uranium ions increased to 55%. Therefore, 0.1 M Cyanex 272 was chosen for the study of other variables. The percentages of extraction and stripping of thorium and rare earth metals are shown in Table 2.6.

(a) [Acidic organophosphorous] (M)

(b) [Acidic organophosphorous] (M)
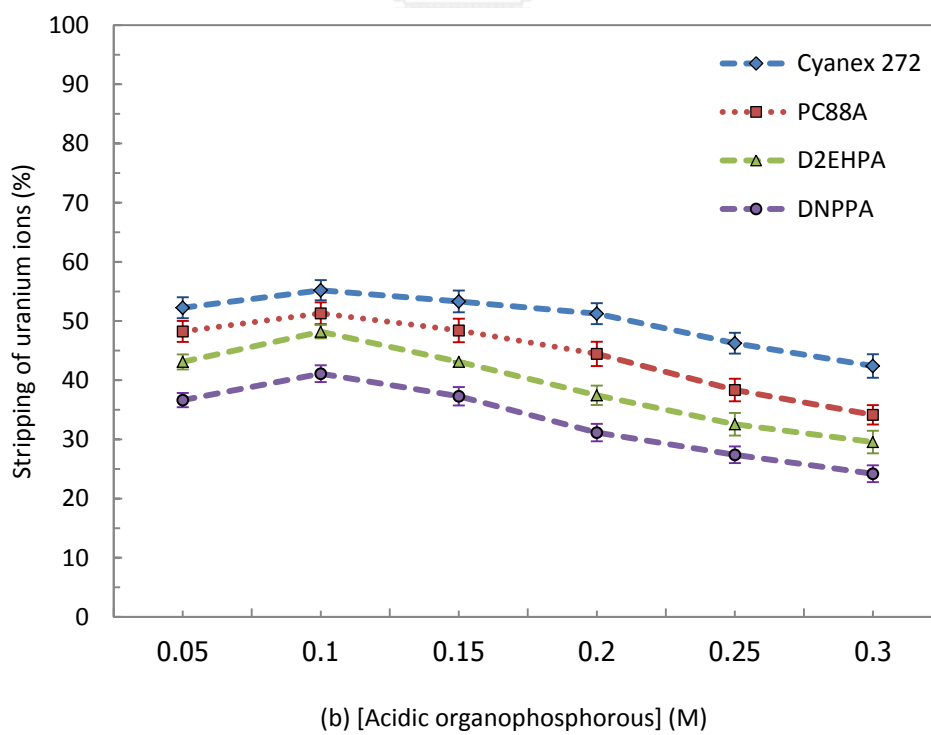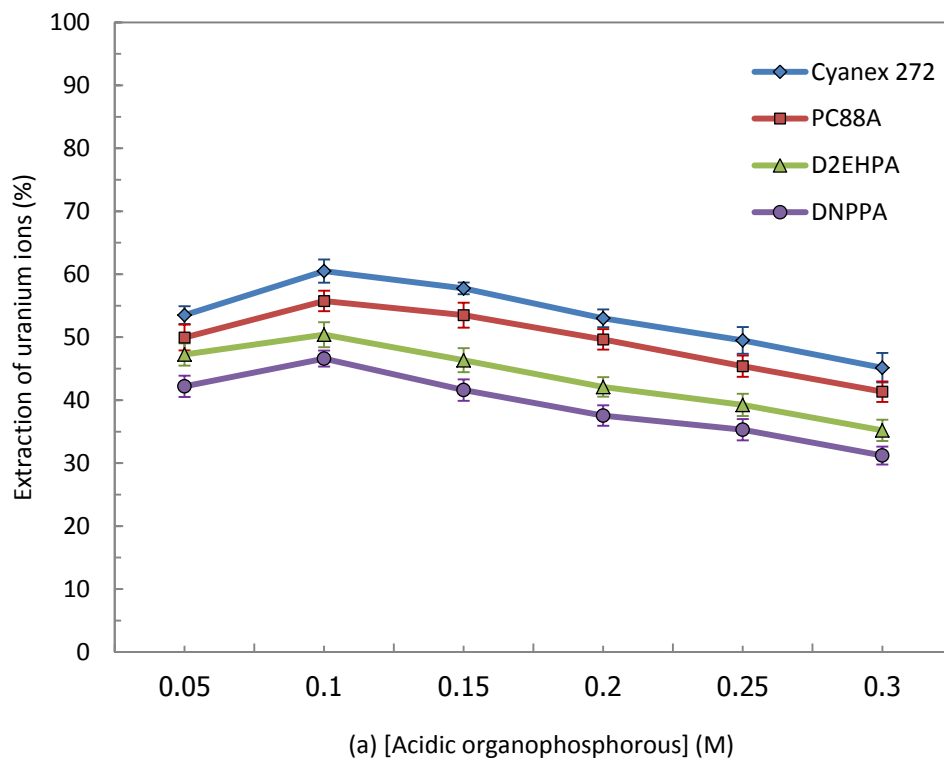
Figure 2.2 Percentage of uranium ions vs concentration of acidic organo-phosphorous (a) extraction (b) stripping (feed pH = 5; H_2SO_4 stripping solution = 2 M; flow rate = 100 mL/min for both feed and stripping solutions; temperature = 30°C).

Table 2.5 Validation of overall mass transfer coefficient (K) of uranium ions across HFSLM as of acid uptake constant (pK_a) of acidic organo-phosphorous solution

Acidic organo-phosphorous	pK_a	K (10^4 cm/s)	Ref.
Cyanex 272	8.7	9.15	[32]
PC88A	7.1	8.89	[32]
D2EHPA	4	5.65	[38]
DNPPA	2.5	4.51	[38]

Note: feed pH = 5; extractants = 0.1 M acidic organo-phosphorous; H_2SO_4 stripping solution = 2 M; flow rate = 100 mL/min for both feed and stripping solutions; temperature = 30°C.

Table 2.6 The percentages of extraction and stripping of thorium and rare earth metals

Metal ions	Th		RE	
Extractants	% Extraction	% Stripping	% Extraction	% Stripping
Cyanex 272	2.45	1.45	8.45	5.45
PC88A	1.58	0.93	7.58	4.23
D2EHPA	1.11	0..53	5.11	3.53
DNPPA	0.89	0.18	2.89	1.58

Note: feed pH = 5; extractants = 0.1 M acidic organo-phosphorous; H_2SO_4 stripping solution = 2 M; flow rate = 100 mL/min for both feed and stripping solutions; temperature = 30°C.

2.5.2 Effect of type and concentration of neutral donors

The effect of different concentrations of neutral donors was studied from 0.05 M to 0.3 M. Results are shown in Fig. 2.3. The extractability of uranium ions across HFSLM for the different extractants followed the order: TOPO > Cyanex 923 > TBP > TEHP. The results record the relative basicity (K_H) of the neutral donors [24, 39] as shown in Table 2.7. The extraction of uranium ions using the neutral donor extractant is shown in Eq. (2.3):

$$UO_{2(aq)}^{2+} + 2NO_{3(aq)}^{-} + 2S_{(org)} \rightleftharpoons UO_2(NO_3)_2 \cdot 2S_{(org)} \qquad (2.3)$$
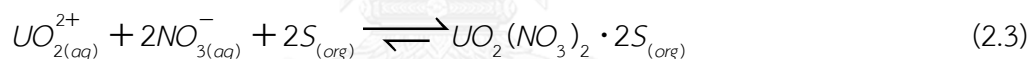
When concentration of TOPO increased to 0.1 M, percentages of extraction and stripping of uranium ions increased. Le Chatelier noted that extraction of uranium ions increased when concentration of the extractant increased. Further, when viscosity was excessive, the percentage of uranium ions extraction decreased. Stokes and Einstein also observed that when viscosity was high, extraction of metal ions decreased. Chakrabarty et al. [40] stated that viscosity of the membrane phase increases when extractant concentration is increased, resulting in a decrease of flux. Therefore, 0.1 M TOPO was selected in order to study other variables.

(a)

(b)
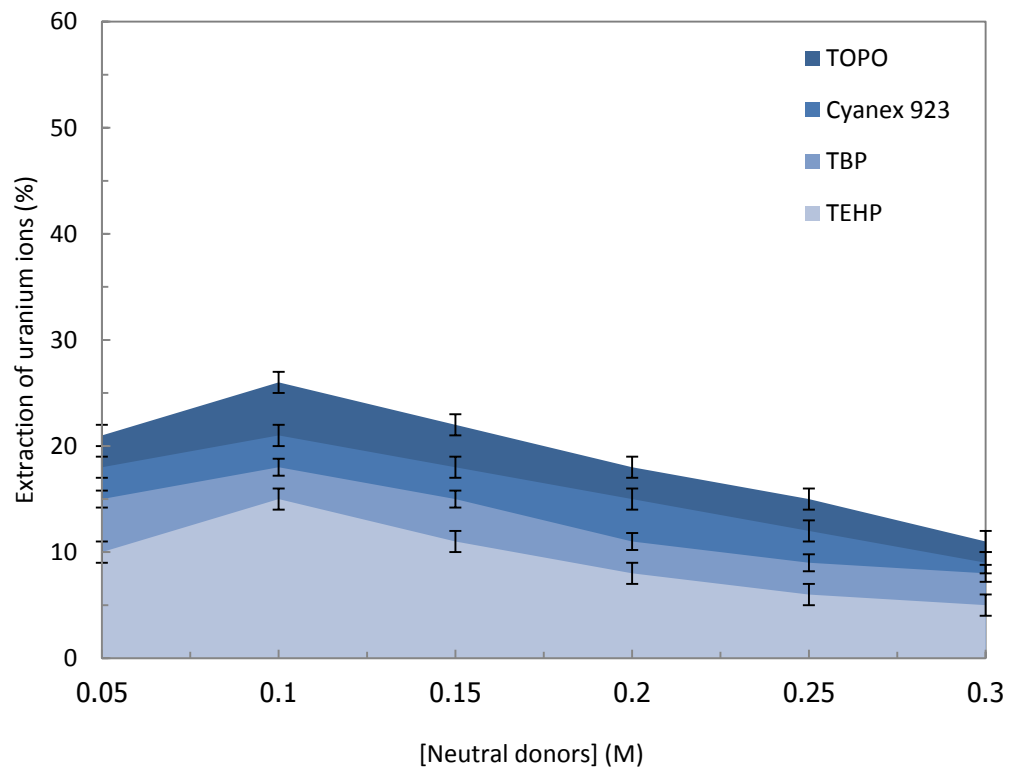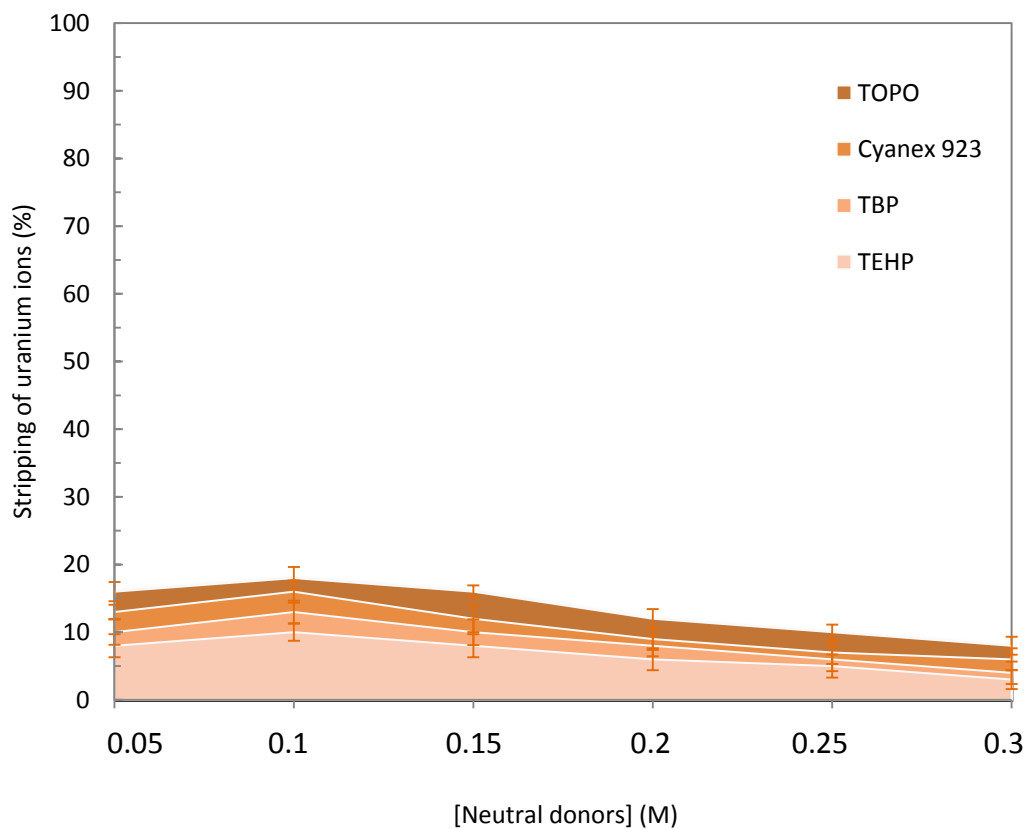
Figure 2.3 Percentage of uranium ions vs concentration of neutral donors (a) extraction (b) stripping (feed pH = 5; H_2SO_4 stripping solution = 2 M; flow rate = 100 mL/min for both feed and stripping solutions; temperature = 30°C).

Table 2.7 Validation of overall mass transfer coefficient (K) of uranium ions across HFSLM as of basicity (K_H) of neutral donors

Neutral donors	K_H	K (10^4 cm/s)	Ref.
TOPO	8.9	3.18	[41]
Cyanex 923	8.3	3.06	[42]
TBP	0.16	2.64	[38]
TEHP	0.16	2.58	[38]

Note: Feed pH = 5; extractants = 0.1 M neutral donor; H_2SO_4 stripping solution = 2 M; flow rate = 100 mL/min for both feed and stripping solutions; temperature = 30℃.

2.5.3 Effect of synergistic extractant concentration

This study was investigated further by generating a dimensional surface plot from the concentration effect data. For synergistic extractants, the mixture of acidic organo-phosphorous solution and neutral donors can be expressed by the following Eq. (2.4):

$$UO_2^{2+}{}_{(aq)} + 2(H_2A_2)_{(org)} + 2S_{(org)} \rightleftharpoons UO_2(A_2H)_2 \cdot 2S_{(org)} + 2H_{(aq)}^+ \qquad (2.4)$$
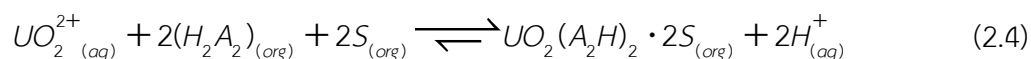
The percentage of extraction and synergistic coefficient is as shown in Table 2.8 where a synergistic coefficient > 1 indicated synergistic reaction.

From the data, the highest percentage of extraction for synergistic separation occurred when TOPO was added into Cyanex 272. The order of synergism was in accordance with the basicities of these neutral donors as TOPO (K_H = 8.9)>Cyanex 923 (K_H = 8.3)>TBP (K_H = 0.16)~TEHP (K_H = 0.16) where K_H = acid uptake constant. Similar observations were reported during supported liquid membrane (SLM) studies of U(VI) [24].

As shown in Fig. 2.4, percentages of extraction and stripping of uranium ions increased when concentration of the synergistic extractant increased. This corresponds to chemical kinetics that the rate of uranium ions stripping increased when concentration of stripping solution was increased. Maximum extraction of uranium ions was attained at concentrations of Cyanex 272 and TOPO in the synergistic extractant mixture of 0.1 M and 0.1 M, respectively. The highest percentages of extraction and stripping obtained were 90% and 85%, respectively. Thereafter, the percentage of extraction and stripping of uranium ions decreased. This was due to excessive viscosity from the high concentration.
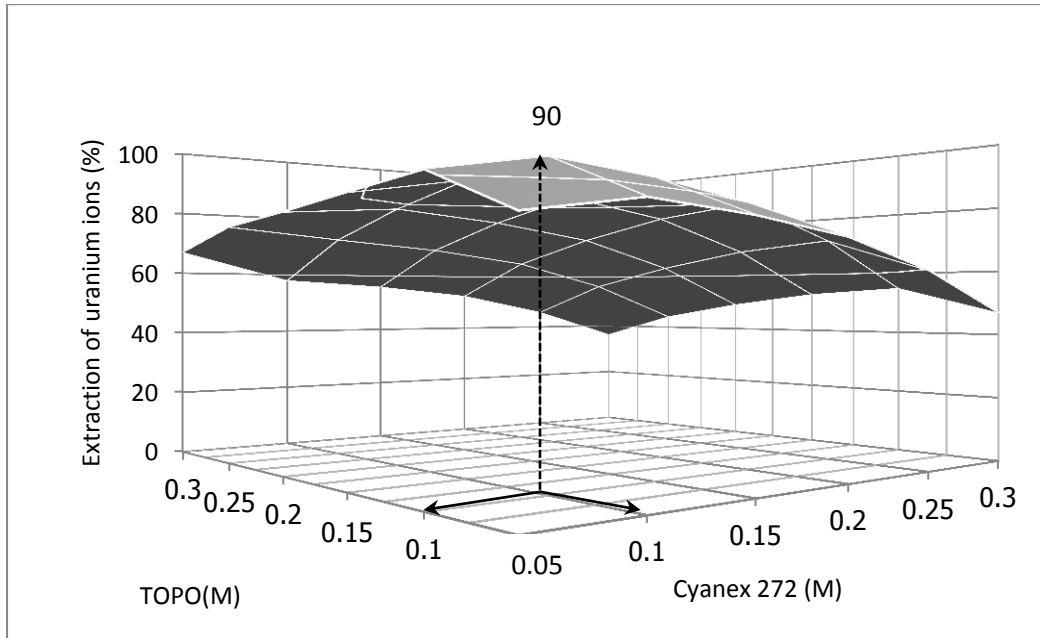
(a)
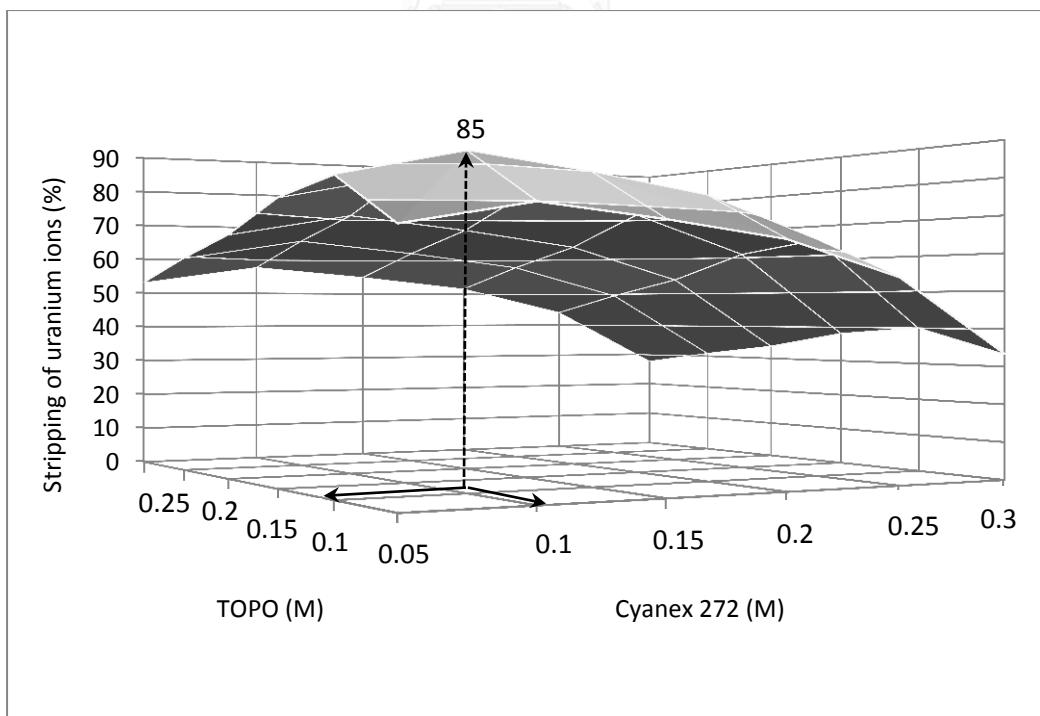
(b)

Figure 2.4 Percentage of uranium ions vs concentration of synergistic extractants (a) extraction (b) stripping (feed pH = 5; H_2SO_4 stripping solution = 2 M; flow rate = 100 mL/min for both feed and stripping solutions; temperature = 30°C).

Table 2.8 Validation of overall mass transfer coefficient, the percentage of extraction and synergistic coefficient (*S.C.*) of synergistic extraction

Synergistic extractant	*S.C.*	% Ex	K (10^3 cm/s)
0.1 M Cyanex 272 + 0.1 M TOPO	4.32	90	1.433
0.1 M Cyanex 272 + 0.1 M Cyanex 923	3.59	85	1.414
0.1 M Cyanex 272 + 0.1 M TBP	2.14	71	1.061
0.1 M Cyanex 272 + 0.1 M TEHP	1.58	64	0.984

Note: feed pH = 5; synergistic extractants = 0.1 M acidic organo-phosphorous + 0.1 M neutral donors; H_2SO_4 stripping solution = 2 M; flow rate = 100 mL/min for both feed and stripping solutions; temperature = 30°C.

2.5.4   Effect of stripping concentration

Stripping investigations were carried out with regard to the liquid membrane consisting of the synergistic extractant. The effect of different concentrations of H_2SO_4 stripping solution was studied from 0.5 – 3 M. Results in Fig. 2.5 show that there was an increase in the percentage of uranium ion stripping. This corresponds to chemical kinetics that the rate of uranium ion stripping increases when concentration of stripping solution is increased. Optimum percentages for the extraction and

stripping of uranium ions were obtained at 2 M H_2SO_4 since concentration of stripping solution higher than 2 M can degrade the polypropylene hollow fibers [43]. Thus, 2 M H_2SO_4 was recommended for further studies.
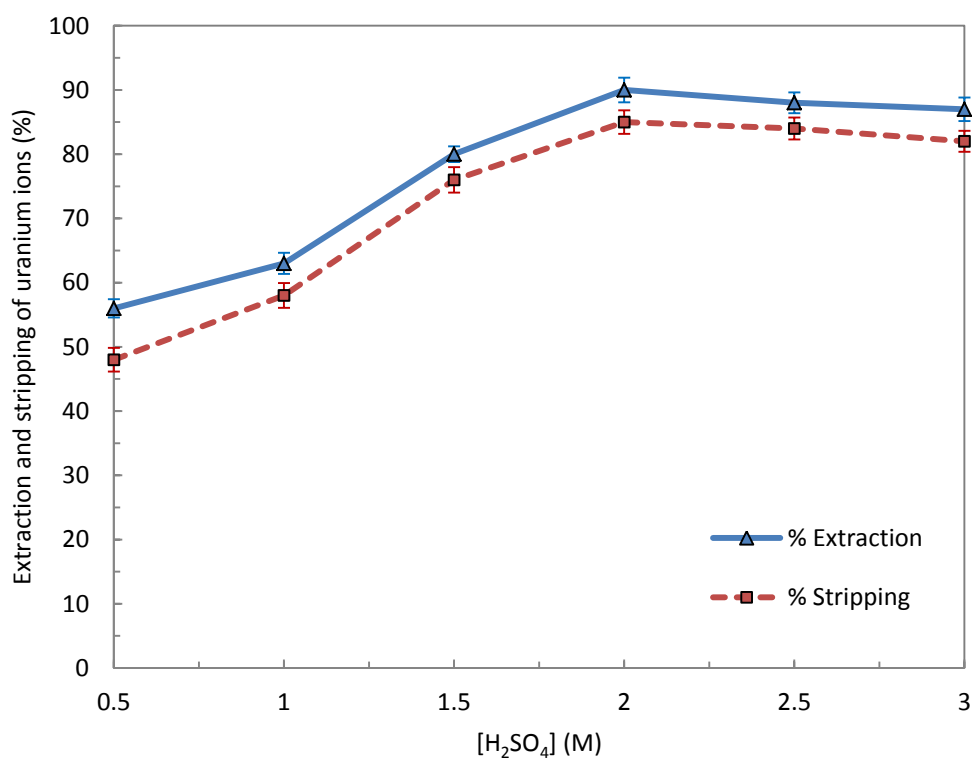
Figure 2.5 Percentage of uranium ions vs concentration of H_2SO_4 stripping solution (feed pH = 5; synergistic extractants = 0.1 M Cyanex 272 + 0.1 M TOPO; flow rate = 100 mL/min for both feed and stripping solutions; temperature = 30°C).

2.5.5   Effect of flow rate for both feed and stripping solutions

Equal flow rates of feed and stripping solutions were studied. The results are shown in Fig. 2.6. Maximum extraction and stripping – 90% and 85%, respectively – were obtained at 100 mL·min^{-1}. However, at flow rates greater than 100 mL/min. due to the resident time of the solution in the hollow fiber module, percentages of extraction and stripping of uranium ions decreased. This was in agreement with an earlier report by Yang et al [44].
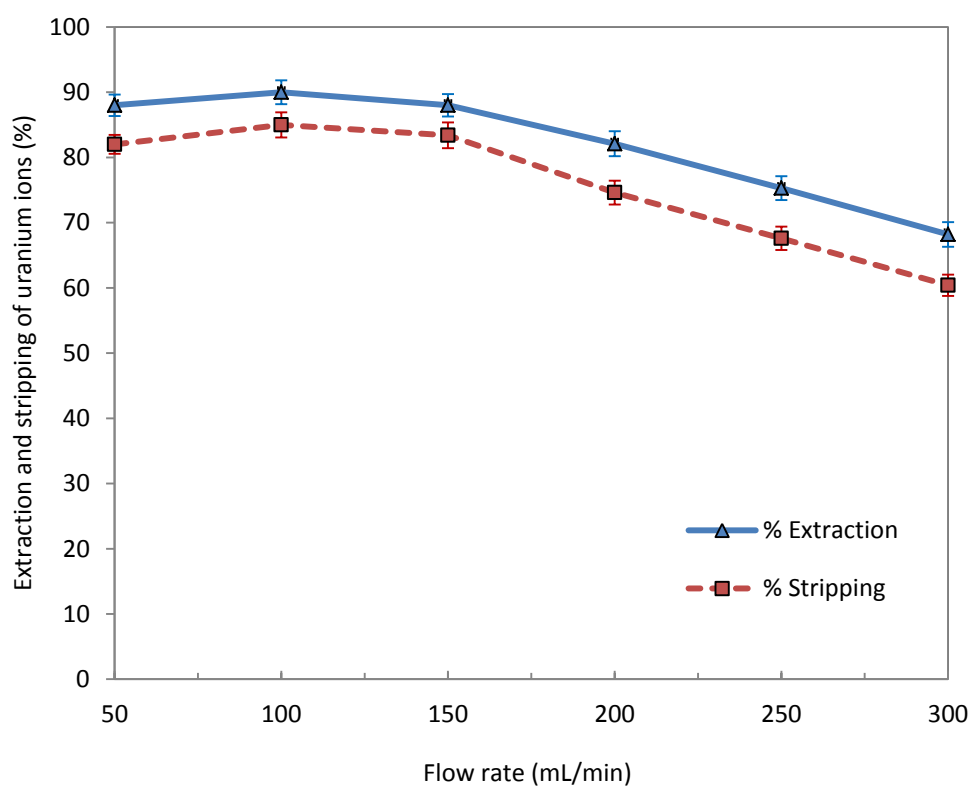
Figure 2.6 Percentage of uranium ions vs flow rate of both feed and stripping solutions (feed pH = 5; synergistic extractants = 0.1 M Cyanex 272 + 0.1 M TOPO; H_2SO_4 stripping solution = 2 M; temperature = 30°C).

2.5.6   Effect of operating cycle

The effect of operating time was investigated using optimum conditions for synergistic extractant. In a once through operation, the percentage of extraction and stripping of uranium ions reached 90% and 85%, respectively. To further enhance performance, the cycle mode of extraction and stripping was repeated. Thus, following a fourth cycle, the cumulative extraction and stripping of uranium ions rose to 95% and 90%, respectively as shown in Fig. 2.7. This indicated that the extractability of uranium ions extraction and stripping was observed to improve with repetition of the extraction cycle mode.
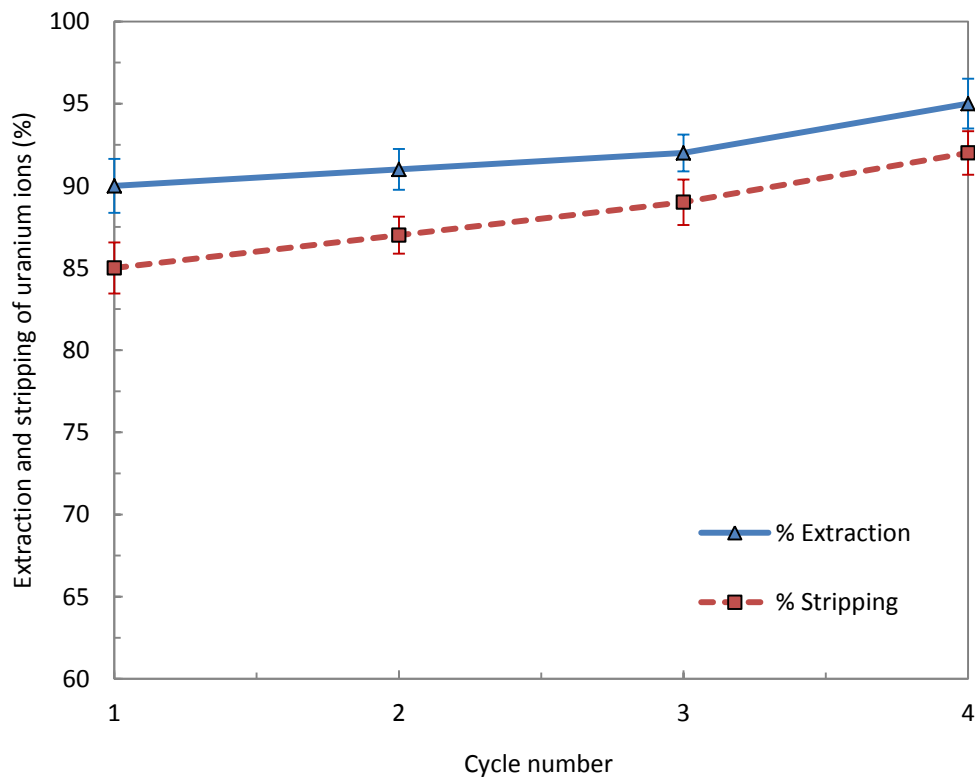
Figure 2.7 Percentage of uranium ions vs number of cycles (feed pH = 5; synergistic extractants = 0.1 M Cyanex 272 + 0.1 M TOPO; H_2SO_4 stripping solution = 2 M; flow rate = 100 mL/min for both feed and stripping solutions; operating time = 240 min for 4 cycles; temperature = 30°C).

2.5.7   Mass transfer coefficient

Values of the mass transfer coefficients can be calculated applying optimum conditions as shown in Table 2.9. From this table, the fractional resistance due to extraction reaction proved to be the highest in value. This indicated that the mass

transfer resistance from the extraction was dominant. From Table 2.9, the mass transfer coefficient due to chemical reaction was found to have the least value. The controlling step is the chemical reaction.

Table 2.9 Mass transfer coefficients and relative resistance of uranium ions overall mass transfer resistance under the optimum conditions of synergistic reaction

Feed phase		Chemical reaction		Membrane		Between of hollow	
k_{af} (cm/s)	Δ_{af} (%)	k_e (cm/s)	Δ_e (%)	K_m (cm/s)	Δ_m (%)	k_o (cm/s)	Δ_o (%)
5.82×10^{-4}	4.96	4.67×10^{-5}	59.61	5.49×10^{-3}	0.63	1.01×10^{-4}	34.80

Note: feed = pH 5; synergistic extractants = 0.1 M Cyanex 272 + 0.1 M TOPO; H_2SO_4 stripping solution = 2 M; flow rate = 100 mL/min for both feed and stripping solutions; temperature = 30°C.

2.6 Conclusion

Optimum conditions for synergistic extraction were found to be at 0.1 M Cyanex 272 + 0.1 M TOPO in the liquid membrane and 2 M H_2SO_4 in the stripping solution. The flow rates of both feed and stripping solutions were 100 mL·min^{-1}. Performance was considerably enhanced by running the operation in repeated cycle mode. After the fourth cycle, the cumulative extraction and stripping of uranium ions reached 95% and 90%, respectively. Fractional resistance of extraction reaction

proved to be the highest in value. This indicated that the mass transfer resistance from the extraction was dominant. The controlling step is the chemical reaction.

2.7 Acknowledge

2.8 Nomenclatures

aq the species in the aqueous phase

k_{af} mass transfer coefficient in the feed solution (cm/s)

k_{as} mass transfer coefficient for the stripping solution (cm/s)

k_e mass transfer coefficient due to the extraction reaction (cm/s)

k_m mass transfer coefficient of the membrane phase (cm/s)

k_o mass transfer coefficient in the shell side between hollow fibers (cm/s)

k_s mass transfer coefficient due to the stripping reaction (cm/s)

K overall mass transfer coefficient (cm/s)

L fiber module length (cm)

org the species in the organic liquid membrane phase

R overall mass transfer resistance (s/cm)

$S.C.$ the synergistic coefficient

2.9   References

[1]   A.W. Lothongkum, P. Ramakul, W. Sasomsub, S. Laoharochanapan, U. Pancharoen, Enhancement of uranium ion flux by consecutive extraction via hollow fiber supported liquid membrane, J. Taiwan Inst. Chem. Eng. 40 (2009) 518-523.

[2]   B. Suanmamuang, S. Laoharochanapan, Office of Atoms for Peace, Bangkok Thailand Institute of Nuclear Technology, Thailand, (2002).

[3]   G.D. Clayton, F.E. Clayton, Patty'sIndustrial Hygiene and Toxicology, Ed. Wiley-Interscience, New York, USA 4th (1994).

[4]   R.D. Ambashta, M.E.T. Sillanpää, Membrane purification in radioactive waste management: a short review, J Environ Radioactivity. 105 (2012) 76-84.

[5]   E.P. Horwitz, M.L. Dietz, R. Chiarizia, H. Diamond, A.M. Essling, D. Graczyk, Separation and preconcentration of uranium from acidic media by extraction chromatography, Anal Chim Acta. 266 (1992) 25-37.

[6]   R. Ganesh, K.G. Robinson, L. Chu, D. Kucsmas, G.D. Reed, Reductive precipitation of uranium by Desulfovibrio desulfuricans: evaluation of cocontaminant effects and selective removal, Water Research 33 (1999) 3447-3458.

[7]   J.E. Quinn, D. Wilkins, K.H. Soldenhoff, Solvent extraction of uranium from saline leach liquors using DEHPA/Alamine 336 mixed reagent, Hydrometallurgy, 134–135 (2013) 74-79.

[8]   M. Boufatit, H. Ait-Amar, W.R. Mc Whinnie, Extraction of uranium from non-complexing medium in chloroform using polymethylene bis-(acylpyrazolols) as extractants, Chem. Eng. Proc.: Process Intensification, 42 (2003) 743-749.

[9]   A. Aziz, S. Jan, F. Waqar, B. Mohammad, M. Hakim, W. Yawar, Selective ion exchange separation of uranium from concomitant impurities in uranium materials and subsequent determination of the impurities by ICP-OES, J. Rad. Nucl. Chem. Art. 284 (2010) 117-121.

[10] J. Korkisch, G.E. Janauer, Ion exchange in mixed solvents: Adsorption behaviour of uranium and thorium on strong-base anion-exchange resins from mineral acid-alcohol media separation methods for uranium and thorium, Talanta, 9 (1962) 957-985.

[11] R.K. Malhotra, K. Satyanarayana, Estimation of trace impurities in reactor-grade uranium using ICP-AES, Talanta, 50 (1999) 601-608.

[12] C.H. Lee, M.Y. Suh, K.S. Choi, J.S. Kim, Y.J. Park, W.H. Kim, Determination of Ru, Rh, Pd, Te, Mo and Zr in spent pressurized water reactor fuels by ion exchange and extraction chromatographic separations and inductively coupled plasma atomic.

[13] T. Franken, Liquid membranes-academic exercise or industrial separation process, Membrane Technology, 85 (1997) 6-10

[14] L. Boyadzhiev and Z.. Lazarova, Membrane Separation Technology: Principles and Applications, R.D. Noble and S.A. Stern (eds.). Elsevier, Amsterdam,1994.

[15] P. Ramakul, W. Pattavekongka, U. Pancharoen, M. Hronec, Selective separation of trivalent and tetravalent lanthanide from mixture by hollow fiber supported liquid membrane, J. Chin. Inst. Chem. Eng. 36 (2005) 459-465.

[16] P. Ramakul, T. Prapasawad, U. Pancharoen, W. Pattaveekongka, Separation of radioactive metal ions by hollow fiber-supported liquid membrane and permeability analysis, J. Chin. Inst. Chem. Eng. 38 (2007) 489-494.

[17] C. Fontàs, C. Palet, V. Salvadó, M. Hidalgo, A hollow fiber supported liquid membrane based on Aliquat 336 as a carrier for rhodium(III) transport and preconcentration, J. Memb. Sci. 178 (2000) 131-139.

[18] S. Panja, P.K. Mohapatra, S.C. Tripathi, P.M. Gandhi, P. Janardan, Supported liquid membrane transport studies on Am(III), Pu(IV), U(VI) and Sr(II) using irradiated TODGA, J. Haz. Mater. 237-238 (2012) 339-346.

[19] S. Panja, P.K. Mohapatra, S.C. Tripathi, V.K. Manchanda, Facilitated transport of uranium(VI) across supported liquid membranes containing T2EHDGA as the carrier extractant, J. Haz. Mater. 188 (2011) 281-287.

[20] S.D. Dogmane, R.K. Singh, D.D. Bajpai, J.N. Mathur, Extraction of U(VI) by cyanex-272, J. Rad Nucl Chem. 253 (2002) 477-482.

[21] A. Rao, P. Kumar, K.L. Ramakumar, Separation of uranium from different uranium oxide matrices employing supercritical carbon dioxide extraction, J. Rad. Nucl. Chem. 285 (2010) 247-257.

[22] S. Biswas, P.N. Pathak, D.K. Singh, S.B. Roy, Comparative Evaluation of Tri-n-butyl Phosphate (TBP) and Tris(2-ethylhexyl) Phosphate (TEHP) for the

Recovery of Uranium from Monazite Leach Solution, Sep. Sci. Technol. 48 (2013) 2013-2019.

[23] J.M. Joshi, P.N. Pathak, A.K. Pandey, V.K. Manchanda, Study on synergistic carriers facilitated transport of uranium(VI) and europium(III) across supported liquid membrane from phosphoric acid media, Hydrometallurgy, 96 (2009) 117-122.

[24] S. Biswas, P.N. Pathak, S.B. Roy, Carrier facilitated transport of uranium across supported liquid membrane using dinonyl phenyl phosphoric acid and its mixture with neutral donors, Desalination, 290 (2012) 74-82.

[25] J.C.B.S. Amaral, C.A. Morais, Thorium and uranium extraction from rare earth elements in monazite sulfuric acid liquor through solvent extraction, Min. Eng. 23 (2010) 498-503.

[26] U. Pancharoen, A.W. Lothongkum, S. Chaturabul, Mohamed El-Amin (Ed.), Mass Transfer in Multiphase Systems and its Applications, InTech, India (2011), p. 499-524.

[27] M.A. Leveque, Les lois de la transmission de chaleur par convection (or the laws of heat transmission by convection). Ann. Mines 13, 201 - 239.

[28] N. M. Kocherginsky, Q. Yang, Big carrousel mechanism of copper removal from ammoniacal wastewater through supported liquid membrane. Sep. Purif. Technol. 54 (2007) 104–116.

[29] M. Bidabadi, A. Haghiri, A. Rahbari, The effect of Lewis and Damköhler numbers on the flame propagation through micro-organic dust particles, Int. J. Therm. Sci. 49 (2010) 534–542.

[30] P. Ramakul, W. Pattaweekongka,U. Pancharoen, Mass transfer modeling of membrane carrier system for extraction of Ce(IV) from sulfate media using hollow fiber supported liquid membrane Korean J. Chem. Eng. 23 (2006), 85-92.

[31] P. Kandwal, S. Dixit, S. Mukhopadhyay, P.K. Mohapatra, Chemical Engineering Journal 174 (2011) 110–116.

[32] S. Biswas, P.N. Pathak, S. Pal, S.B. Roy, P.K. Tewari, V.K. Manchanda, Uranium Permeation from Nitrate Medium Across Supported Liquid Membrane Containing Acidic Organophosphorous Extractants and their Mixtures with Neutral Oxodonors, Sep. Sci. Technol. 46 (2011) 2110-2118.

[33] T. Wannachod, N. Leepipatpiboon, U. Pancharoen, K. Nootong, Synergistic effect of various neutral donors in D2EHPA for selective neodymium separation from lanthanide series via HFSLM, J. Ind. Eng. Chem. 20 (2014) 4152–4162.

[34] K. Cheng, K. Choi, J. Kim, I.H. Sung, D.S. Chung, Sensitive arsenic analysis by carrier-mediated counter-transport single drop microextraction coupled with capillary electrophoresis, Microchemical J.106 (2013) 220-225.

[35] Y. Tang, W. Liu, J. Wan, Y. Wang, X. Yang, Two-stage recovery of S-adenosyl-methionine using supported liquid membranes with strip dispersion, Process Biochemistry, 48 (2013) 1980-1991.

[36] T. Wannachod, N. Leepipatpiboon, U. Pancharoen, S. Phatanasri, Mass transfer and selective separation of neodymium ions via a hollow fiber supported liquid membrane using PC88A as extractant, J. Ind. Eng.Chem. 21 (2015) 535–541.

[37] C. Sella, A. Becis, G. Cote, D. Bauer, Diphasicacido-basic properties of di(octyl-phenyl) phosphoric acid (DOPPA, Sol.t Ext. Ion Exch. 13 (1995) 715-729.

[38] M. Anitha, D.N. Ambare, M.K. Kotekar, D.K. Singh, H. Singh, Studies on Permeation of Nd (III) through Supported Liquid Membrane Using DNPPA + TOPO as Carrier, Sep. Sci. Technol. 48 (2013) 2196-2203.

[39] N.S. Awwad, Equilibrium and kinetic studies on the extraction and stripping of uranium(VI) from nitric acid medium into tri-phenylphosphine oxide using a single drop column technique, Chem. Eng. Proc.: Process Intensification 43 (2004) 1503-1509.

[40] K. Chakrabarty, K.V. Krishna, P. Saha, A.K. Ghoshal, Extraction and recovery of lignosulfonate from its aqueous solution using bulk liquid membrane, J Memb. Sci. 330 (2009) 135-144.

[41] J.N. Mathur, K.L. Nash, Thermodynamics of extraction of Am(III) and Eu(III) from nitrate and thiocyanate mediawith octyl(phenyl)-N,Ndiisobutylcarbamoyl methylphosphine oxide, Sol. Ext. Ion Exch. 16 (1998) 1341-1356..

[42] P. Naik, P. Dhami, S. Misra, U. Jambunathan, J. Mathur, Use of organo-phosphorus extractants impregnated on silica gel for the extraction chromatographic separation of minor actinides from high level waste solutions, J. Rad. Nucl. Chem. Art. 257 (2003) 327-332.

[43] S. Suren, T. Wongsawa, U. Pancharoen, T. Prapasawat, A.W. Lothongkum, Uphill transport and mathematical model of Pb(II) from dilute synthetic lead-containing solutions across hollow fiber supported liquid membrane, Chem. Eng. J. 191 (2012) 503-511.

[44] Q. Yang, N.M. Kocherginsky, Copper recovery and spent ammoniacal etchant regeneration based on hollow fiber supported liquid membrane technology: From bench-scale to pilot-scale tests, J. Memb. Sci. 286 (2006) 301-309.

CHAPTER 3

Synergistic effect of various neutral donors in D2EHPA for selective neodymium separation from lanthanide series via HFSLM

Thanaporn Wannachod[a], Natchanun Leepipatpiboon[b], Ura Pancharoen[a],* and Kasidit Nootong[a],**

[a]*Department of Chemical Engineering, Faculty of Engineering, Chulalongkorn University, Patumwan, Bangkok 10330, Thailand*

[b]*Chromatography and Separation Research Unit, Department of Chemistry, Faculty of Science, Chulalongkorn University, Patumwan, Bangkok 10330, Thailand*

3.1 Abstract

The separation of Nd(III) from lanthanide series via hollow fiber supported liquid membrane (HFSLM) using synergistic extractant was investigated. Optimum extraction and stripping obtained were 94.5% and 85.1% using D2EHPA and TOPO mixtures (0.5:0.5 M/M) as the synergistic extractant. Reaction order for both extraction and stripping were first-order with rate constants of 1.444 and 1.338 min^{-1}, respectively. The experimental results were used to correlate with the models. Results showed that the concentration of Nd(III) from the experiment fitted in well with the model results. The average deviation was 1.95% and 2.18% for predictions in both feed and stripping sides, respectively.

.

Keywords: synergistic; neodymium; lanthanide; hollow fiber; liquid membrane

3.2 Introduction

Lanthanide elements occur together in nature in some minerals e.g. bastnasite, monazite and xenotime. Lanthanide elements have gained great attention in the last few decades owing to their unique properties and wide range of applications such as

in metallurgy, the ceramic industry and nuclear fuel control [1]. These metal ions have been used for additives to steel or alloys, permanent magnets, hydrogen storage materials, magneto-optic storage discs, electro or cathode rays and household batteries [2-4]. Neodymium, for example, is one of the most abundant rare earths. Currently, it is of commercial interest since it is the base for the most common solid-state lasers which are used in material processing, medicine and related fields [5].

Solvent extraction is employed in order to separate and purify rare earth elements on an industrial scale e.g. selective separation of La, Ce with PC88A by counter-current mixer-settler extraction column [6], separation of Yb(III) by mixtures of Cyanex272 and HEH/EHP in chloride media [7] etc. The ability of solvent extraction to separate Nd(III) from the feed solution and to perform the difficult separations required has been extensively demonstrated in the process of developmental work and in commercial applications. Consequently, solvent extraction plays an important role as a separation and concentration technique. Organo-phosphorous compound extractants, such as di-2-ethylhexyl phosphoric acid (D2EHPA), N,N,N'N'- tetraoctyl diglycolamide (TODGA), 2-ethylhexyl phosphonic acid mono-2-ethylhexyl ester (PC88A), tributyl phosphate (TBP) and trioctyl phoshine oxide (TOPO), are widely

used for this purpose [6, 8-12]. Solvent extraction is well known as an effective method to separate rare earths. However, the extraction process is very difficult because a large number of stages are required to produce high-purity metals from an acidic leaching solution of minerals [13].

Several liquid ion exchangers, which use an alternative separation technology, have been used in order to extract metallic species. The most widely used are phosphoric acid-based alkyl phosphorus reagents such as bis (2-ethylhexyl) phosphoric acid (D2EHPA) and 2-ethylhexyl-2-ethylhexyl phosphonic acid (EHEHPA). The above are used in the separation and purification of metal cations of different valence [14]. Some authors have investigated the separation of middle rare earths by a combination of electrochemical reduction and solvent extraction [15-17].

Even using the extractants, as mentioned earlier, separation and purification is still known to be difficult. This is because of their similar chemical and physical properties, especially the neighboring rare earth elements. There is a growing interest, therefore, in the development of new extractants and extraction systems for the separation of rare earth elements as a group or from one another.

The development of more efficient techniques is necessary for a stable supply of rare earths at commercially viable prices. The technique employed in this study is separation via hollow fiber supported liquid membrane (HFSLM). It is the technique that has carrier-mediated transport through HFSLM where simultaneous extraction and stripping process of target ions occurs in a single-step operation. High selectivity is obtainable from this technique by controlling (1) the extraction and stripping equilibrium at the interfaces and (2) the kinetics of transported species under non-equilibrium mass transfer process [18, 19]. One of the most important advantages of such a system is the possibility for selectivity and its ability to tune the transport by controlling the pH of the aqueous feed and/or receiving phases. The HFSLM process has several advantages, such as low energy consumption and a lower amount of extractant solution used [20]. It also has a larger mass transfer per unit of surface area [21]. HFSLM offers unique simultaneous extraction and recovery applications [22]. This method is suggested as a viable technique for achieving metal extraction at very low concentrations [23]. HFSLM is very a promising method for the separation and concentration of such species from aqueous streams because it combines both extraction and stripping processes. The application of HFSLM was considered for this

study following previous success with precious metals [24] and with radio metal separation by research groups [25-27].

Synergistic extraction systems have been applied to separate rare earth elements numerous times [11]. Consequently, it was observed that there was a large increase in extraction efficiency [28]. In addition, a few synergistic systems have shown improved separation among trivalent rare earth elements [29]. By using HFSLM, Ramakul et al. [30] successfully separated La(III) and Nd(III) using HTTA and TOA. Pei et al. [8] studied Nd(III) on a novel flat renewal supported liquid membrane with D2EHPA. Previous successful separations of rare earths are summarized in Table 3.1.

Table 3.1 Summary of previous research on lanthanides separation, using single extractant and synergistic extractants

Authors	Metal	Extractants	Diluents	Stripping	Method	% Ex	Ref.
Pei et al.	Nd	D2EHPA	Kerosene	HNO_3	LM	92.9	[8]
El-Nadi et al.	La, Nd	TOPO and TRPO	Kerosene	H_2SO_4	L-L	97, 81	[11]
Desouky et al.	Y	Primene-JMT	Kerosene	HNO_3	L-L	97.8	[31]
Gaikwad et al.	Y	PC-88A	Toluene	HCl	FSLM	N/A	[32]
El-Nadi et al.	Pr, Sm	Cyanex 923	Chloroform	H_2SO_4	L-L	98, 98	[33]
Pei et al.	Eu	D2EHPA	Kerosene	HNO_3	LM	94.2	[34]
Wang et al.	Y	CA12 and Cyanex 272	Kerosene	HCl	L-L	95	[35]
Wang et al.	Sm	Cyanex 272, 8-hydroxyquinoline	Heptane	HCl	L-L	N/A	[36]
This study	Nd	D2EHPA, TOPO, TBPO, TPPO and TBP	Heptane	H_2SO_4	HFSLM	94.5	

Note: L-L: Liquid-liquid extraction, LM: Liquid membrane, FSLM: Flat sheet supported liquid membrane and HFSLM: Hollow fiber supported liquid membrane.

In the present work, the possible enhancement of selective separation was investigated via the concept of synergistic effect. The synergistic nature was arbitrarily created by an introduction of a mixture of an acidic extractant with a neutral one. In this study, the acidic extractant was D2EHPA while the neutral donor extractants used were TOPO, TBPO, TPPO and TBP. The separation of Nd(III) by the HFSLM

process is governed by several parameters. The feed solution for the study was supplied in nitrate solutions – the digestion product of monazite ores processing where it contained Nd(III) 100 mg/L, Gd(III) 45 mg/L and Y(III) 28 mg/L. The choice of extractant, organic diluent and stripping solution is vital for the success of the separation of Nd(III) as in previous works [8, 11, 36].

3.3 Theory

The HFSLM system consists of a feed solution (containing metal ions) and a stripping solution. Both feed and stripping phases are separated by a supported liquid membrane embedded with one type of organic extractant or a mixture of two types of extractant to enhance the separation. The target metal ions react with the extractant at the feed membrane interface to form complex species. Subsequently, the complex species diffuse across the liquid membrane to react with the stripping solution, at the opposite interface of the membrane. Then, the complex species are stripped into the stripping phase. Thus, the target metal ions can be extracted and stripped simultaneously in a single step, as shown in Fig. 3.1. The driver in this transportation mechanism is the concentration gradient of hydrogen ions, H^+, between the feed and stripping phases.
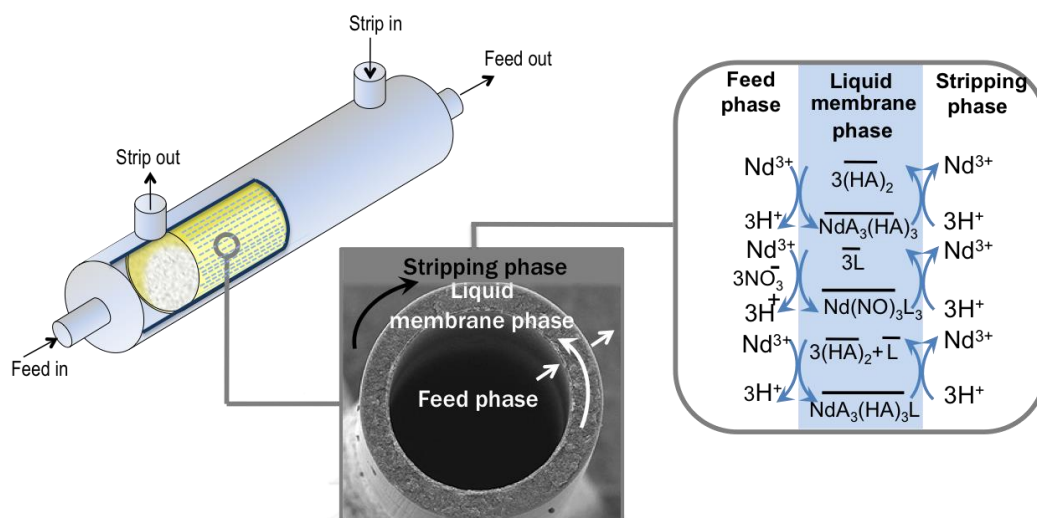
Figure 3.1 Schema of Nd(III) transport across HFSLM.

Phospho-organic extractants have functional groups with strong electron-donor oxygen atoms. They can form complexes of a diverse structure and also have the ability to interact with one another, creating various associated molecules [37]. Acid phospho-organic extractants in solvents used for the extraction of metal ions occur in dimer form: $2(HA) \rightarrow (HA)_2$.

For the 1st extractant, the extraction reaction of Nd(III) with D2EHPA $((HA)_2)$ is as shown in Eq. (3.1) as reported earlier [8].

$$Nd^{3+} + 3(\overline{HA})_2 \underset{}{\overset{k_{Ex}}{\rightleftharpoons}} \overline{NdA_3(HA)_3} + 3H^+ \tag{3.1}$$
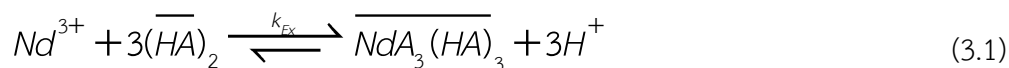
where the overbar represents the species in the liquid membrane phase, $(HA)_2$ is the dimer from of D2EHPA and k_{Ex} is the reaction rate constant of extraction.

For the 2nd extractant, the extraction reaction of Nd(III) with neutral donor ligand (L=TOPO, TBPO, TPPO and TBP) is shown in Eq. (3.2). The neutral donor (L) captures the inorganic anion (NO_3^-) in the feed phase to form the 2nd extractant. Subsequently, it reacts with Nd(III) to produce complex ions ($\overline{Nd(NO_3)_3 \cdot L_3}$). The numbers of stoichiometry in this present work were determined by slope analysis method. The obtained stoichiometric numbers agreed with the results reported earlier by El-Nadi [38].
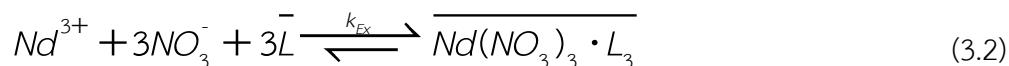
$$Nd^{3+} + 3NO_3^- + 3\overline{L} \underset{}{\overset{k_{Ex}}{\rightleftharpoons}} \overline{Nd(NO_3)_3 \cdot L_3} \tag{3.2}$$

For synergistic extractants, the mixture of D2EHPA and the neutral donor ligand can be expressed by the following Eq. (3.3). Again, the stoichiometric numbers

were also determined by slope analysis method and appeared to agree with the results reported earlier by Anitha [39].
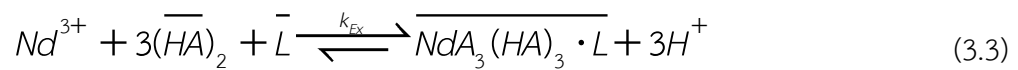
$$Nd^{3+} + 3\overline{(HA)_2} + \overline{L} \underset{}{\overset{k_{Ex}}{\rightleftharpoons}} \overline{NdA_3(HA)_3 \cdot L} + 3H^+ \tag{3.3}$$

The stripping reaction, due to 1st extraction reaction (1st extractant), is shown in Eq. (3.4).

$$\overline{NdA_3(HA)_3} + 3H^+ \underset{}{\overset{k_{St}}{\rightleftharpoons}} Nd^{3+} + 3\overline{(HA)_2} \tag{3.4}$$
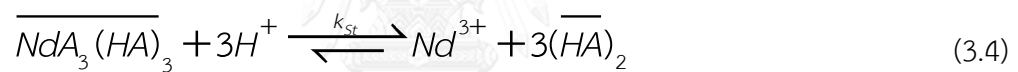
where k_{St} is the reaction rate constant of stripping.

The stripping reaction, due to 2nd extraction reaction (2nd extractant), is shown in Eq. (3.5).

$$\overline{Nd(NO_3)_3 \cdot L_3} + 3H^+ \underset{}{\overset{k_{St}}{\rightleftharpoons}} Nd^{3+} + 3NO_3^- + 3\overline{L} + 3H^+ \tag{3.5}$$
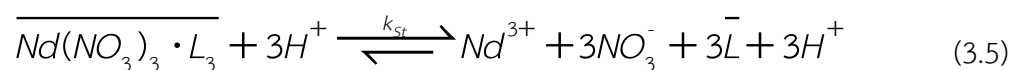
The stripping reaction, due to the synergistic reaction (mixed extractants), is shown in Eq. (3.6).

$$\overline{NdA_3(HA)_3 \cdot L} + 3H^+ \xrightleftharpoons{k_{St}} Nd^{3+} + 3\overline{(HA)_2} + \overline{L} \tag{3.6}$$
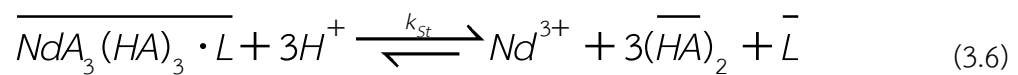
Luo et al. [40] determined the synergistic coefficient (*S.C.*) in terms of the distribution coefficient:

$$S.C. = \frac{K_{d12}}{K_{d1} + K_{d2}} \tag{3.7}$$

If S.C. > 1, synergism is present.

For S.C. = 1, there is no synergism.

If S.C. < 1, an antagonistic effect happens.

where K_{d12} is the distribution coefficient of the synergistic system to extract the specified ions, K_{d1} is the distribution coefficient of D2EHPA and K_{d2} is the distribution coefficient of the neutral donor.

The distribution coefficient (K_d) for Nd(III) extraction can be calculated by [41]:

$$K_{d1} = \frac{\left[\overline{NdA_3(HA)_3}\right]}{\left[Nd^{3+}\right]} \qquad (3.8\text{-a})$$

and

$$K_{d2} = \frac{\left[\overline{Nd(NO_3)\cdot L_3}\right]}{\left[Nd^{3+}\right]} \qquad (3.8\text{-b})$$

then

$$K_{d12} = \frac{\left[\overline{NdA_3(HA)_3 \cdot L}\right]}{[Nd^{3+}]} \qquad (3.8\text{-c})$$

where [Nd^{3+}] is the initial concentration of Nd(III) in the feed phase, $\left[\overline{NdA_3(HA)_3}\right]$,

$\left[\overline{Nd(NO_3)\cdot L_3}\right]$ and $\left[\overline{NdA_3(HA)_3 \cdot L}\right]$ are the concentrations of complex species

in the liquid membrane phase.

The percentages of Nd(III) extraction and stripping from experiments were calculated by Eqs. (3.9) and (3.10), respectively:

$$Extraction\ (\%) = \frac{[C]_{f,in} - [C]_{f,out}}{[C]_{f,in}} \times 100 \tag{3.9}$$

$$Stripping\ (\%) = \frac{[C]_{s,out} - [C]_{s,in}}{[C]_{f,in}} \times 100 \tag{3.10}$$

where $[C]_{f,in}$, $[C]_{s,in}$ denote the initial concentration in the feed and stripping phases and $[C]_{f,out}$, $[C]_{s,out}$ denote the concentration in the feed and stripping phases.

The separation factor S_F(AB) is the ratio of concentrations A and B in the permeate and retentate [42]. This was calculated as in Eq. (3.11):

$$S_F = \frac{\left(C_A / C_B \right)_{permeate}}{\left(C_A / C_B \right)_{raffinate}} \tag{3.11}$$

where C_A and C_B are the concentrations of Nd(III) and Gd(III) or Y(III).

3.3.1   Model for Nd(III) transport through HFSLM

Chaturabul et al. [43] modeled the metal ion transport in both feed and stripping phases based on chemical reaction. The extraction reaction is summarized in Eq. (3.3). The reaction rate of extraction with respect to target metal concentration (C_{Af}) is described as in Eq. (3.12).

$$-r_f = k_{Ex} C_{Af}^n (x,t) \qquad (3.12)$$

where x is the longitudinal axis of the hollow fiber in the feed phase, k_{Ex} is the extraction rate constant, t is the extraction time, C_{Af} is the concentration of metal ions in the feed solution (mg/L) and n is the reaction order of extraction.

The stripping reaction is summarized in Eq. (3.6). The reaction rate of stripping with respect to target metal concentration (C_{As}) is described as in Eq. (3.13).

$$+r_s = k_{St} C_{A_s}^m (\overline{x}, t) \tag{3.13}$$

where $\overline{x}$ = L-x, is the longitudinal axis of the hollow fiber in the stripping phase, k_{St} is the stripping rate constant, C_{As} is the concentration of metal ions in the stripping solution and m is the reaction order of stripping.

The following assumption for the model in the feed phase is that perfect mixing occurs within the sheer small cross sectional area of the inner hollow fiber tube. In consequence, there is no variation in ion concentration across the cross-sectional area but only in the axial direction, arising from reaction flux along the hollow fiber tube.

A theoretical model was developed for predicting the outlet concentration of Nd(III) at any time in the feed phase by Chaturabul et al. [43]. The model equation was derived from mass conservation where the conventional as well as reaction flux was taken into account, as shown in Eq. (3.14).

$$-\frac{q}{A_f}\frac{\partial C_{Af}(x,t)}{\partial x} - r_{Af}(x,t) = \frac{\partial C_{Af}(x,t)}{\partial t} \tag{3.14}$$

where $r_{Af}(x,t)$ and $C_{Af}(x,t)$ are the reaction rate and the concentration of Nd(III) at any time, respectively.

In the feed phase model [43], the complete set of solutions was as follows:

For the Case n = 1, the solution of Eq. (3.14) can be expressed as:

$$\overline{C}_{Af}(L,t) = \exp(\tau_f k_f) \cdot \overline{C}_{Af}(0,t-\tau_f) \cdot u(t-\tau_f) \tag{3.15}$$

where $u(t-\tau_f)$ is a unit shifting function

$$\overline{C}_{Af}(x,t) = C_{Af}(x,t) - C_{Af}(x,0)$$

$$\tau_f = \frac{A_f L}{q_f}$$

$$A_f = 35000 \times \pi r_i^2$$

where $\overline{C}_{Af}(0, t-\tau_f)$ is the concentration of Nd(III) in the feed reservoir (mg/L), k_f is the reaction rate constants of extraction, A_f is the cross-sectional area of hollow fiber (cm^2), L is the length of hollow fiber (cm), q_f is a volumetric flow rate in the feed phase (mL/min), t is time (min) and r_i is the inner radius of the hollow fiber (cm).

A key assumption for the model, in the stripping phase, is possible given that the operation is isothermal at constant pressure and volume. Complete mixing occurs in each thin segment of the flow moving frame. The transport direction for the metal complex is in radial direction from the feed phase to the stripping phase. Due to the very thin liquid membrane thickness, it is presumed that the reaction occurs only in the axial direction of the hollow fibers [24, 43]. The stripping reaction takes place very fast at the contact surface between the liquid membrane and the stripping phases, along the length of the hollow fiber module. The forward reaction of stripping is assumed to occur more than its backward reaction. Thus, the overall reaction of stripping is irreversible [43]. As a result, once the metal ion complex decomposes to the original ions, the metal ions will only then be transferred to the stripping phase.

In the stripping phase model [43], solution to outlet concentration at any time is based on the reaction flux. The model replicates assumptions earlier deployed in the feed phase. The complete set of solutions is subsequently obtained as follows:

For the Case m = 1:

$$\overline{C}_{As}(L,t) = \exp(\tau_s k_s) \cdot \overline{C}_{As}(0, t - \tau_s) \cdot u(t - \tau_s)$$

(3.16)

where $u(t - \tau_s)$ is a unit shifting function

$$\overline{C}_{As}(x,t) = C_{As}(x,t) - C_{As}(x,0)$$

$$\tau_s = \frac{A_s L}{q_s}$$

$$A_s = 35000 \cdot \left(\frac{\sqrt{3}}{4} d_0^2 - \frac{\pi r_0^2}{2} \right)$$

where $\bar{C}_{As}(0, t - \tau_s)$ is the concentration of Nd(III) in the stripping reservoir (mg/L), k_s is the reaction rate constants of stripping, A_s is the cross-sectional area in the stripping phase (cm^2), L is the length of hollow fiber (cm). q_s is the volumetric flow rate in the stripping phase (mL/min), t is time (min), d_0 is the outer diameter (cm) and r_0 is the outer radius of the hollow fiber (cm).

Kandwal et al. [44] developed the principle of facilitated diffusional transport mechanism. Eq. (3.17) has been used in order to obtain the time variation of metal ion concentration in both feed and stripping solutions,

$$\ln\left(\frac{C_t}{C_0}\right) = \frac{V}{V_f}\left(e^{-\frac{2\varepsilon}{RV}\left(\frac{K_d L}{K_d \Delta_{aq} + \Delta_{org}}\right)} - 1\right)t \tag{3.17}$$

where $\quad \Delta_{aq} = \dfrac{R\varepsilon d_{aq}}{(R - d_{aq})D_{aq}} \quad$ and $\quad \Delta_{org} = \dfrac{d_{org}\tau}{D_{org}}$

Since

C_t	=	metal concentration at any time "t" (mg/L),
C_0	=	metal concentration at time t = 0 (mg/L) ,
V	=	volumetric flow rate (mL/min),
V_f	=	volume of feed solution in reservoir (mL),
K_d	=	distribution coefficient of the metal ion (-),
L	=	the length of fiber (cm),
R	=	the inner radius of hollow fiber (cm),
Δ_{aq}	=	the aqueous phase resistance (cm),
Δ_{org}	=	the organic phase resistance (cm),
ε	=	the porosity of hollow fiber (%),
τ	=	the tortuosity factor membrane (-),
d_{aq}	=	the thickness of aqueous diffusion layer (cm),
d_{org}	=	the thickness of membrane diffusion layer (cm),
D_{aq}	=	the aqueous diffusion coefficient (-) and
D_{org}	=	the membrane diffusion coefficient (-).

The mathematical model was validated by the percentage of standard deviation (S.D. (%)) obtained from the model and experimental results. The standard deviation is as follows:

$$\% \; S.D. = 100 \times \sqrt{\dfrac{\displaystyle\sum_{i=1}^{n}\left\{\left(\dfrac{D_{Exp.}}{D_{Model}}\right) - 1\right\}^{2}}{N - 1}} \tag{3.18}$$

where $D_{Exp.}$ is the experimental data, D_{Model} is the model calculated value from the mathematical model and N is the number of experimental points.

3.4 Experimental

3.4.1 Chemicals and reagents

The feed solution contained Nd(III) 100 mg/L, Gd(III) 45 mg/L and Y(III) 28 mg/L in nitric acid solution. By courtesy of the Rare Earth Research and Development Center, Office of Atoms for Peace, Bangkok, Thailand, the feed solutions for study were supplied in nitrate solutions – the digestion product of monazite ores processing. The liquid membrane phase was a solution of synergistic extractants – D2EHPA mixed with donor (TOPO, TBPO, TPPO or TBP) – in heptane (analytical

reagent grade) obtained from Merck (Germany). The chemical structure is shown in

Fig. 3.2. The stripping solution, sulfuric acid (QRec), was dissolved in deionized water.

All reagents used in this experiment were of GR grade.
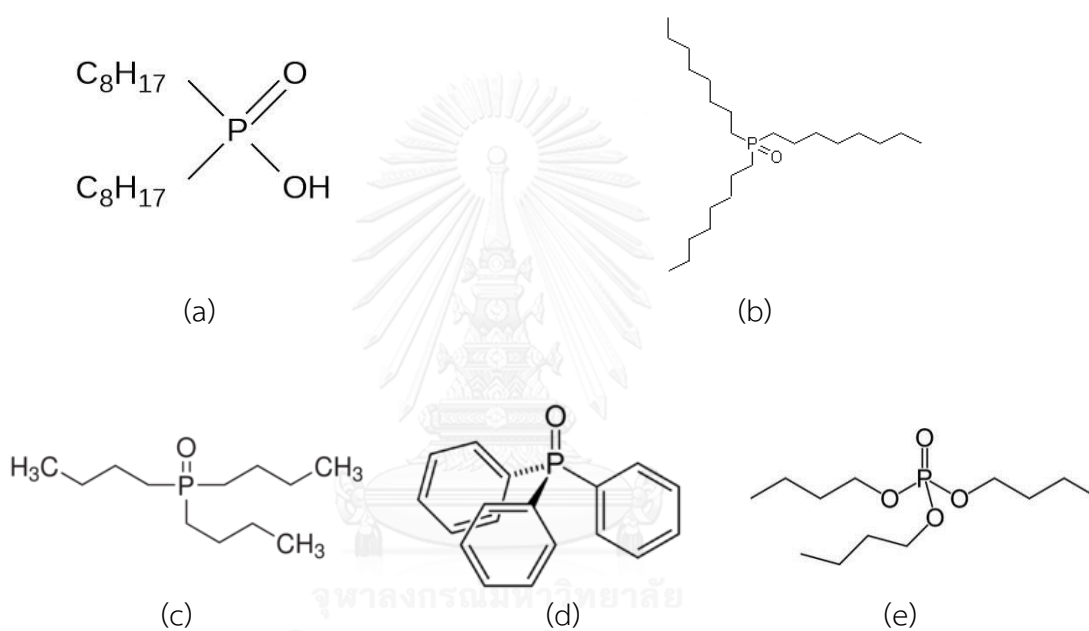
Figure 3.2 The structures of the extractants: (a) D2EHPA (di(2-ethylhexyl) phosphoric acid), (b) TOPO (trioctyl phosphine oxide), (c) TBPO (tributyl phosphine oxide), (d) TPPO (triphenylphosphine oxide) and (e) TBP (tributyl phosphate).

3.4.2   Apparatus

The HFSLM Liqui-Cel Extra-Flow membrane contactor was manufactured by Hoechst Celanese, USA. The module uses Celgard micro-porous polypropylene fibers that are woven into a fabric. Properties of the hollow fiber module are as shown in Table 3.2. The concentration of metal ions in the feed and stripping solutions was analyzed by inductively coupled plasma spectrometry (ICP).

Table 3.2 Properties of the hollow fiber module

Property	Description
Material	Polypropylene
Inside diameter of hollow fiber	0.024 cm
Outside diameter of hollow fiber	0.03 cm
Effective length of hollow fiber	15 cm
Number of hollow fibers	35,000
Average pore size	3×10^{-6} cm
Porosity	30%
Effective surface area	1.4_c
Area per unit volume	29.3 cm^2/cm^3
Module diameter	6.3 cm
Module length	20.3 cm
Contract area	30%
Tortuosity factor	2.6
Operating temperature	273–333 K

3.4.3 Procedure

The single module operation is shown in Fig. 3.3. The selected organic carrier D2EHPA, neutral donors (TOPO, TBPO, TPPO and TBP) and synergistic extractant (D2EHPA + neutral donor) were dissolved individually in heptane (0.5 L). Then, the extractant was simultaneously pumped into the tube and shell sides of the hollow fiber module for 40 min. to ensure that the extractant was entirely embedded in the micro-pores of the hollow fibers. Subsequently, 5 L of both feed solution and stripping solution were fed counter-currently into the tube side and shell side, respectively, of the single-module operation.
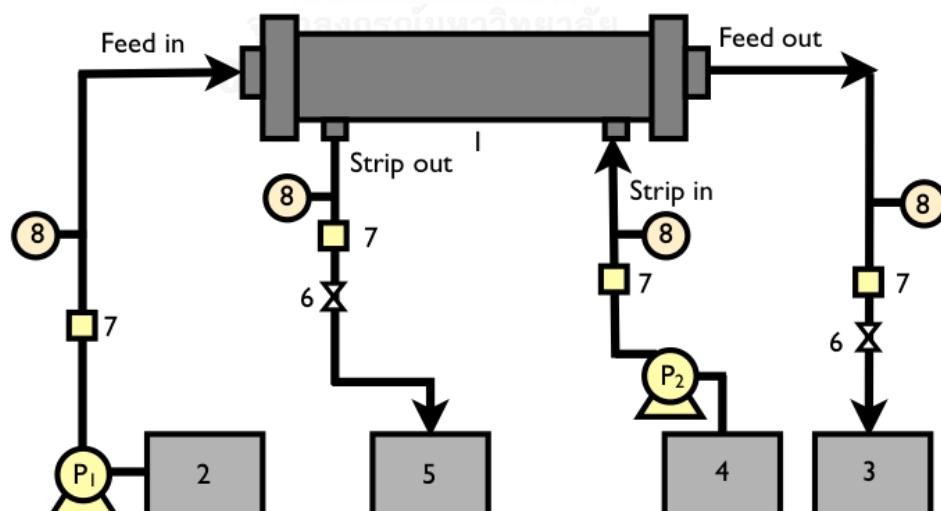
Figure 3.3 Shows the schematic representation of the counter-current flow diagram for continuous operation in HFSLM: (1) HFSLM (2) Feed in reservoir (3) Feed out reservoir (4) Stripping in reservoir (5) Stripping out reservoir (6) Flow regulator valve (7) Flow indicator (8) Pressure indicator

3.5   Results and discussion

3.5.1   Effect of the concentration of D2EHPA

The concentration of D2EHPA was studied in the range of 0.1 – 0.7 M. Consequently, the increase in Nd(III) extraction corresponded to an increase in the extractant concentration, as shown in Fig. 3.4(a). The highest percentage of Nd(III) extraction was obtained at a concentration of 0.5 M. This proved to be the optimized concentration for use in further runs as a baseline for future study with neutral donors. The highest extraction of Nd(III) obtained by the D2EHPA extractant in a single-module operation was 81.5% which reciprocated stripping percentage at 69.1%. To further enhance performance, the extraction cycle mode was repeated. As a result, the cumulative Nd(III) extraction and stripping rose to 87% and 83%, respectively, following the fourth cycle which provides the results in Fig. 3.4(b). The selectivity of Nd(III) stripping was also observed to improve with repetition of the extraction cycle mode. The percentages of extraction of Gd(III) and Y(III) were 13% and 8% and stripping of Gd(III) and Y(III) were 7% and 4% respectively.

From this study, extraction and stripping of lanthanides followed the sequence Nd(III)> Gd(III)>Y(III). This was in agreement with an earlier report by Anitha et al. [39]. Thus, when extractant concentration increased more than 0.5 M, no significant change in Nd(III) extraction was observed. This can be attributed to the fact that the viscosity of the liquid membrane becomes higher when extractant concentration is increased. This, in turn, impedes the mass transfer of complex ions confirming Nernst's equation (Eq. (3.19)) where viscosity (η) is inversely to the diffusion coefficient ($\mathscr{D}$):

$$D = \frac{k_B T}{6\pi\eta r} \tag{3.19}$$

where k_B is Boltzmann's constant, η is the viscosity of the liquid membrane, r is the radius and T is the temperature.

(a)
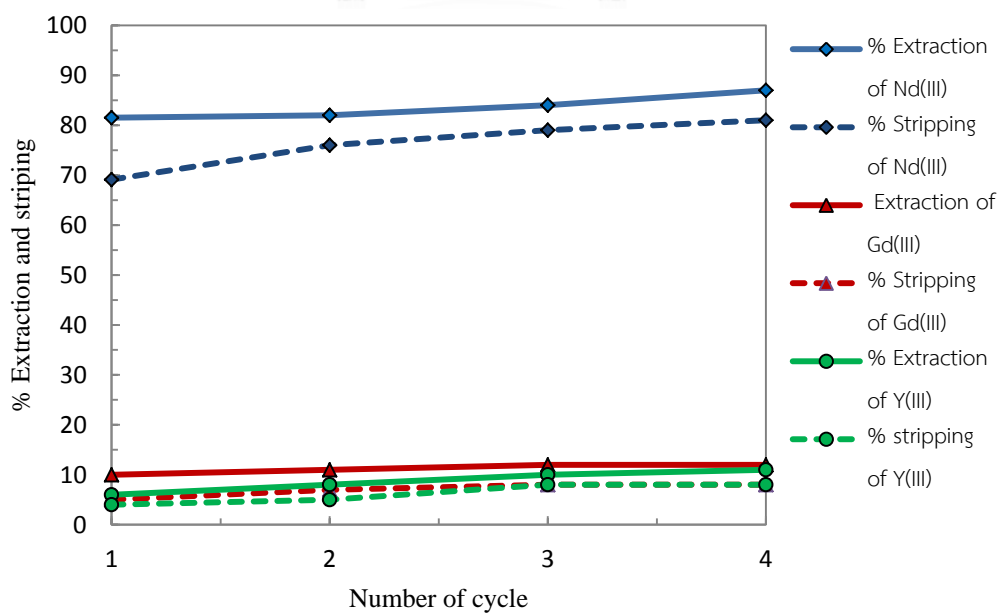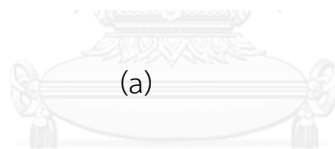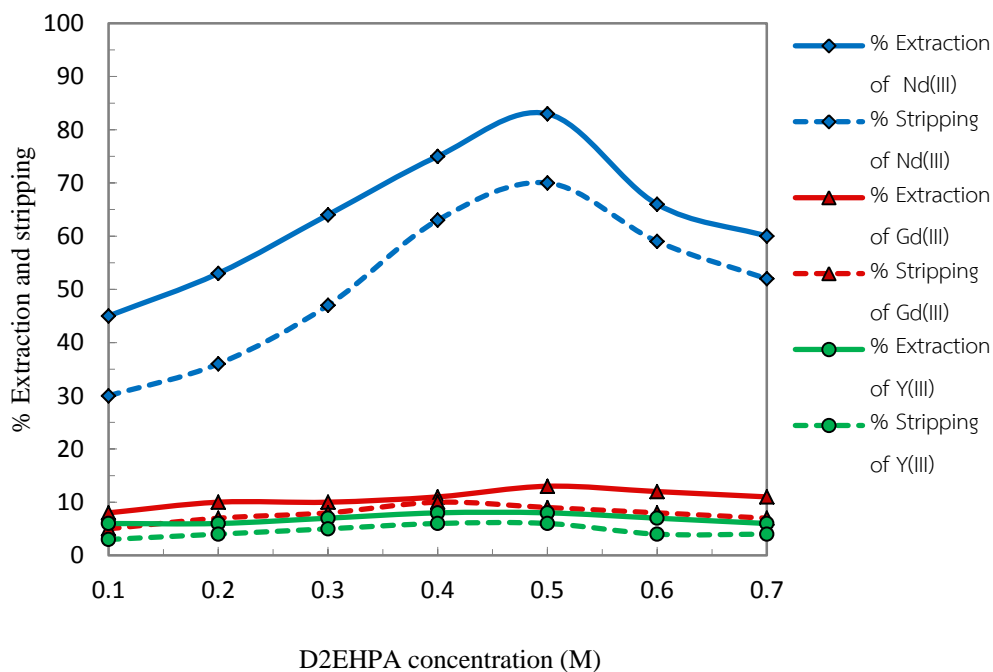
(b)

Figure 3.4 (a) The effect of concentration of D2EHPA on extraction and stripping percentages of lanthanide (Feed = pH 4.5; stripping = 1 M H_2SO_4; flow rate = 100 mL/min. for both feed and stripping solutions), (b) The number of cycle on extraction and stripping percentages of lanthanide (Feed = pH 4.5; extractant = 0.5 M; stripping = 1 M H_2SO_4; flow rate = 100 mL/min. for both feed and stripping solutions).

3.5.2   Effect of concentration of neutral donors

The effect of different neutral donors (organo-phosphorus) bases on the extraction of Nd(III) were studied. The concentration of D2EHPA was studied in the range of 0.1 – 0.7 M. As shown in Fig. 3.5, extraction increased when concentration increased up to 0.5 M. Higher than 0.5 M, no significant change in Nd(III) extraction (or less fluxes) was observed. This was because the extractant solution became more viscous at the higher concentration; hence impeding the effective mass transfer.

Extraction of Nd(III) followed the sequence TOPO>TBPO>TPPO>TBP corresponding to the order of relative basicity (K_H) – which is the nitric acid uptake equilibrium constant – of individual neutral donor i.e. TOPO (K_H = 8.9), TBPO (K_H=7.4), TPPO (K_H=7.1), TBP (K_H=0.16)), K_H= acid uptake constant. A somewhat similar trend was seen in the synergistic extraction of other transition metals and actinides [25,45].

The extraction percentage achieved by neutral donors was fairly low compared with an acidic extractant such as D2EHPA in the preceding case. The extraction percentage of rare earth metals by a solvating extractant is very low in the pH range e.g. between 2 to 6. Usually, a solvating extractant (TOPO, TBPO, TPPO, TBP) is extracted at a high pH. Kumbarsa et al [46] successfully extracted rare earth metals at a value of pH 8.

Neutral donors were chosen for synergistic reaction since the lone electron pair, available from the phosphorus-oxygen bond, has the ability to bridge with D2EPHA to form synergistic extractants. The synergistic extractants are a combination of prime (D2EPHA) and supplementary (neutral donor) extractants. Thus, overall extraction was enhanced by introducing the third extraction reaction in addition to the original reaction mechanisms by individual prime extractants and individual supplementary extractants. Examples of supplementary extractants were TOPO, TBPO, TPPO and TBP.

(a) Neutral donors concentration (M)

(b) Neutral donors concentration (M)
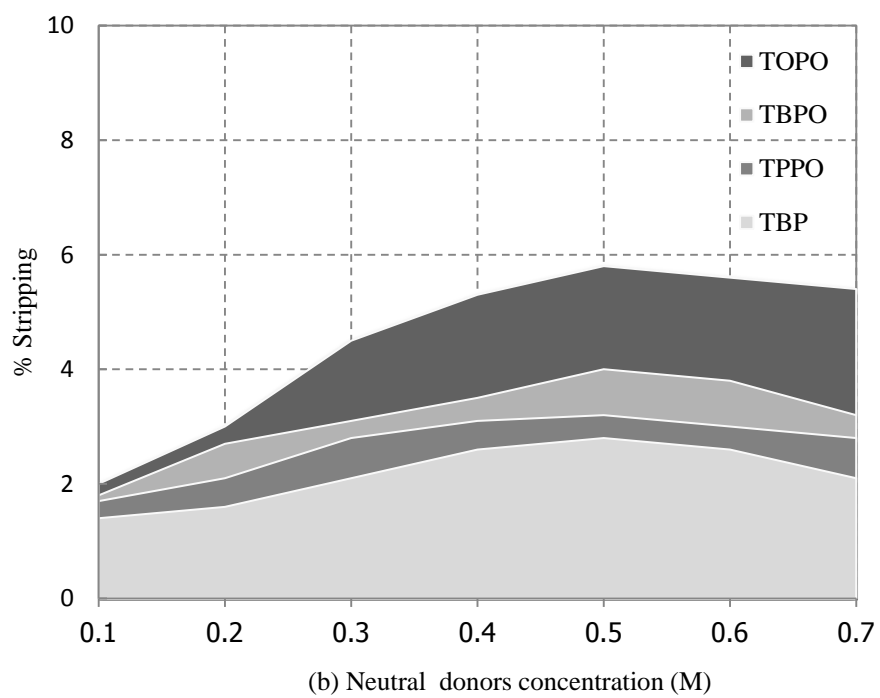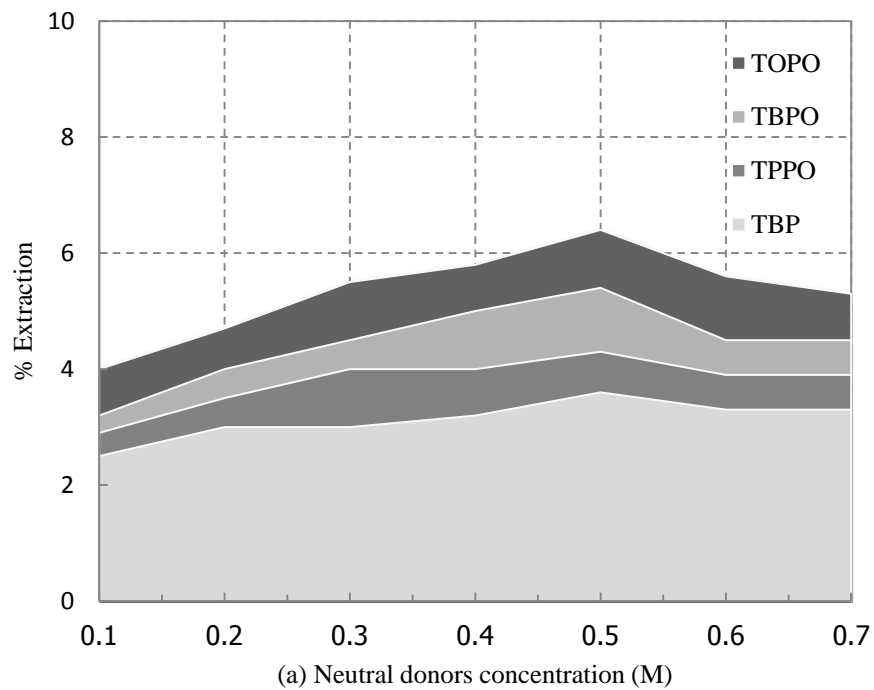
Figure 3.5 Effect of neutral donor concentration on percentages of (a) extraction and (b) stripping of Nd(III) (Feed = pH 4.5; stripping = 1 M H_2SO_4; flow rate = 100 mL/min. for both feed and stripping solutions).

3.5.3   Effect of pH of feed solution on the synergistic extractability

Based on the transport mechanism of Nd(III) across the HFSLM system, the concentration gradient of hydrogen ions between feed and stripping solutions is a prominent driving force. In this work, the pH of feed solution in the range of 2 to 6 was studied, as shown in Fig. 3.6. The results indicated that when the pH value increased, the synergistic coefficients increased and the highest was achieved at pH 4.5. This could be explained by the fact that in the pH range of 2.8 to 4.5, the higher pH (lower H^+ concentration) brings the stronger driving force. However, when pH was higher than 4.5, the synergistic coefficient decreased because the extraction was governed by a cation exchange reaction in which protons are released [47]. Thus, the feed solution pH of 4.5 was considered as the optimum pH condition in the feed phase and it will be used in the further experiments.
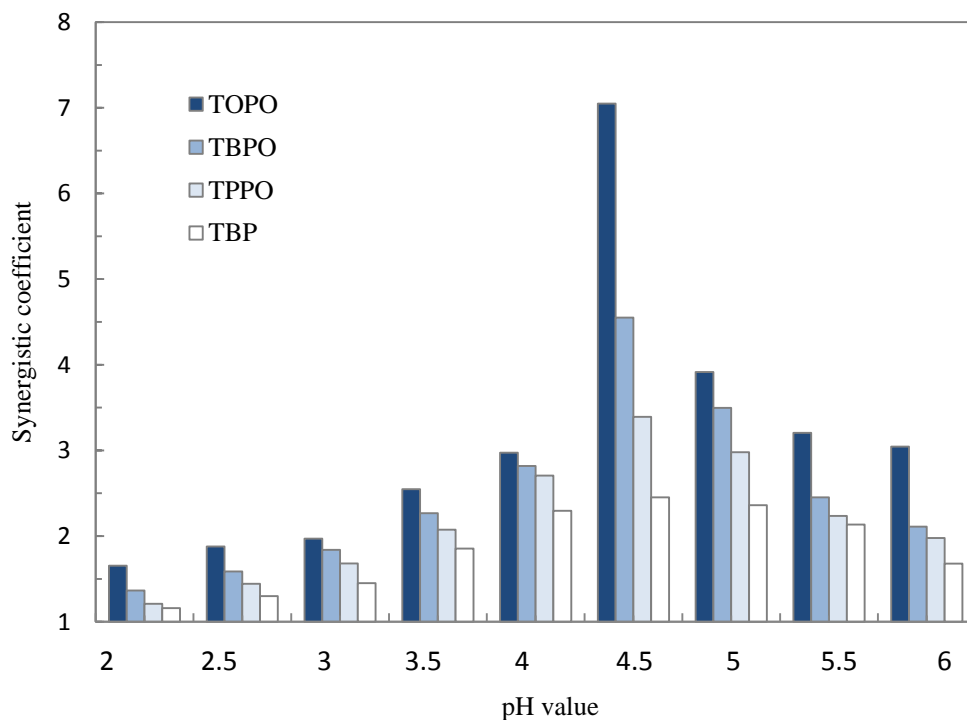
Figure 3.6 Effect of pH on the synergistic coefficient (Extractant = 0.5 M D2EHPA and 0.5 M of neutral donor; stripping = 1 M H_2SO_4; flow rate = 100 mL/min. for both feed and stripping solutions).

3.5.4   Effect of the synergistic extractant on Nd(III) extraction and stripping

The investigation was expanded by generating a dimensional surface plot from the concentration effect data. Synergistic separation occurred by adding TOPO to D2EHPA. As shown in Fig. 3.7, the percentages of Nd(III) extraction and stripping increased when the concentration of TOPO in the synergistic extractant increased.

This could be explained by Le Chatelier's principle whereby extraction increased when concentration of the extractant increased. Maximum Nd(III) extraction was attained at concentrations of D2EHPA and TOPO in the synergistic extractant mixture of 0.5 M and 0.5 M, respectively. The highest percentages of extraction and stripping obtained were 94.5% and 85.1%, respectively.

Further, the percentage of Nd(III) extraction then decreased due to the excessive viscosity from the high concentration. According to the molecular kinetic interpretation by Stokes and Einstein, an increase in high viscosity leads to a lower diffusion coefficient, resulting in lower extraction. Chakrabarty et al. [48] also observed that the viscosity of the membrane phase increases when the extractant concentration is increased, resulting in a decrease of flux.
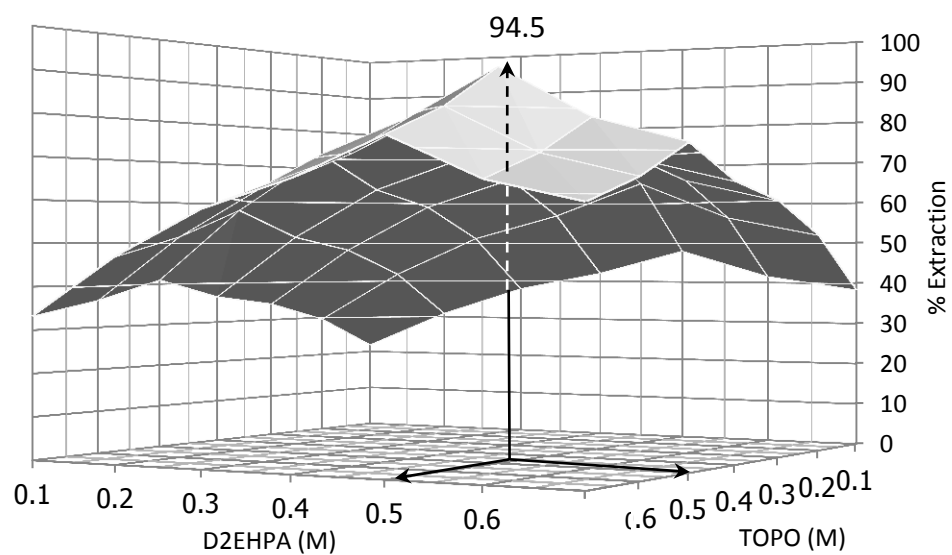
(a)
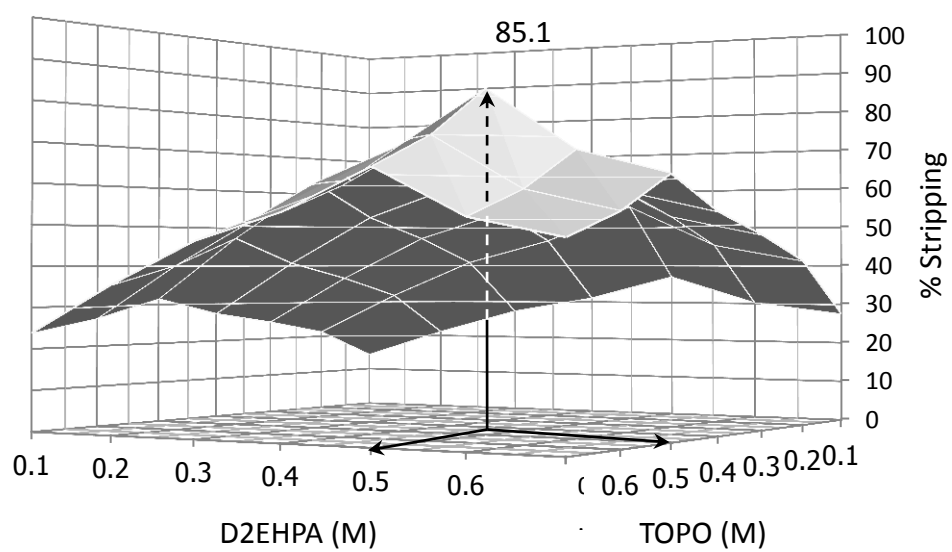
(b)

Figure 3.7 Effect of synergistic extractant on (a) extraction yield and (b) stripping yield (Feed = pH 4.5; stripping = 1 M H_2SO_4; flow rate = 100 mL/min. for both feed and stripping solutions).

The influence of the synergistic extractant compositions are shown in Fig. 3.8. Increasing the concentration of TOPO from 0.1 to 0.5 M was found to increase the synergistic coefficient. The optimized condition for concentration of D2EHPA: TOPO was 0.5M: 0.5M.

The formation of new bonds in the organic phase between D2EHPA and neutral donors may be the reason for the increased synergistic reaction whereby some extractant molecules are polymerized through hydrogen bonds [49]. Theoretically, after the point corresponding to maximum extraction, the fluxes decrease at higher extractant concentration because the viscosity of the film between the feed solution and liquid membrane increased and obstructed the mass transfer [50].
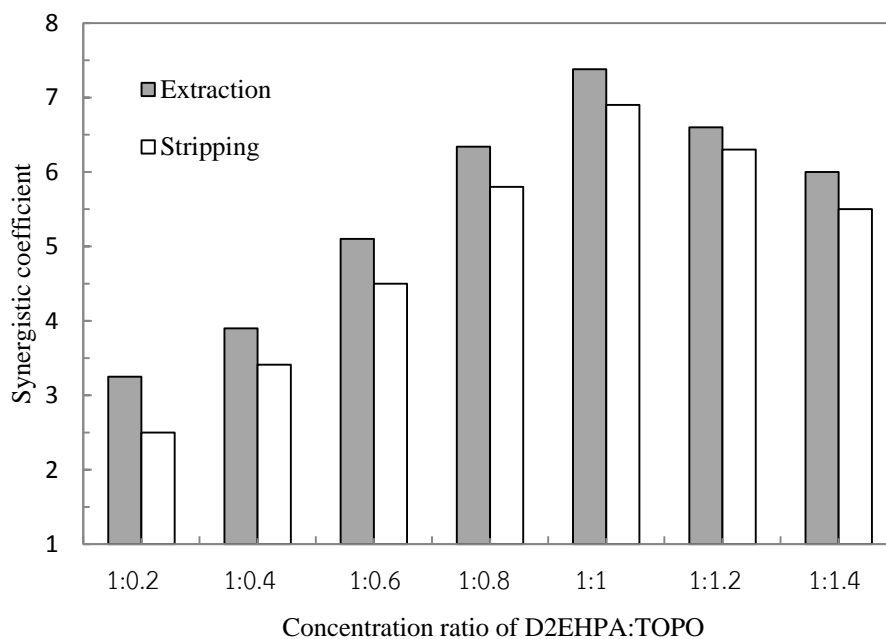
Figure 3.8 Effect of the synergistic extractant on the synergistic coefficient of extraction and stripping (Feed = pH 4.5; stripping = 1 M H_2SO_4; flow rate = 100 mL/min. for both feed and stripping solutions).

3.5.5   Effect of concentration of stripping solutions

Stripping investigations were carried out with regard to the organic solution consisting of the usual mixture of 0.5 M D2EHPA and 0.5 M TOPO. Furthermore, the effect of different concentrations of mineral acids on the stripping of metal ions was investigated. The results given in Fig. 3.9 show that when the concentration of stripping solution increased up to 1 M, the percentage of stripping decreased due to the concentration polarization. This can be explained by the fact that the stripping of

metal ions was obstructed by concentration polarization when the concentration of stripping increased up to 1 M [51]. Thus, optimum percentage of Nd(III) stripping was obtained at 1 M sulfuric acid. Similar trends were reported previously where stripping percentage reduced significantly.
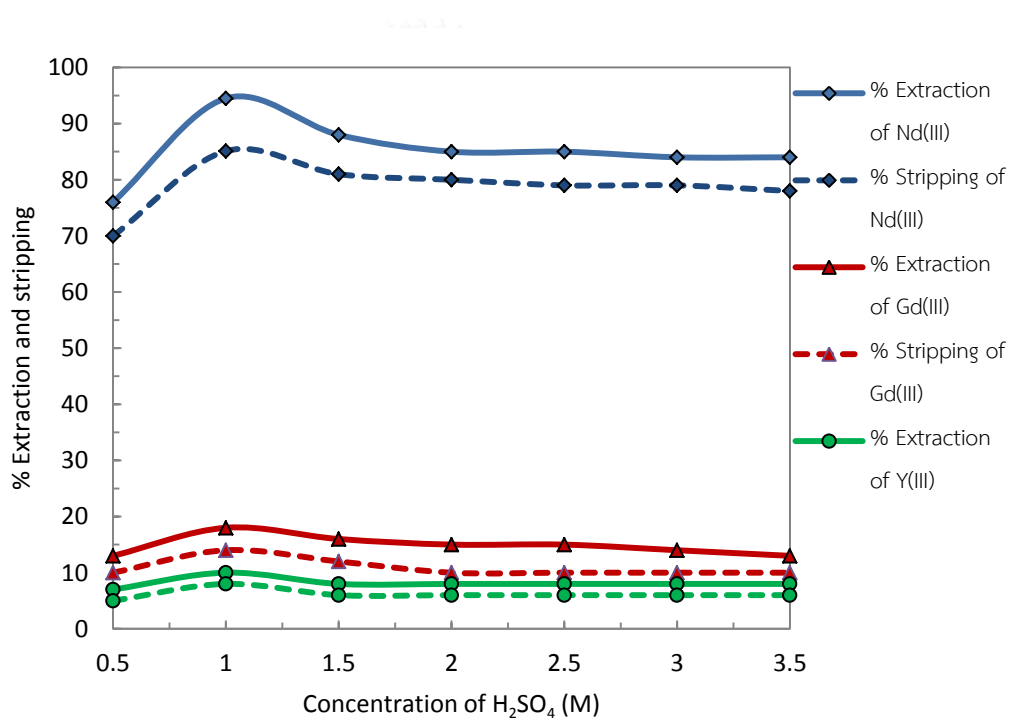
Figure 3.9 Effect of concentration of stripping (Feed = 4.5; Extractants = 0.5 M D2EHPA and 0.5 M TOPO; flow rate = 100 mL/min. for both feed and stripping solutions).

3.5.6   Effect of the flow rate of feed and stripping solutions

The influence of flow rates was investigated using Nd(III) in nitric solution as feed solution. Flow rates of feed and stripping solutions were varied from 50 to 350 mL/min. as shown in Fig. 3.10. In this experiment, optimum percentages of Nd(III) extraction and stripping were obtained at flow rates of both feed and stripping solutions of 100 mL/min. using a single-module operation for 70 min. The highest percentages of Nd(III) extraction and stripping obtained were 94.5% and 85.1%, respectively. However, percentages of Nd(III) extraction and stripping decreased when flow rates of feed and stripping solutions increased due to the resident time of the solution in the hollow fiber module. This was in agreement with an earlier report by Yang et al. [52].
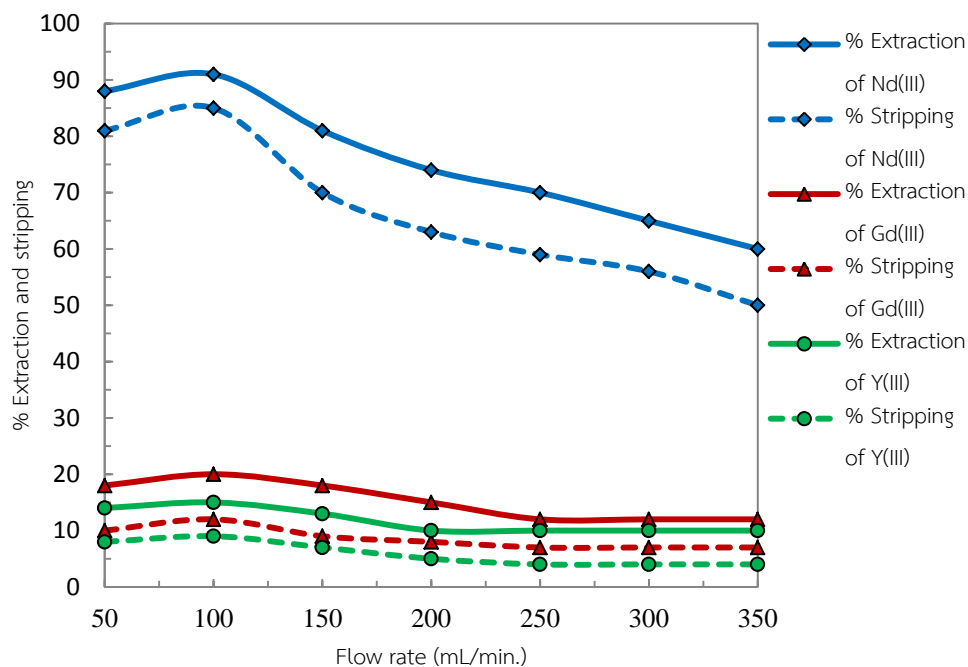
Figure 3.10 Effect of flow rate (Feed = pH 4.5; Extractants = 0.5 M D2EHPA and 0.5 M TOPO; stripping = 1 M H$_2$SO$_4$).

3.5.7   Separation factor

The separation factor is an important parameter in separation chemistry. Under the same experimental conditions, the separation factors for the pair of rare earths Nd/Gd and Nd/Y are shown in Table 3.3, using experimental conditions similar to those used in Fig. 3.7. Although the separation factor values between these rare earths are not high, the synergistic extractant can be of some use in the extraction of these elements, particularly for moderate separation of Nd(III) from lanthanide.

Table 3.3 The separation factor for validation at 0.5 M D2EHPA

[TOPO] (M)	0.1	0.2	0.3	0.4	0.5	0.6	0.7
S_F (Nd/Gd)	8.33	7.76	10.84	22.91	55.09	16.91	15.04
S_F (Nd/Y)	13.39	13.84	14.42	37.23	121.43	35.97	32.56

3.5.8   Reaction order and reaction rate constants

As shown in Table 3.4, the highest R^2 of D2EHPA denoted first-order reactions. The reaction rate constants of D2EHPA for extraction (k_f) and stripping (k_s) were determined from the slopes of the integral concentration of Nd(III) plotted against time and were found to be 0.9207 and 0.7149 min^{-1}, respectively. For neutral donors, the highest R^2 denoted second-order reactions for the concentration of only one reactant. The reaction rate constants of neutral donors for extraction (k_f) and stripping (k_s) were determined from the slopes of the integral of Nd(III) plotted against time and were found to be TOPO>TBPO>TPPO>TBP.

Table 3.4 Analysis of reaction order and reaction rate constants of extraction and stripping of Nd(III) using a single extractant.

Reaction order	Relationship	k_f	k_s	R^2 Ext.	Str.
		Determination		R^2	
D2EHPA					
0	C vs. time	0.5045 mg/L.min	0.4963 mg/L.min	0.8351	0.8795
1	ln (C$_0$/C) vs. time	0.9207 min^{-1}	0.7149 min^{-1}	0.9869*	0.9841*
2	1/C vs. time	0.0407 L/mg.min	0.0383 L/mg.min	0.8895	0.8991
TOPO					
0	C vs. time	0.2415 mg/L.min	0.2184 mg/L.min	0.8539	0.7982
1	ln (C$_0$/C) vs. time	0.0045 min^{-1}	0.0034 min^{-1}	0.7175	0.9368
2	1/C vs. time	0.0029 L/mg.min	0.0021 L/mg.min	0.9941*	0.9968*
TBPO					
0	C vs. time	0.1655 mg/L.min	0.1587 mg/L.min	0.7886	0.7905
1	ln (C$_0$/C) vs. time	0.0038 min^{-1}	0.0029 min^{-1}	0.9106	0.9215
2	1/C vs. time	0.0023 L/mg.min	0.0018 L/mg.min	0.9956*	0.993*
TPPO					
0	C vs. time	0.1235 mg/L.min	0.1109 mg/L.min	0.7745	0.7892
1	ln (C$_0$/C) vs. time	0.0026 min^{-1}	0.0021 min^{-1}	0.8764	0.9126
2	1/C vs. time	0.0015 L/mg.min	0.0048 L/mg.min	0.9987*	0.9959*
TBP					
0	C vs. time	0.0991 mg/L.min	0.0842 mg/L.min	0.7942	0.8217
1	ln (C$_0$/C) vs. time	0.0018 min^{-1}	0.0015 min^{-1}	0.8974	0.8981
2	1/C vs. time	0.0005 L/mg.min	0.0003 L/mg.min	0.9882*	0.9873*

* Best fit

In Table 3.5 (synergistic extractant of D2EHPA and neutral donor), the reaction rate constants of synergistic extraction (k_f) and stripping (k_s) were again determined from the slopes of the integral concentration of Nd(III) plotted against time and were found to be TOPO>TBPO>TPPO>TBP.

Table 3.5 Analysis of reaction order and reaction rate constants of extraction and stripping of Nd(III) using synergistic extractant.

Reaction order		Determination		R^2	
D2EHPA	Relationship	k_f	k_s	Ext.	Str.
TOPO					
0	C vs. time	1.8312 mg/L.min	1.7381 mg/L.min	0.9071	0.9145
1	ln (C_0/C) vs. time	1.4448 min^{-1}	1.3382 min^{-1}	0.9892*	0.9841*
2	1/C vs. time	0.2861 L/mg.min	0.2786 L/mg.min	0.8621	0.8714
TBPO					
0	C vs. time	0.6154 mg/L.min	0.5736 mg/L.min	0.7983	0.8006
1	ln (C_0/C) vs. time	0.9991 min^{-1}	0.8284 min^{-1}	0.9971*	0.9918*
2	1/C vs. time	0.2691 L/mg.min	0.2548 L/mg.min	0.8825	0.7914
TPPO					
0	C vs. time	0.5935 mg/L.min	0.5309 mg/L.min	0.8815	0.8796
1	ln (C_0/C) vs. time	0.9419 min^{-1}	0.7914 min^{-1}	0.9876*	0.9888*
2	1/C vs. time	0.2511 L/mg.min	0.2158 L/mg.min	0.7980	0.7871
TBP					
0	C vs. time	0.5136 mg/L.min	0.4692 mg/L.min	0.8756	0.8673
1	ln (C_0/C) vs. time	0.9321 min^{-1}	0.7435 min^{-1}	0.9859*	0.9914*
2	1/C vs. time	0.2431 L/mg.min	0.2239 L/mg.min	0.7914	0.7543

* Best fit

The highest extraction and stripping of Nd(III) from the experiments of the synergistic reaction were observed when using 0.5 M of D2EHPA and 0.5 M of TOPO in the liquid membrane and 1M sulfuric acid in the stripping solution. The integral concentrations of Nd(III) were plotted against time, as shown in Fig. 3.11. This was done in order to determine the reaction order (n) and the reaction rate constant of extraction (k_f) as well as stripping (k_s). It is well known that rates of chemical changes may control transport kinetics through the liquid membrane, depending on transport mechanisms. As shown in Fig. 3.11, the synergistic reaction rate constant of extraction and stripping was found to be 1.4448 min^{-1} (R^2 > 0.98) and 1.3382 min^{-1}, respectively. Best-fit result was obtained from the integrated first-order rate law at the semi-natural logarithm plot between Nd(III) concentration and time.

(a)

(b)
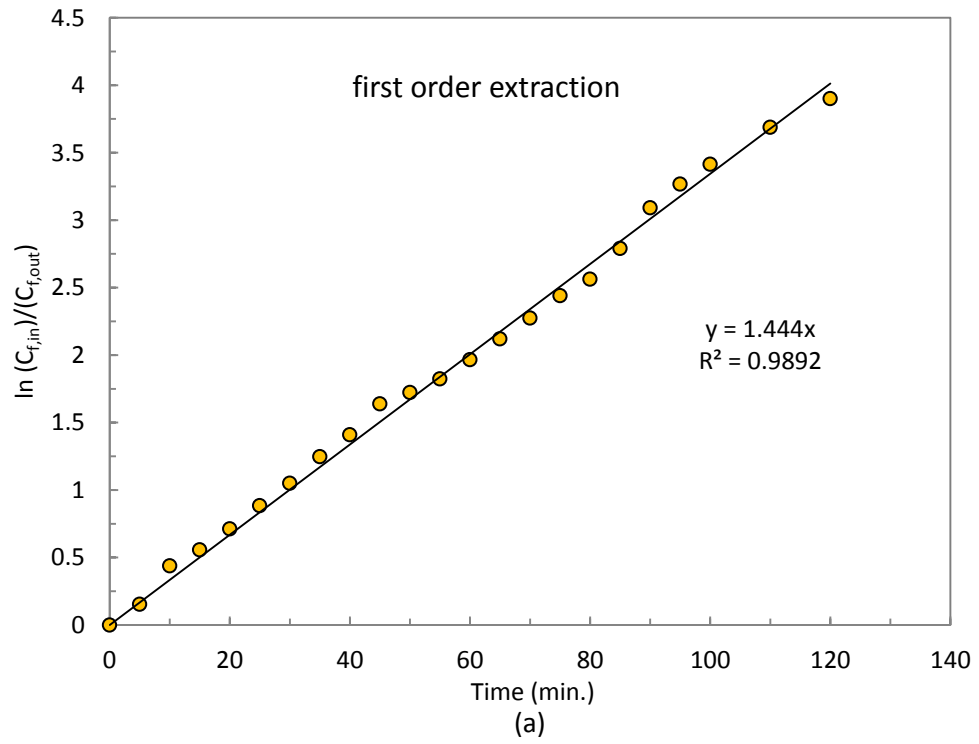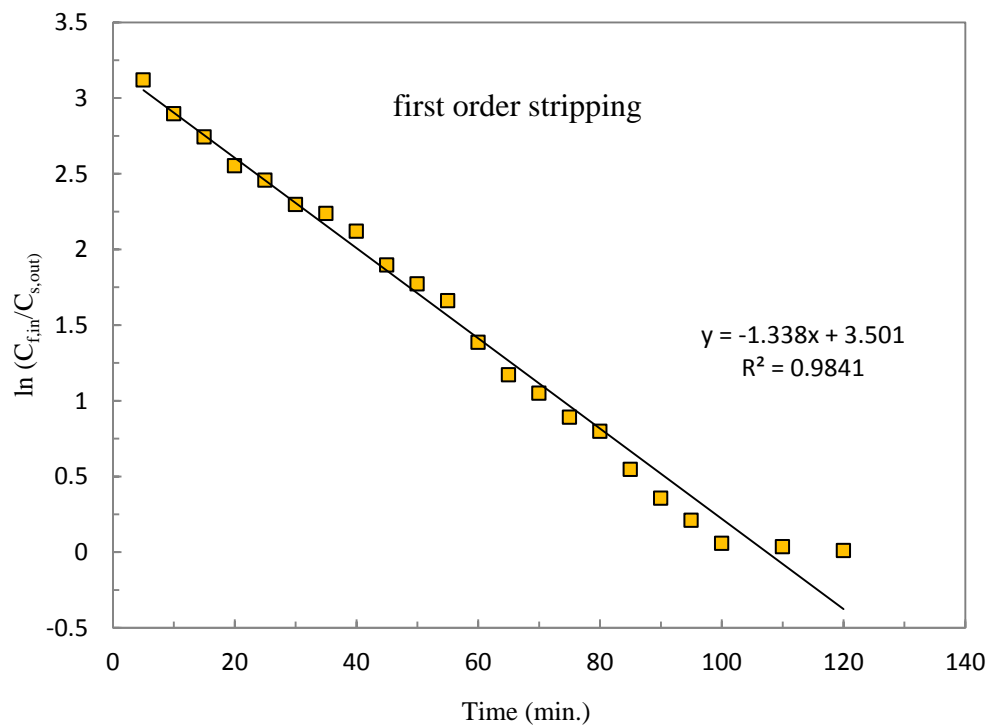
Figure 3.11 Integral concentrations of Nd(III) reaction (a) extraction and (b) stripping.

3.5.9   Model for extraction and stripping of Nd(III)

In Fig. 3.12 the concentration of Nd(III), at any time, from both feed and stripping solutions as calculated in Eqs. (3.15), (3.16) and (3.17) shows the comparison of concentration of Nd(III) in feed solutions obtained from experimental results and from the models. The model of Chaturabul et al. [43] was developed based on chemical reactions (neglecting diffusion); results of extraction and stripping were in

good agreement with the experimental data at an average standard deviation of 1.95% and 2.18%, respectively. Kandwal et al. [44] developed a facilitated diffusional transport mechanism (neglecting chemical reactions); average standard deviations for extraction and stripping were 9.81% and 8.54% respectively. These results indicated that the transport of complex species in the liquid membrane phase was influenced by the chemical reaction.
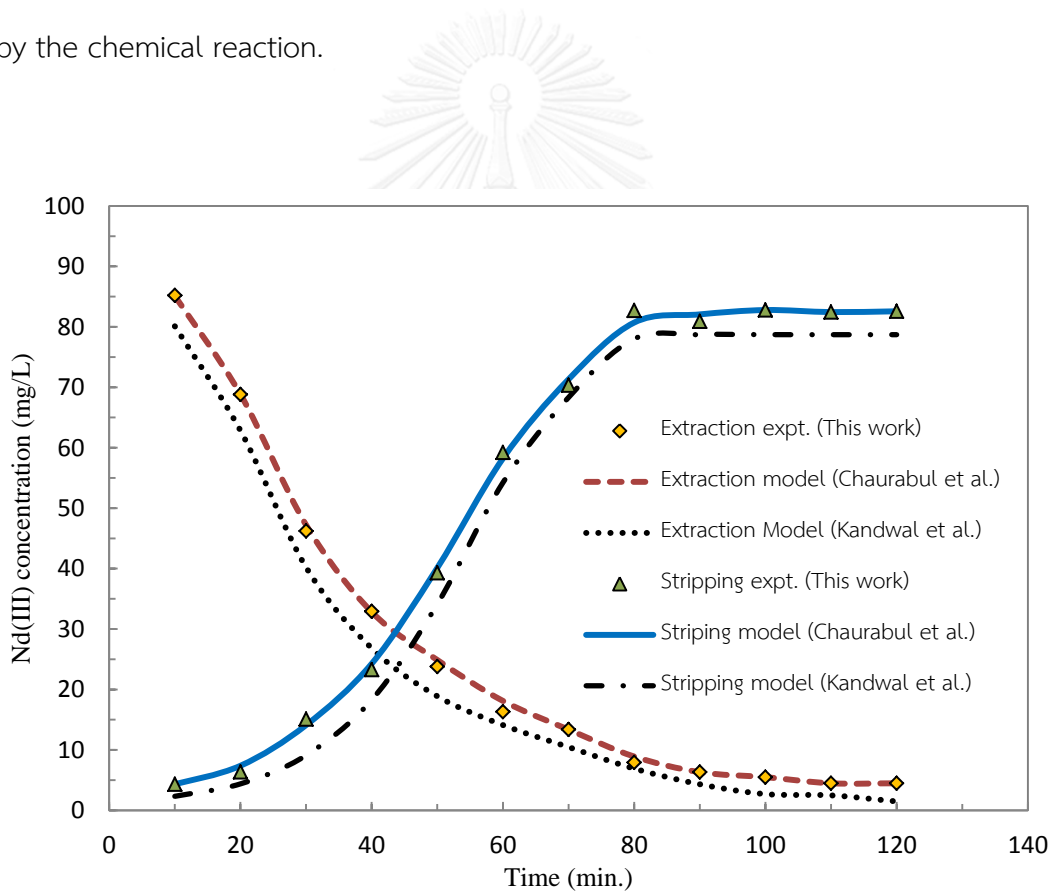
Figure 3.12 The model computation results against experimental data.

3.6   Conclusion

It was observed that HFSLM, hollow fiber supported liquid membrane, can be used to separate Nd(III) from Y(III) and Gd(III). The percentages of extraction and stripping were found to be 87% and 83%, following the fourth cycle. When a neutral donor was added to D2EHPA, the percentages of extraction and stripping increased considerably. Extraction of Nd(III) followed the sequence TOPO>TBPO>TPPO>TBP. The percentages of extraction and stripping of the synergistic reaction were found to be 94.5% and 85.1%, respectively. Optimum conditions for the synergistic reaction were found at pH 4.5 in the feed (nitrate solution), 0.5 M D2EHPA and 0.5 M TOPO in the liquid membrane, 1 M H_2SO_4 in the stripping solution and an operating flow rate of 100 mL/min. The system appeared to obey a pseudo-first-order rate equation in which both extraction and stripping depended on the concentration of only one reaction. The extraction and stripping reaction rate constant of the synergistic reaction for Nd(III) were found to be 1.4448 and 1.3382 min^{-1}.

Consequently, the reaction flux model, based on the chemical reaction, for predicting the concentration of Nd(III) proved to be in good agreement with the experimental data. Average standard deviations were 1.95% and 2.18% for

predictions in feed and stripping solution. This indicated that the extraction and stripping reactions at the liquid membrane interfaces were important factors that governed the rate of Nd(III) transport across the liquid membrane phase.

3.7   Acknowledgements

3.8   References

[1]   T.P. Rao, V.M. Biju, Crit. Rev. Anal. Chem. 30 (2000) 179-220.

[2]   J-L. Sabot, P. Maestro, Lanthanides, in Encyclopedia of Chemical Technology, pp. 1091, Wiley Interscience Publication, New York, 1996.

[3]   P. Maestro, D. Huguenin, J. Alloy. Comp. 225 (1995) 520-528.

[4]   D. Fontana, L. Pietrelli, J. Rare Earth. 27 (2009) 830-833.

[5]   N.E. El-Hefny, Chemical Engineering and Processing: Process Intensification, 46 (2007) 623-629.

[6]   A.A. Ahmed, N. Susumu, K. Fumio, T. Katsuroku, Sep. Puri. Technol. 26 (2002) 265-272.

[7]   Y. Xiong, X. Wang, D. Li, Sep. Sci. Technol. 40 (2005) 2325-2336.

[8]   L. Pei, L. Wang, G. Yu, J. Rare Earth. 30 (2012) 63-68.

[9]   P.V. Vernekar, A.W. Patwardhan, A.V. Patwardhan, S.A. Ansari, P.K. Mohapatra, V.K. Manchanda, Sep. Sci. Technol.. 48 (2012) 1003-1014.

[10] M.-S. Lee, J.-Y. Lee, J.-S. Kim, G.-S. Lee, Sep. Puri. Technol. 46 (2005) 72-78.

[11] Y.A. El-Nadi, Hydrometallurgy, 119-120 (2012) 23-29.

[12] A.M. El-Kot, J. Radioanal. Nucl. Chem. 170 (1993) 207-214.

[13] D.F. Koch, A Rare earth Extraction and Separation, Mater. Australasia, (1987).

[14] M.H.I. Baird, Science and Practice of Liquid-Liquid Extraction, Oxford, Claredon Press (1992).

[15] S.A. Sayed, K.A. Rabie, I.E. Salama, Sep. Puri. Technol. 46 (2005) 145-154.

[16] C.A. Morais, V.S.T. Ciminelli, Hydrometallurgy, 60 (2001) 247-253.

[17] L. Jelinek, Y. Wei, T. Arai, M. Kumagai, J. Alloy. Comp. 451 (2008) 341-343.

[18] X.-J. Yang, A.G. Fane, Sep. Sci. Technol. 34 (1999) 1873-1890.

[19] I.M. Coelhoso, M.M. Cardoso, R.M.C. Viegas, J.P.S.G. Crespo, Sep. Puri. Technol. 19 (2000) 183-197.

[20] A.W. Lothongkum, U. Pancharoen, T. Prapasawat, Roles of facilitated transport through HFSLM in engineering applications, Mass Transfer in Chemical Engineering Process, in: J. Markos, InTech, 2011, pp. 177-204 .

[21] U. Pancharoen, W. Poonkum, A.W. Lothongkum, J. Alloy. Comp. 482 (2009) 328-334.

[22] P. Ramakul, T. Supajaroon, T. Prapasawat, U. Pancharoen, A.W. Lothongkum, J. Ind. Eng. Chem. 15 (2009) 224-228.

[23] A.W. Lothongkum, P. Ramakul, W. Sasomsub, S. Laoharochanapan, U. Pancharoen, J. Taiwan Inst. Chem. Eng. 40 (2009) 518-523.

[24] T. Wongsawa, N. Leepipatpiboon, N. Thamphiphit, U. Pancharoen, A.W. Lothongkum, Chem. Eng. J. 222 (2013) 361-373.

[25] J.M. Joshi, P.N. Pathak, A.K. Pandey, V.K. Manchanda, Hydrometallurgy, 96 (2009) 117-122.

[26] A. Bhattacharyya, P.K. Mohapatra, V.K. Manchanda, Sep. Puri. Technol. 50 (2006) 278-281.

[27] S.A. Ansari, D.R. Prabhu, R.B. Gujar, A.S. Kanekar, B. Rajeswari, M.J. Kulkarni, M.S. Murali, Y. Babu, V. Natarajan, S. Rajeswari, A. Suresh, R. Manivannan, M.P. Antony, T.G. Srinivasan, V.K. Manchanda, Sep. Puri. Technol. 66 (2009) 118-124.

[28] M. Atanassova, Proc. Estonian Acad. Sci. Chem. 55 (2006) 202-211.

[29] M. Atanassova, V.M. Jordanov, I.L. Dukov, Hydrometallurgy, 63 (2002) 41-47.

[30] P. Ramakul, U. Pancharoen, Korean J. Chem. Eng. 20 (2003) 724-730.

[31] O.A. Desouky, A.M. Daher, Y.K. Abdel-Monem, A.A. Galhoum, Hydrometallurgy, 96 (2009) 313-317.

[32] A.G. Gaikwad, A.M. Rajput, J. Rare Earth. 28 (2010) 1-6.

[33] Y.A. El-Nadi, J. Rare Earth. 28 (2010) 215-220.

[34] L. Pei, L. Wang, G. Yu, J. Rare Earth. 29 (2011) 7-14.

[35] Y. Wang, W. Liao, D. Li, Sep. Puri. Technol. 82 (2011) 197-201.

[36] X. Wang, M. Du, H. Liu, Sep. Puri. Technol. 93 (2012) 48-51.

[37] B. GajdaJ, M.B. Bogacki, Physicochem. Probl. MI.41 (2007) 145-152.

[38] Y.A. El-Nadi, N.E. El-Hefny, J.A. Daoud, Solvent Extraction and Ion Exchange, 25 (2007) 225-240.

[39] M. Anitha, D.N. Ambare, M.K. Kotekar, D.K. Singh, H. Singh, Separ. Sci. Tech. 48 (2013) 2196-2203.

[40] F. Luo, D. Li, P. Wei, Hydrometallurgy, 73 (2004) 31-40.

[41] V. Jedinakova, P. Vanura, J. Zilkova, V. Bilek, F. Touati, J. Radioanal. Nucl. Chem. 162 (1992) 267-276.

[42] W.J. Koros, Y.H. Ma, T. Shimidzu, Terminology for membranes and membrane propcesses (1996).

[43] S. Chaturabul, K. Wongkaew, U. Pancharoen, Sep. Sci. Technol. 48 (2012) 93-104.

[44] P. Kandwal, S. Dixit, S. Mukhopadhyay, P.K. Mohapatra, Chem. Eng. J. 174 (2011) 110-116.

[45] S. Banerjee, S. Basu, J. Radioanal. Nucl. Chem. 262 (2005) 733-737.

[46] R.A. Kumbasar, O. Tutkun, Hydrometallurgy, 75 (2004) 111-121.

[47] B. Guezzen, M.A. Didi, Int. J. Chem. 4 (2012) 32-41.

[48] K. Chakrabarty, K.V. Krishna, P. Saha, A.K. Ghoshal, J. Membr. Sci. 330 (2009) 135-144.

[49] E. Keshavarz Alamdari, D. Moradkhani, D. Darvishi, M. Askari, D. Behnian, Miner. Eng. 17 (2004) 89-92.

[50] S. Suren, T. Wongsawa, U. Pancharoen, T. Prapasawat, A.W. Lothongkum, Chem. Eng. J. 191 (2012) 503-511.

[51] M. Li, Z. He, L. Zhou, Hydrometallurgy, 106 (2011) 170-174.

[52] Q. Yang, N.M. Kocherginsky, J. Membr. Sci. 286 (2006) 301-309.

CHAPTER 4

Mass transfer and selective separation of neodymium ions via a hollow fiber supported liquid membrane using PC88A as extractant

Thanaporn Wannachod[a], Natchanun Leepipatpiboon[b], Ura Pancharoen[a,*], Suphot Phatanasri[a,* *]

[a] *Department of Chemical Engineering, Faculty of Engineering, Chulalongkorn University, Patumwan, Bangkok 10330, Thailand*

[b] *Chromatography and Separation Research Unit, Department of Chemistry, Faculty of Science, Chulalongkorn University, Patumwan, Bangkok 10330, Thailand*

4.1 Abstract

The mass transfer of Nd(III) via hollow fiber supported liquid membrane was studied. At pH 4.5 using 0.5 M 2-ethylhexyl phosphonic acid mono-2-ethylhexyl ester as the extractant and 1 M H_2SO_4 as the stripping solution, optimum extraction and stripping reached 98% and 95%. Mass transfer resistance due to chemical reaction proved to be of the highest value i.e.$1/K_e = 5.871 \times 10^2$ s/cm. This indicated that the mass transfer resistance from the extraction was the most important. Further, the mass transfer model fitted in well with the experimental data. Average deviation in the feed side was below 5%.

Keywords: Mass transfer; Neodymium; Selectivity; Hollow fiber; Liquid membrane

4.2 Introduction

Rare earth metals, alone or in the form of mischmetal, are of increasing economic importance. The performance of alloys can be greatly improved by the addition of an appropriate amount of rare earth metals or their compounds [1]. For example, when an amount of rare earth elements is added to steel, the plasticity, heat resistance, toughness, oxidation resistance, abrasive resistance and corrosion

resistance of the steel can be increased. Rare earths can be used to make pyrophoric alloys, permanent magnetic materials, dyeing materials, superconducting materials, luminescent materials, trace element fertilizers, and so on. Rare earth metals have not only been widely used in the petrochemical industry and in metallurgy, glass ceramics, fluorescent materials, electronic materials, medicine and agriculture, but also have gradually penetrated into many other areas of modern science and technology. With the ever more extensive application of rare earth elements, their separation and enrichment has become increasingly important [2]. Due to their similar chemical nature owing to the common oxidation state of (III), rare earth metals are very difficult to separate from each other [3].

In recent years, the separation of ions at a very low concentration has been the focus of liquid membrane techniques. The use of a membrane in combination with a chemical or biological treatment process is attractive for wastewater treatment [4]. In particular, hollow fiber supported liquid membrane (HFSLM) is an excellent system for the extraction of metal ions at very low concentration from various solutions. This method allows for both simultaneous extraction and stripping of target ions in one single-step operation [5]. The many advantages of HFSLM over traditional methods include lower energy consumption, lower capital and operating

costs, and less solvent used. It also offers a higher mass transfer rate per unit surface area [6].

The application of HFSLM was considered for this study following the previous success of radioactive, alkali metal and lanthanide metal separation by various research groups [7-10]. For example, Wannachod et al. reported on the separation of Pr(III) from mixed rare earth metals via HFSLM using Cyanex 272 as the extractant [8]. Kandwal et al. separated Cs(I) ions from nitrate media across a HFSLM. Calix-[4]-bis(2,3-naphtho)-crown-6 was used as the extractant and distilled water as the stripping solution [9]. Serajet et al. applied the HFSLM technique to separate actinides and lanthanides from high-level waste using N,N,N',N'-tetraoctyl diglycolamide (TODGA) as the carrier [10]. Acidic organo-phosphorus extractants, such as di-(2-ethylhexyl) phosphoric acid (D2EHPA) and 2-ethylhexyl phosphonic acid mono-2-ethylhexyl ester (PC88A), are widely used for this purpose [11, 12].

Compared with D2EHPA, PC88A is preferred for separating rare earth elements due to its high separation factor [13]. Previous successful separations of rare earths are summarized in Table 4.1. In this work, the separation of neodymium ions from rare earth metals is studied alongside the investigation of the related mass transfer.

Table 4.1 Summary of previous research on rare earth metals separation

Authors	Metals	Extractants	Diluents	Stripping	Methods	% Ex	Ref.
Liang et al.	Nd	D2EHPA	Kerosene	HNO_3	LM	93	[2]
Saleh et al.	La(III)	Cyanex 272	Toluene	HNO_3	L-L	N/A	[14]
Lee et al.	Nd	PC88A	Kerosene	HCl	L-L	N/A	[15]
Wu et al.	Nd	8-hydroxyquinoline	Heptane	H_2SO_4	L-L	N/A	[16]
Fontana et al.	Sm, Eu, Gd, Tb	HEHEPA	Kerosene	HCl	L-L	N/A	[17]
Wang et al.	Y	CA12, Cyanex 272	Kerosene	HCl	L-L	92.9	[18]
Desouky et al.	Y	Primene-JMT	Kerosene	HNO_3	L-L	N/A	[19]
El-Nadi et al.	Pr, Sm	Cyanex 923	Chloroform	H_2SO_4	L-L	98/98	[20]
Liang et al.	Eu	D2EHPA	Kerosene	HCl	LM	94.2	[21]
Gaikwad et al.	Y	PC88A	Toluene	HCl	FSLM	N/A	[22]
This study	Nd(III)	PC88A	Octane	H_2SO_4	HFSLM	91.5	

Note: L-L = liquid–liquid extraction; LM = liquid membrane; FSLM = flat sheet supported liquid membrane; HFSLM = hollow fiber supported liquid membrane.

4.3 Theory

4.3.1 Transport of Nd(III) across the liquid membrane phase

The organic extractant dissolved in solvent solution is trapped in the hydrophobic micro-pores of hollow fibers as the liquid membrane. The feed solution, containing neodymium ions, and the stripping solution are generally fed counter-currently into the tube and shell sides of the hollow fiber module, respectively. The transport of neodymium ions across the liquid membrane phase is presented in Fig. 4.1. Extraction at the feed–liquid membrane interface takes place when the organic

extractant (PC88A; $(HA)_2$) reacts with the neodymium ions in the feed phase to form

the complex species $(\overline{NdA_3(HA)_3})$ and hydrogen ions, as shown in Eq. (4.1) [17]:

$$Nd^{3+} + 3\overline{(HA)_2} \xrightleftharpoons{k_{Ex}} \overline{NdA_3(HA)_3} + 3H^+ \qquad (4.1)$$
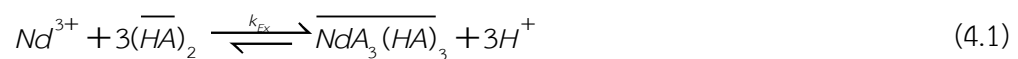
The overbar denotes the species in the liquid membrane phase.

Subsequently, the complex species diffuses across the liquid membrane phase

to the liquid membrane–stripping interface due to the concentration gradient

between the two interfaces. Then, the stripping reaction occurs, as in Eq. (4.2). Thus,

neodymium ions are released into the stripping phase. Finally, the neodymium ions

and hydrogen ions are counter-transported across the liquid membrane phase.

$$\overline{NdA_3(HA)_3} + 3H^+ \xrightleftharpoons{k_{St}} Nd^{3+} + 3\overline{(HA)_2} \qquad (4.2)$$
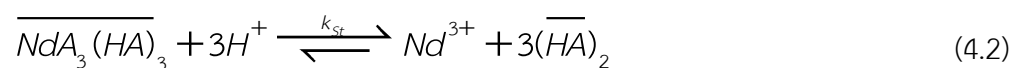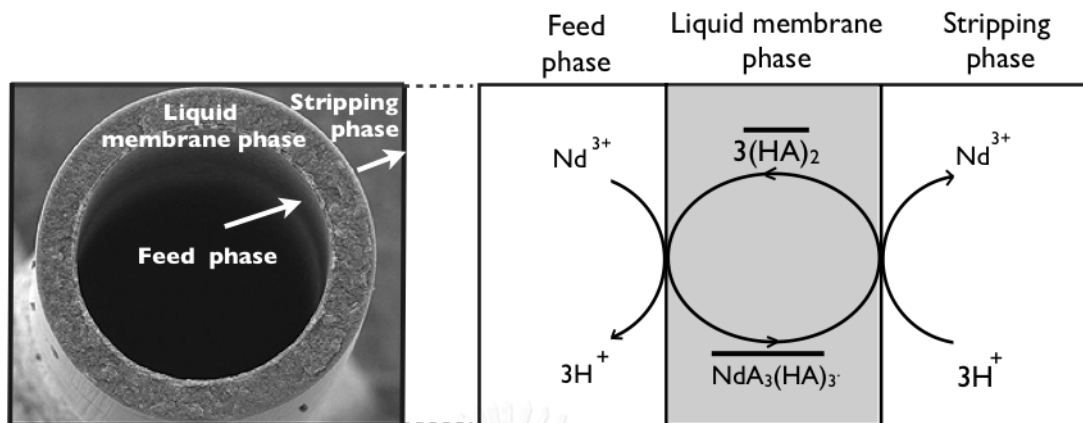
Figure 4.1 Transport of Nd(III) across the HFSLM.

In this research, the extractability of Nd(III) was determined by the percentage of extraction as follows in Eqs. (4.3) and (4.4):

$$Extraction \ (\%) = \frac{[C]_{f,in} - [C]_{f,out}}{[C]_{f,in}} \times 100 \qquad (4.3)$$

$$Stripping \ (\%) \ = \frac{[C]_{s,out} - [C]_{s,in}}{[C]_{f,in}} \times 100 \qquad (4.4)$$

where $[C]_{f,in}$, $[C]_{s,in}$ denote the initial concentrations in the feed and stripping phases, and $[C]_{f,out}$, $[C]_{s,out}$ denote the outlet concentrations in the feed and stripping phases.

4.3.2 Partition coefficient

The partition coefficient of neodymium between the liquid membrane phase and the feed phase can be calculated as in Eq. (4.5):

$$p_f = \frac{[NdA_3(HA)_3]_o}{[Nd^{3+}]_f} \tag{4.5}$$

where $[NdA_3(HA)_3]_o$ is calculated as in Eq. (4.6) which describes the partition equilibrium between the feed solution and liquid membrane solution:

$$[NdA_3(HA)_3]_o = \frac{V_a}{V_o}([Nd^{3+}_{initial}] - [Nd^{3+}]_f) \tag{4.6}$$

4.4 Mass transfer coefficient of complex species across LM phase

Neodymium transport from the feed to the organic membrane phase is given as in Eq. (4.7) [23]:

$$d\frac{[Nd^{3+}]_f}{dt} = -\frac{A}{V_a}J \qquad (4.7)$$

The flux through the supported liquid membrane can be described as in Eq. (4.8):

$$J = K[Nd^{3+}]_f \qquad (4.8)$$

Therefore, the overall mass transfer coefficient of neodymium ions can be determined by the permeability coefficient of Nd(III) in the feed phase, as described by Danesi [24] as in Eq. (4.9):

$$\ln\frac{[Nd^{3+}]_f}{Nd^{3+}_{initial}} = -\frac{KA}{V_a}t \qquad (4.9)$$

where V_a is the volume of the feed solution (cm^3) and A is the effective surface (cm^2).

Eq. (4.9) can be utilized to evaluate the overall mass transfer coefficient from the experimental data. The mass transfer coefficient of complex species across the liquid membrane phase is determined based on the overall mass transfer coefficient (K) of neodymium ion transport in a radial direction from the feed phase to the stripping phase. The overall mass transfer coefficient of neodymium ions represents the mass transfer resistance in the feed phase, the interfacial resistance of the extraction, the liquid membrane phase, the shell-side resistance, the resistance of the stripping reaction, and the strip-side resistance. The reciprocal of the overall mass transfer coefficient [25] can be expressed as:

$$\frac{1}{K} = \frac{1}{K_a} + \frac{1}{K_e} + \frac{1}{p_f K_m} + \frac{1}{p_f K_o} + \frac{1}{p_f K_s} + \frac{1}{(p_f / K_s)K_{as}} \qquad (4.10)$$

where K_a is the mass transfer coefficient in the feed phase, while K_e and K_s are the mass transfer coefficients of reaction for neodymium ions in the feed and stripping phases, respectively. K_m is the mass transfer coefficient of complex species in the liquid membrane phase; K_o is the mass transfer coefficient in the shell side between the hollow fibers; and K_{as} is the mass transfer coefficient for the aqueous stripping solution. The mass transfer resistance of Nd(III) in the stripping phase in Eq. (4.10) can be neglected since the process is instantaneous [25]. Thus:

$$\frac{1}{K} = \frac{1}{K_a} + \frac{1}{K_e} + \frac{1}{p_f K_m} + \frac{1}{p_f K_o} \tag{4.11}$$

The mass transfer coefficient of neodymium in the aqueous phase can be calculated using the Lévêque equation, based on the Sherwood (Sh) and Schmidt correlations (Sc) [26]:

$$Sh = 1.62 \left(\frac{d_i}{L} \text{Re} \, Sc \right)^{0.33} \tag{4.12}$$

where

$$\text{Re} = \frac{4Q_f}{\mu \pi d_i}$$

$$Sh = \frac{K_f d_i}{D_f}$$

$$Sc = \frac{\upsilon}{D_f}$$

The experimental *Re* value was 29.51, as calculated by the procedure as in [27], which was far below 2700, indicating that the flow inside the hollow fibers was laminar. Accordingly, the mass transfer coefficient in the aqueous phase [28] is given by:

$$K_a = 1.62 \frac{D_f}{d_i} \left(\frac{d_i^2 \upsilon_f}{L D_f} \right)^{0.33} \tag{4.13}$$

The mass transfer coefficient in the membrane phase can be calculated accordingly:

$$K_m = \frac{D_m \varepsilon d_{lm}}{\delta \eta d_o} \tag{4.14}$$

The mass transfer coefficient on the shell sides of two hollow fibers can be estimated based on the Sherwood and Schmidt correlations [29] as in Eq. (4.15):

$$K_o = 1.25 \frac{D_m}{d_h^{0.07}} \left(\frac{d_h \upsilon_s}{\upsilon L} \right)^{0.93} \left(\frac{\upsilon}{D_m} \right)^{0.33} \tag{4.15}$$

where

$$Sh = \frac{K_o d_h}{D_m} = 0.56 Re^{0.62} Sc^{0.33}$$

$$Re = \frac{d_h \upsilon_s}{\upsilon}$$

$$Sc = \frac{\upsilon}{D_m}$$

The hydraulic diameter of the intermediate region between the shell sides of two hollow fibers is calculated [29] as in Eq. (4.16):

$$d_h = \frac{d_a^2 - d_i^2 - nd_0^2}{nd_0} \tag{4.16}$$

4.5   Experimental

4.5.1   Materials

Nitrate solution from monazite processing was used as the feed solution. The source of mixed rare earths for study (supplied in nitrate solution) was the digestion product of monazite ore processing, courtesy of the Rare Earth Research and Development Centre, Office of Atoms for Peace, Bangkok, Thailand. Properties of the feed solutions are shown in Table 4.2. The liquid membrane was composed of 2-ethylhexyl phosphonic acid mono-2-ethylhexyl ester (PC88A) and a diluent. Sulfuric acid was used as the stripping solution. All chemicals were of GR grade and obtained from Merck, Germany.

Table 4.2 Properties of feed solutions (nitrate solution from monazite processing)

Metal ions	Y	La	Ce	Pr	Nd	Sm	Eu	Gd	Dy	Yb
Concentration (mg/L)	13.6	12.8	1.8	23	106.7	1.3	0. 3	7.7	2.5	0.2

4.5.2   Apparatus

The HFSLM (Liqui-Cel$^®$ Extra-Flow membrane contactor) was manufactured by Membrane (formerly Hoechst Celanese), USA. The module uses Celgard micro-porous polypropylene fibers that are woven into a fabric. The properties of the hollow fiber module are shown in Table 4.3. The concentrations of metal ions in the feed and stripping solutions were analyzed by inductively coupled plasma spectrometry (ICP).

Table 4.3 Properties of the hollow fiber module

Properties	Description
Material	Polypropylene
Inside diameter of hollow fiber	0.024 cm
Outside diameter of hollow fiber	0.03 cm
Effective length of hollow fiber	15 cm
Number of hollow fibers	35,000
Average pore size	3×10^{-6} cm
Porosity	30%
Effective surface area	1.4×10^{4} cm^2
Area per unit volume	29.3 cm^2/cm^3
Module diameter	6.3 cm
Module length	20.3 cm
Contract area	30%
Tortuosity factor	2.6
Operating temperature	273–333 K

4.5.3   Procedure

A single-module HFSLM operation is shown in Fig. 4.2. The extractant was first dissolved in octane (500 mL). Then the extractant was simultaneously pumped into the tube and shell sides of the hollow fiber module for 40 min. to ensure that the extractant was entirely embedded in the micro-pores of the hollow fibers. Subsequently, 5 L of both feed solution and stripping solution were fed counter-currently into the tube and shell sides, respectively, of the single-module operation. Nd(III) from the nitrate solution moved across the liquid membrane to the stripping phase and was collected in the stripping reservoir. The concentrations of metal ions in samples from the feed and stripping solutions were analyzed by ICP to determine the percentages of extraction and stripping.
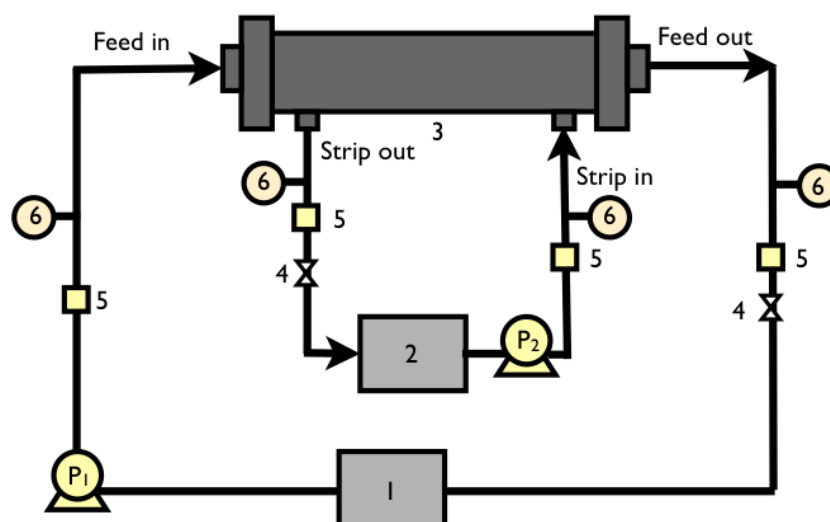
Figure 4.2 Schema representation of the counter-current flow diagram for continuous HFSLM operation: (1) feed reservoir (2) stripping reservoir (3) HFSLM (4) flow regulator valve (5) flow indicator and (6) pressure indicator.

4.6 Results and discussion

4.6.1 Influence of pH of feed solution

The pH is an important factor for consideration in separating Nd(III) from mixed rare earths. PC88A exhibits good performance in the extraction of metal cations from an acidic solution. The influence of feed solution pH was studied by varying the pH in a range of 2.0–5.0. As shown in Fig. 4.3, percentages of extraction and stripping steadily increased, reaching a maximum at pH 4.5 and the highest Nd(III) extraction and stripping of about 91.5% and 88.1%, respectively were obtained. However, at feed solution pH of 5.0, percentages of extraction and stripping declined slightly due to the equilibrium reaction at the feed–liquid membrane interface [30]. Thus, a feed solution pH of 4.5 was chosen to study further variables.

(a)

(b)
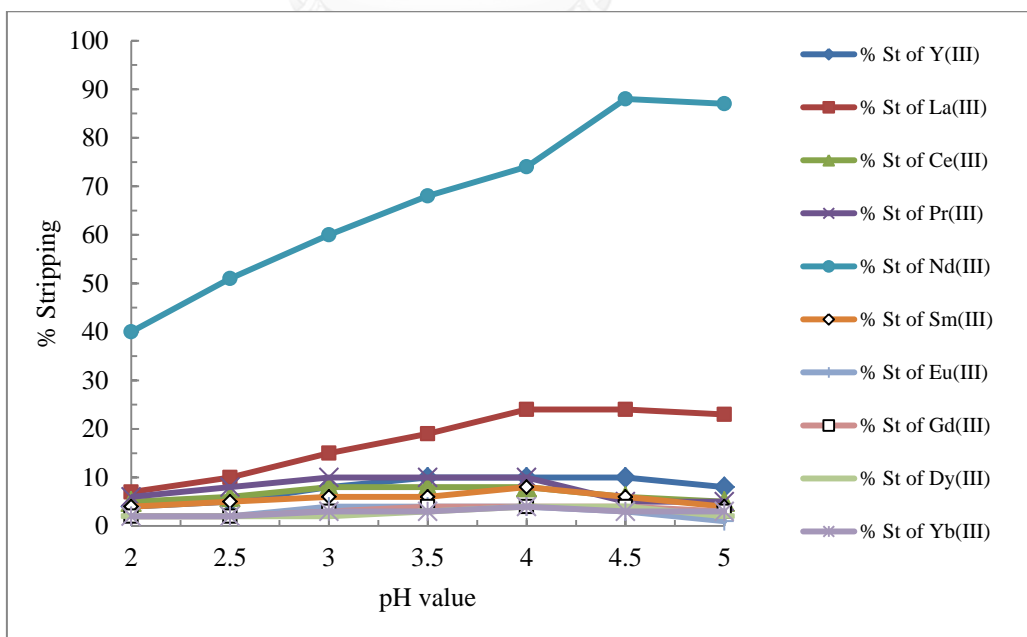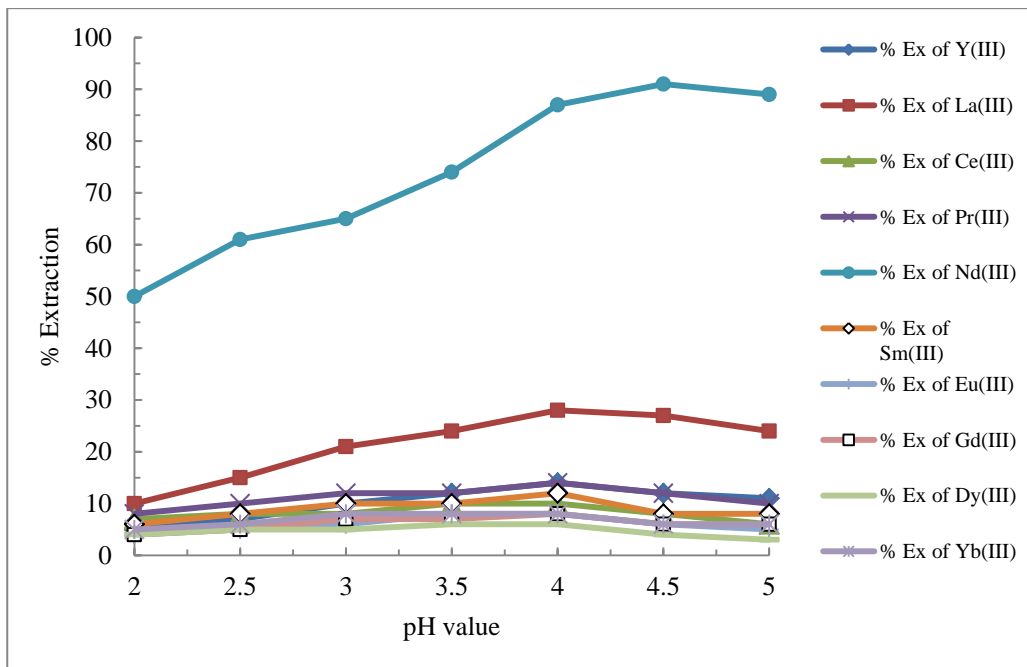
Figure 4.3 Influence of pH of feed solution on: (a) extraction and (b) stripping. (Extractant = 0.5 M PC88A; stripping = 1 M H_2SO_4; flow rate = 100 mL/min for both feed and stripping solutions.)

4.6.2   Influence of extractant concentration

The influence of the concentration of PC88A is demonstrated in Fig. 4.4. Generally, reaction rate increases as the concentration of the extractant increases. Fig. 4.4 shows that percentages of extraction increased when the concentration of the extractant increased up to 0.5 M. However, extraction of Nd(III) decreased when the concentration was higher than 0.5 M. This was due to an increase in liquid membrane viscosity that obstructed the mass transfer in the liquid membrane phase, corresponding to our previous findings [31]. Thus, optimum concentration of the extractant was found to be 0.5 M.
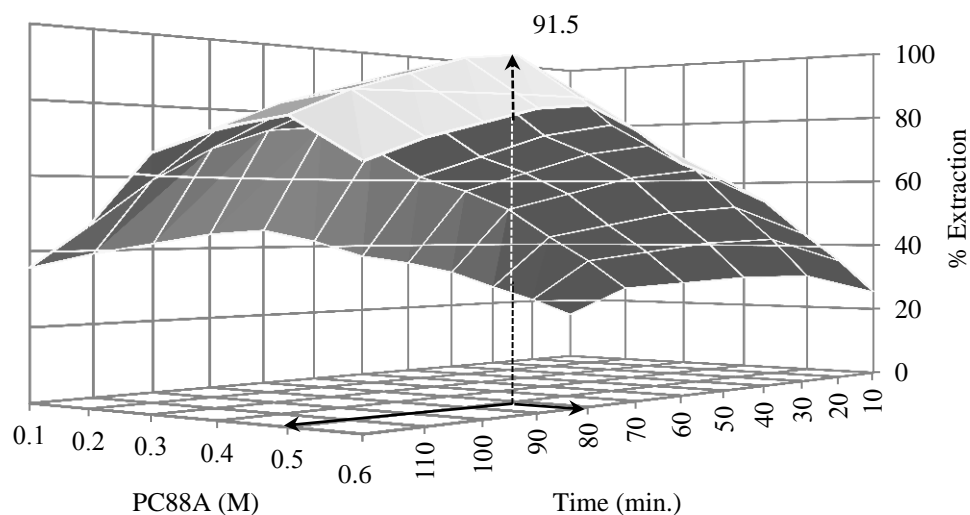
Figure 4.4 Influence of concentration of PC88A. (Feed = pH 4.5; stripping = 1 M H$_2$SO$_4$; flow rate = 100 mL/min for both feed and stripping solutions.)

4.6.3   Influence of stripping solution concentration

In regard to the concentration of stripping solution (Fig. 4.5), percentages of stripping increased up to 1 M; the percentages then remained constant at concentrations higher than 1 M (excess stripping solution). This indicated that the amount of Nd(III) in the stripping solution was limited due to the amount of complex species that reacted with the stripping solution at the liquid membrane–stripping interface. Thus, the optimum stripping solution concentration was found to be 1 M.
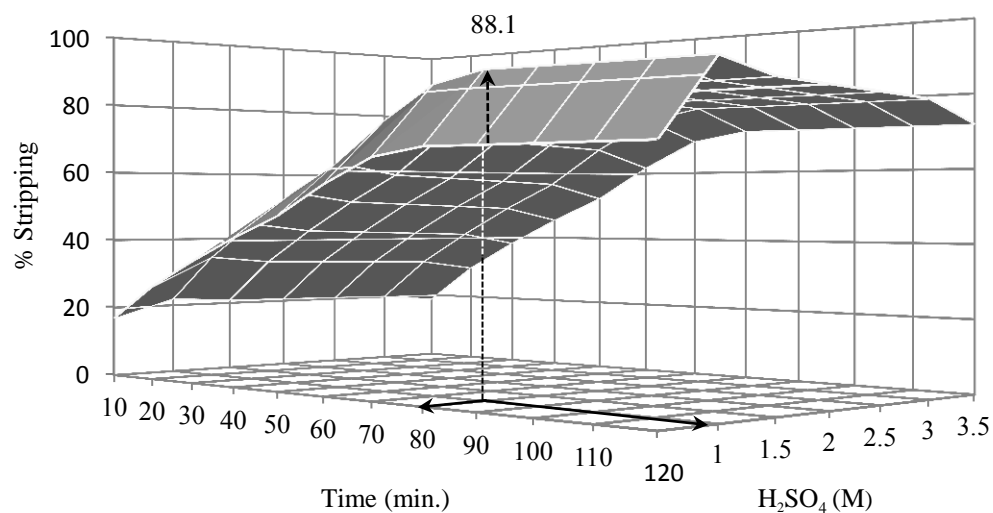
Figure 4.5 Influence of concentration of H_2SO_4. (Feed = pH 4.5; extractant = 0.5 M PC88A; flow rate = 100 mL/min for both feed and stripping solutions.)

4.6.4   Influence of flow rates of feed and stripping solutions

Equal flow rates of feed and stripping solutions were studied, as shown in Fig. 4.6. Maximum extraction and stripping of 91.5% and 88.1% respectively were obtained at 100 mL/min. However, percentages of Nd(III) extraction and stripping decreased at flow rates greater than 100 mL/min due to the resident time of the solution in the hollow fiber module. This was in agreement with an earlier report by Yang et al. [32].
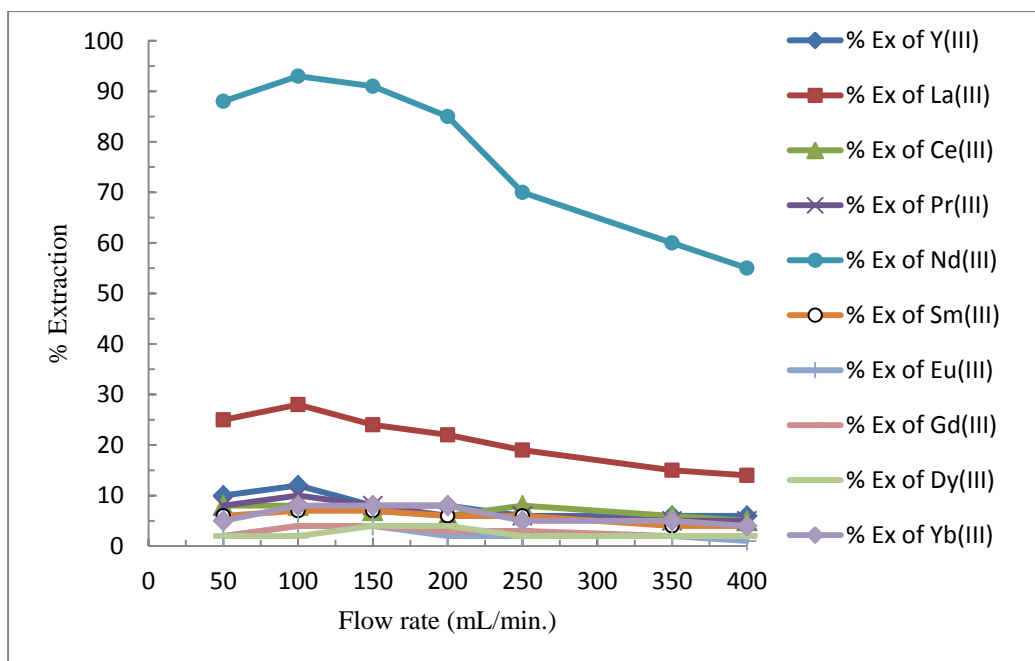
(a)
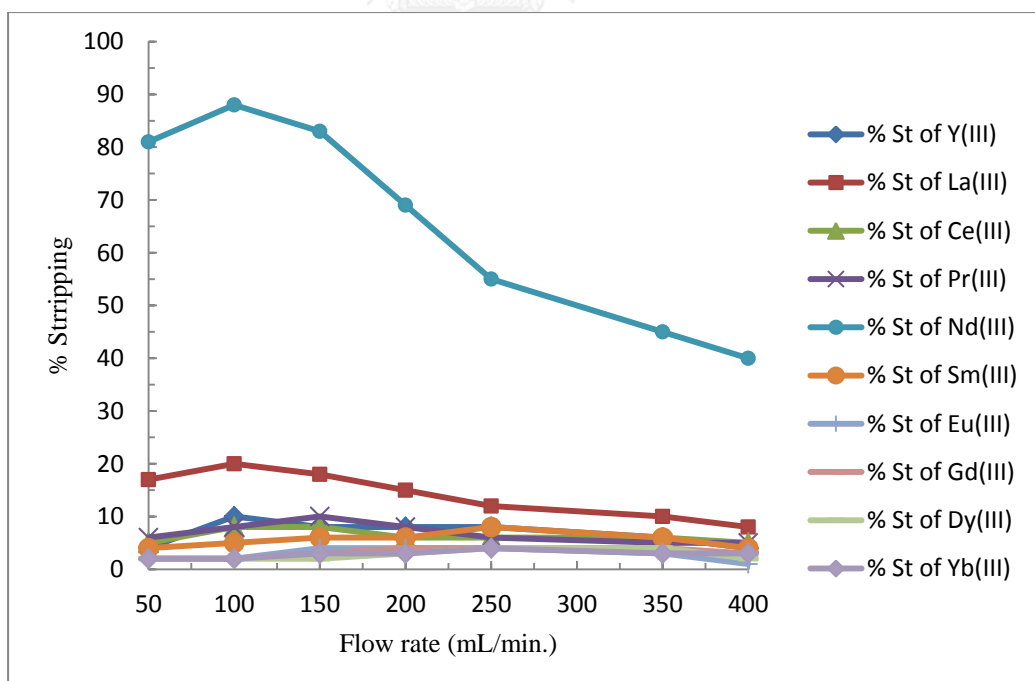
(b)

Figure 4.6 Influence of flow rate on: (a) extraction and (b) stripping. (Feed = pH 4.5; extractant = 0.5 M PC88A; stripping = 1 M H_2SO_4; flow rate = 100 mL/min for both feed and stripping solutions.)

4.6.5   Influence of operating cycle

In a once-through operation, an extraction yield of Nd(III) of 91.5% was attained while the percentage of stripping was 88.1%. To further enhance performance, the operation was carried out in repeat cycle mode. Subsequently, the cumulative Nd(III) extraction and stripping rose to 98% and 95%, respectively, following the fourth cycle, over a total of 320 min.

The selectivity of Nd(III) stripping was also observed to improve with repetition of the extraction cycle. The selectivity index was calculated from Eq. (4.17). Selectivity indices of 0.56, 0.75, 0.84 and 0.93 were obtained after the first, second, third and fourth cycles, respectively.

$$Selectivity \ index \ = \ \frac{C_{out,s}^{Nd(III)}}{\sum_{i=1}^{n} C_{out,s}^{i}}, \quad \text{for Nd(III)} \tag{4.17}$$

where $C_{out,s}^{Nd(III)}$ is the outlet stripping concentration of Nd(III) (ppm) and $C_{out,s}^{i}$ is the outlet stripping concentration of component i (ppm).

4.6.6   Mass transfer resistance

The values of mass transfer resistance were calculated employing optimum conditions. The values for the four individual transfer resistances were calculated: $1/K_m = 0.285 \times 10^2$, $1/K_a = 0.966 \times 10^2$, $1/K_o = 1.896 \times 10^2$ and $1/K_e = 5.871 \times 10^2$ s/cm. The overall mass transfer resistance was determined experimentally and was found to be $1/K = 9.018 \times 10^2$ s/cm. The mass transfer resistances from the extraction reaction, the shell side and feed side proved to be much higher than that from the membrane phase. This indicated that mass transfer in the membrane phase had little effect on the overall mass transfer process.

4.6.7   Mass transfer modelling of Nd(III) through the HFSLM

The neodymium ions (Nd^{3+}) diffuse through the layer of the feed phase toward the feed–membrane interface where they instantly react with PC88A to form a complex. The complex diffuses across the membrane phase and reaches the

membrane–stripping interface where de-complexing occurs by reacting with perchlorate. Finally, neodymium ions diffuse through the stagnant layer of the stripping phase to the stripping solution.

The diffusion process is explained by Fick's law. The mass transfer flux is presented by the following equation estimating the neodymium concentration in the feed solution [9]:

$$\ln\left(\frac{C_t}{C_0}\right) = \frac{V}{V_f}\left(e^{-\frac{2\varepsilon}{RV}\left(\frac{K_d L}{K_d \Delta aq + \Delta org}\right)} - 1\right)t \tag{4.18}$$

where

$$\Delta_{aq} = \frac{R\varepsilon d_{aq}}{(R - d_{aq})D_{aq}} \quad \text{and} \quad \Delta_{org} = \frac{d_{org}\tau}{D_{org}}$$

and

C_t =   metal concentration at any time t (mg/L)

C_0 =   metal concentration at time t = 0 (mg/L)

V	=	volumetric flow rate (mL)
V_f	=	volume of feed solution in reservoir (mL)
K_d	=	distribution coefficient of the metal ions (-)
L	=	length of fiber (cm)
R	=	inner radius of hollow fiber (cm)
Δ_{aq}	=	aqueous phase resistance (cm)
Δ_{org}	=	organic phase resistance (cm)
ε	=	porosity of hollow fiber (%)
τ	=	membrane tortuosity factor (-)
d_{aq}	=	thickness of aqueous diffusion layer (cm)
d_{org}	=	thickness of membrane diffusion layer (cm)
D_{aq}	=	aqueous diffusion coefficient (-)
D_{org}	=	membrane diffusion coefficient (-)

The mathematical model was validated by the percentage of standard deviation (% S.D.) obtained from the model and experimental results. The standard deviation [33] was obtained as follows using Eq. (4.19):

$$\% \, S.D. = 100 \times \sqrt{\frac{\sum\limits_{i=1}^{n}\left\{\left(\dfrac{D_{Exp.}}{D_{Model}}\right) - 1\right\}^{2}}{N - 1}} \qquad (4.19)$$

where $D_{Exp.}$ is the experimental data, D_{Model} is the calculated value from the mathematical model and N is the number of experimental points.

Fig. 4.7 illustrates the comparison of concentrations of neodymium ions from the experimental data and theoretical values estimated using Eq. (4.18).
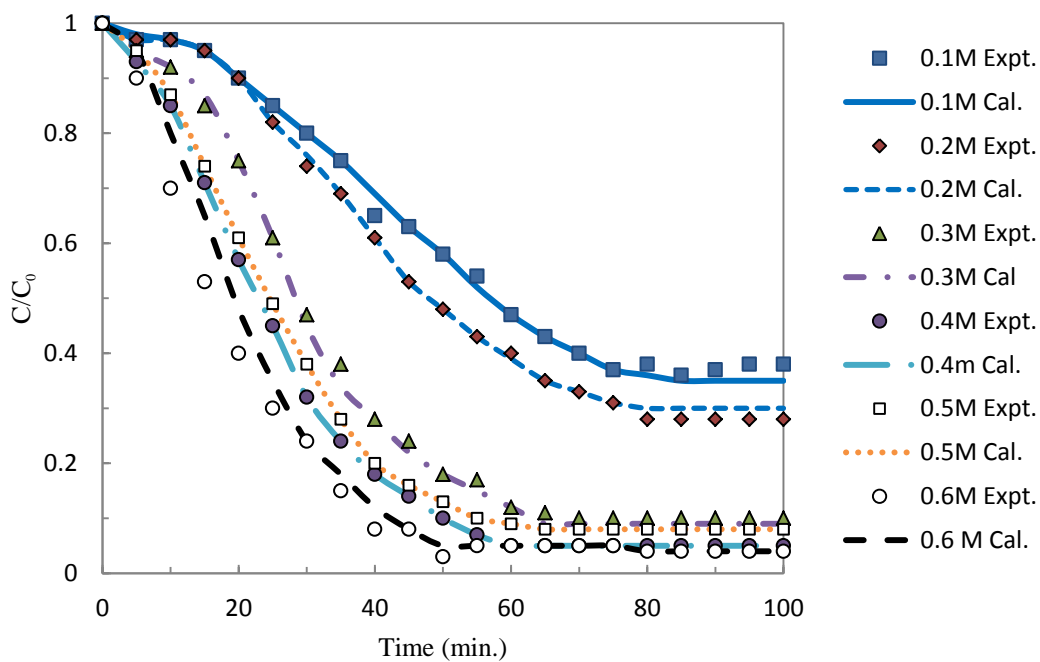
Figure 4.7 Concentration of neodymium ions in the feed solution (experimental and model calculated values) plotted as a function of time, at different concentrations of PC88A. (Feed = pH 4.5; stripping solution, 1 M H_2SO_4; flow rate = 100 mL/min for both feed and stripping solutions.)

The results indicated that when the concentration of PC88A was lower than 0.6 M, the mass transfer model proved satisfactory, as demonstrated in Fig. 4.7. However, when the concentration of PC88A was more than 0.5 M, the mass transfer model performed poorly. This discrepancy is likely due to the assumption that the initial concentration of PC88A was low. When the concentration of PC88A is higher than 0.5 M, the viscosity of the liquid membrane is very high. This results in the obstruction of mass transfer while the metal-complex accumulates in the liquid membrane. Moreover, the free PC88A molecules are difficult to transport so as to react with the neodymium ions. Therefore, a concentration of PC88A higher than 0.5 M causes the system to be out of sync. The average deviation in the feed side was below 5%.
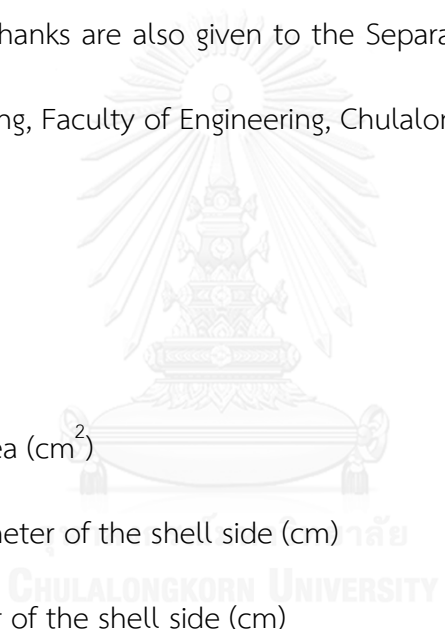
4.7 Conclusion

The mass transfer of Nd(III) via hollow fiber supported liquid membrane containing PC88A as carrier was studied. Optimum extraction and stripping of 91.5% and 88.1% respectively were obtained with a feed solution of pH 4.5, using 0.5 M PC88A in octane as the extractant and 1 M H_2SO_4 as the stripping solution. Flow rates of both feed and stripping solutions were 100 mL/min. Performance was considerably enhanced by running the operation in repeat cycle mode. After the fourth repeat cycle, cumulative extraction and stripping of Nd(III) reached 98% and 95%, respectively. Under optimal operating conditions, the membrane resistance, the aqueous solution in the feed phase resistance, the organic phase shell-side resistance, the extraction reaction resistance and the overall mass transfer resistance were as follows, $1/K_m = 0.285 \times 10^2$, $1/K_a = 0.966 \times 10^2$, $1/K_o = 1.896 \times 10^2$, $1/K_e = 5.871 \times 10^2$ and $1/K = 9.018 \times 10^2$ s/cm, respectively. The overall mass transfer resistance was governed by the resistance resulting from extraction reaction as well as the shell-side resistance. The mass transfer model fitted in well with the experimental data when the concentration of PC88A was lower than 0.6 M.
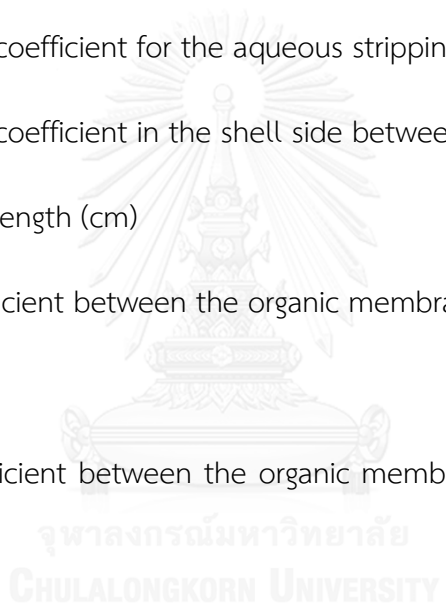
4.8   Acknowledgements

4.9   Nomenclature

A   membrane area (cm^2)

d_h hydraulic diameter of the shell side (cm)

d_i inner diameter of the shell side (cm)

d_{lm} log-mean diameter of the membrane (cm)

d_o outer diameter of the membrane (cm)

D_a diameter of the fiber tube

D_f diffusivity of Nd(III) in the aqueous feed solution (cm^2/s)

D_m diffusivity of Nd(III) extractant complex in the organic membrane phase

J   flux of Nd(III) through the supported liquid membrane phase (cm^2/s)

K   overall mass transfer coefficient (cm/s)

K_a mass transfer coefficient in the aqueous feed solution (cm/s)

K_e mass transfer coefficient due to the extraction reaction (cm/s)

K_m mass transfer coefficient of the membrane phase (cm/s)

K_s mass transfer coefficient due to the stripping reaction (cm/s)

K_{as} mass transfer coefficient for the aqueous stripping solution (cm/s)

K_o mass transfer coefficient in the shell side between hollow fibers (cm/s)

L   fiber module length (cm)

p_f partition coefficient between the organic membrane phase and the aqueous feed solution

p_s partition coefficient between the organic membrane phase and the stripping solution

Re   Reynolds number

v_f linear velocity of feed solution in the tube side (cm/s)

v_s linear velocity of stripping solution in the shell side (cm/s)

V_a volume of the aqueous feed solution (cm^3)

V_o volume of the organic membrane solution (cm^3)

Sh   Sherwood number

Sc   Schmidt number

t time (s)

ν kinematic viscosity of organic phase (cm^2/s)

4.10 References

[1] S. Benltoufa, F. Falaya, S. BenNasrallah, J. Eng. Fibers. Fabrics. 3 (2008) 47-54.

[2] L. Pei, L. Wang, G. Yu, J. Rare. Earth. 30 (2012) 63-68.

[3] M. Anitha, D.N. Ambare, M.K. Kotekar, D.K. Singh, H. Singh, Sep. Sci. Technol. 48 (2013) 2196-2203.

[4] V. Mavrov, E. Bélières, Desalination, 131 (2000) 75-86.

[5] I.M. Coelhoso, M.M. Cardoso, R.M.C. Viegas, J.P.S.G. Crespo, Sep. Puri.Technol. 19 (2000) 183-197.

[6] M.F. San Román, E. Bringas, R. Ibañez, I. Ortiz, J. Chem.Tech. Biotechnol. 85 (2010) 2-10.

[7] S. Panja, P.K. Mohapatra, S.C. Tripathi, P.M. Gandhi, P. Janardan, Journal of Hazardous Materials, 237–238 (2012) 339-346.

[8] P. Wannachod, S. Chaturabul, U. Pancharoen, A.W. Lothongkum, W. Patthaveekongka, J. Alloy. Comp. 509 (2011) 354-361.

[9]   P. Kandwal, S. Dixit, S. Mukhopadhyay, P.K. Mohapatra, Chem. Eng. J. 174 (2011) 110-116.

[10] S.A. Ansari, P.K. Mohapatra, V.K. Manchanda, Industrial & Engineering Chemistry Research, 48 (2009) 8605-8612.

[11] G.S. Lee, M. Uchikoshi, K. Mimura, M. Isshiki, Sep. Puri. Technol. 71 (2010) 186-191.

[12] S.N. Bhattacharyya, K.M. Ganguly, Hydrometallurgy, 32 (1993) 201-208.

[13] N.V. Thakur, D.V. Jayawant, N.S. Iyer, K.S. Koppiker, Hydrometallurgy, 34 (1993) 99-108.

[14] M.I. Saleh, M.F. Bari, B. Saad, Hydrometallurgy, 63 (2002) 75-84.

[15] M.-S. Lee, J.-Y. Lee, J.-S. Kim, G.-S. Lee, Sep. Puri. Technol.46 (2005) 72-78.

[16] D. Wu, Q. Zhang, B. Bao, Hydrometallurgy, 88 (2007) 210-215.

[17] D. Fontana, L. Pietrelli, J. Rare Earth. 27 (2009) 830-833.

[18] X. Wang, M. Du, H. Liu, Sep. Puri.Technol. 93 (2012) 48-51.

[19] O.A. Desouky, A.M. Daher, Y.K. Abdel-Monem, A.A. Galhoum, Hydrometallurgy, 96 (2009) 313-317.

[20] Y.A. El-Nadi, J.Rare Earth. 28 (2010) 215-220.

[21] L. Pei, L. Wang, G. Yu, J. Rare. Earth. 29 (2011) 7-14.

[22] A.G. Gaikwad, A.M. Rajput, J. Rare Earth. 28 (2010) 1-6.

[23] W.S.W. Ho, B. Wang, Industrial & Engineering Chemistry Research, 41 (2002) 381-388.

[24] P.R. Danesi, J. Memb. Sci. 20 (1984) 231-248.

[25] Y. Tang, W. Liu, J. Wan, Y. Wang, X. Yang, Process Biochemistry, 48 (2013) 1980-1991.

[26] S.R. Wickramasinghe, M.J. Semmens, E.L. Cussler, J. Memb. Sci.69 (1992) 235-250.

[27] J.L. Hoffman, Biochemistry, 25 (1986) 4444-4449.

[28] M.-C. Yang, E.L. Cussler, AIChE Journal, 32 (1986) 1910-1916.

[29] A. Baudot, J. Floury, H.E. Smorenburg, AIChE Journal, 47 (2001) 1780-1793.

[30] T. Wongsawa, N. Leepipatpiboon, N. Thamphiphit, U. Pancharoen, A.W. Lothongkum, Chem. Eng. J. 222 (2013) 361-373.

[31] S. Suren, T. Wongsawa, U. Pancharoen, T. Prapasawat, A.W. Lothongkum, Chem. Eng. J. 191 (2012) 503-511.

[32] Q. Yang, N.M. Kocherginsky, J. Membr. Sci. 286 (2006) 301-309.

[33] T. Pirom, K. Wongkaew, T. Wannachod, U. Pancharoen, N. Leepipatpiboon, J. Ind. Eng. Chem. 20 (2014) 1532–1541.

CHAPTER 5

The separation of Nd(III) from mixed rare earths via hollow fiber supported liquid membrane and mass transfer analysis

Thanaporn Wannachod[a], Vanee Mohdee[a], Sira Suren[a], Prakorn Ramakul[b], Ura Pancharoen[a,*] and Kasidit Nootong[a,**]

[a]*Department of Chemical Engineering, Faculty of Engineering, Chulalongkorn University, Patumwan, Bangkok 10330, Thailand*

[b]*Department of Chemical Engineering, Faculty of Engineering and Industrial Technology, Silpakorn University, Nakhon Pathom 73000, Thailand*

5.1 Abstract
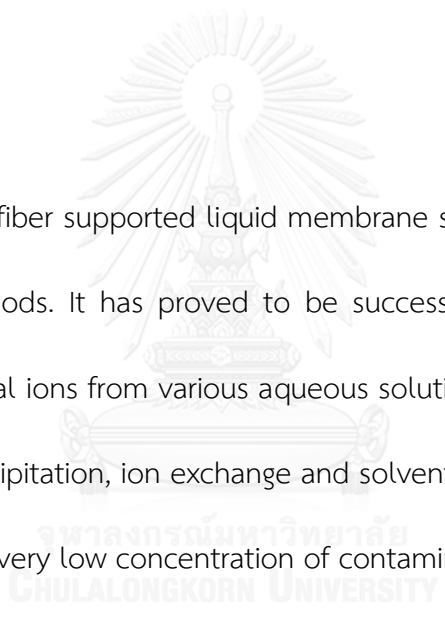
The separation of Nd(III) via hollow fiber supported liquid membrane (HFSLM) and mass transfer analysis was studied. At pH of 4.5, 0.5 M DNPPA as extractant, 3 M H_2SO_4 as stripping solution, flow rates of feed and stripping solutions of 100 mL/min and temperature of feed and stripping solutions of 313 K. optimum extraction and stripping reached 98% and 95%. The mass transfer due to chemical reaction is the mass transfer–controlling step. The experiment data fitted in well with the mass transfer model. The average deviation in the feed side was below 2%.

Keywords: Temperature, Mass transfer; Separation; Neodymium; Hollow fiber.

5.2 Introduction

Currently, high purity rare earth oxides are in great demand for the production of steel or alloys, permanent magnets, hydrogen storage materials, electro or cathode ray luminescence etc. [1-3]. Neodymium (Nd) is used in medicine and in the field of solid state lasers [4]. The purification and separation of rare earth metals are difficult because of their similar chemical and physical properties. Recently, the introduction of new extractants and extraction systems has caused renewed interest in the separation of these rare earth metals. Acidic organo-phosphorous extractants,

such as diethylhexyl phosphoric acid (D2EHPA) [5, 6], 2–ethylhexyl phosphoric acid mono–2–ethylhexyl ester (PC88A) [7-9], N,N,N'N'- tetraoctyl diglycolamide (TODGA)[10], bis(2,2,4–trimethyl pentyl) phosphonic acid (Cyanex 272) [11, 12] and dinonyl phenyl phosphoric acid (DNPPA) [13] are widely used for this purpose. Moreover, DNPPA is a more effective extractant compared to PC88A and D2EHPA [13].

HFSLM, hollow fiber supported liquid membrane system, has many advantages over traditional methods. It has proved to be successful in separating a very low concentration of metal ions from various aqueous solutions. Traditional methods, for example such as precipitation, ion exchange and solvent extraction have been found to be ineffective at a very low concentration of contaminated metal ions. The HFSLM system can extract and strip target ions in a single–step operation with high selectivity [14, 15]. It has lower energy consumption, lower capital and operating costs and less solvent is used [16]. Furthermore, HFSLM has a high surface area [17, 18]. HFSLM can be applied in many industries, such as chemical, food and pharmaceutical processing [17,19,20]. Many researchers have applied the HFSLM system to separate various target species e.g. metal ions [21-25], organic compounds [26-27] and enantiomers [28].

Temperature has an important role to play in the separation of metal ions by means of liquid membrane processes [29-33]. Few works have focused on the influence of temperature on the separation of metal ions using the HFSLM system. Therefore, this work investigates the influence of temperature on the extraction and stripping of Nd (III) via HFSLM using DNPPA as the extractant [34]. Moreover, the influence of the pH of feed solution, the concentration of the extractant DNPPA and stripping solution, the flow rates of both feed and stripping solutions and mass transfer analysis were investigated.

5.3 Theory

5.3.1   Mass transfer of neodymium (III) ions across HFSLM

Neodymium (III) ions in feed solution diffuse across the layer of the feed phase towards the feed–liquid membrane interface. Consequently, an instant reaction takes place with DNPPA forming an organo-metal complex (Fig. 5.1) which diffuses across the liquid membrane phase to the liquid membrane-stripping interface. At this stage, de-complexing occurs throughout the stripping solution. Then, the neodymium (III) ions are released through the layer of the stripping phase to the stripping solution.
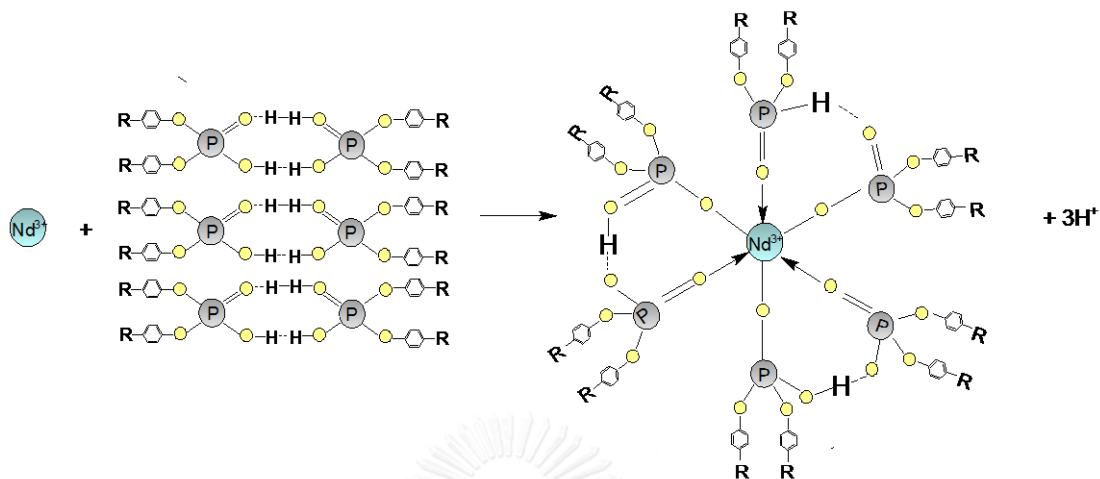
Figure 5.1 Schematic representation of Nd (III) with DNPPA to form the complex species

The overall mass transfer coefficient of neodymium ions represents the mass transfer resistance in the feed solution (tube side), the extraction reaction, the liquid membrane phase, the stripping reaction, and stripping solution (shell side) [35].

The mass transfer resistance of Nd(III) in the stripping phase can be neglected since the process is instantaneous [36] and can be defined as follows:

$$\frac{1}{K} = \frac{1}{k_t} + \frac{1}{k_e} + \frac{1}{k_m m_f (\ln r_o / r_i)}$$

(5.1)

Yang and Kocherginsky research [35] proved that the flow rates of feed and stripping solution at 100 mL/min. remained laminar. The mass transfer coefficients of Nd (III) in the aqueous phase can be calculated from Sherwood–Graetz correlations [37] and by using the Lévêque equation [38] as expressed:

$$k_t = 1.62 \frac{D_{Nd,a}}{2r_i} \left(\frac{4r_i^2 v_t}{L D_{Nd,a}} \right)^{0.33} \tag{5.2}$$

For the liquid membrane phase, the mass transfer coefficient can be calculated by [39] as in Eq. (5.3):

$$k_m = \frac{\varepsilon D_m}{\tau r_i \ln(r_o / r_i)} \tag{5.3}$$

The mass transfer coefficient due to extraction reaction (k_e) can be approximated as follows [35] in Eq. (5.4):

$$k_e = \frac{1}{k_{ex}[Nd^{3+}]_{fi}[(HA)_2]_{fi}^2 - k_{st}[NdA_3(HA)_3]_o[H^+]^3} \tag{5.4}$$

5.4 Experimental

5.4.1 The feed solution and reagents

The feed solution i.e. the digestion product of monazite ores processing obtained from the courtesy of the Rare Earth Research and Development Centre, Office of Atoms for Peace, Bangkok, Thailand, was supplied in nitrate solutions. The properties of feed solution (Table 5.1) were analyzed by ICP. DNPPA was used as an extractant and n-dodecane was used as the diluent. Reagent grade H_2SO_4 was used as the stripping solution. All chemicals were of GR grade

Table 5.1 Compositions of feed solutions (nitrate solution from monazite processing at pH 4.5)

Metal ions	Y	Nd	Sm	Eu	Gd	Dy	Yb
Concentration (mg/L)	13.6	106.7	1.3	0. 3	7.7	2.5	0.2

5.4.2 Apparatus

The hollow fiber module from Liqui–Cel[®] (Hoechst Celanese, Bridgewater, NJ) consisting of 35,000 micro-porous polypropylene fibers which are woven into fabric

and wrapped around a central feeder tube in order to supply the shell–side fluid

was used to study the separation of Nd (III).

5.4.3   Procedure

The liquid membrane containing the extractant (DNPPA) mixed with n-

dodecane was circulated along the tube and shell sides of the hollow fibers

simultaneously until it filled in the hollow fiber micro-pores with a total volume of

about 50 mL. Subsequently, both feed solution and stripping solution were fed

counter–currently into the tube and shell sides of the hollow fibers, respectively

(flow rate = 100 mL/min). The sample of both feed and stripping solutions, each of

10 mL, were collected every 10 min. All samples collected from the experiment

were analyzed by an inductively coupled plasma spectrometry (ICP). The detection

limits with the ICP system were about 0.5–10 pg mL^{-1} [40].

5.5   Results and discussion

5.5.1   Effect of pH of feed solution

The pH value is an important factor for the separation of Nd(III) from mixed rare

earths. DNPPA exhibits good performance in the extraction of metal cations from an

acidic solution [34]. The influence of pH of feed solution was studied by varying the pH in a range of 2.0–5.0. Percentages of Nd(III) extraction and stripping steadily increased and reached a maximum at pH 4.5 where the highest extraction and stripping of Nd(III) was obtained reaching 85.5% and 70.1% respectively. Operating time was 70 min. When feed solution was higher than pH 4.5, percentages of extraction and stripping declined slightly due to the equilibrium reaction at the feed–liquid membrane interface [41]. At a higher pH, lanthanum ion is hydrolysed and precipitation of hydroxyl compound resulted [42]. Thus, a feed solution of pH 4.5 was chosen to study further variables.

The percentages of extraction and stripping of rare earth metals decreased following the trend: Nd>Sm>Eu>Gd>Dy>Yb>Y. As the lanthanide atomic number increased, the percentage of extraction and stripping decreased. This was because of the formation of a stronger complex in the lanthanide series which arose due to a decrease in ionic radii from La to Lu and can be explained by an increase in the stability of the complexes formed with extract [34].

5.5.2   Effect of DNPPA concentration

The extractant, diluent and stripping solution chosen is vital for the success of the separation of Nd(III) as reported in previous work [13, 34]. The percentages of Nd(III) extraction increased when the concentration of the extractant increased up to 0.5 M. Then, the percentage of Nd(III) extraction decreased. This was because of an increase in liquid membrane viscosity that obstructed mass transfer in the liquid membrane phase, corresponding to previous findings [43].

5.5.3   Effect of H_2SO_4 concentration

The effect of concentration of the stripping solution (H_2SO_4) on the extraction and stripping of Nd(III) was studied by varying the concentration of H_2SO_4 from 1 – 7 M. The percentage of Nd(III) stripping increased when the concentration of H_2SO_4 was increased. This corresponds to chemical kinetics. However, when the concentration of H_2SO_4 was higher than 3 M, percentages of extraction and stripping of Nd(III) decreased due to the concentration gradient. This was because there is a higher ion concentration in the region near the membrane compared to the bulk of solution [44]. Thus, 3 M H_2SO_4 was recommended. Under this condition, percentages of extraction and stripping of Nd(III) were found to be 85.5% and 70.1%, respectively.

5.5.4   Effect of temperature

The effect of temperature in the feed and stripping solutions on the extraction and stripping of neodymium (III) ions was studied in the range of T 293–313 K. The percentages of extraction and stripping of Nd(III) increased when the temperature increased as shown in Fig. 5.2. The highest percentages of extraction and stripping of 98% and 95% respectively were noted at T = 313 K.
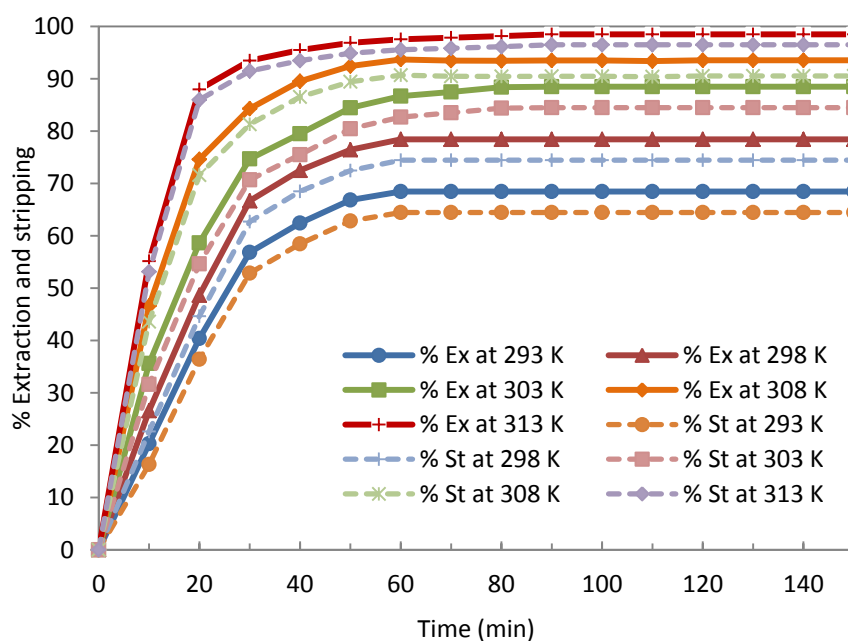
Figure 5.2 Effect of temperature on the extraction yield and the stripping yield (feed = pH 4.5; extractant = 0.5 M DNPPA; stripping = 3 M H_2SO_4; flow rate = 100 mL/min. for both feed and stripping solutions)

5.5.5   The mass transfer coefficient

The mass transfer coefficients are shown in Table 5.2. When temperature was increased, the mass transfer increased due to endothermic reaction [45]. From Table 5.2, the mass transfer due to chemical reaction was found to have the least value. Thus, the mass transfer due to chemical reaction proved to be the mass transfer–controlling step.

Table 5.2 The effect of temperature on mass transfer coefficient of Nd(III) ions

Temperature (K)	k_t (cm/s)	k_m (cm/s)	k_e (cm/s)	K (cm/s)
293	3.89×10^{-4}	4.15×10^{-4}	5.11×10^{-5}	1.83×10^{4}
298	4.15×10^{-4}	4.85×10^{-4}	5.85×10^{-5}	1.94×10^{4}
303	5.67×10^{-4}	5.18×10^{-4}	5.42×10^{-5}	2.01×10^{4}
308	6.12×10^{-4}	5.69×10^{-4}	6.31×10^{-5}	2.14×10^{4}
313	6.58×10^{-4}	6.21×10^{-4}	7.18×10^{-5}	2.25×10^{4}

Note: feed = pH 4.5, extractant = 0.5 M DNPPA; stripping = 3 M H_2SO_4; flow rate = 100 mL/min for both feed and stripping solutions

5.5.6   Validation of the model with the experimental results

The results of the experiments whereby temperatures of both feed and stripping solutions varied between T 293–313 K, using circulating flows of both feed and stripping solutions, were used to validate the model prediction. K_F was

determined from Eq. 5.1. The concentration of Nd(III) in the feed solution from the model results in accordance with Eq. (5.5) is shown in Fig. 5.3 where the experimental results are compared to those obtained from the model. The results show that the concentration of Nd(III) in feed solution increased when the temperature was increased. Thus, the concentration of Nd(III) in the feed solution as predicted by the model fitted in well with the experimental results. Average percent deviation for predictions in the feed phase is shown in Table 5.3.

$$ln\left(\frac{C}{C_0}\right) = -\varepsilon \frac{A}{V_F} K_F t \qquad (5.5)$$
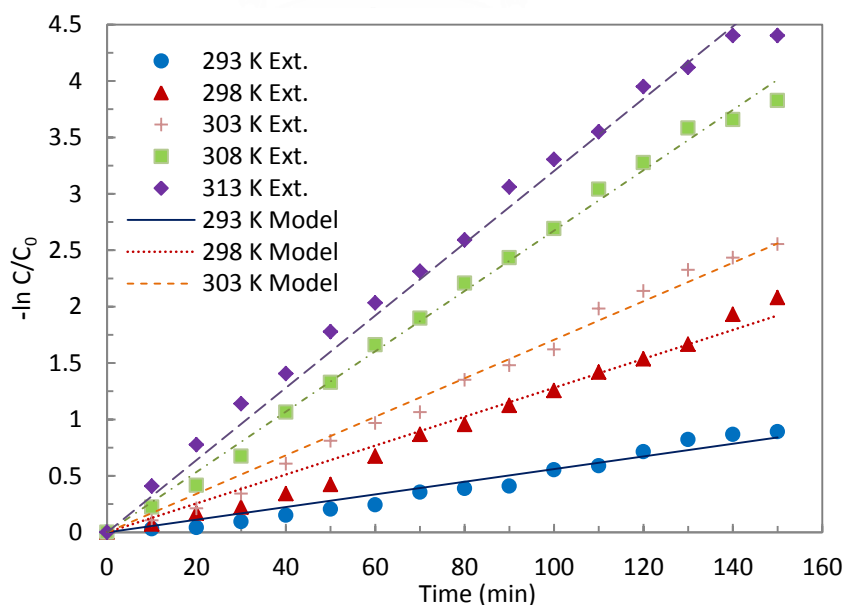
Figure 5.3 Nd (III) transport experiment with model

Table 5.3 The average standard deviation

Temperature (K)	293	298	303	308	313
% S.D. Feed side	1.91	1.89	1.81	1.75	1.64

5.6 Conclusion
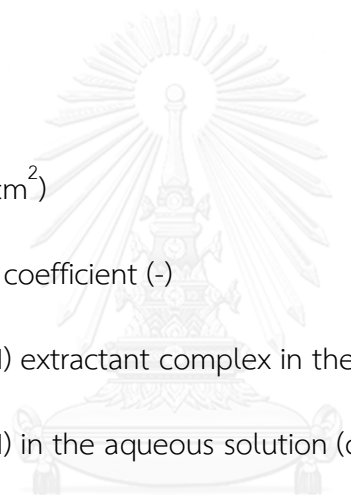
It was found that the HFSLM system could successfully separate a very low concentration of Nd(III) from mixed rare earths. When the temperature was increased, the mass transfer and the percentage of extraction and stripping increased. Optimum percentages of extraction and stripping of 98% and 95% were obtained at a temperature of feed and stripping solutions of 313 K using a feed solution of pH 4.5, 0.5 M DNPPA as extractant, 3 M H_2SO_4 as stripping solution, and equal flow rates of both feed and stripping solutions of 100 mL/min. The mass transfer due to chemical reaction proved to be the controlling step. The model results proved to be in good agreement with the experimental data. Average percent deviation for predictions in feed sides was below 2%.

5.7 Acknowledgements

5.8 Nomenclature

A membrane area (cm^2)

D_{aq} aqueous diffusion coefficient (-)

D_m diffusivity of Nd (III) extractant complex in the membrane phase (cm^2/s)

$D_{Nd,a}$ diffusivity of Nd (III) in the aqueous solution (cm^2/s)

K overall mass transfer coefficient (cm/s)

k_{as} mass transfer coefficient for the stripping solution (cm/s)

k_e mass transfer coefficient due to the extraction reaction (cm/s)

k_{ex} forward constants in the extraction reaction (min^{-1})

k_m mass transfer coefficient of the membrane phase (cm/s)

k_s mass transfer coefficient in the shell side

k_{ss} mass transfer coefficient due to the stripping reaction (cm/s)

k_{st} reverse constants in the extraction reaction (min^{-1})

k_t mass transfer coefficient in the tube side (cm/s)

m_f partition coefficient between the membrane and the feed phase (-)

r_i inner radius of the hollow fiber (cm)

r_o outer radius of the hollow fiber (cm)

t time (s)

v_f linear velocity of feed solution in the tube side (cm/s)

V_f volume of the feed solution (cm^3)

V_m volume of the membrane solution (cm^3)

ε porosity of hollow fiber (%)

τ tortuosity factor membrane (-)

ν kinematic viscosity of organic phase (cm^2/s)

5.9   References

[1]   P.M. J-L. Sabot, Lanthanides, in Encyclopedia of chemical technology, Wiley Interscience Publication, New York, (1996).

[2]   P. Maestro and D. Huguenin, J. Alloys Comp. 225 (1995) 520-528.

[3]   D. Fontana and L. Pietrelli, J. Rare Earths, 27 (2009) 830-833.

[4]   N.E. El-Hefny, Process Intensification, 46 (2007) 623-629.

[5]   L. Pei, L. Wang, G. Yu, J. Rare Earths, 30 (2012) 63-68.

[6]   A.M. El-Kot, J. Radioanal. Nucl. Chem.170 (1993) 207-214.

[7]   D. Wu, Q. Zhang, B. Bao, Hydrometallurgy, 88 (2007) 210-215.

[8]   M.-S. Lee, J.-Y. Lee, J.-S. Kim, G.-S. Lee, Sep. Purif. Technol. 46 (2005) 72-78.

[9]   A.A. Abdeltawab, S. Nii, F. Kawaizumi, K. Takahashi, Sep. Purif. Technol. 26 (2002) 265-272.

[10]   P.V. Vernekar, A.W. Patwardhan, A.V. Patwardhan, S.A. Ansari, P.K. Mohapatra, V.K. Manchanda, Sep. Sci. Technol. 48 (2012) 1003-1014.

[11]   P. Wannachod, S. Chaturabul, U. Pancharoen, A.W. Lothongkum, W. Patthaveekongka, J. Alloys Comp. 509 (2011) 354-361.

[12]   Y.A. El-Nadi, Hydrometallurgy, 119–120 (2012) 23-29.

[13]   S. Biswas, P.N. Pathak, S.B. Roy, Desalination, 290 (2012) 74-82.

[14]   I.M. Coelhoso, M.M. Cardoso, R.M.C. Viegas, J.P.S.G. Crespo, Sep. Purif. Technol. 19 (2000) 183-197.

[15]   P.C. Rout, K. Sarangi, Hydrometallurgy., 133 (2013) 149-155.

[16]   M.F. San Roman, E. Bringas, R. Ibanez, I. Ortiz, J. Chem. Tech. Biotechnol. 85 (2010) 2-10.

[17]   N.M. Kocherginsky, Q. Yang, L. Seelam, Sep. Purif. Technol. 53 (2007) 171-177.

[18]   P.K. Mohapatra, V.K. Manchanda, Liquid membrane-based separations of actinides. In: Pabby, A.K., Rizvi, S.S.H., Sastre, A.M. (Eds.), Handbook of

Membrane Separations: Chemical, Pharmaceutical, Food and Biotechnological Applications. CRCPress, pp. 883–918., (2009).

[19] B.F. Jirjis, S. Luque, Chapter 9 - Practical aspects of membrane system design in food and bioprocessing applications, in: Z.F. Cui, H.S. Muralidhara (Eds.) Membrane Technology, Butterworth-Heinemann, Oxford, 2010, pp. 179-212.

[20] Z. Lazarova, B. Syska, K. Schügerl, J. Membr. Sci. 202 (2002) 151-164.

[21] S. Heng, K.L. Yeung, M. Djafer, J.-C. Schrotter, J. Membr. Sci. 289 (2007) 67-75.

[22] W. Kit Chan, J. Jouët, S. Heng, K. Lun Yeung, J.-C. Schrotter, J Solid State Chem 189 (2012) 96-100.

[23] K.F. Lam, H. Kassab, M. Pera-Titus, K.L. Yeung, B. Albela, L. Bonneviot, J Phys. Chem. C 115 (2010) 176-187.

[24] P.V. Vernekar, Y.D. Jagdale, A.W. Patwardhan, A.V. Patwardhan, S.A. Ansari, P.K. Mohapatra, V.K. Manchanda, Chem. Eng. Res. Des. 91 (2013) 141-157.

[25] S. Gupta, M. Chakraborty, Z.V.P. Murthy, J. Ind. Eng. Chem. 20 (2014) 2138-2145.

[26] M.S. Manna, P. Saha, A.K. Ghoshal, J. Membr. Sci., 471 (2014) 219–226.

[27] P. Praveen, K.-C. Loh, Chem. Eng. J. 255 (2014) 641-649.

[28] K. Tang, C. Zhou, X. Jiang, Science in China Series B: Chemistry, 46 (2003) 96-103.

[29] L. Chimuka, M.M. Nindi, M.E.M. ElNour, H. Frank, C. Velasco, J. High Resolut. Chromatogr. 22 (1999) 417–420.

[30] L. Chimuka, M. Michel, E. Cukrowska, B. Buszewski, J. Sep. Sci. 32 (2009) 1043–1050.

[31] A.O. Saf, S. Alpaydin, A. Sirit, J. Membr. Sci. 283 (2006) 448–455.

[32] B. N. Kumar, B. Ramachandra Reddy, M. Lakshmi Kantam, J. Rajesh Kumar and Jin Young Lee, Sep. Sci. Technol. 49 (2014) 130–136.

[33] P.R. Zalupski, K.L. Nash, L.R. Martin, J. Solution Chem. 39 (2010) 1213–1229.

[34] M. Anitha, D.N. Ambare, M.K. Kotekar, D.K. Singh, H. Singh, Sep. Sci. Technol. 48 (2013) 2196-2203.

[35] Q. Yang, N.M. Kocherginsky, J. Membr. Sci. 286 (2006) 301-309.

[36] Y. Tang, W. Liu, J. Wan, Y. Wang, X. Yang, Process Biochemistry, 48 (2013) 1980-1991.

[37] N.M. Kocherginsky, Q. Yang, Sep. Purif. Technol.54 (2007) 104-116.

[38] L.L. M.A. Leveque, De la, transmission de chaleur par convection, Ann. Mines, 13 (1928) 201-239.

[39] G.R.M. Breembroek, A. van Straalen, G.J. Witkamp, G.M. van Rosmalen, J. Membr. Sci.146 (1998) 185-195.

[40] W.R Pedreira, J.E.S Sarkis, C.A da Silva Queiroz, C Rodrigues, I.A Tomiyoshi, A Abrão, J Solid State Chem. 171(2003) 3–6.

[41] T. Wongsawa, N. Leepipatpiboon, N. Thamphiphit, U. Pancharoen, A.W. Lothongkum, Chem. Eng. J. 222 (2013) 361-373.

[42] M. Idiris Saleh, Md. Fazlul Bari, Bahruddin Saad, Hydrometallurgy, 63(2002)75-84.

[43] S. Suren, T. Wongsawa, U. Pancharoen, T. Prapasawat, A.W. Lothongkum, Chem. Eng. J. 191 (2012) 503-511.

[44] T. Wannachod, N. Leepipatpiboon, U. Pancharoen, K. Nootong, J. Ind. Eng. Chem. 20(2004) 4152–4162.

[45] Q. Jia, Z. Li, W. Zhou, H. Li, , J. Chem. Tech Biotechnol, 84 (2009) 565-569.

CHAPTER 6

Optimization of synergistic extraction of neodymium ions from monazite leach solution treatment via hollow fiber supported liquid membrane using response surface methodology

Thanaporn Wannachod, Phupairum Phuphaibul, Vanee Mohdee, Ura Pancharoen* and Suphot Phatanasri**

Department of Chemical Engineering, Faculty of Engineering, Chulalongkorn University, Patumwan, Bangkok 10330, Thailand

6.1 Abstract

The extraction of neodymium ions from monazite leach solution was achieved by synergistic extraction via hollow fiber supported liquid membrane (HFSLM). Applying the results from central composite design (CCD) experiments, further optimization experiments were carried out using response surface methodology (RSM). Validation tests revealed optimum performance at 0.1 M Cyanex 272 and 0.05 M TOPO, 4 M HNO_3 as the stripping solution and flow rates of both feed and stripping solutions were 100 mL/min. The extraction of neodymium ions reached a maximum of 98%. Results indicated that the highest fractional resistance was a chemical reaction. This showed that mass transfer resistance due to chemical reaction was dominant for transport of neodymium ions through the hollow fiber supported liquid membrane system.

Keywords: Synergistic; Extraction; Neodymium; Optimization; HFSLM

6.2 Introduction

Rare earth metals (REMs) consist of fourteen lanthanides and three elements which are Sc, Y and La. Thus, the total number of REMs is 17. They are divided conventionally into two groups: the light group (Sc, La, Ce, Pr, Nd, Pm, Sm, Eu, Gd)

and the heavy group (Y, Tb, Dy, Ho, Er, Tm, Yb, Lu) (Hnghag, 2004). Currently, neodymium, one of the most abundant of rare earth metals, is of commercial interest as it is the basis for the most common solid-state lasers used in material processing such as in medicine (Wu et al., 2007). Neodymium is also used as raw material for high-strength permanent magnets (Nd–B–Fe) (Xie et al., 2014) and it costs less than samarium-cobalt permanent magnets (Lee et al., 2005). Rare earth elements have very similar chemistry and this makes them difficult to separate.

Various methods can be used to recover these metals from aqueous solutions. Traditional methods, for example such as ion exchange, precipitation and solvent extraction have been found to be ineffective at a very low concentration of contaminated metal ions. Regarding this, hollow fiber supported liquid membrane (HFSLM) has been employed. Several studies have highlighted the use of HFSLM for separating various trace metal ions from aqueous solutions. The HFSLM system allows for both simultaneous extraction and stripping of target metal ions in a single-step operation, with high selectivity (Coelhoso et al., 2000).

Many advantages of HFSLM over traditional methods include lower energy consumption, lower capital and operating costs and less extractant used (San Román

et al., 2010). HFSLM has a high surface area per unit volume for mass transfer (Kocherginsky et al., 2007). Therefore, it has been used to separate metal ions, toxic ions, radioactive and lanthanide metal ions. Different properties of two extractants can be combined to enhance extraction of some metal ions. Therefore, synergistic extraction has been applied to separate metal ions. Ansari et al. (Ansari et al., 2009) applied HFSLM for the separation of actinides and lanthanides from high-level waste: 0.1M N,N,N',N'–tetraoctyl diglycolamide (TODGA) and 0.5 M N,N–dihexyl octanamide (DHOA) dissolved in normal paraffinic hydrocarbon (NPH) was used as the carrier. Pancharoen et al. (Ramakul et al., 2009) also reported on the separation of Y(III) from mixed rare earths via HFSLM. Cyanex 272 and TBP in kerosene were used separately as extractants. The results demonstrated that this system was most efficient in separating Y(III) from the mixed rare earths. Previous successful research on the separation of rare earth metals is summarized below in Table 6.1.

To investigate the relationship between various determinants, response surface methodology (RSM) was employed. RSM, utilizing a group of mathematical and statistical techniques, is most useful for designing experiments, evaluating the effect of factors and finding the optimal condition for a particular response. A central composite design (CCD) helps to fit the collected data with an empirical, second-

order polynomial model. Moreover, CCD together with a second-order polynomial model provides an adequate representation of most continuous response surfaces over a relatively broad factor domain (Khanmohammadi et al., 2014).

Table 6.1 Summary of previous research on rare earth metals ions separation

Authors	Metals	Extractants	Diluents	Stripping	Method	% Ex	Ref.
Wu et al.	Nd	8-hydroxy quinoline	Heptane	H_2SO_4	L–L	N/A	(Wu et al., 2007)
Lee et al.	Nd	PC88A	Kerosene	HCl	L–L	N/A	(Lee et al., 2005)
Saleh et al.	La	Cyanex 272	Toluene	HNO_3	L–L	N/A	(Saleh et al., 2002)
Fontana et al.	Sm, Eu, Gd, Tb	HEHEPA	Kerosene	HCl	L–L	N/A	(Fontana, 2009)
Wang et al.	Y	CA12 + Cyanex 272	Kerosene	HCl	L–L	92.9	(Wang et al., 2012)
Desouky et al.	Y	Primene–JMT	Kerosene	HNO_3	L–L	N/A	(Desouky et al., 2009)
El-Nadi et al.	Pr, Sm	Cyanex 923	Chloroform	H_2SO_4	L–L	98,98	(El-Nadi, 2010)
Pei et al.	Eu	D2EHPA	Kerosene	HCl	LM	94.2	(Pei et al., 2011)
Gaikwad et al.	Y	PC88A	Toluene	HCl	FSLM	N/A	(Gaikwad, 2010)
El-Nadi et al.	La, Nd	TOPO + TRPO	Kerosene	H_2SO_4	L–L	97, 81	(El-Nadi, 2012)
Wannachod et al.	Nd	Cyanex 272 +TOPO	Octane	H_2SO_4	HFSLM	98	This study

Note: FSLM = flat sheet supported liquid membrane; HFSLM = hollow fiber supported liquid membrane; L–L = liquid–liquid extraction and LM = liquid membrane.

The separation of neodymium ions by synergistic extractants has been studied in detail, using octane as a diluent and HNO_3 as a stripping solution. Feed solution was obtained from the digestion of product from monazite ore processing, courtesy of the Rare Earth Research and Development Center, Office of Atoms for Peace, Bangkok, Thailand. The choice of extractant, diluent and stripping solution was vital for the success of separation in previous works (Anitha et al., 2013; Biswas et al., 2012). The type of acidic organo-phosphorus and neutral donors, the concentration of synergistic extractants, the concentration of the stripping solution, the flow rate of both feed and stripping solutions, the cycle of operating as well as flow patterns were studied.

In this work, the separation of neodymium ions from monazite leach solution using synergistic extractants was investigated. An investigation of the related mass transfer of neodymium ions was also undertaken. The objective is to find the optimum conditions for synergistic extractants. RSM was employed to identify the optimal conditions for high extraction yield of neodymium ions.

6.3 Theoretical

The hollow fiber module system contains hollow fibers aligned horizontally; within them an extractant is embedded. An extractant, which dissolves in the organic solution as the liquid membrane, can be used singly or as a mixture of two types of extractant. The target metal ions diffuse across the liquid membrane from the feed phase to the stripping phase. The feed and stripping solutions flow counter–currently in the tube and shell sides of the hollow fibers, respectively.

6.3.1 Transport of neodymium ions across the liquid membrane phase

The descriptive schematic mechanisms were the counter transport mechanisms via HFSLM. The concentration profile for the system is shown in Fig. 6.1. The driving force of the process is the proton concentration gradient in the feed solution and the stripping solution. The gradient of proton concentration yielded high enrichment factors for metal ions (Cheng et al., 2013). Neodymium ions in the feed solution are transported to the interface between the feed phase and the liquid membrane phase. Subsequently, the neodymium ions react with the extractant to form complex species. Then, the complex species diffuse to the interface between the liquid membrane phase and the stripping phase by the concentration gradient. H^+

from the stripping phase diffuses to the liquid membrane-stripping interface. The hydrogen ions react with the complex species at the liquid membrane-stripping interface. Thereupon, neodymium ions are released together with the extractant. Neodymium ions transfer into the stripping phase while the extractant diffuses back to the liquid membrane phase by the concentration gradient and reacts again with the metal ions. Thus, the target metal ions can be extracted and stripped simultaneously in a single step.
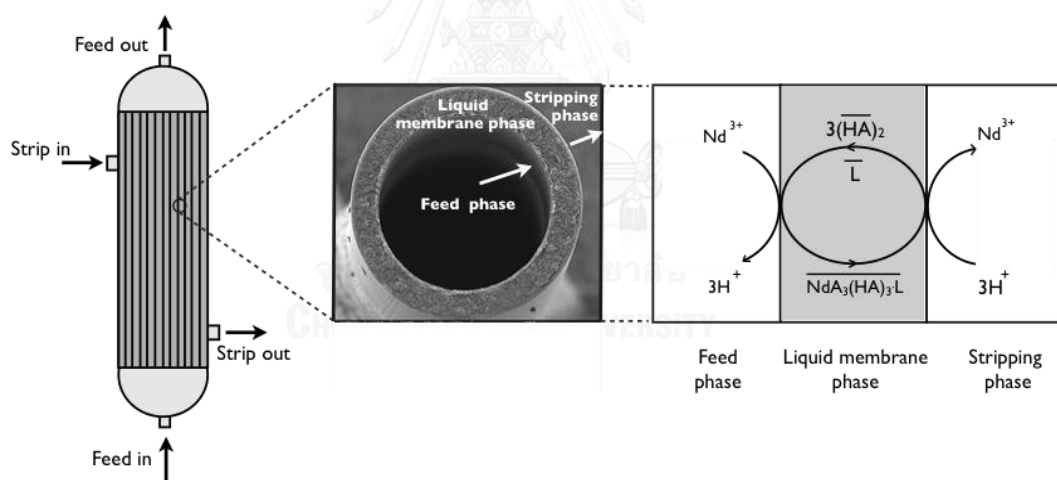
Figure 6.1 Schematic mechanism of neodymium ions transport across the liquid membrane phase using synergistic extractants of acidic organo-phosphorous (H_2A_2) and neutral donors (L)

For the 1st extractant, the extraction of neodymium ions from feed solution by acidic organo-phosphorous (H_2A_2) is shown in Eq. (6.1) as reported earlier (Pei et al., 2012):

$$Nd_{(aq)}^{3+} + 3(HA)_{2(org)} \xrightleftharpoons[k_{st}]{k_{ex}} NdA_3(HA)_{3(org)} + 3H_{(aq)}^{+} \qquad (6.1)$$
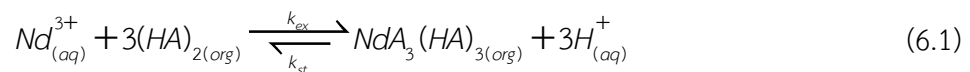
where k_{ex} and k_{st} denote the forward and the reverse constants in the extraction reaction, respectively.

For the 2nd extractant, the extraction of neodymium ions from feed solution by neutral donors (L) is shown in Eq. (6.2). The neutral extractant captures both Nd^{+3} and NO$_3^-$ from the feed phase and forms the second extracted species or compound. Subsequently, it reacts with neodymium ions to produce complex ions ($Nd(NO_3)_3 \cdot L_3$). The numbers of stoichiometry in this present work were determined by slope analysis method. The stoichiometric numbers obtained agreed with the results reported earlier by El–Nadi et al. (El-Nadi et al., 2007):

$$Nd_{(aq)}^{3+} + 3NO_{3(aq)}^{-} + 3L_{(org)} \xrightleftharpoons[k_{st}]{k_{ex}} Nd(NO_3)_3 \cdot L_{3(org)} \qquad (6.2)$$
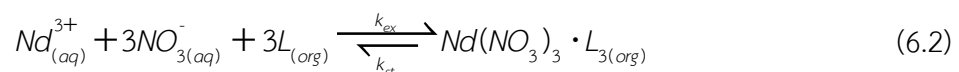
For synergistic extractants, the extraction of neodymium ions can be expressed by the following Eq. (6.3). Again, the stoichiometric numbers were determined by slope analysis method and appeared to agree with the results as reported earlier by Anitha et al. (Anitha et al., 2013):
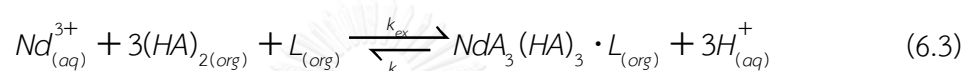
$$Nd^{3+}_{(aq)} + 3(HA)_{2(org)} + L_{(org)} \underset{k_{st}}{\overset{k_{ex}}{\rightleftharpoons}} NdA_3(HA)_3 \cdot L_{(org)} + 3H^+_{(aq)} \qquad (6.3)$$

where (aq) is the species in the aqueous phase and (org) is the species in the liquid membrane phase.

The complex species continuously react with hydrogen ions at the membrane–stripping interface to strip neodymium ions to the stripping phase. Thus, the stripping reaction, due to 1st extraction reaction (1st extractant), is shown in Eq. (6.4):

$$NdA_3(HA)_{3(aq)} + 3H^+_{(aq)} \underset{k'_{ex}}{\overset{k'_{st}}{\rightleftharpoons}} Nd^{3+}_{(aq)} + 3(HA)_{2(org)} \qquad (6.4)$$
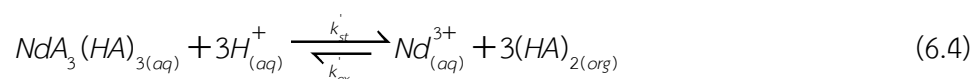
where k'_{ex} and k'_{st} represent the forward and the reverse constant in the stripping reaction, respectively.

The stripping reaction, due to 2nd extraction reaction (2nd extractant), is shown in Eq. (6.5):

$$Nd(NO_3)_3 \cdot L_{3(org)} \xrightleftharpoons[k'_{ex}]{k'_{st}} Nd^{3+}_{(aq)} + 3HNO^-_{3(aq)} \qquad (6.5)$$
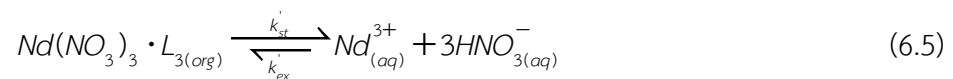
The stripping reaction, due to the synergistic reaction, is shown in Eq. (6.6):

$$NdA_3(HA)_3 \cdot L_{(org)} + 3H^+_{(aq)} \xrightleftharpoons[k'_{ex}]{k'_{st}} Nd^{3+}_{(aq)} + 3(HA)_{2(org)} + L_{(org)} \qquad (6.6)$$
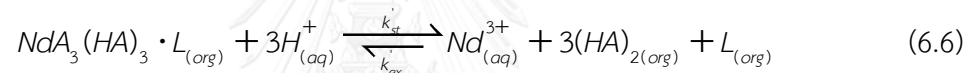
6.3.2   Synergistic coefficient

Luo et al. (Luo et al., 2004) defined the synergistic coefficient (*S.C.*) in terms of the distribution coefficient:

$$S.C. = \frac{D_{12}}{D_1 + D_2} \qquad (6.7)$$

If S.C.   > 1, synergism is present.

If S.C.   < 1, an antagonistic effect happens.

For S.C. = 1, there is no synergism.

where D_1 is the distribution coefficient of acidic organo-phosphorous, D_2 is the distribution coefficient of the neutral donor and D_{12} is the distribution coefficient of the synergistic system.

6.3.3 Mass transfer coefficient of neodymium ions via HFSLM

The overall mass transfer coefficient of neodymium ions represents the mass-transfer resistances in the tube side, the interfacial resistance of the extraction, the liquid membrane phase resistance, the shell–side resistance, the resistance of the stripping reaction and the strip–side resistance (Tang et al., 2013):

$$\frac{1}{K_{total}} = \frac{1}{k_{af}} + \frac{1}{k_e} + \frac{1}{m_f k_m} + \frac{1}{m_s k_o} + \frac{1}{m_s k_s} + \frac{1}{(m_s / k_s)k_{as}} \tag{6.8}$$

Eq. (6.8) can be simplified by neglecting the transport resistances involving the stripping reaction which were negligible because the stripping reaction was almost instantaneously completed during the HFSLM process as in Eq. (6.9):

$$\frac{1}{K_{total}} = \frac{1}{k_{af}} + \frac{1}{k_e} + \frac{1}{m_f k_m} + \frac{1}{m_s k_o} \tag{6.9}$$

or

$$R = R_{af} + R_e + R_m + R_o$$

The relative contribution of each resistance to the overall resistance to mass transfer was obtained as follows:

$$\Delta_i (\%) = \frac{R_i}{R_{af} + R_e + R_m + R_o} \tag{6.10}$$

where Δ_i is the fractional resistance.

The partition coefficient of neodymium ions between the liquid membrane phase and the feed phase can be calculated by:

$$m_f = \frac{[NdA_3(HA)_3 \cdot L]}{[Nd^{3+}]_f} \tag{6.11}$$

where k_{af} is the mass transfer coefficient in the feed solution; k_e is the mass transfer coefficient due to the extraction reaction; k_m is the mass transfer coefficient of complex species in the liquid membrane phase whereas k_o is the mass transfer coefficient in the shell side between the hollow fibers; k_s is the mass transfer coefficient owing to stripping reaction and k_{as} is the mass transfer coefficient for the stripping solution.

The mass transfer coefficients of neodymium ions in the feed solution can be calculated using Lévêque equation (Leveque, 1928), based on Sherwood–Graetz correlations (Kocherginsky and Yang, 2007):

$$k_{af} = 1.62 \frac{D_{Nd,a}}{2r_i} \left(\frac{4r_i^2 v_t}{L D_{Nd,a}} \right)^{0.33} \qquad (6.12)$$

where v_t is the linear velocity of feed solution in the tube side (cm/s) and r_i is the inner radius of the feed side (cm). The $D_{Nd,a}$ is the diffusion coefficient of neodymium ions in aqueous solution, equal to 5.48×10^{-5} cm^2/s.

In the hollow fiber operation, metal ions in the complex, occurring at the feed–liquid–membrane interface, are stripped out continuously by the stripping agent at the liquid–membrane–stripping interface. Therefore, the total reaction as in Eq. (6.13), the extraction equilibrium constant ($K_{ex,f}$) of neodymium ions extracted can be written as:

$$K_{Ex,f} = \frac{k_{ex}}{k_{st}} = \frac{[NdA_3(HA)_3 \cdot L]_o [H^+]^3}{[Nd^{3+}]_{fi} [(HA)_2]_{fi}^2} \tag{6.13}$$

The mass transfer coefficient due to extraction reaction rate can be approximated as follows (Yang and Kocherginsky, 2006):

$$\frac{1}{k_e} = \frac{1}{k_{ex}[Nd^{3+}]_{fi}[(HA)_2]_{fi}^2 - k_{st}[NdA_3(HA)_3 \cdot L]_o[H^+]^3} \tag{6.14}$$

The mass transfer coefficient in the liquid membrane phase can be expressed by (Breembroek et al., 1998):

$$k_m = \frac{\varepsilon D_m}{\tau r_i \ln(r_o / r_i)} \tag{6.15}$$

where D_m is the diffusivity of neodymium ions in the liquid membrane solution (cm^2/s), r_o is the outer radius of the membrane (cm), r_i is the inner radius of the membrane (cm), ε is the porosity of the hollow fiber and τ is the tortuosity of the hollow fiber.

The mass transfer coefficient on the shell side of two hollow fibers can be calculated by (Baudot et al., 2001):

$$k_o = 1.25 \frac{D_{Nd,a}}{d_h^{0.07}} \left(\frac{d_h v_s}{\upsilon L} \right)^{0.93} \left(\frac{\upsilon}{D_{Nd,a}} \right)^{0.33} \tag{6.16}$$

where v_s is the linear velocity of stripping solution in the shell side (cm/s) and υ is the kinetic viscosity (cm^2/s).

The hydraulic diameter of hollow fibers is calculated by (Baudot et al., 2001):

$$d_h = \frac{d_a^2 - d_i^2 - nd_0^2}{nd_0} \tag{6.17}$$

6.4   Experimental

6.4.1   Feed solution and reagents

The feed solution as supplied by courtesy of the Rare Earth Research and Development Centre, Office of Atoms for Peace, Bangkok, Thailand, was supplied in nitrate solutions i.e. the digestion product of monazite ores processing. The feed solution contained Y 16.3 mg/L, Nd 106.7 mg/L, Sm 16.3 mg/L, Eu 0.3 mg/L, Gd 7.7 mg/L, Dy 2.5 mg/L and Yb 0.2 mg/L in nitric acid solution. TOPO, Cyanex 272, Cyanex 923, TBP and TEHP were obtained from Cytec Canada. PC88A, D2EHPA and DNPPA were from BASF and used as the extractants. These were diluted in octane (Aldrich) and used for the preparation of the liquid membrane phase. Reagent grade nitric acid (Merck) was used as the stripping solution. All chemicals were used as received without any further purification. All the chemicals were of GR grade.

6.4.2   Hollow fiber supported liquid membrane system

The extractant was diluted in octane and then circulated throughout the tube and shell sides of the hollow fibers for 40 min. to ensure the extractant sets in the micro-pores of the hollow fibers. Thereafter, the feed solution was pumped into the

tube side. Meanwhile, the stripping solution was pumped counter–currently into the shell side. Then, the neodymium ions in the feed solution diffused across the liquid membrane to the stripping phase and collected in the stripping reservoir. The properties of the hollow fiber module are as shown below in Table 6.2. The concentration of metal ions in samples from the feed and stripping solutions was analyzed by ICP.

Table 6.2 Properties of the hollow fiber module

Properties	Description
Material	Polypropylene
Number of hollow fibers	35,000
Module diameter (cm)	6.3
Module length (cm)	20.3
Inside diameter (cm)	0.024
Outside diameter (cm)	0.03
Effective length (cm)	15
Average pore size (cm)	3×10^{-6}
Porosity (%)	25%
Effective surface area (cm^2)	1.4×10^4
Area per unit volume (cm^2/cm^3)	29.3
Tortuosity factor	2.6
Operating temperature (K)	273 – 333

The extractability of neodymium ions in this research can be calculated by the percentage of extraction and stripping:

$$\%Extraction = \frac{[C]_{f,in} - [C]_{f,out}}{[C]_{f,in}} \cdot 100 \tag{6.18}$$

$$\%Stripping = \frac{[C]_{s,out}}{[C]_{f,in}} \cdot 100 \tag{6.19}$$

where $[C]_{f,in}$ denotes the initial concentration in the feed phase and $[C]_{f,out}$ and $[C]_{s,out}$ denote the outlet concentration in the feed and stripping phases, respectively.

6.4.3   Analytical methods

Inductively coupled plasma spectrometry (ICP) was used: ICP Spectrometer–model Stroflame–ICP M from Spectro Co. can detect the elements of concentrations higher than 1 ppm, in both acidic and basic states.

The analyzing method comprised of:

(1)   Introducing 1 mL of sample into a volumetric flask of 10 mL

(2)   Adding 1% (v/v) HNO_3 volume to 10 mL and

(3)   Analyzing the amount of neodymium ions in the sample

6.4.4   Experimental design

A central composite design (CCD) was used to optimize the extracted neodymium ions based on the results revealed from the factorial experiments. The F-test analysis of variance with a 95% confidence interval was also used to evaluate statistically the regression significance. The analysis of variance and estimation of the parameters was performed using Design-Expert 9.0.3.1 Trial version (Stat-Ease, Inc., Minneapolis, MN, USA).

6.5   Results and discussion

6.5.1   Effect of types of acidic organo-phosphorous

From a review of the literature, Cyanex 272, PC88A, D2EHPA, and DNPPA show high performance in the extraction of metal ions (Biswas et al., 2011). Thus, they were chosen to study the selective extraction of neodymium (III) ions from monazite

leach solution. The concentration of acidic organo-phosphorus extractants used was 0.1 M. The results showed that the extractability of neodymium ions across HFSLM for different extractants followed: Cyanex 272>PC88A>D2EHPA>DNPPA. The results follow the *pKa* values of the acidic organo-phosphorous extractants–which is the *pKa* values – of individual *pKa* values i.e. Cyanex 272 (*pKa* = 8.7), PC 88A (*pKa* = 7.1), D2EHPA (*pKa*= 4) and DNPPA (*pKa* = 2.5) (Dogmane et al., 2002; Sella et al., 1995). Similar observations have been reported on the extraction of neodymium ions from nitric acid medium using different acidic extractants (Dogmane et al., 2002). Using 0.1 M Cyanex 272, the percentage of extraction and stripping of neodymium ions increased to 75% and 68 %. Therefore, Cyanex 272 was selected in order to study the other variables. The overall transfer coefficient (K_{total}) of neodymium ions across HFSLM as of Cyanex 272, PC 88A, D2EHPA and DNPPA were 6.29×10^{-3} cm/s, 5.84×10^{-3} cm/s, 5.51×10^{-3} cm/s and 5.18×10^{-3} cm/s, respectively.

The percentages of extraction and stripping of rare earth metals are as shown in Table 6.3. The percentage of extraction and stripping decreased when the lanthanide atomic number increased. This was because of the formation of a stronger complex in the lanthanide series which arose due to a decrease in ionic radii

from La to Lu and can be explained by an increase in the stability of the complexes

formed (Anitha et al., 2013).

Table 6.3 The percentages of extraction and stripping of lanthanide ions

Metal ions	Nd	Sm	Eu	Gd	Dy	Yb	Y
% Extraction	75	9.1	8.5	6.3	5.5	4.1	3.9
% Stripping	68	7.8	6.4	4.2	3.8	3.1	2.2

Note: feed = pH 4.5; extractant = 0.1 M acidic organo-phosphorous; stripping = 4 M HNO_3; flow rate = 100 mL/min for both feed and stripping solutions).

6.5.2   Effect of types of neutral donors

From a review of the literature TOPO, Cyanex 923, TBP and TEHP were used in the extraction of lanthanide metals (Biswas et al., 2012). Thus, they were chosen to study the selective extraction of neodymium ions from monazite leach solution. Further, the effect of different types of neutral donors was studied at 0.05 M. The results showed that the percentages of extraction and stripping of neodymium ions across HFSLM for different extractants followed: TOPO>Cyanex 923>TBP>TEHP. The results followed the relative basicity (K_H) of the neutral donors – of individual neutral donor i.e. TOPO (K_H =8.9), Cyanex 923 (K_H =8.3), TBP (K_H =0.16) and TEHP (K_H =0.16) (Naik et al., 2003, Biswas et al., 2012). The overall transfer coefficient (K_{total}) of

neodymium ions across HFSLM as of TOPO, Cyanex 923, TBP and TEHP were 3.54×10^{-3} cm/s, 3.31×10^{-3} cm/s, 2.48×10^{-3} cm/s and 2.15×10^{-3} cm/s, respectively.

6.5.3   Effect of synergistic extractants concentration

The synergistic extraction of neodymium ions was effected using the mixtures of Cyanex 272 and neutral donors (TOPO, Cyanex 923, TBP and TEHP) according to the more than unity synergistic coefficient illustrated in Table 6.4 below. TOPO, as the neutral donor giving the maximum synergistic coefficient of 4.48 along with Cyanex 272, was selected in the next section of study.

Table 6.4 Validation of overall mass transfer coefficient (*K)* of neodymium ions across HFSLM with synergistic coefficient (*S.C.*) of synergistic extraction

Synergistic extractant		*S.C.*	*K*
Acidic organo-phosphorous	Neutral donors		$(10^3$ cm/s)
Cyanex 272	TOPO	4.48	9.18
	Cyanex 923	3.19	8.95
	TBP	2.58	8.52
	TEHP	1.49	7.79

Note: feed = pH 4.5; synergistic extractants = 0.1M acidic organo-phosphorous and 0.05M neutral donors; stripping = 4M HNO_3; flow rate = 100 mL/min for both feed and stripping solutions

To optimize the concentration of synergistic extractants, it was necessary to consider their mutual and interactive effect on the extraction yield of neodymium ions. For this purpose, a centered central composite design (CCD) was employed for the optimization of Cyanex 272 concentration and TOPO concentration for the extraction of neodymium ions via HFSLM. The range and levels of individual variables are given below in Table 6.5.

To determine the regression model for these dependent parameters, a two-factor and five-level CCD with 13 individual design points were chosen in this study. All these 13 experiments were performed by varying initial Cyanex 272 concentration from 0.05 to 0.25 M and TOPO concentration from 0 to 0.2 M at their optimum values. The results of CCD for the two variables A (Cyanex 272 concentration), B (TOPO concentration) are shown accordingly in Table 6.6.

Table 6.5 The levels of different variables in coded and un-coded form for the extraction of neodymium ions

Independent variable	Range and levels				
	-1.414	-1	0	1	1.414
Cyanex 272, A (M)	0.05	0.1	0.15	0.2	0.25
TOPO, B (M)	0	0.05	0.10	0.15	0.20

The percentage of extraction was modeled from the experimental data using a second-order polynomial regression equation:

$$Y = \beta_0 + \sum_{i=1}^{k}\beta_i X_i + \sum_{i=1}^{k}\beta_{ii} X_i^2 + \sum_{i=1}^{k-1}\sum_{j=2}^{k}\beta_{ij} X_i X_j + \varepsilon \tag{6.20}$$

where Y is the result of response of the experiment; β_0 is the general constant coefficient; β_i, β_{ii}, β_{ij} are constant coefficients for the linear, quadratic and interaction effects, respectively; x_i is a code factor for each independent variable, Cyanex 272 concentration (M) or TOPO concentration (M) and ε is a random error.

From Table 6.6 it was observed that both the dependent parameters and their interaction were showing significant effects on the neodymium ions extraction via HFSLM. The following quadratic regression equation can predict the percentage of extraction of neodymium ions:

$$Y = 88.56 - 10.79A - 2.75B + 14.00AB - 14.78A^2 - 17.78B^2 \tag{6.21}$$

In Table 6.6, the experimental design is shown along with the relevant data and predicted responses. In Table 6.7 below, the model coefficients, F values and p values, generated by the software, are given and can be used to evaluate the model. In general, any term having the values of $p < 0.05$ is significant. Table 6.7 also shows that the probability for the regression quadratic model of extraction of neodymium ions is significant ($p < 0.05$). This indicated that the model was statistically good. In addition, the model proved to be a suitable prototype to represent the real relationships among the selected parameters since the predicted R^2 of the model was found to be 0.9815. This indicated that 98.15% of the variability in the response could be explained by the model. Again, the high value of the adjusted R^2 (0.9589) was significant. These results ensured a satisfactory adjustment of the polynomial model to the experimental data. Hence, this well-fitting model for neodymium ions extraction was successfully established.

The influences of Cyanex 272 and TOPO concentration and their interactive effect on neodymium ions extraction via HFSLM are shown below in Fig. 6.2. Fig. 6.2 highlights the three-dimensional surface-contour plots of the influences of Cyanex 272 concentration and TOPO concentration on neodymium ions extraction. It can be seen that neodymium ions extraction increases when Cyanex 272 increases in

concentration from 0.05 to 0.1 M. However, when Cyanex 272 concentration is greater than 0.1 M, neodymium ions extraction was found to decrease. Neodymium ions extraction increased when TOPO concentration increased to 0.05 M. After the peak, the extraction percentages of neodymium ions dropped due to the excessive viscosity of the liquid membrane phase which was in agreement with the findings of Chakrabarty et al. (Chakrabarty, 2009). Therefore, 0.1 M Cyanex 272 and 0.05 M TOPO was chosen to be used for further experiments.

Table 6.6 CCD design matrix along with experimental and predicted values of the extraction yield of neodymium ions via HFSLM

Run no.	A	B	% Extraction	
			Experimental	Predicted
1	0	0	88.5	88.56
2	1	1	58	56.46
3	0	0	88.5	88.56
4	0	0	88.6	88.56
5	0	0	88.4	88.56
6	0	-1.41421	55	56.89
7	0	0	88.8	88.56
8	1.41421	0	41	43.74
9	-1	-1	98	95.54
10	-1	1	54	50.04
11	-1.41421	0	72	74.26
12	0	1.41421	48	49.11
13	1	-1	33	34.96

Table 6.7 ANOVA for response surface quadratic model

Source	Coefficient	Sum of Squares	df	Mean Square	F Value	p-value Prob > F
Model	88.56	5073.13	5	1014.63	10.40	0.0039
A-Cyanex 272	-10.79	930.62	1	930.62	9.54	0.0176
B-TOPO	-2.75	60.50	1	60.50	0.62	0.04568
AB	14.00	784.00	1	784.00	8.04	0.0252
A^2	-14.78	1519.64	1	1519.64	15.58	0.0056
B^2	-17.78	2199.15	1	2199.15	22.54	0.0021
Residual		682.97	7	97.57		
Lack of Fit		682.88	3	227.63	9896.78	< 0.0001
Pure Error		0.092	4	0.023		
Cor Total		5756.10	12			

R^2 = 0.9815 and $Adj\ R^2$ = 0.9586
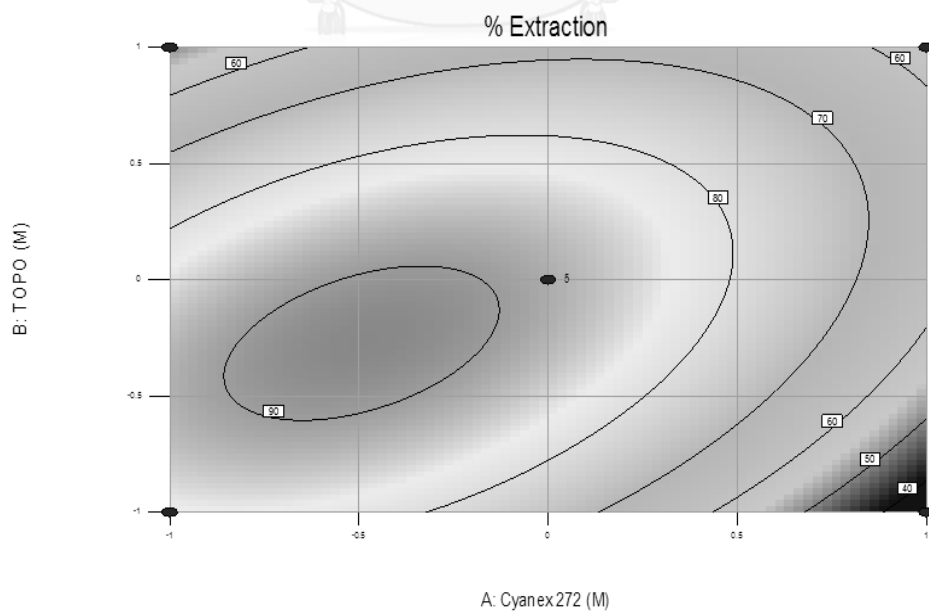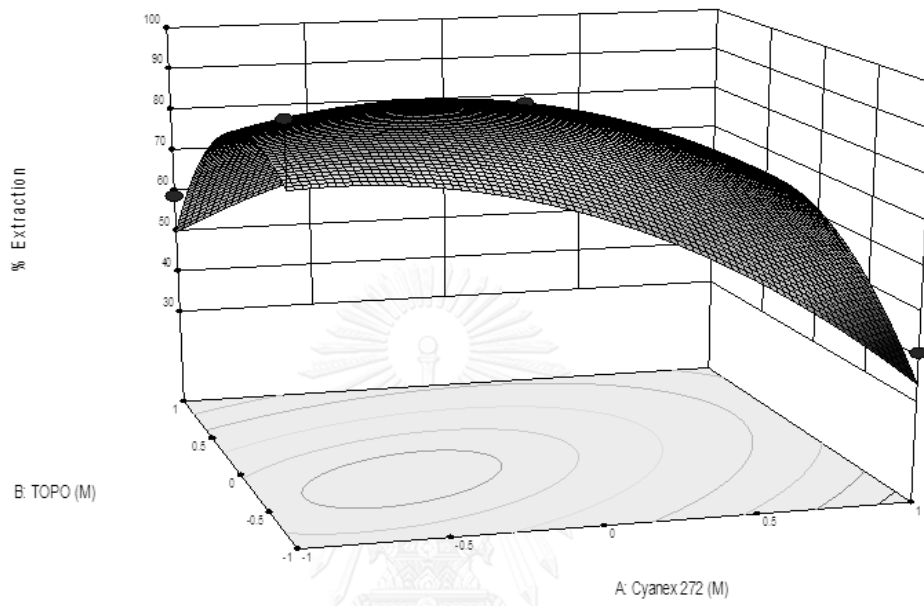
% Extraction

Figure 6.2 Percentage of neodymium ions vs concentration of synergistic extractants (a) extraction and (b) stripping (feed: pH 4.5; stripping: 4M HNO_3; flow rate = 100 mL/min for both feed and stripping solutions).

6.5.4   Effect of stripping concentration

Stripping investigations were carried out with regard to the organic solution consisting of the synergistic extractants. The effect of HNO_3 concentrations on the stripping solution was studied from 1 – 6 M. The results in Fig. 6.3 show that the percentage of stripping of neodymium ions increased. This corresponds to the chemical kinetics whereby the rate of stripping of neodymium ions increase when the concentration of stripping solution is increased. Optimum percentages of extraction and stripping of neodymium ions were obtained at 4 M HNO_3. When concentration was higher than 4 M HNO_3, percentages of extraction and stripping did not improve due to the equilibrium reaction at the feed–liquid membrane interface. Thus, in this study, 4M HNO_3 was recommended. Moreover, as confirmed by Güell et al (Güell et al., 2008), the effectiveness of the HFSLM system under strong acidic conditions was shown under prolonged operation up to 8 consecutive days.

Figure 6.3 Percentage of neodymium ions vs concentration of HNO_3 (feed: pH 4.5; synergistic extractants: 0.1M Cyanex 272 and 0.05M TOPO; flow rate = 100 mL/min for both feed and stripping solutions).

6.5.4 Effect of operating cycle

The effect of operating time was investigated using optimum conditions of the synergistic extractants. In a once–through operation, the percentages of extraction and stripping of neodymium ions reached 95% and 90%, respectively. To further enhance performance, the extraction cycle mode was repeated. As a result,

following the fourth cycle, the cumulative extraction and stripping of neodymium ions rose to 98% and 95%. The results are seen in Fig. 6.4. The selectivity of neodymium ions extraction and stripping was also observed to improve with repetition of the extraction cycle mode.

Figure 6.4   Percentage of neodymium ions vs number of cycles (feed = pH 4.5; synergistic extractants: 0.1M Cyanex 272 and 0.05M TOPO; stripping: 4M HNO_3; flow rate = 100 mL/min for both feed and stripping solutions; operating time: 240 min. for 4 cycles).

6.5.5   Effect of flow patterns of both feed and stripping solutions

The effect of flow patterns of both feed and stripping solutions via the HFSLM system (i.e. single-pass flows of feed and stripping solutions, circulating flows of feed and stripping solutions as well as single-pass flow of feed solution and circulating flow of stripping solution) was studied. The data is as shown in Fig. 6.5. The results indicated that the highest extractability of neodymium ions was achieved by the circulating flows of both feed and stripping solutions, a single-pass flow of feed solution and circulating flow of stripping solution. According to Anita et al. (Anitha et al., 2013), the extraction and stripping of precious metals is due to the relatively slow chemical reactions; long residence times are required. Thus, the circulating flows of feed and stripping solutions through HFSLM were appropriate and are in agreement with an earlier report by Suren et al. (Suren et al., 2012).

(a)
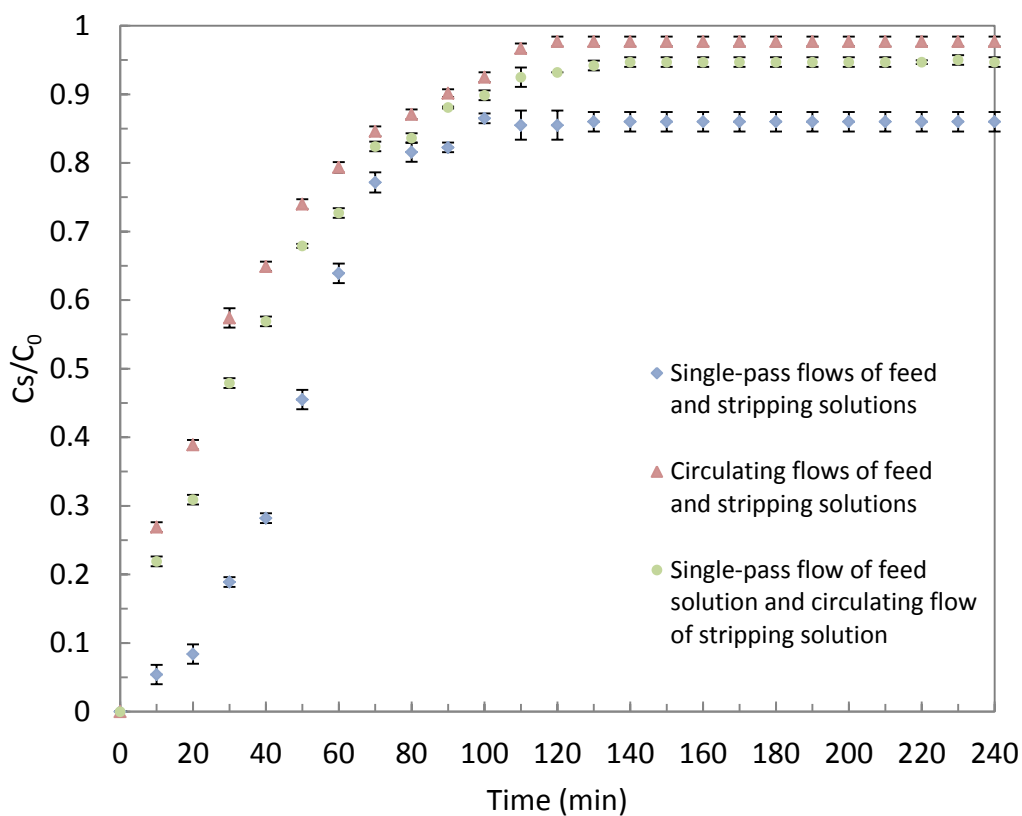
Figure 6.5 Concentration of neodymium ions vs time (a) C_f/C_0 and (b) C_s/C_0 (feed = pH 4.5; synergistic extractants = 0.1 M Cyanex 272 and 0.05 M TOPO; stripping = 4 M HNO_3; flow rate = 100 mL/min for both feed and stripping solutions).

6.5.6 Effect of flow rates of both feed and stripping solutions

Equal flow rates of both feed and stripping solutions were studied. The results are as shown in Fig. 6.6. At 100 mL/min. maximum percentage of extraction and stripping of neodymium ions reached 95% and 90%, respectively. However, at flow rates greater than 100 mL/min. the percentages of extraction and stripping of

neodymium ions decreased owing to the less residence time of the solution in the hollow fiber module. This was in agreement with an earlier report by Yang et al. (Yang and Kocherginsky, 2006).
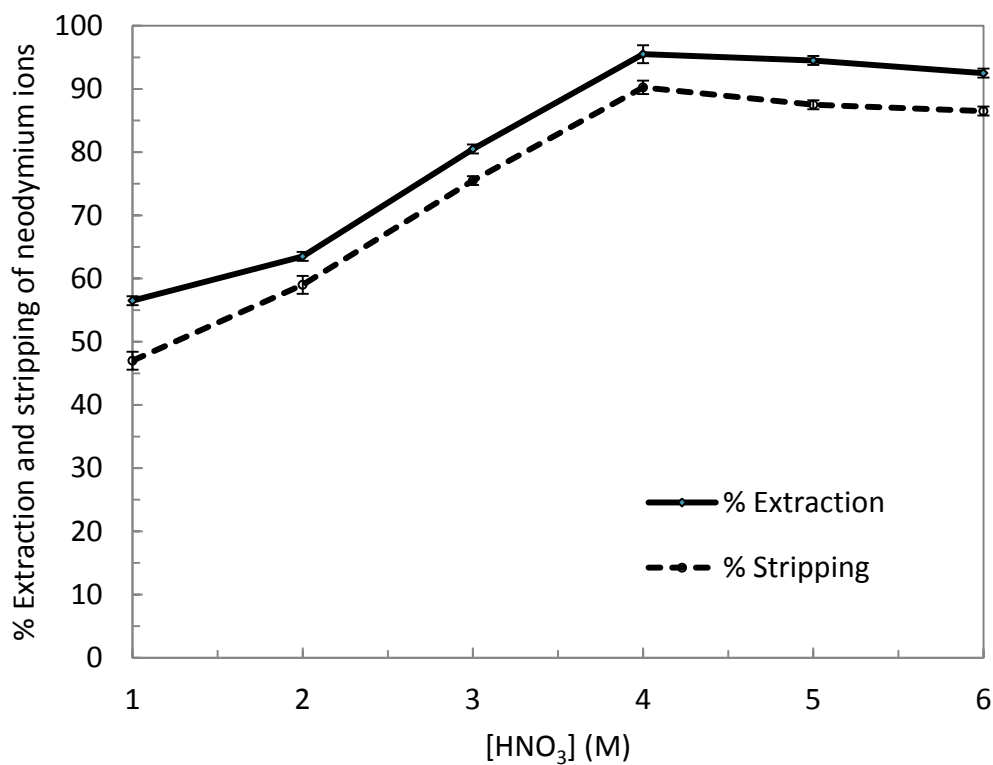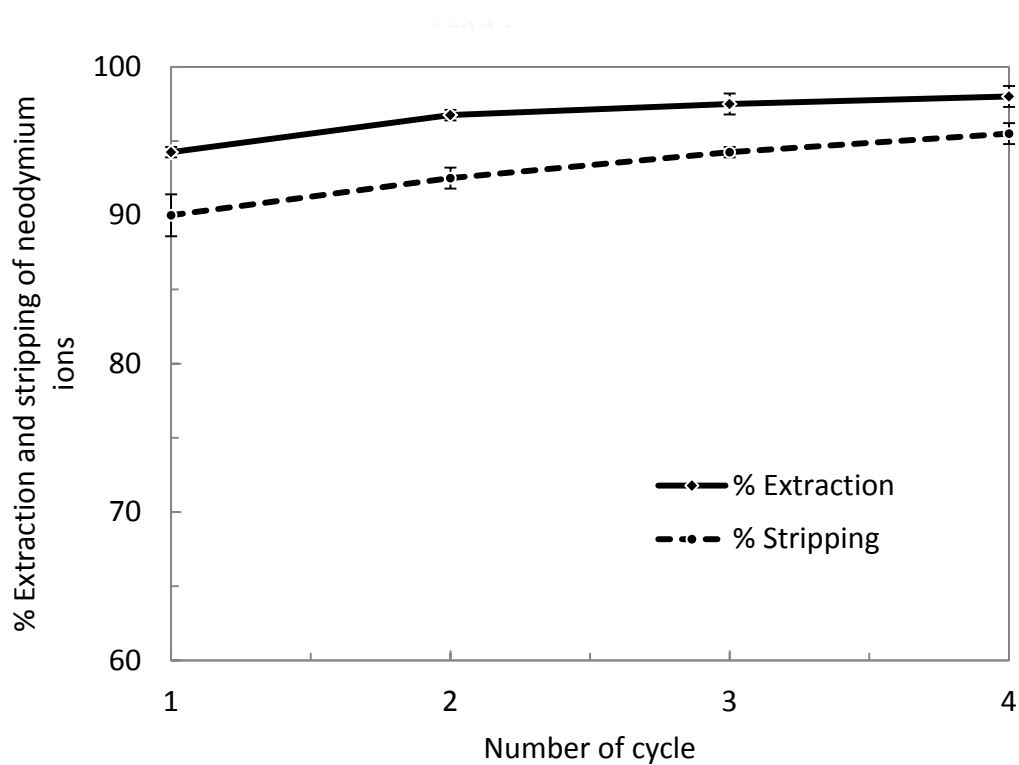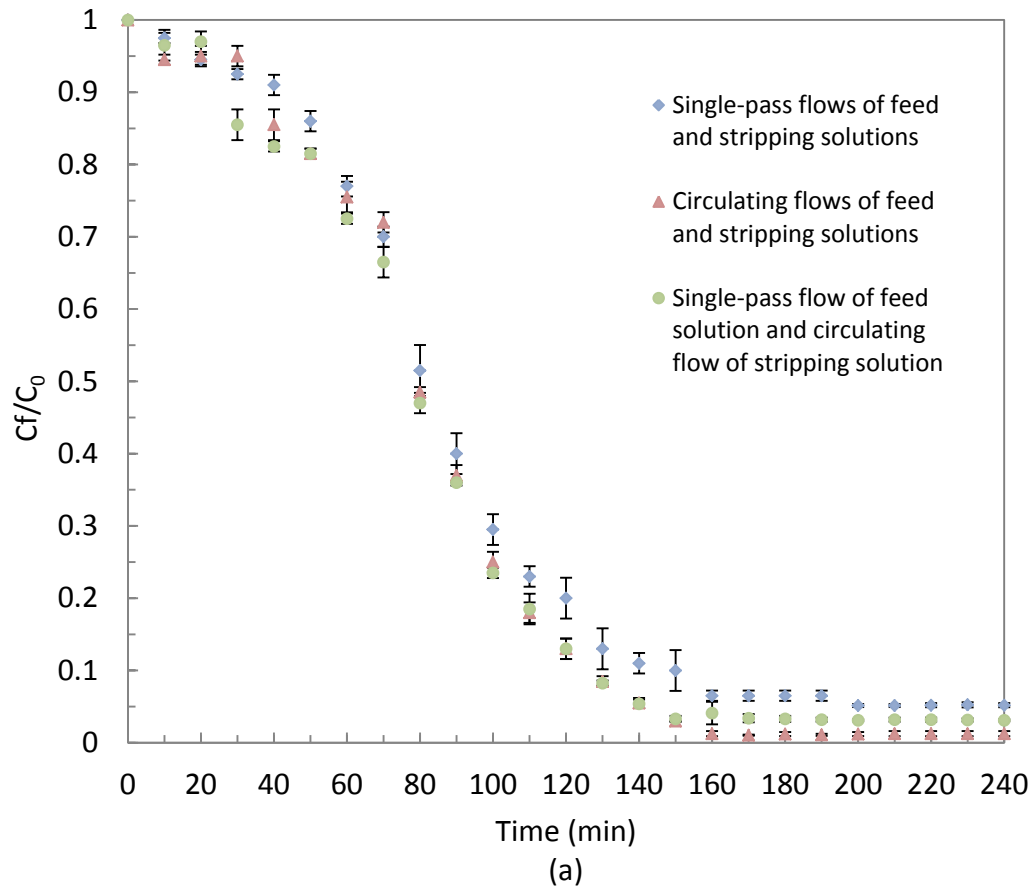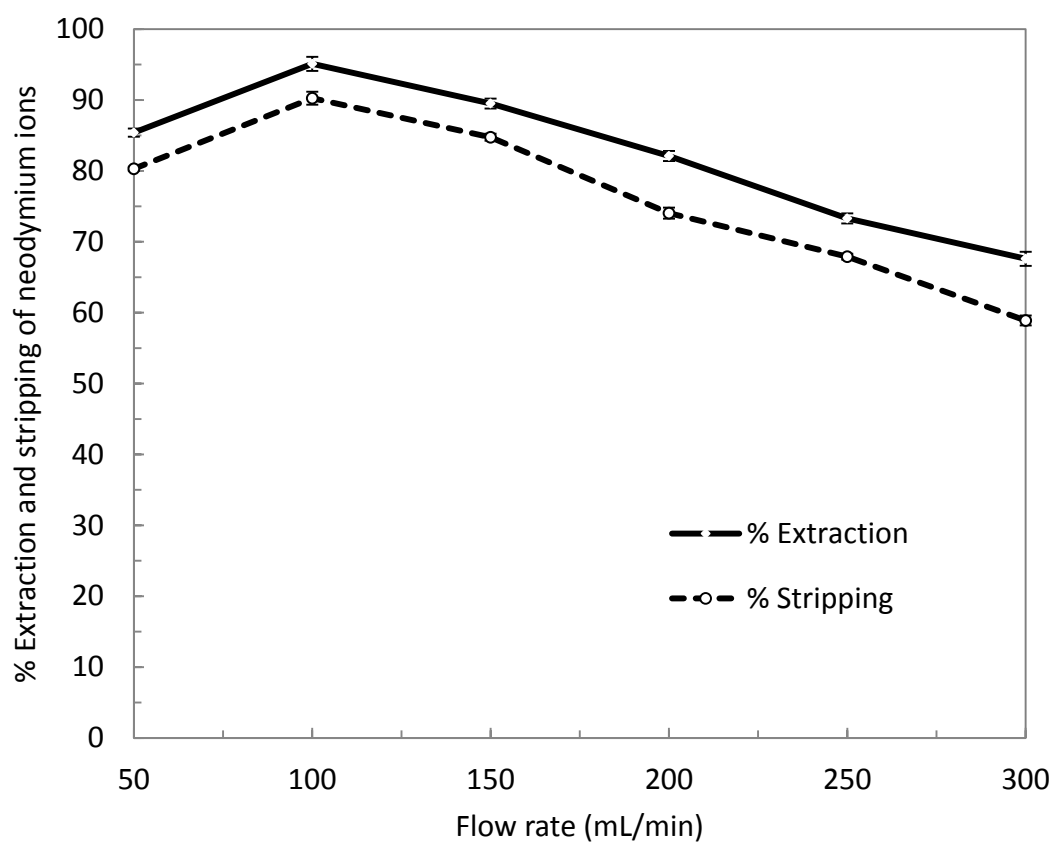

Figure 6.6 Percentage of neodymium ions vs flow rate (feed = pH 4.5; synergistic extractants: 0.1M Cyanex 272 and 0.05M TOPO; stripping: 4 M HNO_3).

6.5.7   Mass transfer coefficients

The values of mass transfer coefficients can be calculated employing optimum conditions. The values of the four individual mass transfer coefficients and the relative contribution of each resistance can be characterized by fractional resistance with respect to the total resistance as shown in Table 6.8. Results show that the highest fractional resistance is a chemical reaction, indicating that mass transfer in the chemical reaction is important as regards the overall mass transfer process.

Table 6.8 The effect of flow rate of both feed and stripping solutions and relative resistance of neodymium ions overall mass transfer resistance

Flow rate (mL/min)	Tube side k_{af} (cm/s)	Δ_t (%)	Membrane k_m (cm/s)	Δ_m (%)	Reaction k_e (cm/s)	Δ_e (%)	Between of hollow k_o (cm/s)	Δ_o (%)
50	3.99×10^{-4}	9.67	5.15×10^{-4}	7.49	5.87×10^{-5}	70.54	3.14×10^{-4}	12.28
100	4.15×10^{-4}	9.16	5.15×10^{-4}	7.38	4.12×10^{-5}	77.95	3.98×10^{-4}	8.06
150	5.67×10^{-4}	6.36	5.15×10^{-4}	7.00	5.15×10^{-5}	76.21	4.25×10^{-4}	9.23
200	6.18×10^{-4}	6.63	5.15×10^{-4}	7.95	5.31×10^{-5}	77.18	4.98×10^{-4}	8.22
250	6.42×10^{-4}	6.67	5.15×10^{-4}	8.32	5.58×10^{-5}	76.81	5.24×10^{-4}	8.18
300	6.98×10^{-4}	7.00	5.15×10^{-4}	9.48	6.49×10^{-5}	75.29	5.95×10^{-4}	8.21

Note: feed = pH 4.5; synergistic extractants = 0.1M Cyanex 272 and 0.05M TOPO; stripping = 4M HNO_3

6.6 Conclusion
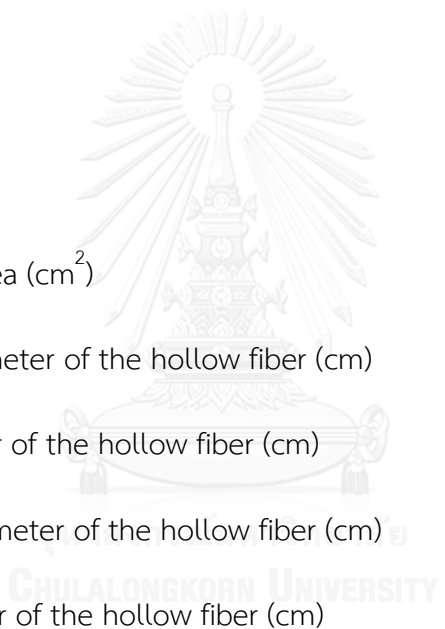
Results show that the HFSLM system could successfully extract neodymium ions from monazite leach solution. A quadratic regression model, predicted by using CCD, revealed the interaction between independent parameters (concentrations of Cyanex 272 and TOPO). The acquired statistical model had an excellent goodness of fit confirmed by the significant regression coefficient ($p<0.05$). The results suggested that the concentration of both Cyanex 272 and TOPO had a significant effect on the extraction of neodymium ions. Performance was considerably enhanced by running the operation in repeated cycle mode. After the fourth repeat cycle, the cumulative extraction and stripping of neodymium ions reached 98% and 95%, respectively. Under optimal operating conditions, the fractional resistance of chemical reaction reached the highest, indicating the control by the chemical reaction for the transport of neodymium ions through the hollow fiber supported liquid membrane.

6.7 Acknowledge

6.8   Nomenclature

A membrane area (cm^2)

d_h hydraulic diameter of the hollow fiber (cm)

d_i inner diameter of the hollow fiber (cm)

d_{lm} log–mean diameter of the hollow fiber (cm)

d_o outer diameter of the hollow fiber (cm)

D_{aq} aqueous diffusion coefficient (-)

D_m diffusivity of neodymium ions extractant complex in the liquid membrane

         phase (cm^2/s)

$D_{Nd,a}$ diffusivity of neodymium ions in the aqueous solution (cm^2/s)

J flux of neodymium ion through the liquid membrane phase ($\mathbf{mg\,/\,cm^2 \cdot s}$)

K_{total} overall mass transfer coefficient (cm/s)

k_{af} mass transfer coefficient in the feed solution (cm/s)

k_e mass transfer coefficient due to the extraction reaction (cm/s)

k_{ex} forward constants in the extraction reaction

k_m mass transfer coefficient of the liquid membrane phase (cm/s)

k_o mass transfer coefficient in the shell side between of the hollow fibers (cm/s)

k_s mass transfer coefficient due to the stripping reaction (cm/s)

k_{as} mass transfer coefficient for the stripping solution (cm/s)

k_{st} reverse constants in the extraction reaction

L fiber module length (cm)

m_f partition coefficient between the liquid membrane and the feed phase (-)

m_s partition coefficient between the liquid membrane and the stripping phase (-)

r_i inner radius of the hollow fiber (cm)

r_o outer radius of the hollow fiber (cm)

R overall mass transfer resistance (s/cm)

Re Reynolds number (-)

Sc Schmidt number (-)

Sh Sherwood number (-)

t time (s)

v_f linear velocity of feed solution in the tube side (cm/s)

v_s linear velocity of feed solution in the shell side (cm/s)

V_f volume of the feed solution (cm^3)

V_m volume of the liquid membrane solution (cm^3)

ε porosity of hollow fiber (%)

τ tortuosity factor membrane (-)

ν kinematic viscosity of organic phase (cm^2/s)

6.9   References

Anitha, M., Ambare, D.N., Kotekar, M.K., Singh, D.K., Singh, H., Studies on Permeation of Nd (III) through Supported Liquid Membrane Using DNPPA + TOPO as Carrier. Separation Science and Technology, 2013, **48(14)**, 2196-2203.

Ansari, S.A., Mohapatra, P.K., Manchanda, V.K., Recovery of Actinides and Lanthanides from High-Level Waste Using Hollow-Fiber Supported Liquid Membrane with TODGA as the Carrier. Industrial & Engineering Chemistry Research, 2009, **48(18)**, 8605-8612.

Baudot, A., Floury, J., Smorenburg, H.E., Liquid-liquid extraction of aroma compounds with hollow fiber contactor. AIChE Journal, 2001, **47(8)**, 1780-1793.

Biswas, S., Pathak, P.N., Pal, S., Roy, S.B., Tewari, P.K., Manchanda, V.K., Uranium Permeation from Nitrate Medium Across Supported Liquid Membrane

Containing Acidic Organophosphorous Extractants and their Mixtures with Neutral Oxodonors. Separation Science and Technology, 2011, **46(13)**, 2110-2118.

Biswas, S., Pathak, P.N., Roy, S.B., Carrier facilitated transport of uranium across supported liquid membrane using dinonyl phenyl phosphoric acid and its mixture with neutral donors. Desalination, 2012, **290(0)**, 74-82.

Breembroek, G.R.M., van Straalen, A., Witkamp, G.J., van Rosmalen, G.M., Extraction of cadmium and copper using hollow fiber supported liquid membranes. Journal of Membrane Science, 1998, **146(2)**, 185-195.

Cheng, K., Choi, K., Kim, J., Sung, I.H., Chung, D.S., Sensitive arsenic analysis by carrier-mediated counter-transport single drop microextraction coupled with capillary electrophoresis. Microchemical Journal, 2013, **106(0)**, 220-225.

Coelhoso, I.M., Cardoso, M.M., Viegas, R.M.C., Crespo, J.P.S.G., Transport mechanisms and modelling in liquid membrane contactors. Separation and Purification Technology, 2000, **19(3)**, 183-197.

Desouky, O.A., Daher, A.M., Abdel-Monem, Y.K., Galhoum, A.A., Liquid–liquid extraction of yttrium using primene-JMT from acidic sulfate solutions. Hydrometallurgy, 2009, **96(4)**, 313-317.

Dogmane, S.D., Singh, R.K., Bajpai, D.D., Mathur, J.N., Extraction of U(VI) by cyanex-272. Journal of Radioanalytical and Nuclear Chemistry, 2002, **253(3)**, 477-482.

El-Nadi, Y.A., Effect of diluents on the extraction of praseodymium and samarium by Cyanex 923 from acidic nitrate medium. Journal of Rare Earths, 2010, **28(2)**, 215-220.

El-Nadi, Y.A., Lanthanum and neodymium from Egyptian monazite: Synergistic extractive separation using organophosphorus reagents. Hydrometallurgy, 2012, **119–120(0)**, 23-29.

El-Nadi, Y.A., El-Hefny, N.E., Daoud, J.A., Extraction of Lanthanum and Samarium from Nitrate Medium by some Commercial Organophosphorus Extractants. Solvent Extraction and Ion Exchange, 2007, **25(2)**, 225-240.

Fontana, D., Pietrelli, L., Separation of middle rare earths by solvent extraction using 2-ethylhexylphosphonic acid mono-2-ethylhexyl ester as an extractant. Journal of Rare Earths, 2009, **27(5)**, 830-833.

Gaikwad, A.G., Rajput, A.M., Transport of yttrium metal ions through fibers supported liquid membrane solvent extraction. Journal of Rare Earths, 2010, **28(1)**, 1-6.

Güell, R., Anticó, E., Salvadó, V., Fontàs, C., Efficient hollow fiber supported liquid membrane system for the removal and preconcentration of Cr(VI) at trace levels. Separation and Purification Technology, 2008, **62(2)**, 389-393.

Hnghag, P., Encyclopedia of the Elements Technical Data. 2004.

Chakrabarty, K., Krishna, K.V., Saha, P., Ghoshal, A.K., Extraction and recovery of lignosulfonate from its aqueous solution using bulk liquid membrane. Journal of Membrane Science, 2009, **330**, 135-144.

Khanmohammadi, M., Khoshfetrat, A.B., Eskandarnezhad, S., Sani, N.F., Ebrahimi, S., Sequential optimization strategy for hyaluronic acid extraction from eggshell and its partial characterization. Journal of Industrial and Engineering Chemistry, 2014, **20(6)**, 4371-4376.

Kocherginsky, N.M., Yang, Q., Big Carrousel mechanism of copper removal from ammoniacal wastewater through supported liquid membrane. Separation and Purification Technology, 2007, **54(1)**, 104-116.

Kocherginsky, N.M., Yang, Q., Seelam, L., Recent advances in supported liquid membrane technology. Separation and Purification Technology, 2007, **53(2)**, 171-177.

Lee, M.-S., Lee, J.-Y., Kim, J.-S., Lee, G.-S., Solvent extraction of neodymium ions from hydrochloric acid solution using PC88A and saponified PC88A. Separation and Purification Technology, 2005, **46(1–2)**, 72-78.

Luo, F., Li, D., Wei, P., Synergistic extraction of zinc(II) and cadmium(II) with mixtures of primary amine N1923 and neutral organophosphorous derivatives. Hydrometallurgy, 2004, **73(1–2)**, 31-40.

Leveque, M.A., De la, L.L., transmission de chaleur par convection. Ann. Mines, 1928, **13**, 201-239.

Naik, P., Dhami, P., Misra, S., Jambunathan, U., Mathur, J., Use of organophosphorus extractants impregnated on silica gel for the extraction chromatographic separation of minor actinides from high level waste solutions. Journal of Radioanalytical and Nuclear Chemistry Articles, 2003, **257(2)**, 327-332.

Pei, L., Wang, L., Yu, G., Separation of Eu(III) with supported dispersion liquid membrane system containing D2EHPA as carrier and HNO3 solution as stripping solution. Journal of Rare Earths, 2011, **29(1)**, 7-14.

Pei, L., Wang, L., Yu, G., Study on a novel flat renewal supported liquid membrane with D2EHPA and hydrogen nitrate for neodymium extraction. Journal of Rare Earths, 2012, **30(1)**, 63-68.

Ramakul, P., Supajaroon, T., Prapasawat, T., Pancharoen, U., Lothongkum, A.W., Synergistic separation of yttrium ions in lanthanide series from rare earths mixture via hollow fiber supported liquid membrane. Journal of Industrial and Engineering Chemistry, 2009, **15(2)**, 224-228.

Saleh, M.I., Bari, M.F., Saad, B., Solvent extraction of lanthanum(III) from acidic nitrate-acetato medium by Cyanex 272 in toluene. Hydrometallurgy, 2002, **63(1)**, 75-84.

San Román, M.F., Bringas, E., Ibaňez, R., Ortiz, I., Liquid membrane technology: fundamentals and review of its applications. Journal of Chemical Technology & Biotechnology, 2010, **85(1)**, 2-10.

Sella, C., Becis, A., Cote, G., Bauer, D., DIPHASIC ACIDO-BASIC PROPERTIES OF DI(OCTYLPHENYL)PHOSPHORIC ACID (DOPPA). Solvent Extraction and Ion Exchange, 1995, **13(4)**, 715-729.

Suren, S., Wongsawa, T., Pancharoen, U., Prapasawat, T., Lothongkum, A.W., Uphill transport and mathematical model of Pb(II) from dilute synthetic lead-containing solutions across hollow fiber supported liquid membrane. Chemical Engineering Journal, 2012, **191(0)**, 503-511.

Tang, Y., Liu, W., Wan, J., Wang, Y., Yang, X., Two-stage recovery of S-adenosylmethionine using supported liquid membranes with strip dispersion. Process Biochemistry, 2013, **48(12)**, 1980-1991.

Wang, X., Du, M., Liu, H., Synergistic extraction study of samarium(III) from chloride medium by mixtures of bis(2,4,4-trimethylpentyl)phosphinic acid and 8-hydroxyquinoline. Separation and Purification Technology, 2012, **93(0)**, 48-51.

Wu, D., Zhang, Q., Bao, B., Solvent extraction of Pr and Nd (III) from chloride-acetate medium by 8-hydroquinoline with and without 2-ethylhexyl phosphoric acid mono-2-ethylhexyl ester as an added synergist in heptane diluent. Hydrometallurgy, 2007, **88(1–4)**, 210-215.

Xie, F., Zhang, T.A., Dreisinger, D., Doyle, F., A critical review on solvent extraction of rare earths from aqueous solutions. Minerals Engineering, 2014, **56(0)**, 10-28.

Yang, Q., Kocherginsky, N.M., Copper recovery and spent ammoniacal etchant regeneration based on hollow fiber supported liquid membrane technology: From bench-scale to pilot-scale tests. Journal of Membrane Science, 2006, **286(1–2)**, 301-309.
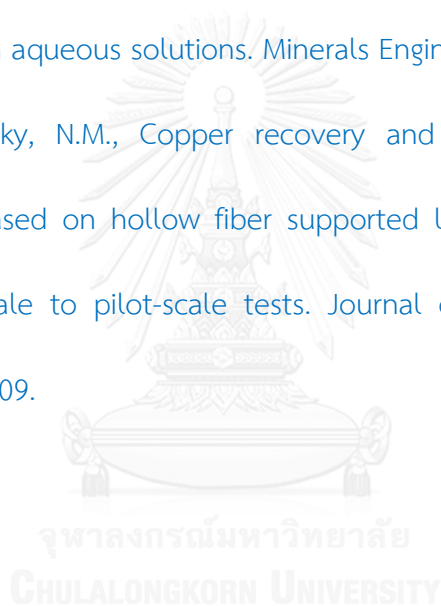
CHAPTER 7

Separation and mass transport of Nd(III) from mixed rare earths via hollow fiber supported liquid membrane: experiment and modeling

Thanaporn Wannachod[a], Natchanun Leepipatpiboon[b], Ura Pancharoen[a],* and Kasidit Nootong[a], **

[a]Department of Chemical Engineering, Faculty of Engineering, Chulalongkorn University, Patumwan, Bangkok 10330, Thailand

[b]Chromatography and Separation Research Unit, Department of Chemistry, Faculty of Science, Chulalongkorn University, Patumwan, Bangkok 10330, Thailand

7.1 Abstract

The separation of Nd(III) from mixed rare earths via hollow fiber supported liquid membrane (HFSLM) was examined. Percentages of extraction and stripping of Nd(III) attained were 95% and 87%, respectively. Optimum condition was achieved using 4.5 pH of feed solution, 0.5 M 2-ethylhexyl-2-ethylhexyl phosphoric acid (HEHEPA) dissolved in octane as the extractant and 4 M HNO_3 of stripping solution. The flow rates of both feed and stripping phase were 100 mL/min. A mathematical model was developed on the conservation of mass which consisted of convection, diffusion, reaction and accumulation. The model results prediction proved to be in good agreement with the experimental data at an average Standard Deviation of 1.9% and 1.2%, respectively.

7.2 Introduction

Rare earth metals (REMs) consist of the three elements that is Sc, Y, La and fourteen lanthanides, namely, from cerium to lutetium. The total number of REMs is thus 17. They are divided conventionally into two groups: the light group (Sc, La, Ce,

Pr, Nd, Pm, Sm, Eu, Gd) and the heavy group (Y, Tb, Dy, Ho, Er, Tm, Yb, Lu) [1].
Neodymium, for example, is one of the most abundant rare earth elements.
Neodymium is of current commercial interest as it is the basis for the most common
solid state lasers used in material processing such as in medicine [2]. Neodymium is
also the raw material used for high-strength permanent magnet (Nd-B-Fe) and it costs
less than samarium-cobalt permanent magnet [3].

The use of membrane in combination with a chemical or biological treatment
process is attractive for waste water treatment. It answers the demand for efficient,
compact and discreet treatment units suitable for densely populated areas where
both the land cost and sensitivities are high [4]. Membrane technology has attracted
the attention of many researchers for metal removal and wastewater treatment.
Yeung's team was one team of potential group researchers [5-7]. Their work
successfully demonstrated the MCM-41 (LUS-type) membranes. LUS membranes can
enhance high selectivity to Cu(II) for the Cu(II)/Au(III) system [7]. Recent studies have
investigated the use of hollow fiber supported liquid membrane (HFSLM) for
separating various trace metal ions from aqueous solutions. The HFSLM system
allows for both simultaneous extraction and stripping process of target ions in one
single-step operation [8]. Advantages of HFSLM over traditional methods include

lower energy consumption, lower capital and operating cost and less extractant used [9]. HFSLM has a high surface area per unit volume for mass transfer [10]. Therefore, HFSLM was used to separate metal ions, radioactive and lanthanide metals. Pancharoen et al. [11] for example reported on the separation of Ce(IV) and La(III) from sulfate media via HFSLM using trioctyl amide (TOA) as the extractant. Results demonstrated that this system was most efficient in removing Ce(IV) from La(III). Further, Ramakul et al. [12] separated uranium ions from nitrate media across HFSLM. Tri-butyl phosphate (TBP) diluted in kerosene was used as the extractant and sodium hydroxide was applied as a stripping solution. The percentage of uranium ions extraction attained 67% using TBP 5%(v/v). Ansari et al. [13] applied HFSLM for the recovery of actinides and lanthanides from high-level waste. TODGA was used as the carrier.

Since reliable mathematical models provide an understanding of the transport mechanism of target species across liquid membrane, from the feed side to stripping side, they therefore, are required. The models also help in the scale-up of the HFSLM system. Most models have been developed based on the principle of a facilitated diffusional transport mechanism neglecting the chemical reactions in the system. Vernekar et al. [14] developed a model for the transport of Co(II) across

HFSLM based on facilitated diffusional transport, neglecting complexation and de-complexation reactions. The results indicated that the controlling step of Co(II) transport was the diffusion in the liquid membrane phase.

Kandwal et al. [15] established a mathematical model describing the transport of Cs(I) through HFSLM based on facilitated diffusional transport mechanism. Chemical reactions were neglected. The results showed that the mathematical model was acceptable

Yang and Kocherginsky [16] found that the transport of Cu(II) across liquid membrane also depended on chemical reactions. Pancharoen et al. [17] developed a mathematical model describing the transport of Cu(II) via HFSLM. This model was developed based on chemical reaction at the feed-liquid-membrane interface, neglecting the diffusion. The modeled results fitted in well with the experimental data. This confirmed that the transport of Cu(II) via HFSLM was controlled by a chemical reaction. However, this model describes the transport of target ions only in the feed side.

Developing a mathematical model based on chemical reactions leads to a complicated series of differential equations. The concept of Generating Function has been used to solve the series of differential equations in catalytic polymerization which are not easy to solve due to difficulty in integrating. By using this concept, the chemical kinetic problems have been overcome in many cases [18]. Suren et al. [19] developed a mathematical model describing the transport of Hg(II) via HFSLM. This model was developed based on chemical reaction at the feed-liquid-membrane interface, neglecting the diffusion. Therefore, a mathematical model, based on conservation of mass which consisted of convection, diffusion, reaction and accumulation, was developed in this work to describe the transport of target ions across HFSLM from feed side to stripping side.

Previous successful research on the separation of rare earth metals is summarized below in Table 7.1. Examples of the mathematical models developed, describing the transport of target ions, are shown in Table 7.2.

Table 7.1 Summary of previous research on lanthanides

Authors	Metals	Extractants	Diluents	Stripping	Methods	Ref.
Saleh et al.	La	Cyanex 272	Toluene	HNO_3	L-L	[20]
Lee et al.	Nd	PC-88A	Kerosene	HCl	L-L	[21]
Wu et al.	Nd	8-hydroxyquinoline	Heptane	H_2SO_4	L-L	[22]
Fontana et al.	Middle RE	HEHEPA	Kerosene	HCl	L-L	[23]
Desouky et al.	Y	Primene-JMT	Kerosene	HNO_3	L-L	[24]
Nadi et al.	Pr, Sm	Cyanex 923	Octane	H_2SO_4	L-L	[25]
Mangesh et al.	Y	TEHP	Toluene	HCl	L-L	[26]
Liang et a.l	Eu	D2EHPA	Kerosene	HCl	LM	[27]
Liang et al.	Nd	D2EHPA	Kerosene	HNO_3	LM	[28]
Gaikwad et al.	Y	PC-88A	Toluene	HCl	FSLM	[29]

Note: L-L= Liquid-liquid extraction, LM = Liquid membrane, FSLM = Flat sheet and HFSLM = Hollow fiber supported liquid membrane

Table 7.2 Literature reviews of a mathematical model for HFSLM

Authors	Metals	Extractant	Stripping	Considered parameters				Methods	% S.D.		Ref.
				(1)	(2)	(3)	(4)		F	S	
Vernekar et al.	Co	D2EHPA	H_2SO_4	✓	✓	-	-	Successive substitution	N/A	N/A	[14]
Kandwal et al.	Cs	CNC	Di-water	✓	✓	-	-	Integral	10	N/A	[15]
Yang et al.	Cu	LIX54	H_2SO_4	✓	-	✓	-	Empirical correlation	N/A	N/A	[16]
Pancharoen et. al.	Cu	LIX84	H_2SO_4	✓	-	✓	✓	Laplace	2	N/A	[17]
Suren et. al.	Hg	Aliquat336	Thiourea	✓	-	✓	✓	Generating	2	5	[19]
Chaturabul et. al.	Pd	TRHCl–OA	$NaNO_2$	✓	-	✓	✓	Laplace	11	2	[30]
This work	Nd	HEHEPA	H_2SO_4	✓	✓	✓	✓	Generating	1.9	1.2	

Note: (1) convection transport (2) diffusion transport (3) reaction (4) mass accumulation

F = Feed and S = Strip

This work studies the extraction and stripping of Nd(III) from nitrate solution – the digestion product of monazite ores processing. The pH of feed solution, the concentration of extractant 2-ethylhexyl-2-ethylhexyl phosphoric acid (HEHEPA), the concentration of stripping solution and the flow rate of both feed and stripping solutions were investigated. The choice of extractant, organic diluent and stripping solution is vital for the success of the separation of Nd(III) as in previous work. A mathematical model, based on the conservation of mass which consisted of convection, diffusion, reaction and accumulation, was developed to describe the transport of Nd(III) in both feed and stripping sides. The complicated series of differential equations arising from the model was solved by the concept of Generating Function. In order to verify the model equations, the results achieved by the experiment were compared with those obtained from the model.

7.3 Modeling of Nd(III) Transport

7.3.1 Transport of Nd(III) across the liquid membrane phase

The organic extractant, dissolved in diluent, was trapped in the hydrophobic micro-pores of the hollow fibers as the liquid membrane. Then, the feed solution containing target metal ions and stripping solution was fed counter-currently through

the tube and shell sides of the hollow fiber module, respectively. The transport of

Nd(III) across the liquid membrane phase is presented in Fig.7.1.

(a)

(b)
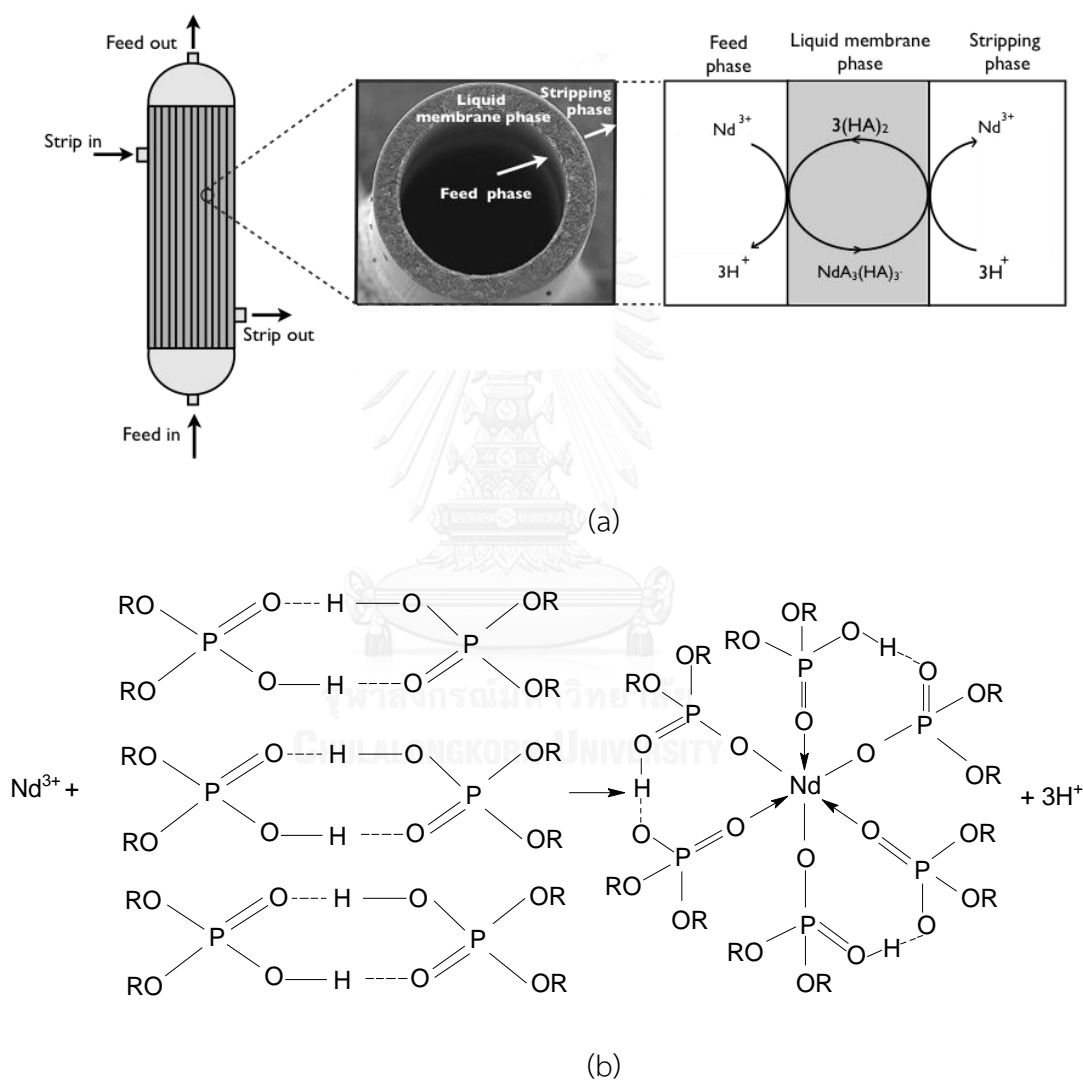
Figure 7.1 (a) Schematic of mass transport of Nd(III) across the liquid membrane phase using HEHEPA as extractant and HNO_3 as the stripping solution (b) Schematic of the chemical reaction of Nd^{3+} with HEHEPA $((RO)_2POOH)$ to form the complex species $(NdA_3(HA)_3)$.

The extraction of Nd(III) from the feed solution with carrier HEHEPA i.e. $(HA)_2$ in octane can be expressed as [23]:

$$Nd^{3+}_{(aq)} + 3(HA)_{2(org)} \xrightleftharpoons{k_{Ex}} NdA_3(HA)_{3(org)} + 3H^+_{(aq)} \qquad (7.1)$$
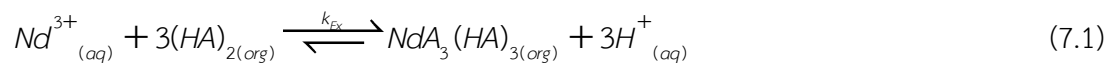
where (aq) represents the species in the aqueous phase and (org) represents the species in the liquid membrane phase, $(HA)_2$ is the dimer form of HEHEPA and k_{Ex} denotes forward reaction percentage constant at the interface between the feed phase and liquid membrane phase.

At the liquid membrane stripping interface, the complex species $NdA_3(HA)_3$ reacts continuously with hydrogen ions from the stripping solution and then releases Nd(III) into the stripping phase as follows:

$$NdA_3(HA)_{3(org)} + 3H^+_{(aq)} \xrightleftharpoons{k_{St}} Nd^{3+}_{(aq)} + 3(HA)_{2(org)} \qquad (7.2)$$
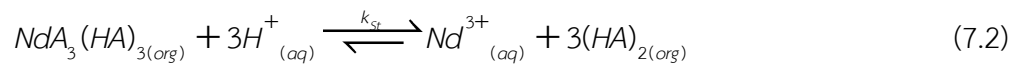
where k_{St} denotes backward reaction percentage constant at the interface between the stripping phase and liquid membrane phase.

In the hollow fiber operation, metal ions in the complex, occurring at the feed–liquid-membrane interface, are stripped out continuously by the stripping agent at the liquid-membrane–stripping interface. Therefore, the total reaction in Eq. (7.1) can be considered as the forward reaction.

The reaction rate of extraction of Nd(III) ($r_{A,Ex}$) can be written as:

$$r_{A,Ex}\left(x,t\right) = -k_{Ex}C_{A,F}^{m}\left(x,t\right) \tag{7.3}$$

where x is any distance along the axis of the hollow fiber in the feed phase, $o \leq x \leq L$, as shown in Fig. 7.2, k_{Ex} is the reaction rate constant of extraction, t is the extraction time, $C_{A,F}$ is the concentration of metal ions in the feed solution (mg/L) and m is the reaction order of extraction.

To strip metal ions, the stripping solution is kept at excess concentration. Therefore, the total reaction of stripping of Nd(III) in Eq. (7.2) can be considered as the forward reaction. Thus, the reaction rate of stripping of Nd(III) ($r_{A,St}$) can be described as follows:

$$r_{A,St}(x,t) = k_{St} C_{A,St}^{n}(x',t) \tag{7.4}$$

where x' is any distance along the axis of the hollow fiber in the stripping phase and equal to $L - x$, as shown in Fig. 7.2, k_{St} is the reaction rate constant of stripping, t is the stripping time, $C_{A,St}$ is the concentration of metal ions in the stripping solution (mg/L) and n is the reaction order of stripping.

7.3.2 Developing a model for neodymium transport via HFSLM

The transport of target ions across HFSLM corresponds to the axial convection, diffusion, extraction reaction and accumulation [31,32].

The mathematical model for the feed phase is developed based on the following assumptions:

1. The system is isothermal at constant pressure and volume in the process of mass transfer.

2. The hollow fiber tube is very small. Thus, the radial-concentration profile of neodymium ions is constant. The diffusion fluxes of Nd(III) in the feed phase exit only in the axial direction.

3. The reaction takes place at the interface between the feed phase and the liquid membrane phase.

4. Only complex species occurring at the interface, not Nd(III), are transported across the liquid membrane phase.

The mathematical model for the stripping phases is developed based on the following assumptions:

1. The system is isothermal at constant pressure and volume in the process of mass transfer.

2. Only neodymium ions from the reaction at the liquid membrane stripping interface transport into the stripping phase [8].

.3. The diffusion of neodymium ions in the stripping phase occurs only in the axial direction.

The mathematical model to describe the transport of metal ions from the feed to stripping phases across the liquid membrane is considered based on conservation of mass at small segments of the hollow fibers, as shown in Fig. 7.2. The conservation of mass at small segments of the hollow fibers is shown in Eq. (7.5).
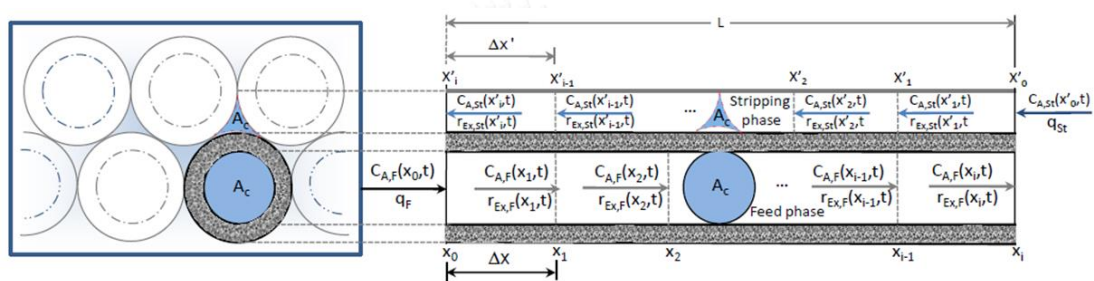
Figure 7.2 Schematic of the transport mechanism of metal ions through small segments of the feed phase (tube side) and stripping phase (shell side)

$$
\begin{bmatrix} \text{Rate of mass} \\ \text{transport into} \\ \text{the system by} \\ \text{convection} \end{bmatrix} - \begin{bmatrix} \text{Rate of mass} \\ \text{transport out of} \\ \text{the system by} \\ \text{convection} \end{bmatrix} + \begin{bmatrix} \text{Rate of mass} \\ \text{transport through} \\ \text{the system by} \\ \text{diffusion} \end{bmatrix} - \begin{bmatrix} \text{Rate of mass} \\ \text{extracted by} \\ \text{extraction} \\ \text{reaction} \end{bmatrix} = \begin{bmatrix} \text{Rate of mass} \\ \text{accumulation} \\ \text{within the} \\ \text{small segment} \end{bmatrix}
$$

(7.5)

In the feed phase, the conservation of mass for metal ions in each small segment (Δx) is described by Eq. (7.6):

$$q_F C_{A,F}\left(x_{i-1},t\right) - q_F C_{A,F}\left(x_i,t\right) + \frac{A_C D_F}{\Delta x}\left[C_{A,F}\left(x_i,t\right) - C_{A,F}\left(x_{i-1},t\right)\right] + r_{A,Ex}\left(x_i,t\right)\cdot V_p$$

$$=V_t \frac{dC_{A,F}\left(x_i,t\right)}{dt} \tag{7.6}$$

where q_F is the volumetric flow rate of the feed solution, i is the number of small segments, V_p is the pore volume of a small segment at the shell of hollow fiber and V_t is the volume of a small segment on the tube side of the hollow fiber.

Solving Eq. (7.6) by the concept of Generating Function, as expressed in detail in Appendix A, the equation for estimating the concentration of metal ions in the outlet feed solution ($C_{A,F}(x_i,t)$) can be expressed as:

$$C_{A,F}\left(x_i,t\right) = -C_{A,F}\left(0,0\right)e^{\frac{-\lambda t q_F}{V_t}}\sum_{l=1}^{i}\frac{1}{(i-l)!}\frac{(\lambda)^l}{(\omega^{-i+2l})}\cdot\left(\frac{tq_F}{V_p}\right)^{i-l} + \frac{V_p\alpha}{q_F\lambda}e^{\frac{-\lambda t q_F}{V_t}}\sum_{l=1}^{i}\frac{\omega^{i-l}}{(i-l)!}\left(\frac{tq_F}{V_p}\right)^{i-l}\sum_{j=1}^{l}\left(\frac{\omega}{\lambda}\right)^{j-1}$$

$$+\frac{V_p\alpha}{q_F\lambda}\sum_{l=1}^{i}\left(\frac{\omega}{\lambda}\right)^{i-l} - C_{A,F}\left(0,0\right)\left(\frac{\omega}{\lambda}\right)^i \tag{7.7}$$

where the detail is shown in Appendix A.

In the case of the stripping phase for a counter-current flow, the conservation of mass of metal ions at segment *i* can be expressed as follows:

$$q_{St}C_{A,St}\left(x_{i-1},t\right) - q_{St}C_{A,St}\left(x_{i},t\right) + \frac{A_{c}D_{St}}{\Delta x}\left[C_{A,St}\left(x_{i},t\right) - C_{A,St}\left(x_{i-1},t\right)\right] + r_{A,St}\left(x_{i},t\right)\cdot V_{p}$$

$$= V_{s}\frac{dC_{A,St}\left(x_{i},t\right)}{dt} \tag{7.8}$$

where q_{St} is the volumetric flow rate of the stripping solution and V_{s} is the volume of a small segment on the shell side of the hollow fiber.

Solving Eq. (7.8) by the concept of Generating Function, as expressed in detail in Appendix A, the equation for estimating the concentration of metal ions in the outlet stripping solution ($C_{A,St}(x_{i}',t)$) is obtained as shown below:

$$C_{A,St}\left(x_{i}',t\right) = -C_{A,St}\left(x_{0}',t\right)e^{\frac{t\theta q_{St}}{V_{s}}}\sum_{l=1}^{i}\frac{1}{(i-l)!}\frac{\theta^{l}}{\delta^{-i+2l}}\cdot\left(\frac{tq_{St}}{V_{p}}\right)^{i-l} - \frac{V_{p}\gamma}{\theta q_{St}}e^{\frac{t\theta q_{St}}{V_{s}}}\sum_{l=1}^{i}\frac{\delta^{i-l}}{(i-l)!}\left(\frac{tq_{St}}{V_{p}}\right)^{i-l}\sum_{j=1}^{l}\left(\frac{\delta}{\theta}\right)^{j-1}$$

$$+\frac{V_p\gamma}{q_{St}\theta}\sum_{l=1}^{i}\left(\frac{\delta}{\theta}\right)^{i-l}+C_{A,St}\left(x_0',0\right)\left(\frac{\delta}{\theta}\right)^{i} \qquad (7.9)$$

where $C_{A,St}(x_0',0)$ is the initial concentration of metal ions in the stripping solution at

position x_0'. The detail in Eq. (7.9) is described in Appendix A.

The outlet concentration of Nd(III) in both feed and stripping phases are

presented as percentages of extraction and stripping. The equations for calculating

percentages of extraction and stripping are shown in Eqs. (7.10) and (7.11)

respectively:

$$\%\ Extraction = \frac{C_{f,in} - C_{f,out}}{C_{f,in}} \times 100 \qquad (7.10)$$

$$\%\ Stripping = \frac{C_{s,out} - C_{s,in}}{C_{f,in}} \times 100 \qquad (7.11)$$

where $C_{f,in}$, $C_{s,in}$ denote the initial concentration in the feed and stripping phases and

$C_{f,out}$, $C_{s,out}$ denote the outlet concentration in the feed and stripping phases.

7.4 Experiment

7.4.1 Reagents and solutions

The Rare Earth Research and Development Center, Office of Atoms for Peace, Bangkok, Thailand, supplied the feed solution. The feed solution was rare earth nitrate solution – the digestion product of monazite ores processing. The initial concentration of the rare earth nitrate solution contained Nd(III) 100 mg/L, Gd(III) 45 mg/L and Y(III) 28 mg/L. HEHEPA, diluted in octane, was used as the extractant. The stripping solution was nitric acid. These reagents were all used, as received, without further purification. All other chemicals used were of GR grade obtained from Merck (Germany).

7.4.2 Apparatus

The hollow fiber module (Liqui-Cel Extra-flow) was used in studying the extraction and stripping of Nd(III). The properties of the hollow fiber module are as shown in Table 7.3. The hydro-phobic polypropylene hollow fibers are woven into fabric and wrapped around a central tube of the module. An inductively coupled plasma spectrometry (ICP) was used to determine the concentration of metal ions.

Table 7.3 Properties of the hollow fiber module

Properties	Descriptions
Material	polypropylene
Inside diameter of hollow fiber	0.024 cm
Outside diameter of hollow fiber	0.03 cm
Effective length of hollow fiber	15 cm
Number of hollow fibers	35,000
Average pore size	3×10^{-6} cm
Porosity	30 %
Effective surface area	1.4×10^{4} cm^2
Area per unit volume	29.3 cm^2/cm^3
Module diameter	6.3 cm
Module length	20.3 cm
Contract area	30%
Tortuosity factor	2.6
Operating temperature	273-333 K

7.4.3 Procedure

The single hollow fiber module (as shown in Fig. 7.3.) was set up for all experiments. About 500 cm^3 of liquid membrane (HEHEPA dissolved in octane) was simultaneously pumped into the shell and tube sides of the hollow fibers for 40 min. This was to ensure that the liquid membrane was entirely embedded in the micro-pores of the hollow fibers. Rare earth nitrates, as the feed solution and

stripping solution, were supplied in counter-current circulating mode, to the tube and shell sides of the hollow fibers. Nd(III) from the nitrate solution moved across the liquid membrane to the stripping phase and was collected in the stripping reservoir. The samples of feed and stripping solutions of 10 mL each were collected every 5 min. An inductively coupled plasma spectrometry (ICP) was used to determine the concentration of metal ions in the samples, from both feed and stripping solutions. The results of the experiment were used in order to verify the validation of the model. The validity of the mathematical model was confirmed by the percentage value of the standard deviation (% S.D.) between the model-calculated value of the mathematical model and the experimental results.

$$\% \ S.D. = 100 \times \sqrt{\frac{\sum_{i=1}^{n}\left\{\left(\dfrac{D_{Exp.}}{D_{Model}}\right) - 1\right\}^2}{N - 1}} \qquad (7.12)$$

where $D_{Exp.}$ is the experimental data, D_{Model} is the model calculated value of the mathematical model and N is the number of experimental points.
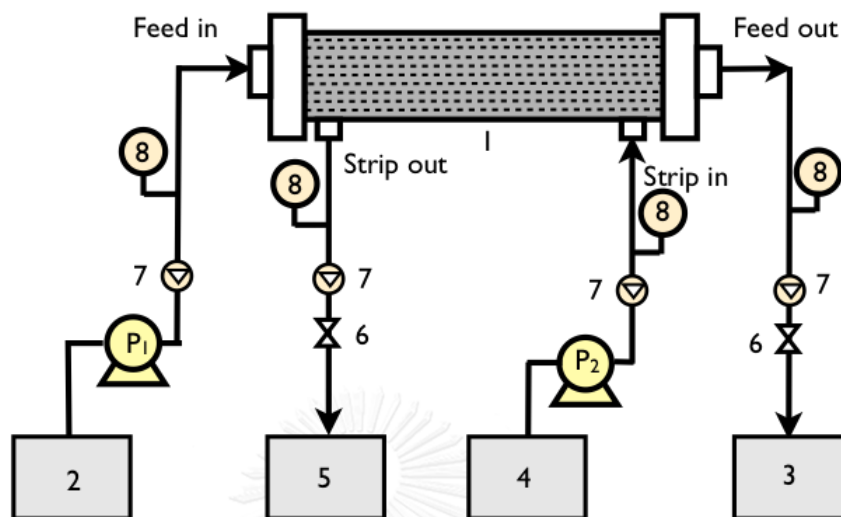
Figure 7.3 Shows the schematic representation of the counter-current flow diagram for continuous operation in HFSLM: (1) HFSLM (2) Feed in reservoir (3) Feed out reservoir (4) Stripping in reservoir (5) Stripping out reservoir (6) Flow regulator valve (7) Flow indicator (8) Pressure indicator

7.5   Results and discussion

7.5.1   Influence of pH of feed solution

By varying the pH of feed solution in Fig.7.4, it was noted that the percentage extraction and stripping of Nd(III) increased when pH was increased to 4.5. This could be explained by the fact that in the pH range 2.8-4.5, the higher pH (lower H^+ concentration) brings the stronger driving force. However, when pH was higher than

4.5, the percentage extraction and stripping of Nd(III) gradually decreased because the extraction was governed by the cation exchange reaction whereby protons are released [33]. Thus, maximum Nd(III) extraction was achieved at 4.5. Thus, the pH of 4.5 was used in the following experiments.
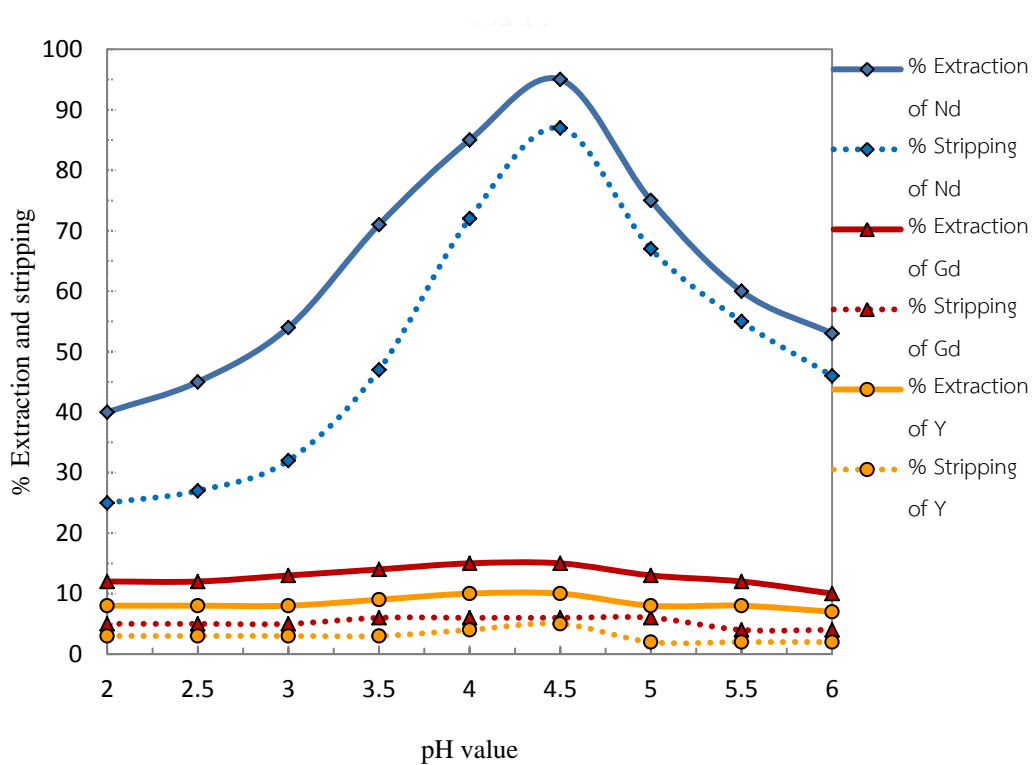

Figure 7.4 Influence of feed solution on the extraction and stripping yield (Extractant = 0.5 M HEHEPA; stripping = 4 M HNO_3; flow rate =100 mL/min. in both feed and stripping solutions; $30\,^{\circ}C$)

7.5.2   Influence of HEHEPA concentration

The influence of the concentration of HEHEPA was demonstrated in Fig. 7.5. Generally, the reaction rate increases as concentration of the extractant increases. From Fig. 7.5, the percentages of extraction and stripping increased when the concentration of the extractant was increased to 0.5 M. However, extraction and stripping of Nd((III) decreased when extractant concentration was higher than 0.5 M. This was due to an increase in liquid membrane viscosity that obstructed the mass transfer in the liquid membrane phase, corresponding to previous works [34, 35]. Thus, optimum concentration of the extractant proved to be 0.5 M.
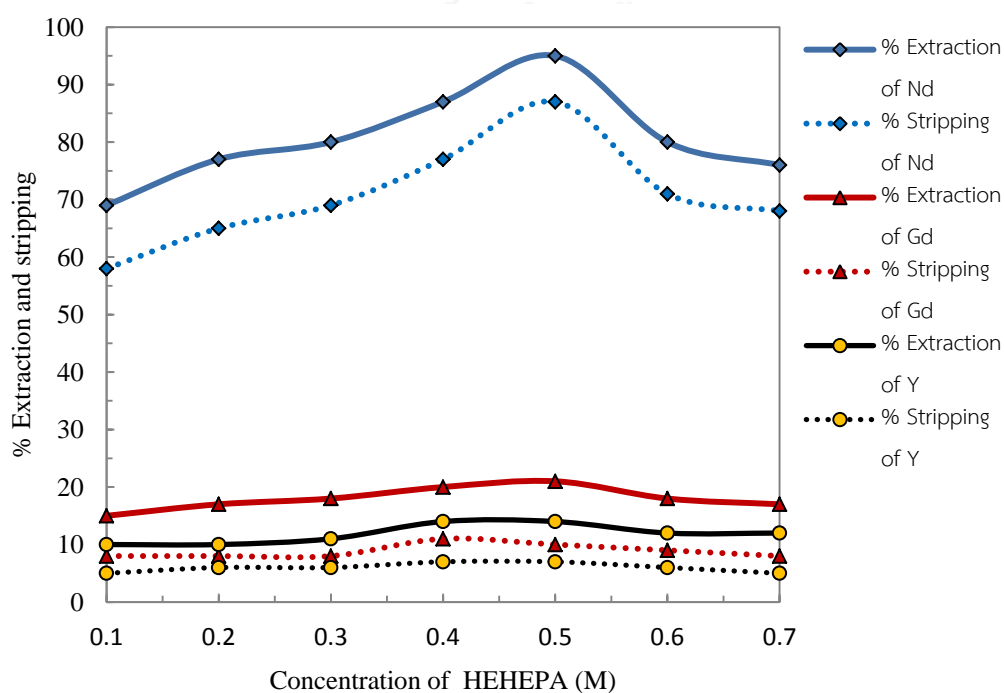
Figure 7.5 Influence of HEHEPA concentration on the extraction and stripping yield (Feed = pH 4.5; stripping = 4 M HNO_3; flow rate =100 mL/min. in both feed and stripping solutions; $30\,^{\circ}C$)

7.5.3 Influence of stripping solution

Stripping investigations were carried out with regard to the organic solution consisting of the HEHEPA in octane. The effect of different concentrations of nitric acid on the stripping solution was studied from 1 – 4.5 M. The results given in Fig. 7.6 show an increase in the percentages of Nd(III) stripping. This complies with the chemical kinetics whereby the rate of Nd(III) stripping increased when the concentration of stripping solution was increased. Thus, optimum percentages and stripping of Nd(III) were obtained at 4 M nitric acid. Similar trends were previously reported by Nadi et al. [36]. Then, at a concentration higher than 4 M (excess stripping solution) percentages remained constant. However, a higher concentration of acid can destroy the polypropylene hollow fibers [8].
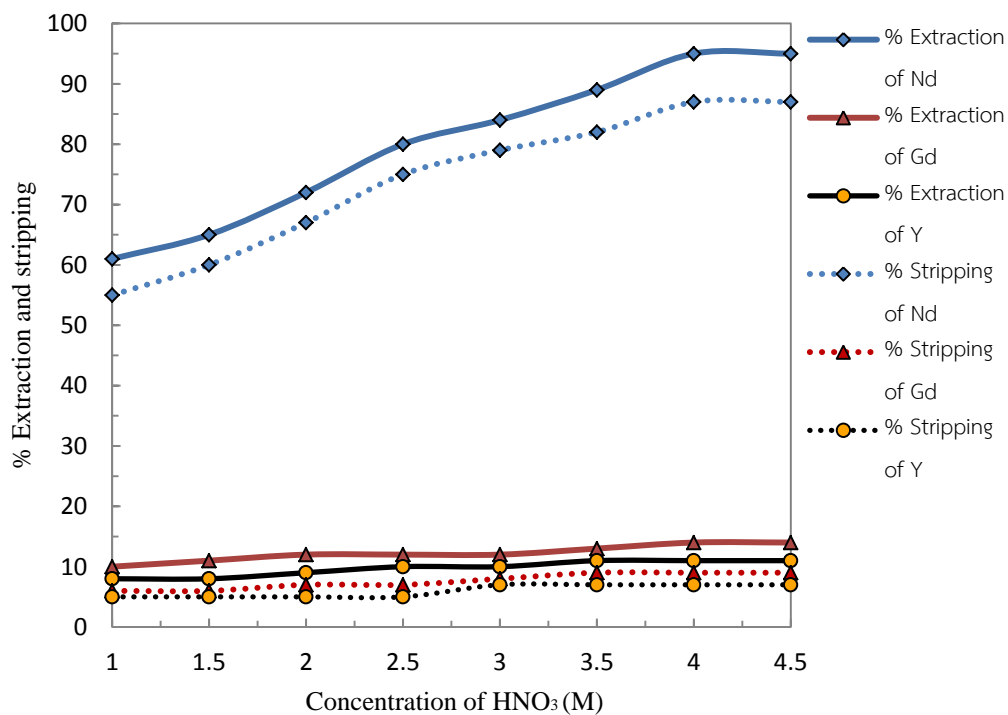
Figure 7.6 Influence of stripping solution on extraction and stripping yield (Feed = pH 4.5; extractant = 0.5 M HEHEPA; flow rate =100 mL/min. in both feed and stripping solutions; $30\,^{\circ}C$)

7.5.4   Influence of flow rates of feed and stripping solutions

The influence of flow rates was investigated using Nd(III) in nitric solution as feed solution. Flow rates of feed and stripping solution varied from 50 to 350 mL/min. as shown in Fig. 7.7. In this experiment, optimum percentages of Nd(III) extraction and stripping were obtained at flow rates of both feed and stripping solutions of 100 mL/min.

It is very important to find an optimal hydrodynamic condition in the HFSLM system for better Nd(III) recovery and scale up process [37]. Volumetric flow rates lower than 50 mL/min were not used in the experiment runs because of too small a volume purified in the unit time. Again, at a flow rate higher than 200 mL/min. the supported liquid membrane could be unstable. Therefore, high flow rates were not employed. It is interesting to note that when the solution in the tube and shell sides was swapped both were recirculated at 100 mL/min. and the fluxes were practically the same. This was probably because the determining step in this case was not transport in both aqueous solutions but in the liquid membrane phase.
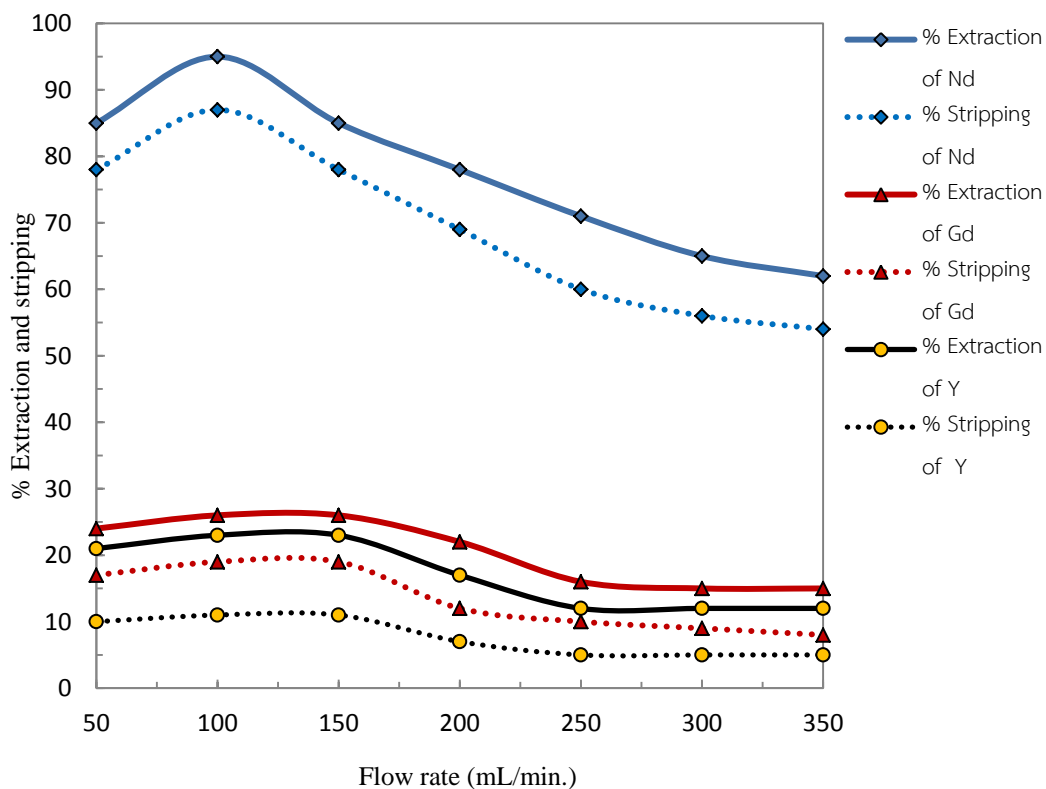
Figure 7.7 Influence of flow rate on extraction and stripping yield (Feed solution = pH 4.5; extractant = 0.5 M HEHEPA; stripping = 4 M HNO_3; $30\,^{\circ}C$)

7.5.5   Parameters used in the model

The reaction order and rate constant of extraction and stripping of Nd(III) were determined in order to calculate the outlet concentration of Nd(III) in both outlet feed and stripping solution as shown in Eqs (7.7) and (7.9), respectively. Results are shown in Table 7.4. Best fit result was obtained from the integrated first-order rate law at the semi-natural logarithm plot between Nd(III) concentration and time. The

linear curve was drawn tangentially along the plot, giving a calculated $R^2 > 0.99$ for extraction and stripping reaction as shown in Fig. 7.8. Thus, the reactions of Nd(III) extraction and stripping were of first-order with reaction rate constants of 1.541 and 1.392 min^{-1}, respectively. Other parameters used in the model were detailed in Table 7.5.

Table 7.4 Analysis of reaction order and rate constants

Reaction order	Determination			R^2	
	Relationship	k_{Ex}	k_{St}	Ext.	Strip.
0	C vs. time	1.7824 mg/L.min	1.6941 mg/L.min	0.8124	0.8171
1	ln (C_o/C) vs. time	1.541 min^{-1}	1.394 min^{-1}	0.9949*	0.9932*
2	1/C vs. time	1.012 L/mg.min	0.981 L/mg.min	0.8842	0.8097

*Best fit

Table 7.5 Values of relevant parameters used in the model.

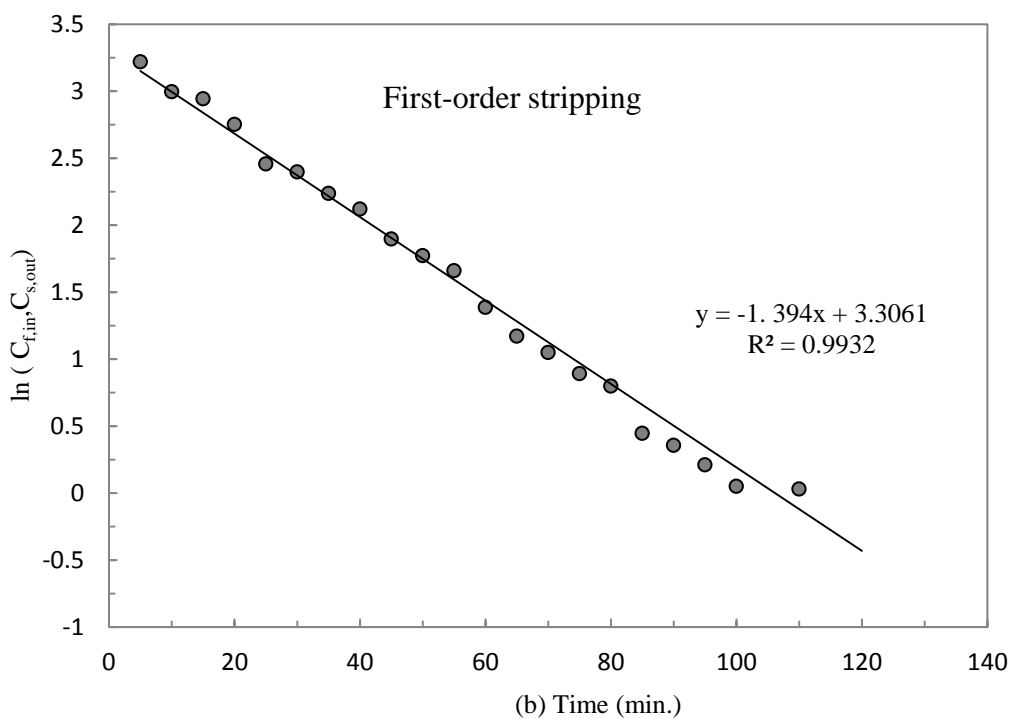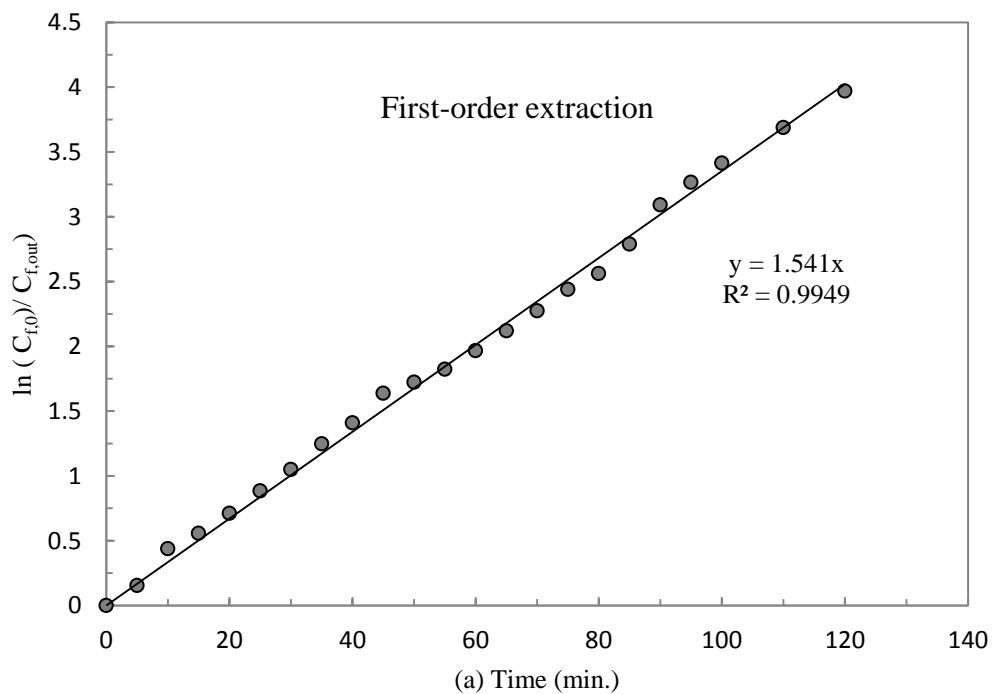| Parameters	Prediction Nd(III)
$C_{A,F(0,0)}$ (mg/L)	100
V_t (cm^3)	4.6×10^{-4}
V_S (cm^3)	3.9×10^{-5}
i (-)	100
A_C (cm^3)	0.16×10^2
A_{St} (cm^3)	0.07×10^2
D_F (cm^2/min)	1.67×10^{-3}
D_{St} (cm^2/min)	2.48×10^{-3}

(a) Time (min.)

(b) Time (min.)

Figure 7.8 (a) Integral concentration of Nd(III) extraction (b) Integral concentration of Nd(III) stripping.

7.5.6   Validation of the model with the experimental results

A mathematical model for Nd(III) transport within HFSLM was developed. It was composed of three flow transport paths. The paths in the feed phase and stripping phase were modeled based on the conservation of mass which consisted of convection, diffusion, reaction and accumulation. The experiment, employing various times for both feed and stripping solution, was carried out in order to validate the model prediction. Total time taken for the experiment was 240 min. The concentrations of Nd(III) in the feed and stripping solution, from both the experimental results and model results, as calculated by Eqs. (7.7) and (7.9), are shown in Fig. 7.9. The results showed that the concentration of Nd(III) in the feed solution decreased with an increase in time. However, concentration of Nd(III) in the stripping solution showed the opposite results. Thus, an operating time for both feed and stripping solutions of 80 min. was recommended. The predicted concentration of Nd(III) as per the model, in both feed and stripping solutions, fitted in well with the experimental results. Average percent deviation of 1.9% and 1.2% for predictions in the feed and stripping phases were noted. These results indicated that all terms of

the conservation of mass were important factors of Nd(III) transport across the liquid membrane phase.
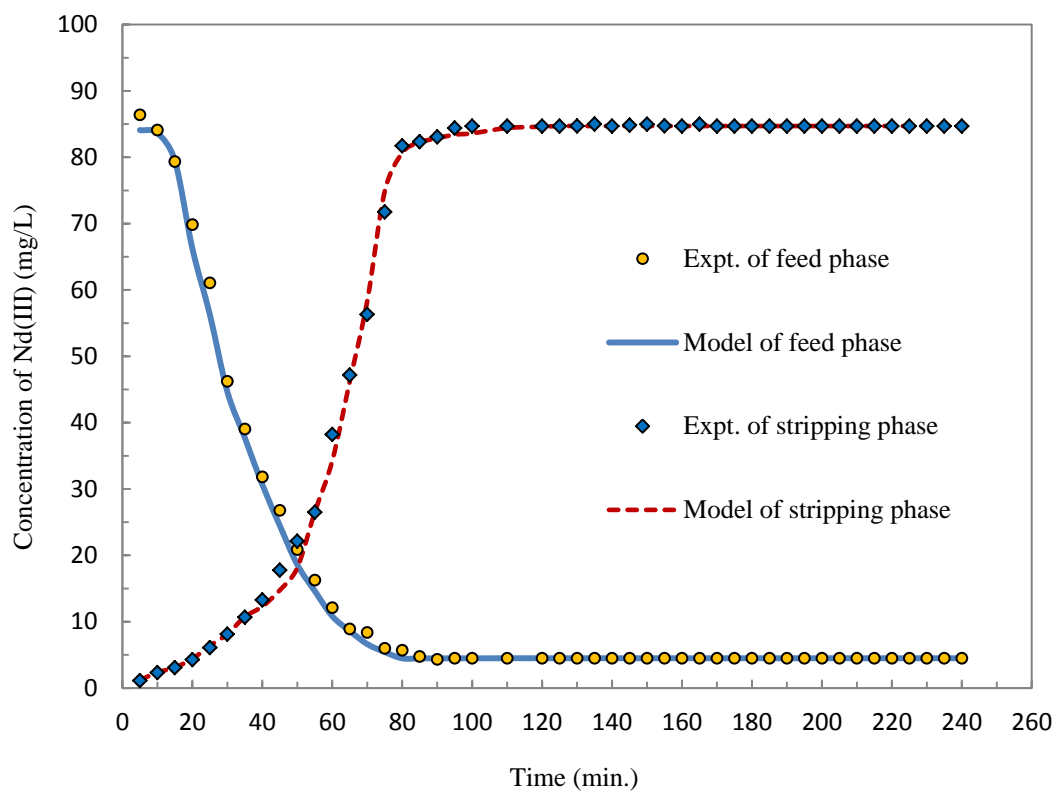

Figure 7.9 Model calculation results against experimental data for the case of varying time

7.5.7   Comparison of models

Fig. 7.10 shows the comparison of concentration of Nd(III) in feed solution obtained from the experimental results and from the models of this work- Kandwal

et al. [38] and Yang et al. [16]. Kandwal et al. developed their model based on the principle of a facilitated diffusional transport mechanism (neglecting mass accumulation and chemical reactions); average standard deviations for extraction and stripping were 9.8% and 8.5%, respectively. The model of Yang et al. was developed based on the chemical reactions (neglecting mass accumulation and diffusion); average standard deviations for extraction and stripping were 10.5% and 9.4%, respectively. The results of the models by Kandwal and Yang et al. did not match the experimental results.

In contrast, the predicted results of this work, based on the conservation of mass consisting of convection, diffusion, reaction and accumulation, were in good agreement with the experimental results. Average percent deviations were 1.9% and 1.2%, respectively for predictions in the feed and stripping phases. This confirmed that the conservation of mass which consisted of convection, diffusion, reaction and accumulation are very important factors in controlling the rate of transport of Nd(III) along the hollow fibers.
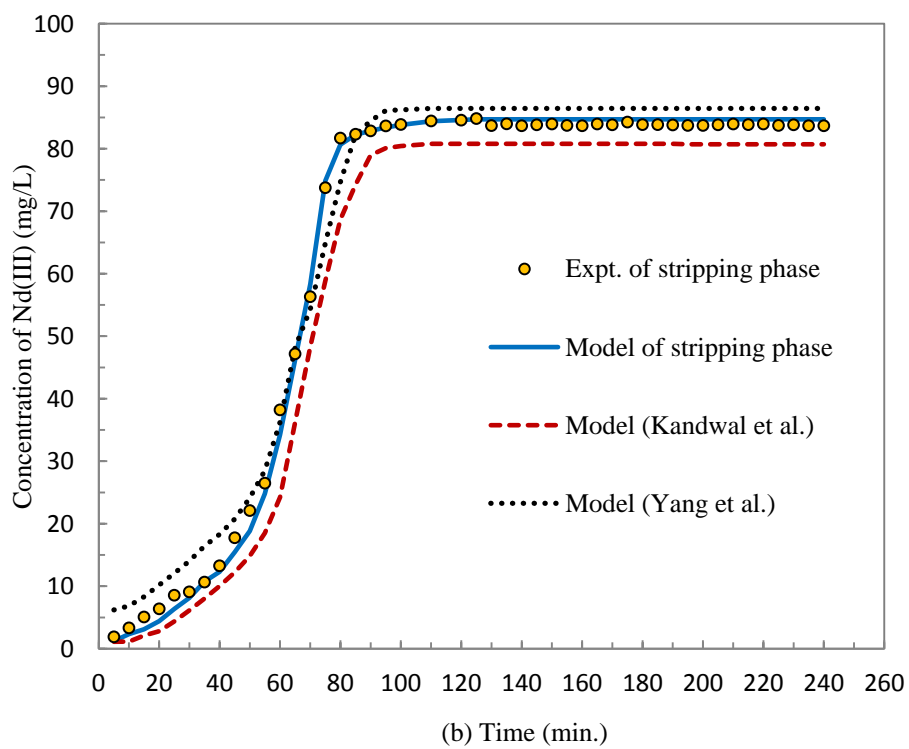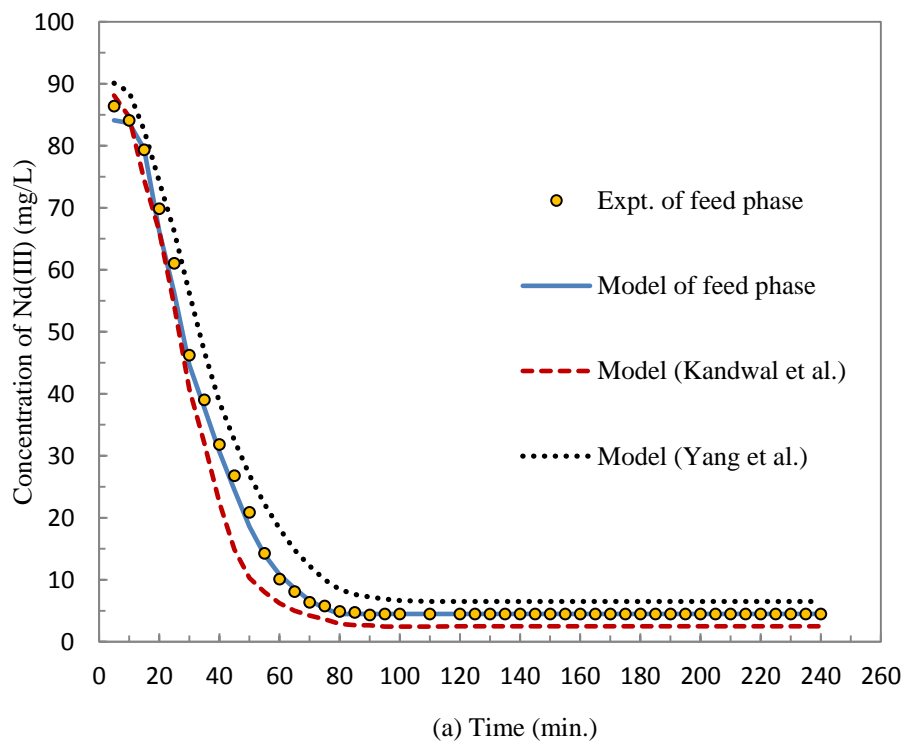
(a) Time (min.)

(b) Time (min.)

Figure 7.10 Comparison of concentration of Nd(III) in the feed and stripping solutions, obtained from experimental results and mathematical model results: (a) Feed solution (b) Stripping solution

7.6 Conclusion

HFSLM can successfully extract Nd(III) at a very low concentration from nitric solution. Percentages of extraction and stripping reached 95% and 87%, respectively. Optimum conditions were achieved using 4.5 pH of feed solution, 0.5 M HEHEPA, 4 M HNO_3, and equal flow rates of both feed and stripping solutions at 100 mL/min. Reaction rate constants for extraction and stripping of Nd(III) were 1.541 and 1.394 min^{-1}. The model developed in this work based on the conservation of mass which consisted of convection, diffusion, reaction and accumulation via HFSLM for the extraction and stripping concentration prediction proved to be in good agreement with the experimental data. Average standard deviations were 1.9% and 1.2% for prediction in feed and stripping sides, respectively. When comparison is made with other models, the model employed in this work rigorously approaches the experimental data more than the others, implying that the combination of parameters of convection, diffusion and reaction is crucial for accurate prediction in this unsteady state model.

7.7   Acknowledgments

Appendix A. The developed-model mathematics and assumptions for metal ion transport through HFSLM

The conservation of mass of metal ions in each small segment for the feed phase is shown as:

$$q_F C_{A,F}\left(x_{i-1},t\right) - q_F C_{A,F}\left(x_i,t\right) + \frac{A_C D_F}{\Delta x}\left[C_{A,F}\left(x_i,t\right) - C_{A,F}\left(x_{i-1},t\right)\right] + r_{A,Ex}\left(x_i,t\right)\cdot V_p$$

$$= V_t \frac{dC_{A,F}(x_i,t)}{dt} \tag{A.1}$$

Linearization of the reaction rate of extraction ($r_{A,Ex}(x_i,t)$) in Eq. (A.1) using the Taylor series gives the following equation:

$$r_{A,Ex}(x_i,t) = -\left[\alpha + \beta C_{A,F}(x_i,t)\right] \tag{A.2}$$

given:

$$\alpha = (1-m)k_{Ex}C_{A,F}^{m}(0,0)$$

$$\beta = m\,k_{Ex}C_{A,F}^{m-1}(0,0)$$

$C_{A,F}(0,0)$ is the initial concentration of metal ions in the feed solution. By substituting Eq. (A.2) into Eq. (A.1) and dividing by the volumetric flow rate, the following equation is obtained:

$$\frac{V_t}{q_F}\frac{dC_{A,F}(x_i,t)}{dt} = (1-\frac{A_C D_F}{q_F \Delta x})C_{A,F}(x_{i-1},t) - (1-\frac{A_C D_F}{q_F \Delta x}+\frac{V_p}{q_F}\beta)C_{A,F}(x_i,t) - \frac{V_p}{q_F}\alpha \tag{A.3}$$

where

$$V_t = \pi r_i^2 \Delta x,$$

$$V_p = \pi (r_o^2 - r_i^2)\Delta x \varepsilon \text{ and } \Delta x = \frac{L}{i}$$

where r_o and r_i are the outer and inner radius of the hollow fibers and L is the effective length of the hollow fibers.

Considering the conservation of mass in segments 1, 2, 3, ..., i based on Eq. (A.3), the following series of differential equations is obtained:

$$\frac{V_t}{q_F}\frac{dC_{A,F}(x_1,t)}{dt} = (1-\frac{A_C D_F}{q_F \Delta x})C_{A,F}(x_0,t) - (1-\frac{A_C D_F}{q_F \Delta x}+\frac{V_p}{q_F}\beta)C_{A,F}(x_1,t) - \frac{V_p}{q_F}\alpha \qquad (A.4)$$

$$\frac{V_t}{q_F}\frac{dC_{A,F}(x_1,t)}{dt} = (1-\frac{A_C D_F}{q_F \Delta x})C_{A,F}(x_1,t) - (1-\frac{A_C D_F}{q_F \Delta x}+\frac{V_p}{q_F}\beta)C_{A,F}(x_2,t) - \frac{V_p}{q_F}\alpha \qquad (A.5)$$

$$\frac{V_t}{q_F}\frac{dC_{A,F}(x_1,t)}{dt} = (1-\frac{A_C D_F}{q_F \Delta x})C_{A,F}(x_2,t) - (1-\frac{A_C D_F}{q_F \Delta x}+\frac{V_p}{q_F}\beta)C_{A,F}(x_3,t) - \frac{V_p}{q_F}\alpha \qquad (A.6)$$

.

.

.

$$\frac{V_t}{q_F}\frac{dC_{A,F}(x_1,t)}{dt} = (1-\frac{A_C D_F}{q_F \Delta x})C_{A,F}(x_{i-1},t) - (1-\frac{A_C D_F}{q_F \Delta x}+\frac{V_p}{q_F}\beta)C_{A,F}(x_i,t) - \frac{V_p}{q_F}\alpha \qquad (A.7)$$

The series of differential equations in Eqs. (A.4)–(A.7) can be solved by using the concept of Generating Function. The definition of Generating Function [39, 40] is:

$$\mathcal{C}_A(Z,t) = C_{A0}Z^0 + C_{A1}Z^1 + C_{A2}Z^2 + ... \qquad (A.8)$$

where

$$\mathcal{C}_A(Z,0) = C_A(x_0,0)Z^0 + C_A(x_1,0)Z^1 + C_A(x_2,0)Z^2 + ... = C_A(x_0,0)Z^0 = C_A(x_0,0) = C_A(0,0)$$

and Z is a complex quantity.

Eq. (A.8) can be represented as:

$$\frac{\partial \mathcal{C}_A(Z,t)}{\partial t} = Z^0 \frac{dC_A(x_0,t)}{dt} + Z^1 \frac{dC_A(x_1,t)}{dt} + Z^2 \frac{dC_A(x_2,t)}{dt} + Z^3 \frac{dC_A(x_3,t)}{dt} + ... \qquad (A.9)$$

By multiplying the series of differential equations in Eqs. (A.4)–(A.7) by Z^1, Z^2, Z^3, ..., Z^j, and then summing them up, the following equation is obtained:

$$\frac{V_p}{q_F}\left[\frac{dC_{A,F}(x_0,t)}{dt}+Z\frac{dC_{A,F}(x_1,t)}{dt}+Z^2\frac{dC_{A,F}(x_2,t)}{dt}+Z^3\frac{dC_{A,F}(x_3,t)}{dt}+...\right]=$$

$$Z\omega\left[C_{A,F}(x_0,t)+ZC_{A,F}(x_1,t)+Z^2C_{A,F}(x_2,t)+...\right]-$$

$$\lambda\left[C_{A,F}(x_0,t)+ZC_{A,F}(x_1,t)+Z^2C_{A,F}(x_2,t)+Z^3C_{A,F}(x_3,t)+...\right]$$

$$-\frac{V_p}{q_F}\alpha\left[Z+Z^2+Z^3+...\right]+\lambda C_{A,F}(x_0,t)$$

(A.10)

where

$$\omega=1-\frac{A_C D_F}{q_F\Delta x}, \quad \lambda=1-\frac{A_C D_F}{q_F\Delta x}+\frac{V_p}{q_F}\beta.$$

From the definition of the Generating Function, Eq. (A.10) can be rewritten as:

$$\frac{V_t}{q_F}\frac{\partial \mathcal{C}_{A,F}(Z,t)}{\partial t}=Z\omega\mathcal{C}_{A,F}(Z,t)-\lambda\mathcal{C}_{A,F}(Z,t)-\frac{V_p}{q_F}\alpha\sum_{j=1}^{i}Z^j+\lambda C_{A,F}(x_0,t)$$

(A.11)

By integrating Eq. (A.11) and using the boundary condition from Eq. (A.8), the following equation is obtained:

$$C_{A,F}(Z,t) = \left[\frac{Z\omega C_{A,F}(0,0)e^{\frac{\omega tq_F}{V_t}Z}}{(\omega Z - \lambda)} - \frac{\frac{V_p\alpha}{q_F}\sum_{j=1}^{i}Z^j}{(\omega Z - \lambda)}e^{\frac{\omega tq_F}{V_t}Z} \right] e^{\frac{-\lambda tq_F}{V_t}} + \frac{\frac{V_p\alpha}{q_F}}{(\omega Z - \lambda)}\sum_{j=1}^{i}Z^j - \frac{\lambda C_{A,F}(0,0)}{(\omega Z - \lambda)}$$

(A.12)

By the distribution of Z function in Eq. (A.12) into polynomial form and using the method of undetermined coefficients, the equation for calculating the concentration of metal ions in the outlet feed solution ($C_{A,F}(x_i,t)$) is achieved:

$$C_{A,F}(x_i,t) = -C_{A,F}(0,0)e^{\frac{-\lambda tq_F}{V_t}}\sum_{l=1}^{i}\frac{1}{(i-l)!}\frac{(\lambda)^l}{(\omega^{-i+2l})}\cdot\left(\frac{tq_F}{V_p}\right)^{i-l} + \frac{V_p\alpha}{q_F\lambda}e^{\frac{-\lambda tq_F}{V_t}}\sum_{l=1}^{i}\frac{\omega^{i-l}}{(i-l)!}\left(\frac{tq_F}{V_p}\right)^{i-l}\sum_{j=1}^{l}\left(\frac{\omega}{\lambda}\right)^{j-1}$$

$$+\frac{V_p\alpha}{q_F\lambda}\sum_{l=1}^{i}\left(\frac{\omega}{\lambda}\right)^{i-l} - C_{A,F}(0,0)\left(\frac{\omega}{\lambda}\right)^i$$

(A.13)

For the stripping phase, mass conservation of metal ions was examined for each small segment in the shell side of hollow fiber as shown below:

$$q_{St}C_{A,St}\left(x'_{i\text{-}1},t\right) - q_{St}C_{A,St}\left(x'_{i},t\right) + \frac{A_{St}D_{St}}{\Delta x'}\left[C_{A,St}\left(x'_{i},t\right) - C_{A,St}\left(x'_{i\text{-}1},t\right)\right] + r_{A,St}\left(x'_{i},t\right)\cdot V_{p}$$

$$=V_{S}\frac{dC_{A,St}\left(x'_{i},t\right)}{dt} \tag{A.14}$$

To linearize the term of $r_{A,St}(x'_{i},t)$ in Eq. (A.14), the Taylor series is applied:

$$r_{A,St}(x'_{i},t) = \gamma + \varphi C_{A,St}(x'_{i},t) \tag{A.15}$$

where:

$$\gamma = (1\text{-}n)k_{St}C_{A,St}^{n}(x'_{0},0)$$

$$\varphi = nk_{St}C_{A,St}^{n\text{-}1}(x'_{0},0)$$

Substituting Eq. (A.15) in Eq. (A.14) and dividing by the volumetric flow rate of stripping solution, the following equation is obtained:

$$\frac{V_S}{q_{St}}\frac{dC_{A,St}(x_i',t)}{dt} = (1 - \frac{A_{St}D_{St}}{q_{St}\Delta x'})C_{A,St}(x_{i-1}',t) - (1 - \frac{A_{St}D_{St}}{q_{St}\Delta x'} - \frac{V_p}{q_{St}}\varphi)C_{A,St}(x_i',t) + \frac{V_p}{q_{St}}\gamma \qquad \text{(A.16)}$$

where

$$V_S = \left(\frac{\sqrt{3}}{4}d_o^2 - \frac{\pi r_o^2}{2}\right)\Delta x'$$

$$\Delta x' = \frac{L}{i}$$

where d_o and r_o are the outer diameter and outer radius of the hollow fibers.

The conservation of mass in the stripping phase at segments 1, 2, 3, ..., i based on Eq. (A.16) can be expressed by the following series of differential equations:

$$\frac{V_S}{q_{St}}\frac{dC_{A,St}(x_1',t)}{dt} = (1 - \frac{A_{St}D_{St}}{q_{St}\Delta x'})C_{A,St}(x_0',t) - (1 - \frac{A_{St}D_{St}}{q_{St}\Delta x'} - \frac{V_p}{q_{St}}\varphi)C_{A,St}(x_1',t) + \frac{V_p}{q_{St}}\gamma \qquad \text{(A.17)}$$

$$\frac{V_S}{q_{St}}\frac{dC_{A,St}(x_1',t)}{dt} = (1 - \frac{A_{St}D_{St}}{q_{St}\Delta x'})C_{A,St}(x_1',t) - (1 - \frac{A_{St}D_{St}}{q_{St}\Delta x'} - \frac{V_p}{q_{St}}\varphi)C_{A,St}(x_2',t) + \frac{V_p}{q_{St}}\gamma \qquad \text{(A.18)}$$

$$\frac{V_S}{q_{St}}\frac{dC_{A,St}(x_1',t)}{dt} = (1-\frac{A_{St}D_{St}}{q_{St}\Delta x'})C_{A,St}(x_2',t) - (1-\frac{A_{St}D_{St}}{q_{St}\Delta x'}-\frac{V_p}{q_{St}}\varphi)C_{A,St}(x_3',t) + \frac{V_p}{q_{St}}\gamma \quad \text{(A.19)}$$

.

$$\cdots\frac{V_S}{q_{St}}\frac{dC_{A,St}(x_1',t)}{dt} = (1-\frac{A_{St}D_{St}}{q_{St}\Delta x'})C_{A,St}(x_{i-1}',t) - (1-\frac{A_{St}D_{St}}{q_{St}\Delta x'}-\frac{V_p}{q_{St}}\varphi)C_{A,St}(x_i',t) + \frac{V_p}{q_{St}}\gamma \quad \text{(A.20)}$$

solving the series of differential equations in Eqs. (A.17)–(A.20) by the same concept described in Eqs. (A.4) – (A.13), the equation for calculating the concentration of metal ions in the outlet stripping solution ($C_{A,St}(x_i',t)$) is obtained as shown in Eq. (A.21):

$$C_{A,St}(x_i',t) = -C_{A,St}(x_0',t)e^{\frac{t\theta q_{St}}{V_s}}\sum_{l=1}^{i}\frac{1}{(i-l)!}\frac{\theta^l}{\delta^{-i+2l}}\cdot\left(\frac{tq_{St}}{V_p}\right)^{i-l} - \frac{V_p\gamma}{\theta q_{St}}e^{\frac{t\theta q_{St}}{V_s}}\sum_{l=1}^{i}\frac{\delta^{i-l}}{(i-l)!}\left(\frac{tq_{St}}{V_p}\right)^{i-l}\sum_{j=1}^{l}\left(\frac{\delta}{\theta}\right)^{j-1}$$

$$+\frac{V_p\gamma}{q_{St}\theta}\sum_{l=1}^{i}\left(\frac{\delta}{\theta}\right)^{i-l}+C_{A,St}(x_0',0)\left(\frac{\delta}{\theta}\right)^i \quad \text{(A.21)}$$

Defining:

$$\delta = (1-\frac{A_{St}D_{St}}{q_{St}\Delta x'}), \quad \theta = (1-\frac{A_{St}D_{St}}{q_{St}\Delta x'}-\frac{V_p}{q_{St}}\varphi)$$

$C_{A,St}(x_0',0)$ is estimated from the experimental mass-transfer flux of metal-ion transport across the liquid membrane phase from the feed phase to the stripping phase $(J_{Nd^{3+},Expt.})$. The experimental mass-transfer flux can be estimated from Eq. (A.22):

$$J_{Nd^{3+},Expt.} = \frac{q_{St}\Delta C_{A,St}}{A}$$ (A.22)

where A is the effective mass-transfer area and $\Delta C_{A,St}$ is the difference in the concentration of metal ions between the outlet and inlet stripping solutions obtained from the experiment.

The experimental mass-transfer flux can also be estimated from Eq. (A.23):

$$J_{Nd^{3+},Expt.} = \frac{V_{St}}{A}\frac{dC_{A,St}}{dt}$$ (A.23)

Applying Eq. (A.23), the following equation is obtained:

$$J_{Nd^{3+},Expt.} = \frac{V_{St,x_i'}}{A} k_{St} C_{A,St}^n (x_i',t) \tag{A.24}$$

where $V_{St,x_i'}$ is the volume of the stripping phase at position x_i'.

Regarding the small segment at position x_0', $C_{A,St}(x_i',t)$ is equal to $C_{A,St}(x_0',0)$ therefore, from Eqs. (A.22) and (A.24), $C_{A,St}(x_0',0)$ in Eq. (A.21) can be calculated, as shown in Eq. (A.25):

$$C_{A,St}(x_0',0) = \left(J_{Nd^{3+},Expt.} \cdot \frac{A_0}{V_{St,x_0'} k_{St}} \right)^{1/n} \tag{A.25}$$

where $V_{St,x_o'}$ is the volume of the stripping phase at position x_0' and

A_0 is the effective mass-transfer area at position x_0'.

The diffusion coefficient of Nd(III) in feed phase and stripping phase is calculated by the Wilke-Change equation [41], as shown in Eq. (A-26);

$$D = \frac{7.4\,x10^{-8}\,(\phi M)^{0.5}\,T}{\eta V_A^{\,0.6}} \tag{A-26}$$

where D is diffusion coefficient (cm^2/s), M is molecular weight of solvent (g·mol^{-1}), T is temperature (K), η is viscosity (cP) and V_A is molar volume of solute (cm^3/mol).

7.8   References

[1]   P. Enghag, Encyclopedia of the ElementsTechnical Data - History - Processing - Applications, John Wiley & Sons, USA, 2004.

[2]   N.E. El-Hefny, Kinetics and mechanism of extraction and stripping of neodymium using a Lewis cell, Chemical Engineering and Processing: Process Intensification, 46 (2007) 623-629.

[3]   J.S. Preston, P.M. Cole, A.C. du Preez, M.H. Fox, A.M. Fleming, The recovery of rare earth oxides from a phosphoric acid by-product. Part 2: The preparation of high-purity cerium dioxide and recovery of a heavy rare earth oxide concentrate, Hydrometallurgy, 41 (1996) 21-44.

[4]   S. Heng, K.L. Yeung, M. Djafer, J.-C. Schrotter, A novel membrane reactor for ozone water treatment, J.Mem. Sci. 289 (2007) 67-75.

[5]   S. Heng, K.L. Yeung, A.N. Julbe, A.D. Ayral, J.C. Schrotter, Preparation ofcomposite zeolite membrane separator/contactor for ozone water treatment, Microporous Mesoporous Maters, 115 (2008) 137–146.

[6]   W.K. Chan, J.T. Jouët, S. Heng, K.L. Yeung, J.C. Schrotter, Membrane contactor/ separator for an advanced ozone membrane reactor for treatment of recalcitrant organic pollutants in water, J. Solid State Chem. 189 (2012) 96–100.

[7]   K. F. Lam,H. Kassab,M. Pera-Titus, K. L. Yeung, B. Albela and L. Bonneviot MCM-41 "LUS": Alumina Tubular Membranes for Metal Separation in Aqueous Solution, J. Phys. Chem. C 2011, 115, 176–187.

[8]   S. Suren, U. Pancharoen, S. Kheawhom, Simultaneous extraction and stripping of lead ions via a hollow fiber supported liquid membrane: Experiment and modeling, J. Ind. Eng. Chem. (2014), 20 (2584-2593).

[9]   M. F. San Roman, E. Bringas, R. Ibanez, L. Ortiz, Liquid membrane technology: fundamentals and review of its applications, J. Chem. Tech. Bio. 85 (2010) 2-10.

[10]   N. M. Kocherginsky, Q. Yang, L. Seelam, Recent advances in supported liquid membrane technology, Sep. .Puri.Technol. 53 (2007) 171-177.

[11]   U. Pancharoen, P. Ramakul, W. Pattaveekongka, Purely Extraction and Separation of Mixture of Cerium(IV) and Lanthanum(III) via Hollow Fiber Supported Liquid Membrane, J. Ind. Eng. Chem., 11 (2005) 692-931.

[12] P. Ramakul, T. Prapasawad, U. Pancharoen, W. Pattaveekongka, Separation of radioactive metal ions by hollow fiber-supported liquid membrane and permeability analysis, J. Chin. Inst. Chem. Eng. 38 (2007) 489-494.

[13] S.A. Ansari, P.K. Mohapatra, V.K. Manchanda, Recovery of Actinides and Lanthanides from High-Level Waste Using Hollow-Fiber Supported Liquid Membrane with TODGA as the Carrier, Ind. Eng. Chem. Res. 48 (2009) 8605-8612.

[14] P.V. Vernekar, Y.D. Jagdale, A.W. Patwardhan, A.V. Patwardhan, S.A. Ansari, P.K. Mohapatra, V.K. Manchanda, Transport of cobalt(II) through a hollow fiber supported liquid membrane containing di-(2-ethylhexyl) phosphoric acid (D2EHPA) as the carrier, Chem. Eng. Res.Des. 91 (2013) 141-157.

[15] P. Kandwal, S. Dixit, S. Mukhopadhyay, P.K. Mohapatra, Mass transport modeling of Cs(I) through hollow fiber supported liquid membrane containing calix-[4]-bis(2,3-naptho)-crown-6 as the mobile carrier, Chem. Eng. J. 174 (2011) 110-116.

[16] Q. Yang, N.M. Kocherginsky, Copper removal from ammoniacal wastewater through a hollow fiber supported liquid membrane system: Modeling and experimental verification, J. Mem. Sci. 297 (2007) 121-129.

[17] U. Pancharoen, T. Wongsawa, A.W. Lothongkum, A Reaction Flux Model for Extraction of Cu(II) with LIX84I in HFSLM, Sep. Sci. Technol. 46 (2011) 2183-2190.

[18] K. McLaughlin, C. Bertolucci, Applications of generating functions to polymerization kinetics. 3. General procedure illustrated for propagation with monomer conversion, J. Math.Chem. 14 (1993) 71-78.

[19] S. Suren, U. Pancharoen, N. Thamphiphit, N. Leepipatpiboon, A Generating Function applied on a reaction model for the selective separation of Pb(II) and Hg(II) via HFSLM, J. Mem. Sci. 448 (2013) 23-33.

[20] M.I. Saleh, M.F. Bari, B. Saad, Solvent extraction of lanthanum(III) from acidic nitrate-acetato medium by Cyanex 272 in toluene, Hydrometallurgy, 63 (2002) 75-84.

[21] M.-S. Lee, J.-Y. Lee, J.-S. Kim, G.-S. Lee, Solvent extraction of neodymium ions from hydrochloric acid solution using PC88A and saponified PC88A, Sep. Pure. Technol. 46 (2005) 72-78.

[22] D. Wu, Q. Zhang, B. Bao, Solvent extraction of Pr and Nd (III) from chloride-acetate medium by 8-hydroquinoline with and without 2-ethylhexyl phosphoric acid mono-2-ethylhexyl ester as an added synergist in heptane diluent, Hydrometallurgy, 88 (2007) 210-215.

[23] D. Fontana, L. Pietrelli, Separation of middle rare earths by solvent extraction using 2-ethylhexylphosphonic acid mono-2-ethylhexyl ester as an extractant, J. Rare Earth. 27 (2009) 830-833.

[24] O.A. Desouky, A.M. Daher, Y.K. Abdel-Monem, A.A. Galhoum, Liquid–liquid extraction of yttrium using primene-JMT from acidic sulfate solutions, Hydrometallurgy, 96 (2009) 313-317.

[25] Y.A. El-Nadi, Effect of diluents on the extraction of praseodymium and samarium by Cyanex 923 from acidic nitrate medium, J. Rare Earth. 28 (2010) 215-220.

[26] M.H. Chhatre, V.M. Shinde, Separation of scandium(III) and yttrium(III) by tris(2-ethylhexyl)phosphate (TEHP), Talanta, 47 (1998) 413-419.

[27] L. Pei, L. Wang, G. Yu, Separation of Eu(III) with supported dispersion liquid membrane system containing D2EHPA as carrier and HNO_3 solution as stripping solution, J. Rare Earth. 29 (2011) 7-14.

[28] L. Pei, L. Wang, G. Yu, Study on a novel flat renewal supported liquid membrane with D2EHPA and hydrogen nitrate for neodymium extraction, J. Rare Earth. 30 (2012) 63-68.

[29] A.G. Gaikwad, A.M. Rajput, Transport of yttrium metal ions through fibers supported liquid membrane solvent extraction, J. Rare Earth. 28 (2010) 1-6.

[30] S. Chaturabul, K. Wongkaew, U. Pancharoen, Selective Transport of Palladium through a Hollow Fiber Supported Liquid Membrane and Prediction Model Based on Reaction Flux, Sep.Sci. Technol. 48 (2012) 93-104.

[31] V.S. Kislik, Liquid Membranes: Principles and Applications in Chemical Separations and Wastewater Treatment, first ed., The Netherlands, 2010.

[32] O.N. Ata, Mathematical modelling of unsteady-state transport of metal ions through supported liquid membrane, Hydrometallurgy, 87 (2007) 148-156.

[33] B. Guezzen, M. A. Didi, Removal of Zn(II) from aqueous acetate solution using di(2-ethylhexyl) phosphoric acid and tribuytphosphate, Int. J. Chem. 4(2012) 32-41.

[34] Y. Kawamura, M. Mitsuhashi, H. Tanibe, H. Yoshida, Adsorption of metal ions on polyaminated highly porous chitosan chelating resin, Ind. Eng. Chem. Res. 32 (1993) 386-391.

[35] B.F. Jirjis, S. Luque, Chapter 9 - Practical Aspects of Membrane System Design in Food and Bioprocessing Applications, in: Z.F. Cui, H.S. Muralidhara (Eds.) Membrane Technology, Butterworth-Heinemann, Oxford, 2010, pp. 179-212.

[36] Y.A. El-Nadi, Lanthanum and neodymium from Egyptian monazite: Synergistic extractive separation using organophosphorus reagents, Hydrometallurgy, 119-120 (2012) 23-29.

[37] Q. Yang, N.M. Kocherginsky, Copper recovery and spent ammoniacal etchant regeneration based on hollow fiber supported liquid membrane technology: From bench-scale to pilot-scale tests, J. Mem.Sci. 286 (2006) 301-309.

[38] P. Kandwal, S. Dixit, S. Mukhopadhyay, P.K. Mohapatra, Mass transport modeling of Cs(I) through hollow fiber supported liquid membrane containing calix-[4]-bis(2,3-naptho)-crown-6 as the mobile carrier, Chem. Eng. J. 174 (2011) 110-116.

[39] K.W. McLaughlin, C.M. Bertolucci, Applications of generating functions to polymerization kinetics. 3.: general procedure illustrated for propagation with monomer conversion, J. Math. Chem.14 (1993) 71-78

[40] Elsevier, Appendix A - Elements of the Theory of Generating Functions, in: Neutron Fluctuations, Elsevier, Amsterdam, 2008, pp. 315-329.

[41] C.R. Wilke, P. Chang, Correlation of diffusion coefficients in dilute solutions, Amer. Ins. Chem. Eng. 1 (1955) 264-270

.

CHAPTER 8

8.1 Conclusion

In this study, it was found that HFSLM can effectively separate Nd(III) from mixed rare earths. The extraction and stripping of Nd(III) ions in a single-step operation via HFSLM application was investigated. As stated earlier in previous Chapters, treatment at this stringent level is hardly achievable by conventional techniques.

8.1.1 Effects of performance

It was observed that HFSLM (hollow fiber supported liquid membrane) can be used effectively to separate Nd(III) from rare earth ions. Optimum conditions for extraction of neodymium (III) ions are as shown in Table 8.1 below. As seen, extraction of neodymium (III) ions reached over 90%. Synergistic separation occurred by adding the neutron donor extractant (TOPO) to the acid extractant (D2EHPA, Cyanex 272). Percentages of Nd(III) extraction and stripping improved when concentration of TOPO in the synergistic extractant increased. H_2SO_4 and HNO_3 were

selected as stripping solutions since they had been reported having outstanding performance for use as stripping solutions for neodymium ions recovery.

In this experiment, optimum percentages of Nd(III) extraction and stripping were obtained at flow rates of both feed and stripping solutions of 100 mL/min. Operating time was 70 min. The temperature in both feed and stripping solutions had an effect on the extraction and stripping of neodymium (III) ions. When the temperature increased, the percentages of extraction and stripping of Nd(III) greatly increased. The highest percentages of extraction and stripping of 98% and 95% respectively were noted at 313 K.

Table 8.1 Summary of research on mixed rare earth ions

Feed	pH	Stripping	Extractant	Diluent	Flow rate	Temp.	% Ex.	% St
U, Th, Re	5	2M H_2SO_4	0.1M Cyanex272 + 0.1 M TOPO	Dodecane	100	30	95	90
Nd	4.5	1M H_2SO_4	0.5 M D2EHPA + 0.5 M TOPO	Heptane	100	30	94.5	85.1
Nd	4.5	1M H_2SO_4	0.5 M PC88A	Octane	100	30	91.5	88.1
Nd	4.5	3M H_2SO_4	0.5M DNPPA	Dodecane	100	20-40	85.5	70.1
Nd	4.5	4M HNO_3	0.1M Cyanex272 + 0.05 M TOPO	Octane	100	30	98	95.5
Nd	4.5	4M HNO_3	0.5 M HEHEPA	Octane	100	30	95	87

8.1.2   Prediction from mathematical model

Alongside the experiments, a mathematical model was developed and presented. The mathematical model was developed on the conservation of mass which consisted of convection, diffusion, reaction and accumulation. The mathematical model was presented in order to predict the concentration of Nd(III) ions from feed and stripping solution. The predicted results showed good agreement with the experimental data. For predictions in feed and recovery solutions, average percent deviations were low at 1.9% and 1.2%, respectively. This confirmed that the conservation of mass which consisted of convection, diffusion, reaction and accumulation were very important factors in controlling the rate of transport of Nd (III) along the hollow fibers. The results imply that the combination of convection, diffusion and reaction is crucial for accurate prediction in this unsteady state model. This robust model with its high accuracy provides a greater understanding of transport mechanism across the feed to the stripping solution; a design scale-up for industrial application could prove useful.

8.1.3   Recommendations for future studies

HFLSM has been widely studied for the separation of metal ions i.e. Nd (III), Hg, Ag and Cu. HFLSM can be considered as a potential good choice for application in the field of separation.

Despite its well-known advantages, the HFLSM system suffers from instability with time. This is mainly due to the loss of carrier and/or membrane solvent from the membrane support which has an influence on both the flux and selectivity of the membrane. However, further study on the stability of the HFSLM should be undertaken for scaling up for industrial application.

REFERENCES

Referrences

[1]   S.F. Benltoufa, Faten; BenNasrallah, Sassi, Capillary Rise in Macro and Micro Pores of Jersey Knitting Structure, Journal of Engineered Fabrics & Fibers (JEFF); Sep2008, Vol. 3 Issue 3, p47, 3 (2008) 47-54.

[2]   L. Pei, L. Wang, G. Yu, Study on a novel flat renewal supported liquid membrane with D2EHPA and hydrogen nitrate for neodymium extraction, Journal of Rare Earths, 30 (2012) 63-68.

[3]   M. Anitha, D.N. Ambare, M.K. Kotekar, D.K. Singh, H. Singh, Studies on Permeation of Nd (III) through Supported Liquid Membrane Using DNPPA + TOPO as Carrier, Separation Science and Technology, 48 (2013) 2196-2203.

[4]   MCT, MCT Redbook: solvent extraction reagents and applications.

[5]   A. Manuel, L.C. Jose, Solvent extraction and membranes, fundamentals and applications in new materials, in, CRC Press, the United States of America, 2008.

[6]   T. Wannachod, N. Leepipatpiboon, U. Pancharoen, K. Nootong, Synergistic effect of various neutral donors in D2EHPA for selective neodymium separation from lanthanide series via HFSLM, Journal of Industrial and Engineering Chemistry, 20 (2014) 4152-4162.

[7] A.O. Adebayo, K. Sarangi, Separation of copper from chalcopyrite leach liquor containing copper, iron, zinc and magnesium by supported liquid membrane, Separation and Purification Technology, 63 (2008) 392-399.

[8] A.W. Lothongkum, P. Ramakul, W. Sasomsub, S. Laoharochanapan, U. Pancharoen, Enhancement of uranium ion flux by consecutive extraction via hollow fiber supported liquid membrane, J. Taiwan Inst. Chem. Eng. 40 (2009) 518-523.

[9] B. Suanmamuang, S. Laoharochanapan, Office of Atoms for Peace, Bangkok Thailand Institute of Nuclear Technology, Thailand, (2002).

[10] G.D. Clayton, F.E. Clayton, Patty'sIndustrial Hygiene and Toxicology, Ed. Wiley-Interscience, New York, USA 4th (1994).

[11] J.G. Malecki, A. Maron´, I. Gryca, M. Serda, Characterization of a PdII complex with (E)-8-hydroxyquinoline-2-carbaldehyde O-benzyl oxime, Mendeleev Communications, 24 (2014) 26-28.

[12] T.W. Chapman, Chapter 8, Extraction – Metals Processing, in: R.W. Rousseau (Ed.) Handbook of Separation Process Technology, John Wiley & Sons, Inc., Canada, 1997, pp. 467–499.

[13] F.d.M. Fábrega, M.B. Mansur, Liquid–liquid extraction of mercury (II) from hydrochloric acid solutions by Aliquat 336, Hydrometallurgy, 87 (2007) 83-90.

[14] K.R. Chitra, A.G. Gaikwad, G.D. Surender, A.D. Damodaran, Studies on ion transport of some rare earth elements through solvating extractants immobilised on supported liquid membrane, Journal of Membrane Science, 125 (1997) 257-268.

[15] D. Wu, Q. Zhang, B. Bao, Solvent extraction of Pr and Nd (III) from chloride-acetate medium by 8-hydroquinoline with and without 2-ethylhexyl phosphoric acid mono-2-ethylhexyl ester as an added synergist in heptane diluent, Hydrometallurgy, 88 (2007) 210-215.

[16] M.S.R.a. E. Bringas, JA. Irabien and I. Ortiz, An overview of the mathematical modelling of liquid membrane separation processes in hollow fiber contactors, In: J. Chem Technol Biotechnol, 84 (2009) 1583-1614.

[17] B. GAJDA, M.B. BOGACKI, The Effect of tributyl phosphate on the extraction of nikel(II) and cobalt(II) ions with di(2-ethylhexyl)phosphoric acid Physicochemical Problems of Mineral Processing, 41 (2007) 145-152.

[18] Y.A. El-Nadi, N.E. El-Hefny, J.A. Daoud, Extraction of Lanthanum and Samarium from Nitrate Medium by some Commercial Organophosphorus Extractants, Solvent Extraction and Ion Exchange, 25 (2007) 225-240.

[19] F. Luo, D. Li, P. Wei, Synergistic extraction of zinc(II) and cadmium(II) with mixtures of primary amine N1923 and neutral organophosphorous derivatives, Hydrometallurgy, 73 (2004) 31-40.

[20] T. Wannachod, T. Wongsawa, P.Ramakul, U. Pancharoen, S. Kheawhom, The synergistic extraction of uranium ions from monazite leach solution via HFSLM and its mass transfer, J. Ind. Eng. Chem., 33 (2016) 246-254.

[21] T. Wannachod, N. Leepipatpiboon, U. Pancharoen, K. Nootong, Synergistic effect of various neutral donors in D2EHPA for selective neodymium separation from lanthanide series via HFSLM, J. Ind. Eng. Chem. 20 (2014) 4152–4162.

[22] T. Wannachod, N. Leepipatpiboon, U. Pancharoen, S. Phatanasri, Mass transfer and selective separation of neodymium ions via a hollow fiber supported liquid membrane using PC88A as extractant, J. Ind. Eng. Chem. 21 (2015) 535–541

[23] T. Wannachod, V. Mohdee, S. Suren, P. Ramakul, U. Pancharoen, K. Nootong, The separation of Nd(III) from mixed rare earth via hollow fiber supported liquid membrane and mass transfer analysis, J. Ind. Eng. Chem. 26 (2015) 214–217.

[24] T. Wannachod, P. Phuphaibul, V. Mohdee, U. Pancharoen, S. Phatanasri, Optimization of synergistic extraction of neodymium ions from monazite leach solution treatment via HFSLM using response surface methodology, Minerals Eng. 77 (2015) 1–9.

[25]   T. Wannachod, N. Leepipatpiboon, U. Pancharoen, K. Nootong, Separation and mass transport of Nd(III) from mixed rare earths via hollow fiber supported liquid membrane: Experiment and modeling, Chem. Eng. J. 248 (2014) 158–167

List of publications

[1] Thanaporn Wannachod, Natchanun Leepipatpiboon, Ura Pancharoen, Kasidit Nootong, Synergistic effect of various neutral donors in D2EHPA for selective neodymium separation from lanthanide series via HFSLM, Journal of Industrial and Engineering Chemistry 20 (2014) 4152–4162.

[2] Thanaporn Wannachod, Natchanun Leepipatpiboon, Ura Pancharoen, Kasidit Nootong, Separation and mass transport of Nd(III) from mixed rare earths via hollow fiber supported liquid membrane: Experiment and modeling, Chemical Engineering Journal 248 (2014) 158–167.

[3] Thanaporn Wannachod, Vanee Mohdee, Sira Suren, Prakorn Ramakul, Ura Pancharoen, Kasidit Nootong, The separation of Nd(III) from mixed rare earth via hollow fiber supported liquid membrane and mass transfer analysis, Journal of Industrial and Engineering Chemistry 26 (2015) 214–217.

[4] Thanaporn Wannachod, Phupairum Phuphaibul, Vanee Mohdee, Ura Pancharoen, Suphot Phatanasri, Optimization of synergistic extraction of neodymium ions from monazite leach solution treatment via HFSLM using response surface methodology, Minerals Engineering 77 (2015) 1–9.

[5] Thanaporn Wannachod, Natchanun Leepipatpiboon, Ura Pancharoen, Suphot Phatanasri, Mass transfer and selective separation of neodymium ions via a hollow fiber supported liquid membrane using PC88A as extractant, Journal of Industrial and Engineering Chemistry 21 (2015) 535–541.

[6] Thanaporn Wannachod, Thidarat Wongsawa, Prakorn Ramakul, Ura Pancharoen, Soorathep Kheawhom, The synergistic extraction of uranium ions from monazite leach solution via HFSLM and its mass transfer, Journal of Industrial and Engineering Chemistry, 33 (2016) 246-254.

[7] Thanaporn Wannachod, Milan Hronec, Tomáš Soták, Katarína Fulajtárová, Ura Pancharoen, Amornchai Arpornwichanop, Liquid-Liquid Equilibrium for Systems

Containing Furfuryl Alcohol–n- Butanol–Water and Salt at T = 298.15 K, Journal of Molecular liquids, 218 (2016) 50-58.

[8]   Thanaporn Wannachod, Milan Hronec, Tomáš Soták, Katarína Fulajtárová, Ura Pancharoen and Amornchai Arpornwichanop, Influence of Salt Concentration on Solubility and Tie-line Data for the System: Water + Formic acid + n-Butanol, Fluid phase equilibria, (2016), impress.

[9]   Thanaporn Wannachod, Milan Hronec, Tomáš Soták, Katarína Fulajtárová, Ura Pancharoen, Amornchai Arpornwichanopa, Influence of Salt on the Solubility and Tie-line Data for Water + Formic acid + Methyl Isobutyl Ketone at T = 298.15 K, Journal of Chemical Engineering Data, (2016), impress.

[10]   Srestha Chaturabul, Thanaporn Wannachod, Natchanun Leepipatpiboon, Ura Pancharoen, Soorathep Kheawhom, Mass transfer resistance of simultaneous extraction and stripping of mercury(II) from petroleum produced water via HFSLM, Journal of Industrial and Engineering Chemistry 21 (2015) 1020–1028.

[11]   Srestha Chaturabul, Thanaporn Wannachod, Vanee Mohdee, Ura Pancharoen, Suphot Phatanasri, An investigation of Calix[4]arene nitrile for mercury(II) treatment in HFSLM application, Chemical Engineering and Processing 89 (2015) 35–40.

[12]   Srestha Chaturabul, Wanchalerm Srirachat, Thanaporn Wannachod, Prakorn Ramakul, Ura Pancharoen, Soorathep Kheawhom, Separation of mercury(II) from petroleum produced water via hollow fiber supported liquid membrane and mass transfer modeling, Chemical Engineering Journal 265 (2015) 34–46.

[13]   Teerapon Pirom, Kraiwith Wongkaew, Thanaporn Wannachod, Ura Pancharoen, Natchanun Leepipatpiboon, Separation of Co(II) and Mn(II) from sulphate media via a HFSLM: Reaction flux model and experimental verification, Journal of Industrial and Engineering Chemistry 20 (2014) 1532–1541.

[14]   Dolapop Sribudda, Thanaporn Wannachod, Prakorn Ramakul, Ura Paancharoen and Suphot Phatanasri, Separation of mercury and arsenic from produced water via hollow fiber contactor: Kinetic and mass transfer analysis, Korean Journal of Chemical Engineering, (2015) 1-10.